UNIVERSIDAD
DE GRANADA

PhD Dissertation

Insights into Conic Optimization
Bridging Theory and Applications

MIGUEL MARTÍNEZ ANTÓN

Supervised by:
PROF. VÍCTOR BLANCO IZQUIERDO, PhD

A thesis submitted in fulfillment of the requirements for the degree of Doctor of Philosophy

in the

PROGRAMA DE DOCTORADO EN MATEMÁTICAS
UNIVERSIDAD DE GRANADA

April 2025

Editor: Universidad de Granada. Tesis Doctorales
Autor: Miguel Martínez Antón
ISBN: 978-84-1195-896-7
URI: https://hdl.handle.net/10481/108327

A mi madre y a mi padre.

A mis hermanas.

A María.

Agradecimientos

Como todos los jóvenes, yo vine
a llevarme la vida por delante.

— Jaime Gil de Biedma
No volveré a ser joven

A la edad de diecisiete años tenía claro que, como todos los jóvenes, yo iba a llevarme la vida por delante. También tenía bastante claro que nadie me iba a ayudar, que iba a hacerlo solo y que así, solo, es como me tocaba hacer las cosas. Hoy, una decada después, no podía estar más equivocado. Estas son las personas que me han quitado la razón.

A quién podría estar más agradecido que a Víctor, el principal artífice de que yo haya llegado a escribir estas palabras. No es necesario mentar su inconmensurable labor científica, su indispensable aportación al desarrollo del presente texto, ni la increíble influencia profesional que ha surtido en mi. Allende la matemática, se encuentra lo humano, y es ahí donde me gustaría detenerme. Has sido la persona que sin atender a un porqué más me ha ayudado y más me ha apoyado, y eso es conmovedor. Me faltará tiempo para agradecértelo, y aun así, te quiero dar las gracias. Solo me has cambiado la vida... Quiero aprovechar para extender el agradecimiento a Ana. Saben los dioses que no es sencillo estar lejos de casa y sin embargo sois como mi familia y de esa manera os aprecio a los dos.

Y empieza así, con esta flor, la primavera: María, mi mejor amiga, que resulta ser mi novia. No es que te dedique esta disertación, es que es tuya. No es posible entender quien soy y, por ende, entender este libro, sin ti. Menuda noche, y menudo paseo más bonito que estamos teniendo. Por supuesto, no todo iban a ser personas y, si hablamos de estos últimos años, tenemos que hablar de Godot. Él me dió un rayo de sol, y solo con luz natural se podía alumbrar una tesis como la que están leyendo.

Macondo es el lugar donde los sueños se hacen realidad, y Santander es mi Macondo. Pero al contrario que en el imaginario de García Márquez, allí lo único extraordinario son mis padres. Ello son los que han hecho magia para que mis sueños cobraran vida. A ellos les quiero agradecer este patrimonio cultural que me han dado, del cual yo he hecho mi reino y el único tesoro que de verdad poseo.

Mis abuelas y abuelos, aquellos que se marcharían no sin antes saber la infancia tan bonita que me regalaron y cómo cada uno iba a marcarme para el resto de mi vida sin ellos. Este también va por ellos.

A mis hermanas: Seila y María Cristina. Es difícil dar una descripción poética de lo que significa tener una hermana, imagínense dos... Así que no lo intentaré. Han sido la medida de todas las cosas durante gran parte de mi vida, tanto, que no se donde terminan ellas y empiezo yo. Luego supongo que esta tesis también se la pueden agenciar. Para mis sobrinos —Luna, Lope y Coral— no tengo agradecimientos sino deseos, y deseo que el contexto de la vida y la obra de su tío algún día les sea de utilidad. Cómo no, a mis otros hermanos: Javi y Josek, mis eruditos a la violeta, estoy seguro que sin vosotros no hubiese sido lo mismo.

Escribía Plutarco sobre el inconveniente de tener muchos amigos. Nunca tuve ese problema. A Diego le agradezco demasiadas cosas, porque en los veranos del Martini y las vistas acojonantes la vida era tan bonita, que parecía de verdad...Y qué decir de Jaime; yo tan pesado con mi capacidad de dilatar el tiempo, y él tan capaz de que cualquier rato se me quede corto.

Granada, ciudad a la que también tengo mucho que agradecer. Podría ser la brisa que entra por el Sacromonte, acaricia la Alhambra, atraviesa el Paseo de los Tristes y llega hasta mi ventana. Pero lo más seguro es que sean los amigos que entre estos muros he conocido y que hacen de éste un lugar especial. María, Fran, Juanjo, Natalia, Marta, Enrique, Andrea y Álvaro. Vosotros habeis hecho este rincón único.

El otro enclave de este doctorado ha sido Toulouse. Agradecer al Dr. Victor Magron la oportunida de trabajar con él y aprender de él y del POP Team, y a todo el LAAS Gang por haber hecho mágico aquel otoño invierno en el sur de Francia.

A todos y cada uno de mis docentes desde el Elena Quiroga hasta las Universidades de Cantabria y Granada, pasando por el Augusto González de Linares. Yo era un humano y vostros me hicisteis persona. Máxime a la profesora Nuria Corral —que sembró el germen para que yo esté investigando en Granada—; y al profesor Manuel Bullejos —sin el cual no hubiese conocido a Víctor y este cuento tendría un final muy diferente—.

Para finalizar, quiero agradecer a las Universidades de Cantabria y Granada, al Programa de Doctorado en Matemáticas por darme la oportunidad y, por último, la acogida del Dpto. de Métodos Cuantitativos para la Economía y Empresa, el Instituto de Matemáticas (IMAG), el Centre National de la Recherche Scientifique – Laboratoire d'Analyse et d'Architecture des Systèmes (LAAS-CNRS), el Institut de Mathématiques de Toulouse (IMT) y a la Red Española de Localización (REDLOCA).

A toda mi familia y mis amigos. Cada uno sabe lo que significa para mí.

UNIVERSIDAD DE GRANADA

PROGRAMA DE DOCTORADO EN MATEMÁTICAS

Sinopsis

Doctor en Filosofía

Reflexiones sobre la Optimización Cónica

Entre la Teoría y las Aplicaciones

por MIGUEL MARTÍNEZ ANTÓN

La presente disertación explora nuevas perspectivas sobre la optimización cónica, abarcando una amplia gama de temas que van desde la optimización lineal sobre secciones de conos hasta aplicaciones en diseño de redes complejas, localización de servicios, detección de fugas o geometría algebraica real. El concepto central del trabajo es la noción matemática de cono, que se explora desde sus orígenes geométricos hasta su uso en la teoría moderna de la optimización. El trabajo se basa, máxime, en el estudio de problemas de optimización cónica, donde se minimiza una función lineal sobre la sección de un cono. Esto generaliza la programación lineal e incluye una amplia gama de problemas de optimización.

Uno de los principales propósitos de esta tesis es introducir una nueva familia de conos, los conos de potencia generalizados, y estudiar el problema de minimizar una función lineal sobre ellos. Se realiza un análisis detallado sobre las representaciones minimales de estos conos, proporcionando un procedimiento para construir representaciones minimales utilizando conos de segundo orden cuando los parámetros definitorios son racionales. La construcción se basa en el concepto de grafos mediados, una estructura combinatoria que desempeña un papel crucial en la derivación de estas representaciones minimales.

La metodología utilizada supone el desarrollo de resultados teóricos sobre las propiedades de los conos de potencia generalizados, el análisis de grafos mediados y la exploración de resultados de complejidad para el

problema de factibilidad sobre conos de orden p. Se derivan nuevas cotas de complejidad, mejorando los resultados existentes y llevando a una mejor comprensión de los desafíos computacionales de la optimización cónica.

Los hallazgos tienen aplicaciones directas en varios dominios. Una aplicación importante se encuentra en los problemas de ubicación de instalaciones, donde se aplica la geometría de los conos de potencia generalizados para desarrollar un modelo de optimización basado en la ley de la gravitación universal de Newton. Además, se presenta un enfoque novedoso para la detección de fugas en redes de tuberías, formulado como un problema entero mixto sobre conos de orden p. Las soluciones a estos problemas son computacionalmente eficientes y demuestran la utilidad práctica de los enfoques propuestos.

En conclusión, la disertación contribuye tanto a los avances teóricos en optimización cónica como a metodologías prácticas para aplicaciones en el mundo real, ofreciendo una perspectiva unificada sobre la optimización, la geometría algebraica y la combinatoria.

UNIVERSIDAD DE GRANADA

PROGRAMA DE DOCTORADO EN MATEMÁTICAS

Abstract

Doctor of Philosophy

Insights into Conic Optimization

Bridging Theory and Applications

by MIGUEL MARTÍNEZ ANTÓN

This dissertation explores novel insights into conic optimization, bridging a diverse set of topics ranging from linear optimization over slices of cones to applications in complex network design, facility location, leak detection, or real algebraic geometry. The central concept of the work is the mathematical notion of cone, which is explored from its geometric origins to its use in modern optimization theory. The work is grounded in the study of conic optimization problems, where a linear function is minimized over a slice of a cone. This generalizes linear programming and encompasses a broad range of optimization problems.

One of the main purposes of this thesis is to introduce a new family of cones, generalized power cones, and study the conic optimization problem of minimizing a linear function over these cones. A detailed analysis is conducted on the minimal representations of these cones, providing a procedure for constructing minimal representations using second–order cones when the defining parameters are rational. The construction is grounded in the concept of mediated graphs, a combinatorial structure that plays a crucial role in deriving the minimal representations.

The methodology involves the development of theoretical results on the properties of generalized power cones, the analysis of mediated graphs, and the exploration of complexity results for the feasibility problem over p–order cones. New complexity bounds are derived, improving upon existing results and leading to a better understanding of the computational challenges in conic optimization.

The findings have direct applications in several domains. A significant application is found in facility location problems, where the geometry of generalized power cones is applied to devise an optimization model based on Newton's universal law of gravitation. Additionally, a novel approach to leak detection in pipeline networks is presented, formulated as a mixed integer p–order cone program. The solutions to these problems are computationally efficient and demonstrate the practical utility of the proposed approaches.

In conclusion, the dissertation contributes to both theoretical advancements in conic optimization and practical methodologies for real-world applications, offering a unified perspective on optimization, algebraic geometry, and combinatorics.

Publications

The contents studied throughout the chapters of this doctoral thesis are based on the following works, where some have been published and others have been submitted for publication in scientific journals of international impact.

BLANCO, V. & MARTÍNEZ-ANTÓN, M. (2025). Optimal Mediated Graphs: The role of Combinatorics in Conic Optimization. Preprint available in: arXiv:2502.03288.

BLANCO, V. & MARTÍNEZ-ANTÓN, M. (2024). On minimal extended representations of generalized power cones. *SIAM Journal on Optimization*, 34(3), 3088-3111. https://doi.org/10.1137/23M1617205.

BLANCO, V., MAGRON, V., & MARTÍNEZ-ANTÓN, M. (2025). On the Complexity of p–Order Cone Programs. Preprint available in: arXiv:2501.09828.

BLANCO, V. & MARTÍNEZ-ANTÓN, M. (2024). Optimal coverage-based placement of static leak detection devices for pipeline water supply networks. *Omega*, 122, 102956. https://doi.org/10.1016/j.omega.2023.102956.

Contents

List of Figures

List of Tables

List of Abbreviations

AGI	**A**rithmetic-**G**eometric **I**nequality
C-MinMG	**C**ontinuous **Min**imal **M**ediated **G**raph **P**roblem
COMP	**C**ontinuous **O**rdered **M**edian Location **P**roblem
CP	**C**onic **P**rogramming
D-MaxMG	**D**iscrete **Max**imal **M**ediated **G**raph **P**roblem
D-MinMG	**D**iscrete **Min**imal **M**ediated **G**raph **P**roblem
GPC	**G**eneralized **P**ower **C**one
GPCP	**G**eneralized **P**ower **C**one **P**rogramming
ILP	**I**nteger **L**inear **P**rogramming
LMI	**L**inear **M**atrix **I**nequality
LP	**L**inear **P**rogramming
ℓ_p**-SVM**	ℓ_p–**S**upport **V**ector **M**achine
MaxMG	**Max**imal **M**ediated **G**raphs
MCLP	**M**aximal **C**overing **L**ocation **P**roblem
MICP	**M**ixed **I**nteger **C**onic **P**rogramming
MILP	**M**ixed **I**nteger **L**inear **P**rogramming
MINLP	**M**ixed **I**nteger **N**on-**L**inear **P**rogramming
Mα**MGP**	**M**inimal α–**M**ediated **G**raph **P**roblem
MinMG	**Min**imal **M**ediated **G**raphs
MIp**OCP**	**M**ixed **I**nteger p–**O**rden **C**one **P**rogramming
MNLCLP	**M**aximal **N**etwork **L**ength **C**overing **L**ocation **P**roblem
MP	**M**athematical **P**rogramming
MISDP	**M**ixed **I**nteger **S**emi-**D**efinite **P**rogramming
MISOCP	**M**ixed **I**nteger **S**econd–**O**rden **C**one **P**rogramming
NLP	**N**on-**L**inear **P**rogramming
p**NMP**	ℓ_p–**N**orm **M**inimization **P**roblem
p**OC**	p–**O**rden **C**one
p**OCP**	p–**O**rden **C**one **P**rogramming
POP	**P**olynomial **O**ptimization **P**roblem
(P)SCLP	**(P**artial) **S**et **C**overing **L**ocation **P**roblem
PSNLCLP	**P**artial **S**et **N**etwork **L**ength **C**overing **L**ocation **P**roblem
PSD	**P**ositive **S**emi-**D**efinite
SDP	**S**emi-**D**efinite **P**rogramming
SF	**S**tandard **F**ormula
SOBS	**S**um **O**f **B**inomial **S**quares
SOC	**S**econd–**O**rden **C**one
SOCP	**S**econd–**O**rden **C**one **P**rogramming
SONC	**S**um **O**f **N**onnegative **C**ircuits
SOS	**S**um **O**f **S**quares

List of Notation

Basics	
$\mathbb{R}, \mathbb{Q}, \mathbb{Z}$	fields and rings
$\mathbb{Z}_+$	nonnegative integers
$\mathbb{N}$	positive integers
$\Omega(n)$	binary support
$\mathbb{R}_+$	nonnegative orthant
$\lvert X \rvert$	cardinality
$\mathbf{0}$	zero vector
$\geq$	componentwise order
$\langle \boldsymbol{x}, \boldsymbol{y} \rangle$	inner product in $\mathbb{R}^n$
Δ_n	standard simplex in $\mathbb{R}^n_+$
$\boldsymbol{e}_i$	standard basis vector
$x^\star$	optimal solution
Matrices	
$\mathbb{R}^{m \times n}$	$m \times n$ real matrices
$[\ ]$	matrix brackets
$\mathcal{S}^n$	$n \times n$ real symmetric matrices
$\mathcal{S}^n_+$	$n \times n$ positive semidefinite matrices
$\langle A, B \rangle$	inner product in $\mathcal{S}^n$
$\mathrm{Tr}(A)$	trace
A^T	matrix transpose
$\mathrm{BlockDiag}(A, B, \ldots)$	block diagonal matrix with blocks A, B, etc.
$\succeq$	Loewner order
$\succeq \mathbf{0}$	positive semidefinite
Geometry and Topology	
$\lVert \boldsymbol{x} \rVert_p$	ℓ_p-norm
$\mathbb{B}_R(\boldsymbol{x})$	ball with center $\boldsymbol{x}$ and radius R
$X \oplus Y$	Minkowski sum
$\dim V$	dimension
V^*	vector space dual
K^*	dual cone
$\mathrm{recc}(X)$	reccesion cone
$\mathcal{K}_p^{n,d}(\boldsymbol{\alpha})$	$(p, \boldsymbol{\alpha})$–power cone
X° or $\mathrm{int}(X)$	interior
$\overline{X}$ or $\mathrm{cl}(X)$	closure
∂X	boundary
$\mathrm{Conv}(X)$	convex hull

Algebra	
$\boldsymbol{x}^{\boldsymbol{\alpha}}, \boldsymbol{\alpha} \in \mathbb{Z}_+^n$	monomial
$\boldsymbol{x}^{\boldsymbol{\alpha}}, \boldsymbol{\alpha} \in \Delta_n$	weighted geometric mean
$\mathbb{R}[\boldsymbol{x}]$	polynomial ring in n variables
$\mathbb{R}[\boldsymbol{x}]_d$	polynomials in n variables, degree at most d
$P_{n,2d}$	nonnegative polynomials in n variables, degree at most $2d$
$\Sigma_{n,2d}$	sum of squares in n variables of degree at most $2d$
$\mathrm{Supp}(p)$	support
$\mathrm{New}(p)$	newton polytope
$p(\mathcal{A}, \boldsymbol{\beta})$	AGI-form
Θ_p	circuit number
$C_{n,2d}$	sonc in n variables of degree at most $2d$
Graph Theory	
$G = (V, E)$	undirected graph or network
$G = (V, A)$	directed graph
$\delta^+(v)$	set of outgoing arcs
$\deg^+(v)$	outdegree
$\delta^-(v)$	set of ingoing arcs
$\deg^-(v)$	indegree
$L^+(G)$	Laplacian

Chapter I

Preface

»—Ven —decían—, célebre Ulises, honra de los griegos, y escucha nuestras voces. Nadie ha pasado jamás sin quedarse a oír la encantadora dulzura de nuestro canto, y quien lo escucha se va no solo embelesado, sino también más sabio [. . .]
»Cantaron estas palabras muy musicalmente, y, como quería seguir oyéndolas, indiqué por señas a mis hombres que me soltaran.

— Homero. *Odisea*, Canto XII

What could they have in common...

- Minimizing a linear (even convex) function over a slice of a cone.
- A family of graphs whose vertices are averages of other vertices.
- Hilbert's 17th problem.
- Facility locations problems.
- Newton's law of universal gravitation.
- Formulae in the first–order theory of the reals.
- Complex network design.
- Leak detection.

Throughout the present dissertation, the reader will figure out novel *insights into conic optimization* which will *bridge* the above topics in a ride from *theory* to *applications*.

The core of this thesis lies on the concept of *cone*. Conic structures are ubiquous in the field of mathematics from the Ancient Greeks geometers to the abstract category theory. The primitive notion of cone is a three-dimensional geometric shape that tapers smoothly from a flat base to a point called the apex that is not contained in the base.

A cone is formed by a set of line segments or rays connecting a common point, the apex, to all of the points on a base. In the case of line segments, the cone does not extend beyond the base, while in the case of rays, it extends infinitely far. The first masterpiece that revolves around cones is the Greek text *Conics* by Apollonius of Perga —inheritor of the conics of Menaechmus—, one of the greatest works of Greek mathematics, along with Euclid's *Elements*, *The Works of Archimedes*, Ptolemy's *Almagest*, *Arithmetica* of Diophantus, and *Synagogue* or *Mathematical Collection* of Pappus. Beginning from the earlier contributions of Euclid, Archimedes and Menaechmus on the topic, Apollonius proved that from a single cone, the three types of conic or quadratic curves can be obtained by varying the inclination of the plane that slices the cone. This fact would be established forever in the collective imagination as the *Apollonius cone*.

Afterwards, with the development of linear algebra and the formalization of analytic geometry, a cone becomes in a subset of a real vector space that is closed under positive scalar multiplication. This meant a broad generalization of the traditional cone in the three-dimensional Euclidean space.

The concept of cone has even come down to category theory. Here, given a category $\mathscr{C}$, the base of a cone is a diagram —a functor from a small category to $\mathscr{C}$—, the apex is an object A of that category, and the rays are arrows from A that commute with the diagram. This is the key to define limits and being able to retrieve *forgotten* algebraic structures via adjunction.

Besides cones, the other large topic of this dissertation is optimization. In its most general and abstract form, an optimization (or decision) problem can be defined as the pursuit of a best element, with regard to some criteria, from some set of available alternatives. When we talk about *mathematical optimization*, this "set of available alternatives" is a (partially or fully) ordered set; the "criteria" is that order; and "a best element" becomes in an optimal (minimal or maximal) element within the ordered set.

Recall, let $(X, \geq)$ be an ordered set.

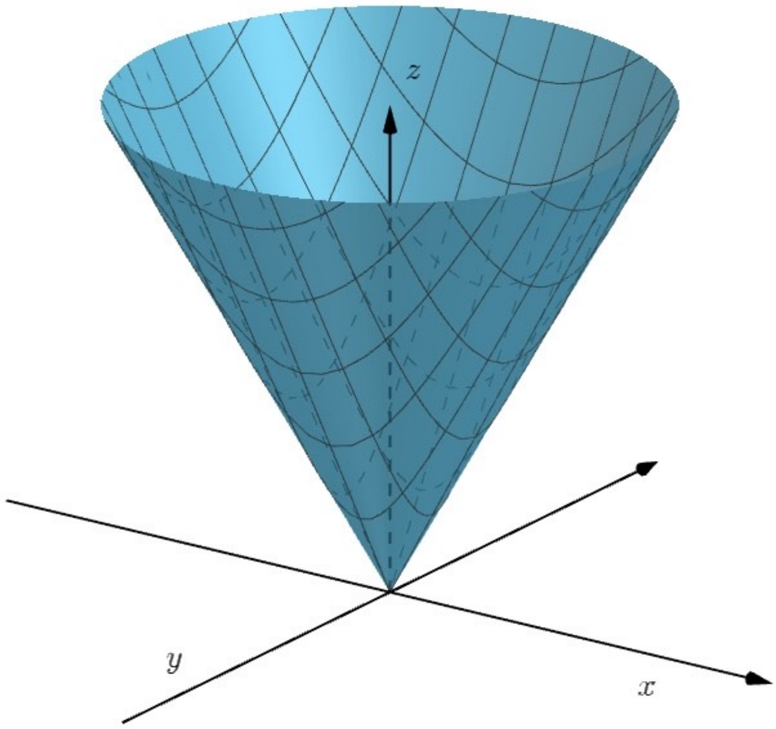

FIGURE 1.1: From Apollonius to Lorentz: the Lorentz or second–order cones represent the multidimensional generalization of the classical Apollonius cone, and they are the heart of this dissertation. Here, its boundary in 3D is drawn.

1. An element $x \in X$ is called *minimal*, if there not exist $y \in X$ such that $y \leq x$ and $x \neq y$.
2. An element $x \in X$ is called *minimum*, if $y \in X$ implies $x \leq y$.

Likewise, the maximal and maximum elements can be defined.

Let $\mathcal{F}$ be a set, $(\mathcal{D}, \leq)$ be an ordered set, and $f : \mathcal{F} \to \mathcal{D}$ be a map. Consider in $\mathcal{F}$ the order, $\leq_f$, induced by f, i.e., for all $x, y \in \mathcal{F}$, $x \leq_f y$ if and only if either $f(x) < f(y)$ or $x = y$. We define the *optimization problem* $\mathcal{P}$,

$$\text{minimize} \quad f(x) \quad \text{subject to} \quad x \in \mathcal{F},$$

as to find a minimal element in $(\mathcal{F}, \leq_f)$ (respectively, a maximal if maximize is used instead of minimize). The set $\mathcal{F}$ is called the *feasible set*. The map f is called the *objective function*. Any $x \in \mathcal{F}$ is called a *feasible solution* and $x^\star \in \mathcal{F}$ stands for a minimal element in $(\mathcal{F}, \leq_f)$ and is called an *optimal solution*. A value $f(x^\star)$ is called an *optimal value*. If $x^\star$ is the minimum, then it is *the* optimal solution. If $\mathcal{F} \neq \emptyset$, the problem is said to be *feasible*; otherwise, it will be *infeasible*.

We are going to focus on the case $\mathcal{D} = \mathbb{R}$ is the field of the reals equipped with the usual order and the feasible region $\mathcal{F}$ is a subset of the Euclidean space $\mathbb{R}^n$. With this status, the concept of mathematical programming arises. When the objective function f is an affine form and the feasible set is defined by $g(x) \geq 0$, where g is also affine, the problem is known as a linear programming problem. Linear programming, developed in the 1940s, has become one of the cornerstones in applied mathematics and operations research today. Its success is based on its geometric intuition, its numerous applications as a subproblem of more complex ones, and its use in modeling problems of all kinds. The constraint inequality "$g(x) \geq 0$" is an inequality between vectors; as such, it requires a definition, and the definition is well known: "$\geq$" must be a partial order compatible with the vector space structure. In the linear programming case, $\geq$, is the componentwise order but what happens if one changes the vector partial order? Optimization meets cones!

The cones that are convex, closed, which has nonempty interior, contain the zero, and do not contain straight lines; are so-called proper cones and they are closely related with vector partial orders. On the one hand, every proper cone K define a vector partial order $\geq_K$ as

$$x \geq_K y \text{ if and only if } x - y \in K, \text{ and}$$
$$x >_K y \text{ if and only if } x - y \in K^\circ.$$

On the other hand, every vector partial order $\geq$ has associated a positive cone defined as the set of vectors x greater or equal to zero, $x \geq 0$, which is a proper cone. Hence, when we are doing linear optimization over an ordered vector space we are minimizing a linear function over a slice of its positive cone. Then, what is conic optimization? Given a proper cone K, it is linear optimization over the ordered vector space defined by the cone, i.e.,

$$\text{minimize} \quad f(x) \quad \text{subject to} \quad g(x) \geq_K 0.$$

Therefore, it can be defined as the problem of minimizing a linear (even convex) function over a slice of a cone. Its development dating back to the 1990s, but it has especially reached a greater degree of maturity in the early years of this century.

Notice that, although we are doing linear optimization, —because of f and g are affine forms—, unless $\geq_K$ is the componentwise order, i.e., K is the nonnegative orthant, then the conic problem is not a linear programming problem, then it becomes in a nonlinear programming problem. The most famous proper cones in conic optimization are the following ones and we refer them as the *big five*:

- nonnegative orthant, which induces componentwise order;
- second–order or Lorentz cone, which is the traditional ice-cream cone;
- cone of positive semidefinite matrices, which induces Loewner order;
- power cone, based on the weighted geometric mean; and
- exponential cone.

Within the wide world of nonlinear optimization, in the last few decades a kind of problems have taken relevance: convex optimization problems. That is due to the vast number of results and the development of algorithms that exploits convexity to solve them efficiently and with guarantees of optimality. A convex optimization problem is one in which the objective function is a convex function and the feasible set is a convex set. That makes conic programming a special sort of convex optimization. In fact, there is a folkloristic belief that all practically relevant convex optimization problems admits a formulation as conic programs involving the big five.

One of the main goals of this thesis is to introduce a new family of proper cones: generalized power cones; and to deal with the conic optimization problem of minimizing a linear function over a slice of this cone. For that purpose, we analyze minimal representations of generalized power cones as simpler cones. We derive some new results on the features of the representations, and we provide a procedure to construct minimal representations by means of second–order cones in case of the parameters that define the cone are rational. The construction is based on the identification of the cones with a graph, the mediated graph.

We provide a unified definition of mediated graphs, a combinatorial structure with multiple applications in mathematical optimization. We study some geometric and algebraic properties of this family of graphs and analyze extremal mediated graphs under the partial order induced by the cardinality of their vertex sets. That is the optimization problem where the objective function is the cardinality of the vertex set and the feasible sets are subsets

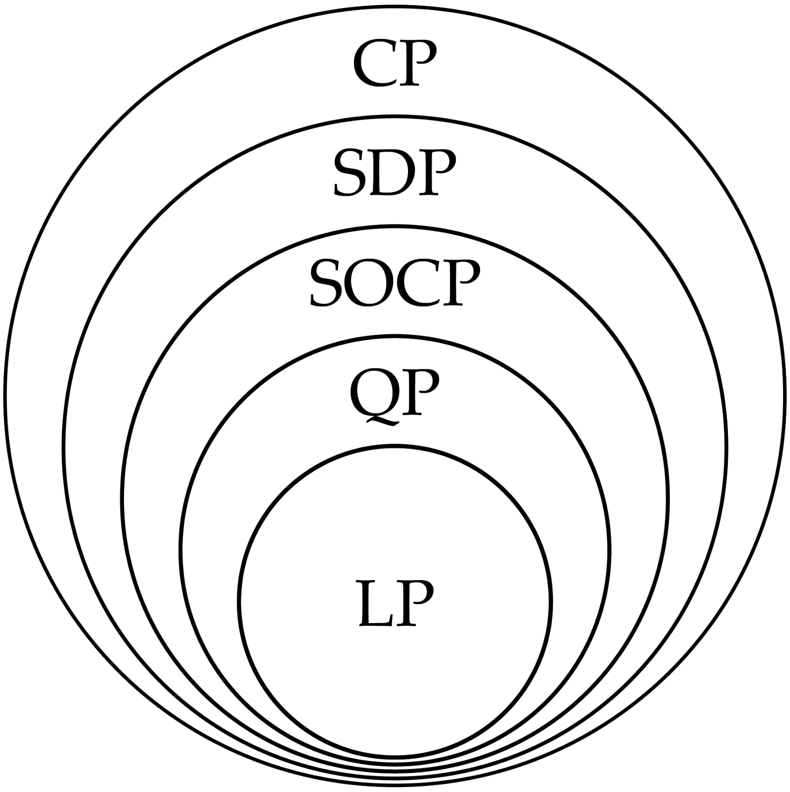

FIGURE 1.2: A hierarchy of convex optimization problems.
LP: linear program, QP: convex quadratic program,
SOCP: second–order cone program,
SDP: semidefinite program, CP: conic program.

of the family of mediated graphs. The solutions of these problems will be optimal mediated graphs and we derive mixed integer linear formulations to compute these challenging graphs.

This geometric graphs can be classified according to the space in which they are embedded. In case that is the entire Euclidean space the optimal graphs will be crucial in conic optimization. But, in case the space is a lattice set then they are strong implications in Hilbert's 17th problem, a legacy of real algebraic geometry which nowadays study the condition for a nonnegative multivariate polynomial is decomposable as sum of squares of polynomials.

Afterwards, we explores novel complexity results for the feasibility problem over p–order cones, a generalization of second–order cones, extending the foundational work of Porkolab and Khachiyan (1997). By leveraging the intrinsic structure of p–order cones, we derive refined complexity bounds that surpass those obtained via standard semidefinite programming reformulations. Our analysis not only improves theoretical bounds but also provides practical insights into the computational efficiency of solving such problems. In addition to establishing complexity results, we derive explicit bounds for solutions when the feasibility problem admits one. For infeasible instances, we analyze their discrepancy quantifying the degree of infeasibility.

Then, we move from theory to applications. First, we examine specific cases of interest, highlighting scenarios where the geometry of p–order cones or problem's structure yields further computational simplifications. These findings contribute to both the theoretical understanding and practical tractability of optimization problems involving p–order cones.

We introduce a new measure in covering location theory based on Newton's law of universal gravitation which can be formulated as a mixed integer generalized power cone program. Furthermore, we provide a mathematical optimization-based framework to determine the location of leak detection devices along a network. Assuming that the devices are endowed with a known coverage area, we analyze two different models. The first model aims to minimize the number of devices to be located in order to (fully or partially) cover the volume of the network. In the second model, the number of devices is given, and the goal is to locate them to provide a coverage volume as broad as possible. Unlike other approaches in the literature, in our models, it is not assumed that the devices are located on the network (vertices or edges) but in the whole space and that the different segments in the networks may be partially covered, which allows for more flexible and realistic coverage. We also derive a method to construct initial solutions as well as a math-heuristic approach for solving the problem for larger instances.

Eventually, we report the results of an extensive battery of experiments to show the validity of our approaches.

The remainder of the present dissertation is structured as follows:

Chapter II: Background

This chapter gathers all the recommended background that could be useful for the reader to explore this thesis. It also sets the notation, definitions, properties, and results that will be used throughout. The topics covered range from the basics of linear algebra, geometry, topology, and complexity, through real algebraic geometry and convexity, to graph theory, and conic and combinatorial optimization.

Chapter III: Mediated Graphs

The content of this chapter is based on the paper

BLANCO, V. & MARTÍNEZ-ANTÓN, M. (2025). Optimal Mediated Graphs: The role of Combinatorics in Conic Optimization. Preprint available in: arXiv:2502.03288.

In Section 3.1, we formally introduce the concept of mediated graphs and establish some fundamental geometric and algebraic properties derived from its definition. Section 3.2 is dedicated to studying optimal (extremal) graphs within the class of mediated graphs under a partial order that we define, based on the cardinality of the vertex set. The identification and computation of these optimal graphs form the core of this part. In Sections 3.2.1 and 3.2.2, we introduce and analyze minimal and maximal mediated graphs, respectively. These sections present the main contributions of this chapter: the development of integer linear programming (ILP) formulations to compute these graphs.

Chapter IV: Conic Algebraic Geometry

What is *conic algebraic geometry*? The term is inheritor of convex algebraic geometry. Blekherman et al. (2012) define convex algebraic geometry as an evolving subject area arising from a synthesis of ideas and techniques from optimization, convex geometry, and algebraic geometry. The central objects of study in this rapidly developing field are convex sets with algebraic structure. Such sets occur naturally, and have been analyzed independently, in convex geometry, real algebraic geometry, optimization, and analysis, but only recently has a unified perspective that systematically takes advantage of the interactions between algebra and convexity emerged. This viewpoint provides rich connections across the mathematical sciences and novel tools for applied mathematics and engineering.

The main contributions of this doctoral thesis taking into account this novel and powerful framework are a *synthesis of ideas and techniques from optimization, convex geometry, and algebraic geometry*, specially conic geometry. That is why, we locate the work within the field of conic algebraic geometry understood as a subfield of the general convex algebraic geometry.

This chapter is splitted in two main sections. The first of them, Section 4.1:

Minimal Representations of Generalized Power Cones, is based on the paper

BLANCO, V. & MARTÍNEZ-ANTÓN, M. (2024). On minimal extended representations of generalized power cones. *SIAM Journal on Optimization*, 34(3), 3088-3111. https://doi.org/10.1137/23M1617205.

Section 4.1.1 is devoted to set the notation and the definition of the main concepts; and seeing possible extensions of the general $(p, \boldsymbol{\alpha})$–power cone by means of simpler $\boldsymbol{\beta}$–power cones and analyzing the complexity between them. In Section 4.1.2, we will show the optimal extended representation of rational $\boldsymbol{\alpha}$–power cone using second–order cones, for this purpose we will introduce the idea of $\boldsymbol{\alpha}$–mediated graph as a special kind of mediated graph, its relationship with these extended representations and address the problem of finding minimal $\boldsymbol{\alpha}$–mediated graphs (M$\boldsymbol{\alpha}$MGP) via combinatorial programming. In Section 4.1.3, we show the implications of the developed theory for conic optimization.

The second large section of the chapter, Section 4.2:

Polynomial Optimization, is due to the implications of discrete minimal mediated graphs for Hilbert's 17th problem, thus real algebraic geometry, and polynomial optimization. Part of this content can be found in

BLANCO, V. & MARTÍNEZ-ANTÓN, M. (2025). Optimal Mediated Graphs: The role of Combinatorics in Conic Optimization. Preprint available in: arXiv:2502.03288.

Section 4.2.1 is due to show how obtain a minimal second–order cone representation of a special cone of sparse polynomials supported on circuits based on continuous minimal mediated graphs and the work of Magron and Wang (2023). Moreover, its implication for unconstrained polynomial optimization. Eventually, in Section 4.2.2, we prove a novel exact and explicit sum of binomial squares decomposition of the above mentioned kind of sparse polynomial, and characterize the intersection of the cone of these polynomials and the cone of sum of squares by means of the optimal solution of our combinatorial optimization problem and the results in Iliman and De Wolff (2016a); Hartzer et al. (2022).

Chapter V: Complexity

This chapter is due to derive different complexity results for the p–order feasibility problem. The content is based on the paper

BLANCO, V., MAGRON, V., & MARTÍNEZ-ANTÓN, M. (2025). On the Complexity of p–Order Cone Programs. Preprint available in: arXiv:2501.09828.

In Section 5.1, we state the notation and main results use to derive the complexity results in this chapter. In this section, we also prove the complexity results that can be derived for the problem by rewriting the problem as a semidefinite programming problem. In Section 5.2, we provide the upper bounds for the feasible solutions and the discrepancy for the p-order feasibility problem. Section 5.3 is devoted to prove the complexity bounds for the p–order feasibility problem. Exploiting the geometry of p–order cones we apply a similar strategy as the one by Porkolab and Khachiyan (1997) to derive new complexity bounds for the problem. We also analyze some particular cases for the value of p, namely, $p = 2$, p nonnegative even integer, and p of the form $\frac{r}{r-1}$ with r nonnegative integer. Finally, in Section 5.4, we extend our complexity results to problems involving several p–order cone constraints.

Chapter VI: Applications

This chapter is the end of the road from theory to practice. It is divided in sections according to the nature of how the theory is applied in each case.

In Section 6.1, we emphasize how the complexity bounds are applied to optimization problems that involve p–order cones. The content can be found in

BLANCO, V., MAGRON, V., & MARTÍNEZ-ANTÓN, M. (2025). On the Complexity of p–Order Cone Programs. Preprint available in: arXiv:2501.09828.

The goal of Section 6.2, **Gravitational Covering Location Problem**, is to propose a novel location problem to optimally locate a given number of facilities in the Euclidean space, and decide their coverage radii based on different features to maximize the overall coverage of a given set of users. The radii will represent an attraction measure based on Newton's law of universal gravitation. We propose a generalized power cone program to solve it. The content can be seen in

BLANCO, V. & MARTÍNEZ-ANTÓN, M. (2024). On minimal extended representations of generalized power cones. *SIAM Journal on Optimization*, 34(3), 3088-3111. https://doi.org/10.1137/23M1617205.

Eventually, Section 6.3:

Network Covering: A Leak Detection Problem, is based on

BLANCO, V. & MARTÍNEZ-ANTÓN, M. (2024). Optimal coverage-based placement of static leak detection devices for pipeline water supply networks. *Omega*, 122, 102956. https://doi.org/10.1016/j.omega.2023.102956.

It provides a mathematical optimization-based framework to determine the location of leak detection devices along a network. Assuming that the devices are endowed with a known coverage area.

In Section 6.3.1, we introduce the problem under analysis and illustrate some of the solutions that can be obtained. Section 6.3.2 is devoted to analyze the problem of locating a single device, which will be helpful in the development of approximation algorithms for the multi-device case. In Section 6.3.3, the general case is analyzed. We provide mixed integer conic programming formulations for the maximal and partial set covering location problems and a deep study of them. We also provide a method to construct initial solutions for the problem based on the geometric properties of the solutions and a math-heuristic approach based on solving, iteratively, single-device instances.

Chapter VII: Computational Experience

After all theoretical and practical development, in this chapter, we report the results of an extensive set of experiments showing the validity and practical utility of our approaches. The computational experiments and results can be found in

BLANCO, V. & MARTÍNEZ-ANTÓN, M. (2025). Optimal Mediated Graphs: The role of Combinatorics in Conic Optimization. Preprint available in: arXiv:2502.03288.

BLANCO, V. & MARTÍNEZ-ANTÓN, M. (2024). On minimal extended representations of generalized power cones. *SIAM Journal on Optimization*, 34(3), 3088-3111. https://doi.org/10.1137/23M1617205.

BLANCO, V. & MARTÍNEZ-ANTÓN, M. (2024). Optimal coverage-based placement of static leak detection devices for pipeline water supply networks. *Omega*, 122, 102956. https://doi.org/10.1016/j.omega.2023.102956.

They are divided in sections depending on the approach whose performance is tested. In Section 7.1, for maximal mediated graphs, we compare our optimization-based method with respect to the enumerative approach proposed by Hartzer et al. (2022). For minimal mediated graphs, we analyze the performance of different domain formulations for which we derive integer linear optimization models. In Section 7.1.3, we show the computational performance of our specific mathematical programming model for compute minimal second–order cone representations. In Section 7.2.1, we have run a series of experiments to analyze the performance of solving the proposed gravitational covering location problem with an optimal second–order cone representation of the generalized power cone with respect to the usual naive representation. Finally, the results of our computational experiments on real-world urban pipeline networks are reported in Section 7.2.2.

Chapter VIII: Conclusion

This PhD dissertation ends in this chapter with the conclusions of the carried out research, and future open lines of work.

Chapter II

Background

— Pues nada, Telva: ¡no la encuentro
a usted en las listas del concejo..!
— ¡Ay, don Rosendo..! ¡Si non me
paez mal..!: Si non toi entre les
«listes»... ¡a lo mejor metiéronme
entre les tontes..!

— Alfonso. *Pinón y Telva*

2.1 Basics

The theoretical foundation on which the present dissertation rests is the so-called Zermelo-Fraenkel set theory, with Choice, ZFC. In this theory, the primitive starting concepts are the *set* and the *membership*, accompanied by the Zermelo-Fraenkel axiomatic system along with the axiom of choice. Based on this theoretical framework, all the constructions and results of this thesis can be deduced.

Given two sets X and Y, one has the following set operators:

- union, $X \cup Y := \{x \mid x \in X \vee x \in Y\}$;
- intersection, $X \cap Y := \{x \mid x \in X \wedge x \in Y\}$;
- subtraction, $X \backslash Y := \{x \mid x \in X \wedge x \notin Y\}$;
- Cartesian product, $X \times Y := \{(x, y) \mid x \in X \wedge y \in Y\}$; and
- exponentiation $X^Y := \{f : Y \to X \mid f \text{ a mapping}\}$.

Given a set X, the notation $|X|$ stands for the cardinality of X. The set $2^X := \{0,1\}^X$ is the power set of X and it is equivalent to the set of all subsets of X. Let $n \in \mathbb{N}$, the set $X^n := X \times \overset{n)}{\cdots} \times X \cong X^{\{1,\dots,n\}}$. Here, $\cong$ stands for the bijection equivalence relation, i.e., $X \cong Y$ if X and Y are bijective sets. In fact, if Y is a finite set, then we can express each element in X^Y as a tuple indexed in Y, i.e., $(x_y)_{y \in Y}$. Specially, each element of X^n can be expressed as $(x_1, \ldots, x_n)$.

Besides, one can define relationships in any set X being the most significative the equivalences and orders.

The notation described below will be followed in general. There may be some deviation where appropriate.

Let $\mathbb{N}$ be the *set of positive integer (natural) numbers*, $\mathbb{Z}$ the *ring of integer numbers*, $\mathbb{Q}$ the *field of rational numbers*, and $\mathbb{R}$ the *field of real numbers*. The notation $\mathbb{Z}_+, \mathbb{Q}_+$, and $\mathbb{R}_+$ stand for the subset of nonnegative numbers in each case. Let $m, n \in \mathbb{N}$, $\mathbb{R}^{m \times n}$ denotes the *set of $m \times n$ real matrices*. Let $\boldsymbol{x} \in \mathbb{R}^n$, $\mathbb{R}[\boldsymbol{x}]$ denotes the *ring of real n-variate polynomials.*

2.1.1 Linear Algebra

We write vectors in bold lower case throughout this thesis. Upper-case letters will be used to represent matrices. Greek letters will typically be used to represent scalars. We work with real vector spaces, mainly, given a natural number n, the n-dimensional real vector space $\mathbb{R}^n$ of vectors with n real components. But also we work with the real vector space $\mathcal{S}^n$ of $n \times n$ real symmetric matrices and the real vector space $\mathbb{R}_d[\boldsymbol{x}]$ of all n-variate real polynomials with degree at most $d \in \mathbb{Z}_+$.

Recall, every real vector space is a real affine space considering the mapping $(\boldsymbol{x}, \boldsymbol{y}) \mapsto \boldsymbol{y} - \boldsymbol{x}$ for every pair of vectors $\boldsymbol{x}, \boldsymbol{y}$. Hence, whenever a vector space is discussed its affine structure will be taken into account and every vector might be seen as an affine point.

A vector is always considered as a column vector, unless otherwise stated. A set of vectors $\boldsymbol{x}_1, \ldots, \boldsymbol{x}_m$ is said to be *linearly dependent* if there are scalars $\lambda_1, \ldots, \lambda_m$, not all zero, such that the *linear combination*

$$\lambda_1 \boldsymbol{x}_1 + \cdots + \lambda_m \boldsymbol{x}_m = \boldsymbol{0}.$$

Otherwise, the set of vector is said to be *linearly independent*. Likewise, a set of affine points $\boldsymbol{x}_0, \boldsymbol{x}_1, \ldots, \boldsymbol{x}_m$ is said to be *affinely dependent* if there are scalars

$\lambda_1, \ldots, \lambda_m$, not all zero, such that the linear combination

$$\lambda_1(\boldsymbol{x}_1 - \boldsymbol{x}_0) + \cdots + \lambda_m(\boldsymbol{x}_m - \boldsymbol{x}_0) = \boldsymbol{0}.$$

Otherwise, the set of points is said to be *affinely independent*. In $\mathbb{R}^n$, the vector inequality $\boldsymbol{x} \geq \boldsymbol{y}$ means $x_j \geq y_j$ for $j = 1, 2, ..., n$ (likewise for the strict order $>$). $\boldsymbol{0}$ represents a vector whose entries are all zeros where it dimension may vary according to other vectors in expressions. Addition of vectors and multiplication of a vector with a scalar are standard. The superscript, T, denotes *transpose* operation. The *inner product* in $\mathbb{R}^n$ is defined as follows:

$$\langle \boldsymbol{x}, \boldsymbol{y} \rangle := \boldsymbol{x}^T \boldsymbol{y} = \sum_{j=1}^{n} x_j y_j \quad \text{for } \boldsymbol{x}, \boldsymbol{y} \in \mathbb{R}^n.$$

For natural numbers m and n, $\mathbb{R}^{m \times n}$ denotes the *vector space of real matrices with m rows and n columns*. For $A \in \mathbb{R}^{m \times n}$, we assume that the row index set of A is $\{1, 2, \ldots, m\}$ and the column index set is $\{1, 2, \ldots, n\}$, but it might be any finite sets. The ith and jth component of A is denoted by a_{ij}. If I is a subset of the row index set and J is a subset of the column index set, then A_I denotes the submatrix of A whose rows belong to I, A_J denotes the submatrix of A whose columns belong to J, A_{IJ} denotes the submatrix of A induced by those components of A whose indices belong to I and J, respectively. If a matrix A has the same index set, I, of cardinality n for rows and columns, A is said to be an $n \times n$ square matrix. If U is a subset of I, then A_U stands for the submatrix of A whose rows and columns belong to I. The identity matrix is denoted by I. The trace of A, denoted by $\mathrm{Tr}(A)$, is the sum of the diagonal entries in A. For matrices $A_i \in \mathbb{R}^{m_i \times n_i}$ for $i \in I$, $\mathrm{BlockDiag}(A_i)_{i \in I}$ represents a matrix in $\mathbb{R}^{\sum_{i \in I} m_i \times \sum_{i \in I} n_i}$ in which the matrices A_i are arranged in diagonal and every other entry is zero. Addition of matrices and multiplication of a matrix with a scalar are standard. The inner product in $\mathbb{R}^{m \times n}$ is defined as follows:

$$\langle A, B \rangle := \mathrm{Tr}(A^T B) = \sum_{i=1}^{m} \sum_{j=1}^{n} a_{ij} b_{ij} \quad \text{for } A, B \in \mathbb{R}^{m \times n}.$$

A square matrix $A \in \mathbb{R}^{n \times n}$ is *symmetric* if $a_{ij} = a_{ji}$ for $i, j = 1, \ldots, n$; i.e, $A^T = A$. The set of $n \times n$ *real symmetric matrices* is denoted as $\mathcal{S}^n$ and is a real vector space of dimension $\binom{n+1}{2} = \frac{1}{2}(n+1)n$.

Real quadratic forms can always be represented in terms of symmetric matrices, i.e., $q(\boldsymbol{x}) = \sum_{i=1}^n \sum_{j=1}^n a_{ij} x_i x_j = \boldsymbol{x}^T A \boldsymbol{x}$, where $a_{ij} = a_{ji}$. They often identify a symmetric matrix with the corresponding quadratic form. If the quadratic form $\boldsymbol{x}^T A \boldsymbol{x}$ takes only nonnegative values, we say that the matrix A is *positive semidefinite* (PSD), and it is denoted by $A \succeq \mathbf{0}$. Similarly, if it takes only positive values (except at the origin, where it necessarily vanishes), then A is *positive definite* denoted by $A \succ \mathbf{0}$.

Given a block-partitioned matrix

$$\begin{bmatrix} A & B \\ B^T & C \end{bmatrix}$$

where A is square and invertible, the *Schur complement* of A is the matrix $C - B^T A^{-1} B$. Similarly, if C is square and invertible, its Schur complement is the matrix $A - BC^{-1}B^T$. Many of the properties of the Schur complement follow quite directly from the two factorizations:

$$\begin{aligned} \begin{bmatrix} A & B \\ B^T & C \end{bmatrix} &= \begin{bmatrix} I & \mathbf{0} \\ B^T A^{-1} & I \end{bmatrix} \begin{bmatrix} A & \mathbf{0} \\ \mathbf{0} & C - B^T A^{-1} B \end{bmatrix} \begin{bmatrix} I & A^{-1}B \\ \mathbf{0} & I \end{bmatrix} \\ &= \begin{bmatrix} I & BC^{-1} \\ \mathbf{0} & I \end{bmatrix} \begin{bmatrix} A - BC^{-1}B^T & \mathbf{0} \\ \mathbf{0} & C \end{bmatrix} \begin{bmatrix} I & \mathbf{0} \\ C^{-1}B^T & I \end{bmatrix}. \end{aligned}$$

Since the factorizations above are congruence transformations, this implies that the following conditions are equivalent:

$$\begin{bmatrix} A & B \\ B^T & C \end{bmatrix} \succeq \mathbf{0} \iff \begin{cases} A \succeq \mathbf{0} \\ C - B^T A^{-1} B \succeq \mathbf{0} \end{cases} \iff \begin{cases} C \succeq \mathbf{0} \\ A - BC^{-1}B^T \succeq \mathbf{0}. \end{cases}$$

A *monomial* in the n variables $x_1, \ldots, x_n$ (abbreviated as $\boldsymbol{x}$) is a formal product $\boldsymbol{x}^{\boldsymbol{\alpha}} := x_1^{\alpha_1} \cdots x_n^{\alpha_n}$, where $\boldsymbol{\alpha} = (\alpha_1, \ldots, \alpha_n) \in \mathbb{Z}_+^n$. A *polynomial* in $\boldsymbol{x}$ with coefficients in $\mathbb{R}$ or a *real polynomial* is a finite linear combination of the form $p := \sum_{\boldsymbol{\alpha} \in \mathcal{A}} c_{\boldsymbol{\alpha}} \boldsymbol{x}^{\boldsymbol{\alpha}}$ where $\mathcal{A} \subset Z_+^n$ is a finite set and $c_{\boldsymbol{\alpha}} \in \mathbb{R}$ for $\boldsymbol{\alpha} \in \mathcal{A}$. An exponent $\boldsymbol{\alpha}$ is in the *support*, $\mathrm{Supp}(p)$, of p if $c_{\boldsymbol{\alpha}} \neq 0$. The *degree* of p is the maximum ℓ_1–norm of the vectors $\boldsymbol{\alpha}$ in the support of p. The *polynomial ring* $\mathbb{R}[\boldsymbol{x}]$ is the set of all polynomials in $\boldsymbol{x}$ with coefficients in $\mathbb{R}$. It is endowed with the two binary operations of addition and multiplication of pairs of polynomials. This commutative ring with identity is also a infinite-dimensional real vector space. Hence, the *set of all n-variate real polynomials with degree at most $d \in \mathbb{Z}_+$*

denoted by $\mathbb{R}_d[x]$ is a real vector space of dimension $\binom{n+d}{n}$.

2.1.2 Geometry and Topology

A *Euclidean space* is an affine space over the reals such that the associated vector space is an *Euclidean vector space*, it means a finite-dimensional inner product space over the real numbers. It follows that $\mathbb{R}^n$ and $\mathcal{S}^n$ are Euclidean spaces regarding the inner products defined in the previous section. Because of the inner product, $\mathbb{R}^n$ becomes in a normed space where the norm is induced by the standard inner product:

$$\|\boldsymbol{x}\|_2 := \sqrt{\boldsymbol{x}^T\boldsymbol{x}}$$

and it is called the *Euclidean or ℓ_2–norm*. Any norm $\|\cdot\|$ makes $\mathbb{R}^n$ for a complete metric space with the distance defined as $d(\boldsymbol{x},\boldsymbol{y}) := \|\boldsymbol{x}-\boldsymbol{y}\|$ and therefore $\mathbb{R}^n$ is also a topological space.

In the present dissertation we are interested in a well-known generalization of the Euclidean norm. Given $p \in \mathbb{R}_+ \cup \{\infty\}$ with $p \geq 1$, the *Hölder or ℓ_p–norm* in $\mathbb{R}^n$ is defined as:

$$\|\boldsymbol{x}\|_p := \begin{cases} \left(\sum_{j=1}^{n} |x_j|^p\right)^{\frac{1}{p}} & \text{if } p < \infty \\ \max_{j=1,\dots,d} |x_j| & \text{if } p = \infty. \end{cases}$$

The ℓ_p–norms are pairwise equivalent, what implies the induced topology is invariant under selection of the parameter p. A (closed) *ℓ_p–ball with center $\boldsymbol{x} \in \mathbb{R}^n$ and radius $R \in \mathbb{R}_+$* is the set

$$\mathbb{B}_R(\boldsymbol{x}) = \{\boldsymbol{y} \in \mathbb{R}^n : \|\boldsymbol{x}-\boldsymbol{y}\|_p \leq R\}.$$

If the inequality is strict we get the open ℓ_p–ball defined as

$$\mathbb{B}_R^\circ(\boldsymbol{x}) := \{\boldsymbol{y} \in \mathbb{R}^n : \|\boldsymbol{x}-\boldsymbol{y}\|_p < R\}.$$

For every p, the latter sets form a basis for the standard topology in $\mathbb{R}^n$. Hence, a subset X of $\mathbb{R}^n$ is *open* if can be written as union of open balls. Otherwise, a subset $X \subset \mathbb{R}^n$ will be *closed* if its complementary $\mathbb{R}^n \backslash X$ is open. A subset will be *bounded* if it is content in some ball. A closed and bounded

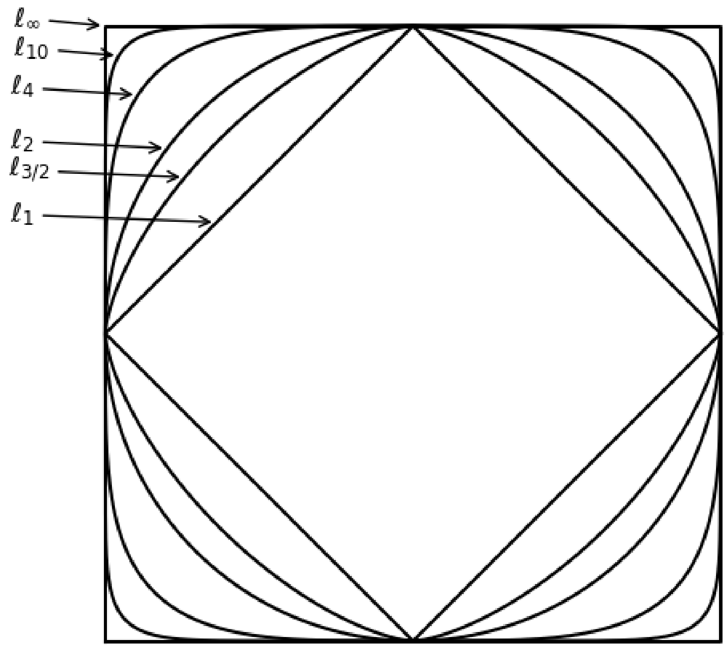

FIGURE 2.1: ℓ_p–norm balls with $p \in \{1, \frac{3}{2}, 2, 4, 10, \infty\}$.

subset is said to be *compact*. Let $\boldsymbol{x} \in X \subset \mathbb{R}^n$ is said to be an *interior point* of X if there exists a ball centered in $\boldsymbol{x}$ content in X. Otherwise, the point $\boldsymbol{x}$ is said to be *exterior*. The set of all interior points of X is known as the *interior* of X, it is denoted as X° or $\mathrm{int}(X)$, and it is the largest open set content in X. Let $\boldsymbol{x} \in \mathbb{R}^n$ be a point, $\boldsymbol{x}$ is called a *closure point* of X if every ball centered in $\boldsymbol{x}$ intersects X. The set of all closure points of X is known as the *closure* of X, it is denoted as $\overline{X}$ or $\mathrm{cl}(X)$, and it is the smallest closed set that contains X. The set $\overline{X} \backslash X^\circ$ is called the *boundary* or *frontier* of X and is denoted as ∂X. For instance, the open ball $\mathbb{B}_R^\circ(\boldsymbol{x})$ is the interior of the (closed) ball, whereas the latter is the closure of the former, i.e., $\mathrm{cl}(\mathbb{B}_R^\circ(\boldsymbol{x})) = \mathbb{B}_R(\boldsymbol{x})$. In both cases, the boundary $\partial\mathbb{B}_R(\boldsymbol{x}) = \{\boldsymbol{y} \in \mathbb{R}^n : \|\boldsymbol{x} - \boldsymbol{y}\|_p = R\}$ is the *sphere of center* $\boldsymbol{x}$ *and radius R*.

Moreover, in the Euclidean space $\mathbb{R}^n$ it can be defined the so-called *Minkowski sum* of two subsets X and Y as the set

$$X \oplus Y := \{\boldsymbol{x} + \boldsymbol{y} \in \mathbb{R}^n \mid \boldsymbol{x} \in X, \boldsymbol{y} \in Y\}.$$

2.1.3 Complexity Estimates

For complexity estimates, we use the bit complexity model. For a nonzero integer $b \in \mathbb{Z}\backslash\{0\}$, we denote by $\tau(b) := \lfloor \log_2(|b|) \rfloor + 1$ the *bit size* of b, with the convention $\tau(0) := 1$. For a rational number $a = \frac{b}{c} \in \mathbb{Q}$, with $b \in \mathbb{Z}, c \in \mathbb{Z}\backslash\{0\}$ and $\gcd(b, c) = 1$, we denote $\max\{\tau(b), \tau(c)\}$ by $\tau(a)$. For the sake of simplicity, all derived complexity estimates are provided while assuming integer input data. It is straightforward to establish similar estimates while assuming rational input data.

For two mappings $g, h : \mathbb{N}^n \to \mathbb{R}_{>0}$, the expression "$g(v) = O(h(v))$" means that there exist integers $b, N \in \mathbb{Z}_+$ such that when all coordinates of v are greater than or equal to N, $g(v) \leq bh(v)$.

2.2 Real Algebraic Geometry

2.2.1 Nonnegative Polynomials and Sums of Squares

Studying nonnegativity of real, multivariate polynomials is a key problem in real algebraic geometry. Since deciding nonnegativity is well-known to be a hard problem both in theory and practice, one is interested in certificates of nonnegativity, i.e., a special structure of real polynomials, which implies nonnegativity and it is easier to test. The classical as well as most common certificate of nonnegativity are *sums of squares* (SOS) (see, e.g., Marshall, 2008; Reznick, 2000). Let n and d be two nonnegative integers we consider in $\mathbb{R}[\mathbf{x}]_{2d}$ the proper cones:

$$P_{n,2d} := \{p \in \mathbb{R}_{2d}[\mathbf{x}] \mid p(\mathbf{x}) \geq 0 \text{ for all } \mathbf{x} \in \mathbb{R}^n\}, \text{ and}$$

$$\Sigma_{n,2d} := \left\{ p \in \mathbb{R}_{2d}[\mathbf{x}] \;\middle|\; p = \sum_{i=1}^{k} \sigma_i^2, \quad \sigma_i \in \mathbb{R}_d[\mathbf{x}] \right\},$$

defined as the *cone of nonnegative polynomials* and *the cone of sum of squares polynomials*, respectively. Nonnegativity of real polynomials and sums of squares has been an active field of research, mainly, due to their relation with polynomial optimization. In the last two decades, polynomial optimization has made a significant impact on both continuous and discrete optimization fundamentally due to its strong connection with semidefinite programming (see Blekherman et al., 2012; Lasserre, 2009). One of the central questions in real algebraic geometry and optimization is understanding the relationship between these two cones.

Since sum of squares implies nonnegativity, i.e., $\Sigma_{n,2d} \subseteq P_{n,2d}$; a natural question is understanding when the converse holds. These studies start when Hilbert (1888) proved that there must be nonnegative polynomials that cannot be represented as sum of squares, in fact, he showed that $\Sigma_{n,2d} \subsetneq P_{n,2d}$ unless $(n, 2d) \in \{(1,k),(k,2),(2,4) : k \in \mathbb{N}\}$; that are univariate polynomials, quadratic polynomials, and bivariate quartics. But, it was not until 1967, almost 80 years later, when Motzkin (1967) offered the first example of nonnegative polynomial that is not sum of squares:

$$M(x,y) = x^4y^2 + x^2y^4 + 1 - 3x^2y^2,$$

in its dehomogenized form. Its nonnegativity follows from monomial substitution $(x^4y^2, x^2y^4, 1)$ into the arithmetic-geometric inequality (AGI) that states

$$\sum_{j=1}^{d} \lambda_j t_j - \prod_{j=1}^{d} t_j^{\lambda_j} \geq 0, \tag{AGI}$$

if $t_j, \lambda_j \geq 0$ and $\sum_{j=1}^{d} \lambda_j = 1$, it means, for nonnegative values of variables t the weighted arithmetic mean is always greater than the weighted geometric mean, regardless of the weights. As early as 1891, Hurwitz (1891) proved that polynomials of the shape:

$$H_{2d}(\boldsymbol{x}) = \sum_{j=1}^{2d} x_j^{2d} - 2d \prod_{j=1}^{2d} x_j$$

are always sums of squares and, with them, he demonstrated the validity of the (AGI) using monomial substitution. From the study of polynomials derived from the (AGI), Reznick (1989) answered the form of a necessary and sufficient condition based on the *Newton polytope* ($\text{New}(p) := \text{Conv}(\text{Supp}(p))$) of nonnegative forms derived from the monomial substitution into (AGI) (AGI-forms).

Given a finite set $\mathcal{A} \subset (2\mathbb{Z})^n$ an affine independent set, and a lattice point $\boldsymbol{\beta}$ in the convex hull of $\mathcal{A}$. The corresponding *AGI-form* is given by

$$p(\mathcal{A}, \boldsymbol{\beta})(\boldsymbol{x}) := \sum_{\boldsymbol{\alpha} \in \mathcal{A}} \lambda_{\boldsymbol{\alpha}} \boldsymbol{x}^{\boldsymbol{\alpha}} - \boldsymbol{x}^{\boldsymbol{\beta}}, \tag{2.1}$$

where the $\boldsymbol{\lambda} \in \mathbb{R}_+^{\mathcal{A}}$ is the vector of barycentric coordinates of $\boldsymbol{\beta}$ (see Section 2.3). In recent years, Iliman and De Wolff (2016a) generalized the concept of AGI-forms to circuit polynomials and connected this with polynomial optimization (Iliman and De Wolff, 2016b).

A polynomial $p \in \mathbb{R}[\boldsymbol{x}]$ is called a *circuit polynomial* (circuit for short) if it is of the form

$$p(\boldsymbol{x}) := \sum_{\boldsymbol{\alpha} \in \mathcal{A}} c_{\boldsymbol{\alpha}} \boldsymbol{x}^{\boldsymbol{\alpha}} + c_{\boldsymbol{\beta}} \boldsymbol{x}^{\boldsymbol{\beta}},$$

where $\mathcal{A} \subset (2\mathbb{Z})^n$ is an affine independent set, $c_{\boldsymbol{\alpha}} > 0$ for $\boldsymbol{\alpha} \in \mathcal{A}$, and $\boldsymbol{\beta} \in \operatorname{Conv}(\mathcal{A})^\circ \cap \mathbb{Z}$.

Let $p \in \mathbb{R}[\boldsymbol{x}]$ be a circuit, the *circuit number* Θ_p is defined as

$$\Theta_p = \prod_{\boldsymbol{\alpha} \in \mathcal{A}} \left(\frac{c_{\boldsymbol{\alpha}}}{\lambda_{\boldsymbol{\alpha}}} \right)^{\lambda_{\boldsymbol{\alpha}}}. \tag{2.2}$$

The nonnegativity of the circuit p can be checked by its circuit number: p is nonnegative if and only if either $|c_{\boldsymbol{\beta}}| \leq \Theta_p$ and $\boldsymbol{\beta} \notin (2\mathbb{Z})^n$, or $c_{\boldsymbol{\beta}} \geq -\Theta_p$ and $\boldsymbol{\beta} \in (2\mathbb{Z})^n$. Let n and d be two nonnegative integers we consider in $\mathbb{R}[\boldsymbol{x}]_{2d}$ the *cone of sum of nonnegative circuit* (SONC) *polynomials*:

$$C_{n,2d} := \left\{ p \in \mathbb{R}_{2d}[\boldsymbol{x}] \;\middle|\; p = \sum_{i=1}^{k} q_i, \quad q_i \text{ is a nonnegative circuit} \right\}.$$

On the other hand, let $\mathcal{A} \subset (2\mathbb{Z})^n$ be an affine independent set. A subset L of $\mathbb{Z}^n$ is said to be an *$\mathcal{A}$–mediated set* if $\mathcal{A} \subseteq L$ and every $\boldsymbol{x} \in L \backslash \mathcal{A}$ is an average of two distinct even points in L, i.e., for all $\boldsymbol{x} \in L \backslash \mathcal{A}$ there exist $\boldsymbol{y} \neq \boldsymbol{z} \in L \cap (2\mathbb{Z})^n$ such that $2\boldsymbol{x} = \boldsymbol{y} + \boldsymbol{z}$.

Reznick (1989) proved that an AGI-form $p(\mathcal{A}, \boldsymbol{\beta})$ is a sum of squares if and only if there is an $\mathcal{A}$-mediated set L that contains $\boldsymbol{\beta}$. Moreover, he provided an algorithm to compute the $\mathcal{A}$-mediated set which contains every $\mathcal{A}$-mediated set. He called it: *maximal mediated set* and denoted it as $\mathcal{A}^*$. Iliman and De Wolff (2016a) generalized the necessary and sufficient condition for nonnegative circuit polynomials, and Hartzer et al. (2022) generalized them for SONC with the following result.

Theorem 2.1. *Let $\mathcal{A} = \{\mathbf{0}, \boldsymbol{\alpha}(1), \ldots, \boldsymbol{\alpha}(n)\} \subset (2\mathbb{Z})^n$ be an affine independent set, $\mathcal{B} \subset \operatorname{Conv}(\mathcal{A})^\circ \cap \mathbb{Z}^d$ be a finite set, and $p = \lambda_0 + \sum_{i=0}^{n} a_i \boldsymbol{x}^{\boldsymbol{\alpha}(i)} + \sum_{\boldsymbol{\beta} \in \mathcal{B}} b_{\boldsymbol{\beta}} \boldsymbol{x}^{\boldsymbol{\beta}}$ be a*

SONC *supported on* $\mathcal{A} \cup \mathcal{B}$ *such that for all* $\boldsymbol{\beta} \in \mathcal{B}$*, either* $b_{\boldsymbol{\beta}} < 0$ *or* $\boldsymbol{\beta} \notin (2\mathbb{Z})^n$*. Then,* p *is sum of squares if and only every* $\boldsymbol{\beta} \in \mathcal{B}$ *satisfies* $\boldsymbol{\beta} \in \mathcal{A}^*$*.*

2.2.2 First–Order Theory of the Reals

The decision problem for the *first-order theory of the reals* is the problem of determining if expressions of a certain form are true or false. Although a more general form is allowed, all allowable expressions can be reduced to the following form.

Definition 2.2. *Given* $k, \omega, d \in \mathbb{Z}_+$*, a* standard formula *in the first-order theory of the reals is an expression of the form*

$$(Q_1 \boldsymbol{x}_1 \in \mathbb{R}^{n_1}) \ldots (Q_\omega \boldsymbol{x}_\omega \in \mathbb{R}^{n_\omega}) P(\boldsymbol{y}, \boldsymbol{x}_1, \ldots, \boldsymbol{x}_\omega), \tag{SF}$$

where:

- $\boldsymbol{y} \in \mathbb{R}^k$ *is a free variables vector;*
- *each* Q_l *(*$l = 1, \ldots, \omega$*) is one of the quantifiers* $\forall$ *or* $\exists$*;*
- $P(\boldsymbol{y}, \boldsymbol{x}_1, \ldots, \boldsymbol{x}_\omega)$ *is a quantifier free boolean formula with* m *atomic predicates of the form*

  $$g_j(\boldsymbol{y}, \boldsymbol{x}_1, \ldots, \boldsymbol{x}_\omega) \lhd_j 0, \quad j = 1, \ldots, m;$$

  where $\lhd_j \in \{<, >, \leq, \geq, =, \neq\}$*, and* g_j *is a real polynomial of degree at most* d*.*

Note that the above formula is in prenex form, i.e., all quantifiers in (SF) appear in front. Formulae with no free variables are called *sentences*. We say $\boldsymbol{y} \in \mathbb{R}^k$ is a *solution of* (SF) if the sentence obtained by substituting $\boldsymbol{y}$ into (SF) is true.

Next, we show three key results of James Renegar from his work on the computational complexity and geometry of the first-order theory of the reals (Renegar, 1992a,b). The first of them provides an upper bound for at least one solution of (SF).

Proposition 2.3. *If a formula* (SF) *has only integer coefficients, each of bit size at most* B*, then every connected component of the set of its solutions intersects the ball* $\{\boldsymbol{y} \in \mathbb{R}^k \mid \|\boldsymbol{y}\|_2 \leq R\}$*, where* R *satisfies* $\log R \leq B(md)^{2^{O(\omega)} k \prod_{l=1}^{\omega} n_l}$*.*

The following result is a quantifier elimination theorem. It provides upper bounds on the complexity of finding an equivalent formula (with the same solutions) that has no quantifiers; the numbers of logical operators, and polynomials; and the degree of the polynomials in the equivalent quantifier free formula.

Theorem 2.4. *There is an algorithm which, given a formula* (SF), *finds an equivalent quantifier free formula of the form*

$$\bigvee_{i=1}^{I} \bigwedge_{j=1}^{J_i} (h_{ij}(\boldsymbol{y}) \lhd_{ij} 0),$$

where:

- $I \leq (md)^{2^{O(\omega)} k \prod_{l=1}^{\omega} n_l}$,
- $J_i \leq (md)^{2^{O(\omega)} k \prod_{l=1}^{\omega} n_l}$,
- $\deg h_{ij}(\boldsymbol{y}) \leq (md)^{2^{O(\omega)} k \prod_{l=1}^{\omega} n_l}$.

The algorithm requires $(rd)^{2^{O(\omega)} k \prod_{l=1}^{\omega} n_l}$ operations and $(rd)^{O(k+\sum_{l=1}^{\omega} n_l)}$ evaluations of the input formula. If the coefficients of the atomic polynomials g_j, $j = 1, \ldots, r$, are integers of bit size at most B, then the algorithm works with numbers of bit size $(B+k)(md)^{2^{O(\omega)} k \prod_{l=1}^{\omega} n_l}$. This bound also holds for the bit size of the coefficients of polynomials h_{ij}.

The last one is a general decision theorem. Set an upper bound on the complexity of the decision problem of the first-order theory of the reals.

Theorem 2.5. *There is an algorithm for the decision problem of the first-order theory of the reals that requires $(md)^{2^{O(\omega)} k \prod_{l=1}^{\omega} n_l}$ operations and $(md)^{O(\sum_{l=1}^{\omega} n_l)}$ evaluations of the input formula. When restricted to sentences involving only polynomials with integer coefficients of bit size at most B, the procedure works with numbers of bit size $B(md)^{2^{O(\omega)} k \prod_l n_l}$.*

Another important result in algebraic computation is the following inequality which is a well-known bound on nonzero roots of univariate polynomials (see, e.g., Mignotte, 1982).

Proposition 2.6. *Let $p(x) = \sum_{k=0}^{d} a_k x^k$ be a univariate polynomial with integer coefficients, and α be a nonzero root of p. Then $|\alpha| \geq \frac{1}{1+h}$, where $h := \max_{0 \leq k \leq d} \{|a_k|\}$ is the* height *of p.*

2.3 Convex Geometry

Here, we summarize some standard definitions, properties, and results of convex sets and cones. For more background, in-depth details, and proofs, the reader is referred to Barvinok (2002); Rockafellar (1970).

A subset C of $\mathbb{R}^n$ is called *convex* if for all $\boldsymbol{x}, \boldsymbol{y} \in C$ we have $\lambda \boldsymbol{x} + (1-\lambda)\boldsymbol{y} \in C$ for all real $0 \leq \lambda \leq 1$, i.e., C is closed under taking segments. For vectors $\boldsymbol{x}_1, \ldots, \boldsymbol{x}_k \in \mathbb{R}^n$ a linear combination $\lambda_1 \boldsymbol{x}_1 + \cdots + \lambda_k \boldsymbol{x}_k$ is said to be a *convex combination* if $\lambda_i \geq 0$ for $i = 1, \ldots, k$ and $\lambda_1 + \cdots + \lambda_k = 1$. Equivalently, a subset C of $\mathbb{R}^n$ is convex if it is closed under taking convex combinations.

Proposition 2.7. *Let C and D be convex sets in the same space. Then $C \cap D$, $C + D$, and $C \times D$ are convex.*

Let $X \subseteq \mathbb{R}^n$ be an arbitrary subset. The *convex hull*, $\mathrm{Conv}(X)$, of X is the smallest convex set containing X. This one coincides with the intersection of all convex sets containing X. Equivalently, $\mathrm{Conv}(X)$ is the set of all convex combinations of points in X,

$$\mathrm{Conv}(X) = \left\{ \sum_{x \in F} \lambda_x \boldsymbol{x} \in \mathbb{R}^n \;\middle|\; F \subseteq X \text{ is a finite set, } \sum_{x \in F} \lambda_x = 1, \text{ and } \lambda_x \geq 0 \right\}.$$

Notice that a point in the convex hull of X can be written in several convex combinations of points in X. Besides, it is unclear how many points are needed to write it down. Carathéodory's theorem yields an upper bound on the number of points of X, which is enough to represent any point in its convex hull. It was proved in Carathéodory (1907).

Theorem 2.8 (Carathéodory's theorem)**.** *Let X be a subset of $\mathbb{R}^n$. Then any point in the convex hull of X can be written as a convex combination of at most $n+1$ points in X.*

If X is a finite subset of $\mathbb{R}^n$ its convex hull is called a *polytope*. Especially, when X is an affinely independent set, the convex hull of X is called a *simplex*. We call *standard simplex*, Δ_n, in $\mathbb{R}^n_+$ to the convex hull of the set $\{\boldsymbol{e}_1, \ldots, \boldsymbol{e}_n\} \subset \mathbb{R}^n_+$, i.e.,

$$\Delta_n := \{(\lambda_1, \ldots, \lambda_n) \in \mathbb{R}^n_+ \mid \lambda_1 + \cdots + \lambda_n = 1\}. \tag{2.3}$$

A direct consequence of Carathéodory's theorem 2.8 is that if a point $\boldsymbol{y}$ lies in the convex hull of a set $X \subseteq \mathbb{R}^n$, then $\boldsymbol{y}$ lies in some simplex generated by finitely many points of X.

Any simplex generated by a set $X \subset \mathbb{R}^n$ possesses the property that for any point $\boldsymbol{y} \in \mathrm{Conv}(X)$ there is only a convex combination that writes down $\boldsymbol{y}$. Hence, one can define the vector of *barycentric coordinates* of $\boldsymbol{y}$ in $\mathrm{Conv}(X)$ as the only vector $\boldsymbol{\lambda} \in \mathbb{R}^X_+$ such that $\boldsymbol{y} = \sum\limits_{x \in X} \lambda_{\boldsymbol{x}} \boldsymbol{x}$ and $\sum\limits_{x \in X} \lambda_{\boldsymbol{x}} = 1$.

Another important type of convex set is the hyperplane. Let $\boldsymbol{a}$ be a nonnull vector of $\mathbb{R}^n$, and b be a real number. The set

$$H := \{\boldsymbol{x} \in \mathbb{R}^n \mid \boldsymbol{a}^T \boldsymbol{x} = b\}$$

is a *hyperplane* in $\mathbb{R}^n$. Relating to the hyperplane, positive and negative closed *half-spaces* are given by

$$H_+ := \{\boldsymbol{x} \in \mathbb{R}^n \mid \boldsymbol{a}^T \boldsymbol{x} \geq b\} \quad \text{and} \quad H_- := \{\boldsymbol{x} \in \mathbb{R}^n \mid \boldsymbol{a}^T \boldsymbol{x} \leq b\}.$$

A half-space can be also seen as the solution set of a *linear inequality* $\boldsymbol{a}^T \boldsymbol{x} \leq b$ (also valid for $\geq$). A set defined by the intersection of finitely many half-spaces (or linear inequalities) is called a *polyhedron*,

$$P := \{\boldsymbol{x} \in \mathbb{R}^n \mid A\boldsymbol{x} \leq \boldsymbol{b}\},$$

where A is a nonnull matrix of $\mathbb{R}^{m \times n}$, and $\boldsymbol{b}$ is a vector of $\mathbb{R}^m$. A bounded polyhedron is a polytope.

The result below is a suitable variant of the fundamental theorem of linear inequalities (see, e.g., Schrijver, 1998).

Proposition 2.9. *Consider a system of linear inequalities:*

$$\boldsymbol{a}_i^T \boldsymbol{x} \leq b_i, \quad i \in M = \{1, \ldots, m\},$$

and let $C \subset \mathbb{R}^n$ be a convex set. If $P = C \cap \{\boldsymbol{x} \in \mathbb{R}^n : \boldsymbol{a}_i^T \boldsymbol{x} \leq b_i, i \in M\}$ is nonempty, then there exists a subset $I \subseteq M$ such that $|I| \leq \min\{m, n\}$ and $\emptyset \neq C \cap \{\boldsymbol{x} \in \mathbb{R}^n : \boldsymbol{a}_i^T \boldsymbol{x} \leq b_i, i \in I\} \subseteq P$.

Convex sets are endowed with a well-defined notion of dimension. Let $C \subseteq \mathbb{R}^n$ be a convex set and let $\mathrm{Aff}(C)$ be its *affine hull*, i.e., the affine linear subspace spanned by C. Then the *dimension* of C is defined by $\dim C :=$

$\dim \mathrm{Aff}(C)$. A compact convex set that is full dimensional in $\mathbb{R}^n$ is called a *convex body*.

Let $C \subseteq \mathbb{R}^n$ be a closed convex set. A subset $F \subseteq C$ is called a *face* of C if for all $\boldsymbol{x}, \boldsymbol{y} \in C$ and any $0 \leq \lambda \leq 1$, if we have $\lambda \boldsymbol{x} + (1-\lambda)\boldsymbol{y} \in F$, then $\boldsymbol{x}, \boldsymbol{y} \in F$. A point $\boldsymbol{x} \in C$ is called an *extreme point* of C if $\{\boldsymbol{x}\}$ is a face of C, i.e., if $\boldsymbol{x} = \lambda \boldsymbol{y} + (1-\lambda)\boldsymbol{z}$ for some $\boldsymbol{y}, \boldsymbol{z} \in C$ and $0 \leq \lambda \leq 1$, then $\boldsymbol{y} = \boldsymbol{z} = \boldsymbol{x}$. The following result is the finite-dimensional version of Krein-Milman theorem. It is also known as Minkowski's theorem.

Theorem 2.10. *Let $C \subset \mathbb{R}^n$ be a compact convex set. Then C is the convex hull of its extreme points.*

For the case of C as a polytope, the extreme points are known as the *vertices* of the polytope.

The theorem of Carathéodory (2.8) was published in 1907. Another crucial result in convex geometry is Helly's theorem. Eduard Helly discovered it in 1913 (Danzer et al., 1963) but was first published by Radon (1921), using Radon's theorem. A second proof was published by König (1922), and Helly's own proof eventually appeared in Helly (1923).

Theorem 2.11 (Helly's theorem)**.** *Suppose $\mathcal{C}$ is a family of at least $n+1$ convex sets in $\mathbb{R}^n$, and $\mathcal{C}$ is finite or each member of $\mathcal{C}$ is compact. Then if each $n+1$ members of $\mathcal{C}$ have a common point, there is a point common to all members of $\mathcal{C}$.*

The above theorem states that if a finite collection of convex sets in $\mathbb{R}^n$ has an empty intersection, then a subcollection of $n+1$ sets with an empty intersection must exist.

A function $f : \mathbb{R}^n \to \mathbb{R}$ is a *convex function* if

$$f(\lambda \boldsymbol{x} + (1-\lambda)\boldsymbol{y}) \leq \lambda f(\boldsymbol{x}) + (1-\lambda) f(\boldsymbol{y}) \text{ for all } \boldsymbol{x}, \boldsymbol{y} \in \mathbb{R}^n, \quad 0 \leq \lambda \leq 1.$$

A function f is convex if and only if its *epigraph* $\{(\boldsymbol{x}, t) \in \mathbb{R}^n \times \mathbb{R} : f(\boldsymbol{x}) \leq t\}$ is a convex set. A function f is *concave* if $-f$ is convex.

The following result is a generalization of von Neumann's saddlepoint theorem. It is crucial in the intimate relationship between convexity and optimization.

Theorem 2.12 (Minimax theorem)**.** *Let $X \subseteq \mathbb{R}^n$ and $Y \subseteq \mathbb{R}^m$ be compact convex sets and $f : X \times Y \to \mathbb{R}$ be a continuous function that is convex in its first argument* *and concave in the second. Then,*

$$\max_{y \in Y} \min_{x \in X} f(\boldsymbol{x}, \boldsymbol{y}) = \min_{x \in X} \max_{y \in Y} f(\boldsymbol{x}, \boldsymbol{y}).$$

Von Neumann's original theorem was motivated by game theory in order to prove the existence of equilibria in the context of two-player zero-sum games (v. Neumann, 1928). In this scenario, X and Y are standard simplices, and the function f is a bilinear form.

2.3.1 Conic Geometry

A cone K is a subset of a real vector space S that is closed under positive scalar multiplication; that is, K is a cone if $\boldsymbol{x} \in K$ implies $\lambda \boldsymbol{x} \in K$ for every positive scalar $\lambda > 0$. In this section, we focus on convex cones that contain the $\mathbf{0}$ defined over $\mathbb{R}^n$. Nevertheless, notice that this content is still valid even if we replace $\mathbb{R}^n$ by any real vector space S, or even by a vector space over any ordered field. This observation will be useful when we state the basis of conic optimization.

For vectors $\boldsymbol{x}_1, \ldots, \boldsymbol{x}_k \in \mathbb{R}^n$ a linear combination $\lambda_1 \boldsymbol{x}_1 + \cdots + \lambda_k \boldsymbol{x}_k$ is said to be a *conic combination* if $\lambda_i \geq 0$ for $i = 1, \ldots, k$.

Definition 2.13 (Convex cone)**.** *A subset K of $\mathbb{R}^n$ is said to be a* convex cone *if it is closed under conic combinations.*

Equivalently, a convex cone is a convex set that is closed under multiplication by nonnegative scalars.

A closed convex cone $K \subseteq \mathbb{R}^n$ is called *pointed* if K does not contain straight lines, i.e., $K \cap (-K) = \{\mathbf{0}\}$ and it is *solid* if it is full-dimensional ($\dim K = n$), i.e., it has a nonnegative interior ($K^\circ \neq \emptyset$). A cone that is convex, closed, pointed, and solid is called a *proper cone*.

Definition 2.14 (Dual cone)**.** *Given a cone $K \subseteq \mathbb{R}^n$, its* dual cone *is the cone*

$$K^* := \{\boldsymbol{y} \in \mathbb{R}^n \mid \langle \boldsymbol{y}, \boldsymbol{x} \rangle \geq 0 \textit{ for all } \boldsymbol{x} \in K\}.$$

Notice that, generally, the dual cone is often defined as a subset of the dual space S^* where S is the real vector space that contains K,

$$K^* := \{\boldsymbol{y} \in S^* \mid \langle \boldsymbol{y}, \boldsymbol{x} \rangle_S \geq 0 \text{ for all } \boldsymbol{x} \in K\},$$

where $\langle \boldsymbol{y}, \boldsymbol{x} \rangle_S := \boldsymbol{y}(\boldsymbol{x})$ is the pairing between an element of the vector space and one of the dual. In the definition of the dual cone for $S = \mathbb{R}^n$ we used the natural identification of the dual space $(\mathbb{R}^n)^*$ with $\mathbb{R}^n$ via the standard inner product. Whether K is a closed convex cone in a real finite dimensional vector space, then $(K^*)^* = K$. A cone K is said to be *self-dual* if $K = K^*$. The dual of a proper cone is also a proper cone. We call $\boldsymbol{x}$ an *interior point* of cone K if and only if for any point $\boldsymbol{y} \in K^*$, $\langle \boldsymbol{y}, \boldsymbol{x} \rangle = 0$ implies $\boldsymbol{y} = \boldsymbol{0}$.

Definition 2.15 (Recession cone). *Let X be a nonempty set in a vector space S. The recession cone of X is defined as:*

$$\operatorname{recc}(X) := \{\boldsymbol{y} \in S \mid \forall \boldsymbol{x} \in X, \quad \forall \lambda \geq 0, \quad \boldsymbol{x} + \lambda \boldsymbol{y} \in X\}.$$

Note that if X is the intersection of a proper cone K and a polyhedron $\{\boldsymbol{x} \in \mathbb{R}^n : \boldsymbol{a}_i^T \boldsymbol{x} \leq b_i, \quad i = 1, \ldots, m\}$ where $\boldsymbol{a}_i \in \mathbb{R}^n$, and $b_i \in \mathbb{R}$ for $i = 1, \ldots, m$. Then, the recession cone is equivalent to

$$K \cap \bigcap_{i=1}^{m} H_i, \tag{2.4}$$

where H_i is the half-space $\{\boldsymbol{x} \in \mathbb{R}^n : \boldsymbol{a}_i^T \boldsymbol{x} \leq 0\}$ for $i = 1, \ldots, m$. If C is a nonempty closed convex subset of a finite-dimensional Hausdorff space (e.g., $\mathbb{R}^n$), then $\operatorname{recc}(C) = \{\boldsymbol{0}\}$ if and only if C is bounded.

Polyhedral Cones

As we have defined the convex hull we can define the conic hull. Let $X \subseteq \mathbb{R}^n$ be an arbitrary subset. The *conic hull*, $\operatorname{Cone}(X)$, of X is the smallest convex cone containing X. Equivalently, $\operatorname{Cone}(X)$ is the set of all conic combinations of points in X,

$$\operatorname{Cone}(X) = \left\{ \sum_{x \in F} \lambda_{\boldsymbol{x}} \boldsymbol{x} \in \mathbb{R}^n \;\middle|\; F \subseteq X \text{ is a finite set, and } \lambda_{\boldsymbol{x}} \geq 0 \right\}.$$

Proposition 2.16. *Let $K \subseteq \mathbb{R}^n$ be a convex cone. The following statements are equivalent:*

1. *K is the conic hull of a finite set of vectors $X \subset \mathbb{R}^n$, i.e., $K = \operatorname{Cone}(X)$.*
2. *K is the intersection of a finite number of half-spaces that have $\boldsymbol{0}$ on their boundary.*

3. *There is some matrix* $A \in \mathbb{R}^{m\times n}$ *such that* $K = \{\boldsymbol{x} \in \mathbb{R}^n : A\boldsymbol{x} \geq \boldsymbol{0}\}$.

The last two statements are the same, and the equivalence between the first two definitions was proved by Weyl (1934) (Mirkil, 1957).

Definition 2.17. *A convex cone* K *of* $\mathbb{R}^n$ *is called a* polyhedral cone *if it satisfies any of the conditions in Proposition 2.16.*

One of the most relevant polyhedral cones is the nonnengative orthant. We denote by $\mathbb{R}^n_+$ the n–dimensional *nonnegative orthant* $\mathbb{R}^n_+ := \{\boldsymbol{x} \in \mathbb{R}^n : \boldsymbol{x} \geq \boldsymbol{0}\}$; that is, the set of all vectors in $\mathbb{R}^n$ with nonnegative entries. This is a proper polyhedral cone and its dual cone is $\mathbb{R}^n_+$, therefore it is self-dual.

Order Cones

Order cones play a crucial, maybe the main, role in the present dissertation. We start defining the second–order (also known as Lorentz) cone (see Figure 1.1).

Definition 2.18 (Second–order cone)**.** *The* second–order cone (SOC) *is defined as*

$$\mathcal{K}_2^{n,1} := \{(\boldsymbol{x}, z) \in \mathbb{R}^n \times \mathbb{R}_+ \mid \|\boldsymbol{x}\|_2 \leq z\},$$

where $\|\cdot\|_2$ *denotes the* ℓ_2 *or Euclidean norm in* $\mathbb{R}^n$*.*

The dual of the second–order cone is itself, therefore it is self-dual, and it is a proper cone.

If we rotate the second–order cone $\mathcal{K}_2^{n,1}$ through an angle of forty-five degrees in the (z, x_n)–plane, we obtain the *rotated quadratic cone*, that we can define, in a rescaled version, as

$$\mathcal{K}_2^{n,2}\left(\frac{1}{2}\right) := \{(\boldsymbol{x}, \boldsymbol{z}) \in \mathbb{R}^n \times \mathbb{R}^2_+ \mid \|\boldsymbol{x}\|_2^2 \leq z_1 z_2\}.$$

Notice that $(\boldsymbol{x}, \boldsymbol{z}) \in \mathcal{K}_2^{n,2}\left(\frac{1}{2}\right)$ if and only if $((2\boldsymbol{x}, z_1 - z_2), z_1 + z_2) \in \mathcal{K}_2^{n+1,1}$. Thus, both cones are equivalents after a rotation and rescaling.

A generalization of second–order cones appears when we replace the euclidean norm with the ℓ_p–norm as the base norm to define the cone.

Definition 2.19 (p–order cone)**.** *Given* $1 \leq p \leq \infty$*, the* p–order cone (pOC) *is defined as*

$$\mathcal{K}_p^{n,1} := \{(\boldsymbol{x}, z) \in \mathbb{R}^n \times \mathbb{R}_+ \mid \|\boldsymbol{x}\|_p \leq z\},$$

where $\|\cdot\|_p$ stands for the ℓ_p or Hölder norm in $\mathbb{R}^n$.

Let p be a value between 1 and ∞, both includes, it is defined the *conjugate* q of p as the number with satisfies $\frac{1}{p} + \frac{1}{q} = 1$, by convention 1 and ∞ are conjugates. The dual of the p–order cone is the q–order cone being q the conjugate of p, also it is a proper cone.

Notice that $\mathcal{K}_p^{0,1}$ equals to $\mathbb{R}_+$.

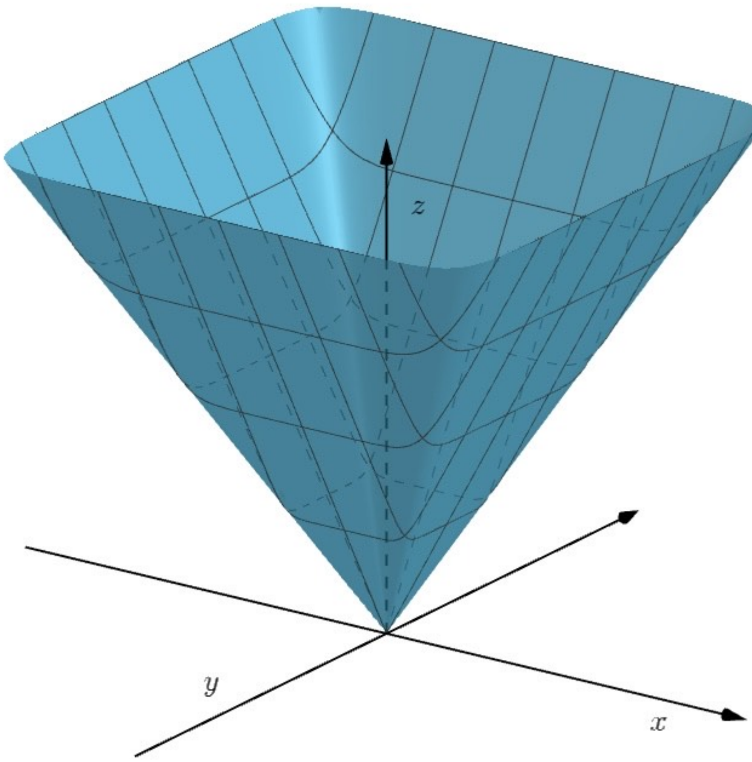

FIGURE 2.2: Boundary of the three-dimensional p–order cone ($p = 10$), i.e., $\mathcal{K}_{10}^{2,1}$.

Cone of Positive Semidefinite Matrices

We denote by $\mathcal{S}_+^n$ the set of all positive semidefinite matrices in $\mathcal{S}^n$. This is a proper cone, called the *positive semidefinite matrix cone* (PSD). The dual of the cone is itself, therefore, it is self-dual.

This family of cones is a matrix generalization of nonnegative orthants and also contains the family of second–order cones.

Let $(\boldsymbol{x}, z) \in \mathbb{R}^{n+1}$ be a vector, the *arrow-shaped* matrix $\operatorname{Arw}(\boldsymbol{x}, z) \in \mathcal{S}^{n+1}$ is defined as:

$$\operatorname{Arw}(\boldsymbol{x}, z) := \begin{bmatrix} zI_n & \boldsymbol{x} \\ \boldsymbol{x}^T & z \end{bmatrix}.$$

Note that by the Schur complement, $(\boldsymbol{x}, z) \in \mathcal{K}_2^{n,1}$ if and only if $\operatorname{Arw}(\boldsymbol{x}, z) \succeq 0$.

Generalized Power Cones

Definition 2.20 ($(p, \boldsymbol{\alpha})$–power cone). *Given* $1 \leq p \leq \infty$, $\boldsymbol{\alpha} \in \Delta_d$, *the* $(n+d)$–*dimensional* $(p, \boldsymbol{\alpha})$–power cone *is defined as*

$$\mathcal{K}_p^{n,d}(\boldsymbol{\alpha}) := \{(\boldsymbol{x}, \boldsymbol{z}) \in \mathbb{R}^n \times \mathbb{R}_+^d \mid \|\boldsymbol{x}\|_p \leq \boldsymbol{z}^{\boldsymbol{\alpha}}\},$$

where $\|\cdot\|_p$ *denotes the* ℓ_p*–norm in* $\mathbb{R}^n$, Δ_d *is the standard simplex, and for any* $\boldsymbol{z} \in \mathbb{R}_+^d$ *and* $\boldsymbol{\alpha} \in \Delta_d$, $\boldsymbol{z}^{\boldsymbol{\alpha}}$ *is the weighted geometric mean of* $\boldsymbol{z}$ *with weights* $\boldsymbol{\alpha}$.

Some particular cases of the $(p, \boldsymbol{\alpha})$–power cones are especially interesting. Specifically, we present the following:

- $\mathcal{K}_p^{n,1}(1) = \mathcal{K}_p^{n,1}$ is the $(n+1)$–dimensional p–order cone for $p \geq 1$.

  In case $p = 2$, $\mathcal{K}_2^{n,1}(1) = \mathcal{K}_2^{n,1}(1)$ is the second–order cone.

- $\mathcal{K}^{1,d}(\boldsymbol{\alpha}) := \mathcal{K}_1^{1,d}(\boldsymbol{\alpha})$ is the $\boldsymbol{\alpha}$*–power cone*.

- $\mathcal{K}_p^{n,2}(\alpha) := \mathcal{K}_p^{n,2}(\alpha, 1-\alpha)$ is the $(d+2)$–dimensional (p, α)*–power cone*, for any $p \geq 1$ and $0 \leq \alpha \leq 1$. In case $d = 1$, $\mathcal{K}^{1,2}(\alpha) := \mathcal{K}_1^{1,2}(\alpha)$ is the α*–power cone*.

- $\mathcal{K}_2^{n,2}\left(\frac{1}{2}\right)$ is the rotated quadratic cone. In case $n = 1$, we obtain the *three-dimensional rotated quadratic cone*

$$\mathcal{K}^{1,2}\left(\frac{1}{2}\right) = \{(x, y, z) \in \mathbb{R}^3 \mid x^2 \leq yz, \quad y, z \geq 0\}.$$

Notice that the latter coincides exactly with the cone $\mathcal{S}_+^2$.

Other Important Cones

A symmetric matrix $X \in \mathcal{S}^n$ is *copositive* if $\boldsymbol{x}^T X \boldsymbol{x} \geq 0$ for all $\boldsymbol{x} \geq \boldsymbol{0}$. The *cone of all copositive matrices*, denoted by $\mathcal{C}_n^*$, is a proper cone in $\mathcal{S}^n$.

The *exponential cone* is a convex set of $\mathbb{R}^3$ defined as the closure (cl) in $\mathbb{R}^3$ of the set of points that satisfy $y \exp\left(\frac{x}{y}\right) \leq z$, and $y > 0$, i.e.,

$$K_{exp} := \operatorname{cl}\left\{(x, y, z) \in \mathbb{R}^3 \mid x \geq y \exp\left(\frac{z}{y}\right), \quad y > 0\right\}.$$

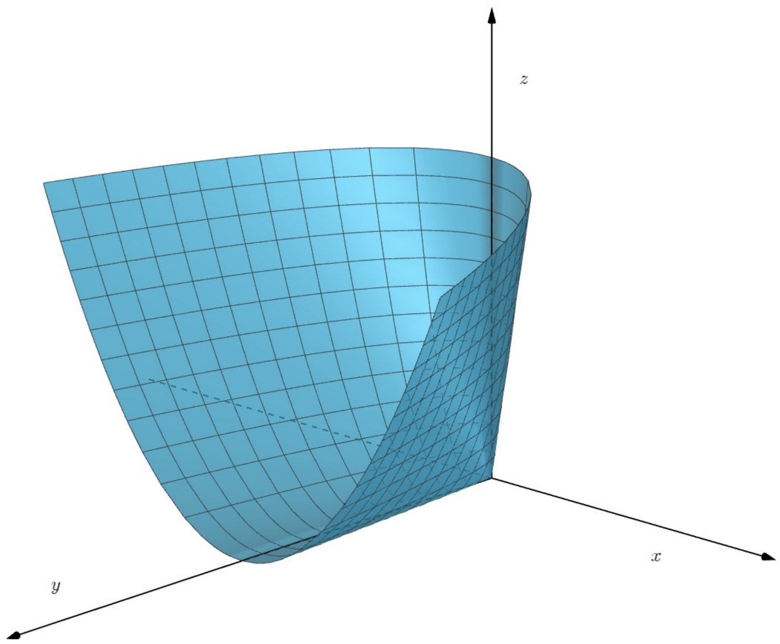

FIGURE 2.3: Boundary of the three-dimensional rotated quadratic cone, $\mathcal{K}^{1,2}\left(\frac{1}{2}\right)$. Equivalently, the 2×2 positive semidefinite matrices, $\mathcal{S}^2_+$.

The *relative entropy cone*

$$\mathcal{RE}_n := \left\{ (\nu, \zeta, \delta) \in \mathbb{R}^n_+ \times \mathbb{R}^n_+ \times \mathbb{R}^n \mid \nu_i \log\left(\frac{\nu_i}{\zeta_i}\right) \leq \delta_i, \quad \forall i = 1, \ldots, n \right\}.$$

Two other important cases are the *hyperbolicity cone* associated with a given hyperbolic polynomial and the *cone of multivariate polynomials that are sums of squares*. This latter cone will play an important role later.

2.4 Conic Programming

Here, we summarize some standard definitions and properties of mathematical optimization with a focus on conic and mixed integer programming. For more background and in-depth details, the reader is referred to Anjos and Lasserre (2011); Ben-Tal and Nemirovski (2001a); Blekherman et al. (2012); Boyd and Vandenberghe (2004); Lee and Leyffer (2011).

Mathematical programming is a language for formally describing tons of optimization problem classes. A *mathematical programming problem* or *mathematical program* (MP) consists of: parameters, encoding the problem input; decision variables, encoding the problem output; one objective function to be minimized; and a set of constraints describing the feasible set (some of these constraints may be bounds or integrality requirements on the decision variables). The objective function and constraints are described by mathematical expressions whose arguments are the parameters and the decision variables. Let $I = \{1, \ldots, n\}$ and $J = \{1, \ldots, m\}$ for some nonnegative integers n and m; and $Z \subseteq I$ be a subset of I. In general, an MP formulation is as follows:

$$\begin{aligned} \text{minimize} \quad & f(\boldsymbol{x}) && \text{(MP)} \\ \text{subject to} \quad & g_j(\boldsymbol{x}) \lhd_j 0, \quad \forall j \in J; \\ & x_i \in \mathbb{Z}, \quad \forall i \in Z; \end{aligned}$$

where $\boldsymbol{x} \in \mathbb{R}^n$ is the vector of *decision variables*; $f : \mathbb{R}^n \to \mathbb{R}$ is the objective function; $g_j : \mathbb{R}^n \to \mathbb{R}$ are real functions and $\lhd_j \in \{\leq, =\}$ for $j \in J$. The set of expressions $g_j(\boldsymbol{x}) \lhd_j 0$ for $j \in J$ is called the *set of constraints* and each of them is a *constraint*. The set of constraints, along with the domain of the variables, shape the feasible set. If $f, g_1, \ldots, g_m$ are affine forms and $Z = \emptyset$, (MP) is a *linear program* (LP). If some of $f, g_1, \ldots, g_m$ is a nonlinear function and $Z = \emptyset$, (MP) is a *nonlinear program* (NLP), and if f is a convex function, $Z = \emptyset$, and the feasible set $\{\boldsymbol{x} \in \mathbb{R}^n : g_j(\boldsymbol{x}) \lhd_j 0, j \in J\}$ is convex, (MP) is a *convex program*. If $f, g_1, \ldots, g_m$ are affine forms and $Z \neq \emptyset$, (MP) is a *mixed integer linear program* (MILP), and if $Z = I$ it is an *integer liner program* (ILP). If some of $f, g_1, \ldots, g_m$ is a nonlinear function and $Z \neq \emptyset$, (MP) is a *mixed integer nonlinear program* (MINLP), and if f is a convex function, $Z \neq \emptyset$, and the feasible set is convex (without consider integrality in the variables), it is a *mixed integer convex program*. If $f, g_1, \ldots, g_m$ are polynomials in $\mathbb{R}[\boldsymbol{x}]$ and $Z = \emptyset$, (MP) is a *polynomial optimization problem* (POP).

A fundamental type of convex program is one whose objective function f is linear and the feasible set is a *slice* of a proper cone, i.e., the intersection between an affine subspace and a proper cone.

Dantzig (1948) carried out an analysis of military operations and proposed that the interrelationships between the activities of a large organization should be viewed as a type of linear program and proposed the *simplex algorithm* to solve them. It was soon recognized that such models could be used in many other contexts, and this brought about the great interest in the theoretical as well as the computational aspects of this field (Vajda, 2009). According to George Dantzig, duality for linear optimization was conjectured by v. Neumann (1928) after himself introduced the problem.

2.4.1 From Linear to Conic Programming

Conic optimization is a branch of convex optimization. The idea is to generalize linear programming, where the associated feasible sets are polyhedra, to the case where the vector of decision variables belongs to a slice of a cone.

Linear Programming

Linear programming is the problem of minimizing a linear function subject to linear constraints.

Definition 2.21 (Linear programs (LP))**.** *Let $A \in \mathbb{R}^{m\times n}$, $\boldsymbol{b} \in \mathbb{R}^m$, and $\boldsymbol{c} \in \mathbb{R}^n$. The standard form* linear programming (LP-P) primal problem *and its* dual problem (LP-D) *are*

$$\begin{aligned} &\textit{minimize} && \boldsymbol{c}^T\boldsymbol{x} && \text{(LP-P)} \\ &\textit{subject to} && A\boldsymbol{x} = \boldsymbol{b}, \\ &&& \boldsymbol{x} \geq \boldsymbol{0}. \end{aligned} \qquad\qquad \begin{aligned} &\textit{maximize} && \boldsymbol{b}^T\boldsymbol{y} && \text{(LP-D)} \\ &\textit{subject to} && A^T\boldsymbol{y} \leq \boldsymbol{c}. \end{aligned}$$

Geometrically, an (LP-P) has a natural interpretation, its feasible set is the intersection of an affine subspace defined by the constraints $A\boldsymbol{x} = \boldsymbol{b}$ and the nonnegative orthant, thus it is a polyhedron. Hence, linear programming corresponds to the minimization of a linear function over a polyhedron. Notice that (LP-D) also corresponds to the maximization of a linear function over a polyhedron. There are very natural and direct algebraic relationships between them.

Weak duality: For any couple of feasible solutions $\boldsymbol{x}, \boldsymbol{y}$ of (LP-P) and (LP-D), respectively, it always holds that

$$\boldsymbol{c}^T\boldsymbol{x} - \boldsymbol{b}^T\boldsymbol{y} = \boldsymbol{x}^T\boldsymbol{c} - (A\boldsymbol{x})^T\boldsymbol{y} = \boldsymbol{x}^T(\boldsymbol{c} - A^T\boldsymbol{y}) \geq 0, \tag{2.5}$$

where the last inequality follows from the constraints $\boldsymbol{x} \geq 0$ and $A^T\boldsymbol{y} \leq \boldsymbol{c}$. Thus, from any feasible dual solution, one can obtain a lower bound on the value of the primal. Conversely, primal feasible solutions give upper bounds on the value of the dual.

Strong duality: If both primal and dual problems are feasible, then they achieve the same optimal value (*zero duality gap*), and there exist optimal feasible solutions $\boldsymbol{x}^\star$ and $\boldsymbol{y}^\star$ such that $\boldsymbol{c}^T\boldsymbol{x}^\star = \boldsymbol{b}^T\boldsymbol{y}^\star$.

Complementary slackness: Strong duality combined with (2.5) implies that at optimality we must have

$$x_i^\star(\boldsymbol{c} - A^T\boldsymbol{y}^\star)_i = 0, \quad i = 1, \ldots, n.$$

That is, there is a correspondence between primal variables and dual inequalities in the sense that whenever a primal variable is nonzero, the corresponding dual inequality must be tight.

Second–Order Cone Programming

Second–order cone programming (SOCP) is the problem of minimizing a linear function subject to linear and quadratic constraints.

Definition 2.22 (Second–order cone programs (SOCP))**.** *Let* $A_i \in \mathbb{R}^{m\times n_i}$, $\boldsymbol{b} \in \mathbb{R}^m$, *and* $\boldsymbol{c}_i \in \mathbb{R}^{n_i}$ *for* $i \in K = \{1, \ldots, k\}$. *The standard form* second–order cone programming (SOCP-P) primal problem *and its* dual problem (SOCP-D) *are*

$$\begin{aligned} \textit{minimize} \quad & \sum_{i=1}^{k} \boldsymbol{c}_i^T \boldsymbol{x}_i \qquad \text{(SOCP-P)} \\ \textit{subject to} \quad & \sum_{i=1}^{k} A_i \boldsymbol{x}_i = \boldsymbol{b}, \\ & \boldsymbol{x}_i \in \mathcal{K}_2^{n_i-1,1}, \quad i \in K. \end{aligned}$$

$$\begin{aligned} \textit{maximize} \quad & \boldsymbol{b}^T\boldsymbol{y} \qquad \text{(SOCP-D)} \\ \textit{subject to} \quad & \boldsymbol{c}_i - A_i^T\boldsymbol{y} \in \mathcal{K}_2^{n_i-1,1}, i \in K. \end{aligned}$$

Geometrically, an (SOCP-P) has a natural interpretation, its feasible set is the intersection of an affine subspace defined by the constraints $A_1\boldsymbol{x}_1 + \cdots + A_k\boldsymbol{x}_k = \boldsymbol{b}$ and a Cartesian product of second–order cones. Notice that (SOCP-D) also corresponds to the maximization of a linear function over a slice of a Cartesian product of Lorentz cones.

Remark 2.23. *Note that in the standard form* (SOCP-P) *each decision variable belongs to one, and only one, second-order cone within the product* $\prod_{i=1}^{k} \mathcal{K}_2^{n_i-1,1}$. *In practice, the same variable usually appears in several SOC constraints (this fact can be fixed by adding more linear constraints), but a more general (and compact) form of SOCP will be as follows. Let* $A \in \mathbb{R}^{m\times n}$, $\boldsymbol{b} \in \mathbb{R}^m$, $\boldsymbol{c} \in \mathbb{R}^n$, *and* $\pi_i : \mathbb{R}^n \to \mathbb{R}^{n_i}$ *be projections, for* $i = 1, \ldots, k$; (SOCP-P) *can be formulated as*

$$\begin{aligned} \textit{minimize} \quad & \boldsymbol{c}^T\boldsymbol{x} \\ \textit{subject to} \quad & A\boldsymbol{x} = \boldsymbol{b}, \\ & \pi_i(\boldsymbol{x}) \in \mathcal{K}_2^{n_i-1,1}, \quad i = 1, \ldots, k. \end{aligned}$$

In case $n_i = 1$ for $i = 1, \dots, k$; then every $\mathcal{K}^{n_i-1,1} = \mathcal{K}_2^{0,1} = \mathbb{R}_+$. Hence, $\prod_{i=1}^{k} \mathcal{K}_2^{n_i-1,1}$ becomes in the nonnegative orthant which implies SOCP generalizes LP.

As SOCP has been defined we can define *p–order cone programming* (pOCP).

Definition 2.24 (p–order cone programs (pOCP))**.** *Let* $1 \leq p \leq \infty$, $A_i \in \mathbb{R}^{m \times n_i}$, $\boldsymbol{b} \in \mathbb{R}^m$, *and* $\boldsymbol{c}_i \in \mathbb{R}^{n_i}$ *for* $i \in K = \{1, \dots, k\}$. *The standard form* p–order cone programming (pOCP-P) primal problem *and its* dual problem (pOCP-D) *are*

$$\begin{aligned} \textit{minimize} \quad & \sum_{i=1}^{k} \boldsymbol{c}_i^T \boldsymbol{x}_i && (p\text{OCP-P}) \\ \textit{subject to} \quad & \sum_{i=1}^{k} A_i \boldsymbol{x}_i = \boldsymbol{b}, \\ & \boldsymbol{x}_i \in \mathcal{K}_p^{n_i-1,1}, \quad i \in K. \end{aligned}$$

$$\begin{aligned} \textit{maximize} \quad & \boldsymbol{b}^T \boldsymbol{y} && (p\text{OCP-D}) \\ \textit{subject to} \quad & \boldsymbol{c}_i - A_i^T \boldsymbol{y} \in \mathcal{K}_q^{n_i-1,1}, i \in K. \end{aligned}$$

where q *is the conjugate of* p.

Semidefinite Programming

Semidefinite programming is a broad generalization of linear programming, where the decision variables are symmetric matrices. A *semidefinite programming* (SDP) problem corresponds to the optimization of a linear function subject to linear matrix inequality constraints. A *linear matrix inequality* (LMI) has the form

$$A_0 + \sum_{i=1}^{m} A_i x_i \succeq 0,$$

where $A_i \in \mathcal{S}^n$ for $i = 0, \dots, m$ are given symmetric matrices.

Definition 2.25 (Semidefinite programs (SDP))**.** *Let* $C, A_i \in \mathcal{S}^n$ *for* $i = 1, \dots, m$; *and* $\boldsymbol{b} \in \mathbb{R}^m$. *The standard form* semidefinite programming (SDP-P) primal problem *and its* dual problem (SDP-D) *are*

$$\begin{aligned} \textit{minimize} \quad & \langle C, X \rangle && (\text{SDP-P}) \\ \textit{subject to} \quad & \langle A_i, X \rangle = b_i, \quad i = 1, \dots, m \\ & X \succeq 0. \end{aligned}$$

$$\begin{aligned} \textit{maximize} \quad & \boldsymbol{b}^T \boldsymbol{y} && (\text{SDP-D}) \\ \textit{subject to} \quad & \sum_{i=1}^{m} A_i y_i \preceq C. \end{aligned}$$

Geometrically, an (SDP-P) has a natural interpretation, its feasible set is the intersection of an affine subspace defined by the constraints $\langle A_i, X \rangle = b_i$

for $i = 1, \ldots, m$; and the cone of positive semidefinite matrices, this kind of slice of $\mathcal{S}^n_+$ is defined as a *spectrahedron*. Hence, semidefinite programming corresponds to the minimization of a linear function over a spectrahedron. Equivalently, a spectrahedron can be also defined as the intersections of finitely many LMI's. Hence, (SDP-D) also corresponds to the maximization of a linear function over a spectrahedron.

When X is a diagonal matrix, (SDP-P) becomes (LP-P) so SDP generalizes LP.

Moreover, we have seen $(\boldsymbol{x}, z) \in \mathcal{K}_2^{n,1}$ if and only if $\mathrm{Arw}(\boldsymbol{x}, z) \succeq 0$, so the constraints $\boldsymbol{x}_i \in \mathcal{K}_2^{n_i-1,1}$ for $i = 1, \ldots, k$ are equivalent to $\mathrm{BlockDiag}(\mathrm{Arw}(\boldsymbol{x}_i)) \succeq 0$ so SDP also generalizes SOCP.

Complexity: Porkolab and Khachiyan (1997) worked on the complexity of semidefinite programming obtaining very celebrated bounds related to this problem via the first–order theory of the reals. They dealt with the *semidefinite feasibility problem* which is defined by the existence of a real $n \times n$ symmetric matrix $X \in \mathcal{S}^n_+$ which is solution for

$$\langle A_i, X \rangle \leq b_i, \quad i = 1, \ldots, m; \quad X \succeq 0, \tag{$\mathbf{F}_{\text{SDP}}$}$$

where $A_1, \ldots, A_m \in \mathcal{S}^n$ are integral $n \times n$ symmetric matrices, $b_1, \ldots, b_m \in \mathbb{Z}$. Their result claims the following.

Theorem 2.26. *Let τ be the maximal bit size of the input data. The feasibility of ($\mathbf{F}_{\text{SDP}}$) can be tested in $mn^{O(\min\{m,n^2\})}$ arithmetic operations over $\tau n^{O(\min\{m,n^2\})}$-bit numbers.*

On the other hand, to know complexity bounds of the interior point method for linear, second–order cone, and semidefinite programming the reader is referred to (Ben-Tal and Nemirovski, 2001a, § 6.6).

Conic Programming

Conic programming (CP) is a general class of convex optimization problems that unifies linear, order, and semidefinite programming. Next, we describe the conic framework followed by the mathematical formulation.

The starting point should be the geometric interpretation. As we have been seeing, one can define a general class of optimization problems where the feasible sets are the intersection of an affine subspace and a proper cone. Consider two real vector spaces S and T, and a linear map $\mathcal{A} : S \to T$. Recall that the *adjoint map* of $\mathcal{A}$ is defined as the unique linear map $\mathcal{A}^* : T^* \to S^*$

that satisfies

$$\langle \mathcal{A}^* \boldsymbol{y}, \boldsymbol{x} \rangle_S = \langle \boldsymbol{y}, \mathcal{A}\boldsymbol{x} \rangle_T, \quad \forall \boldsymbol{x} \in S, \boldsymbol{y} \in T.$$

Definition 2.27 (Conic programs (CP))**.** *Let S and T be a real vector spaces, $\mathcal{A} : S \to T$ be a linear map, $K \subseteq S$ be a proper cone, $\boldsymbol{b} \in T$, and $\boldsymbol{c} \in S^*$. The standard form* conic programming (CP-P) primal problem *and its* dual problem (CP-D) *are*

$$\begin{array}{llc} \textit{minimize} & \langle \boldsymbol{c}, \boldsymbol{x} \rangle_S & \text{(CP-P)} \\ \textit{subject to} & \mathcal{A}\boldsymbol{x} = \boldsymbol{b}, & \\ & \boldsymbol{x} \in K. & \end{array} \qquad \begin{array}{llc} \textit{maximize} & \langle \boldsymbol{y}, \boldsymbol{b} \rangle_T & \text{(CP-D)} \\ \textit{subject to} & \boldsymbol{c} - \mathcal{A}^* \boldsymbol{y} \in K^*. & \end{array}$$

Rapidly, from an algebraic point of view, we notice that the weak duality property holds for conic programs.

Weak duality: For any couple of feasible solutions $\boldsymbol{x}, \boldsymbol{y}$ of (CP-P) and (CP-D), respectively, it always holds that

$$\begin{aligned} \langle \boldsymbol{c}, \boldsymbol{x} \rangle_S - \langle \boldsymbol{y}, \boldsymbol{b} \rangle_T &= \langle \boldsymbol{c}, \boldsymbol{x} \rangle_S - \langle \boldsymbol{y}, \mathcal{A}\boldsymbol{x} \rangle_T \\ &= \langle \boldsymbol{c}, \boldsymbol{x} \rangle_S - \langle \mathcal{A}^* \boldsymbol{y}, \boldsymbol{x} \rangle_S \\ &= \langle \boldsymbol{c} - \mathcal{A}^* \boldsymbol{y}, \boldsymbol{x} \rangle_S \geq 0. \end{aligned}$$

Despite the formal similarities, there are several differences between linear and general conic programming. Beyond the weak duality, there is no strong duality in the general case, i.e., there may be a nonzero duality gap between optimal values of the primal-dual pair. Moreover, optimal solutions *may not be attained*, even if there is zero duality gap.

Strong duality:

1. Let either (CP-P) or (CP-D) be infeasible, and furthermore the other be feasible and has a nonempty interior. Then the other is unbounded.
2. Let (CP-P) and (CP-D) be both feasible, and furthermore one of them has a nonempty interior. Then there is no duality gap at optimality between them, i.e.,

$$\inf\{\langle \boldsymbol{c}, \boldsymbol{x} \rangle_S \mid \mathcal{A}\boldsymbol{x} = \boldsymbol{b}, \boldsymbol{x} \in K\} = \sup\{\langle \boldsymbol{y}, \boldsymbol{b} \rangle_T \mid \boldsymbol{c} - \mathcal{A}^* \boldsymbol{y} \in K^*\}.$$

3. If there is a pair of feasible solutions $\boldsymbol{x} \in K^\circ$ and $\boldsymbol{y} \in (K^*)^\circ$ of (CP-P) and (CP-D), respectively. Then, they achieve the same optimal value (zero duality gap), and there exist optimal feasible solutions $\boldsymbol{x}^\star$ and $\boldsymbol{y}^\star$ such that $\langle \boldsymbol{c}, \boldsymbol{x}^\star \rangle_S = \langle \boldsymbol{y}^\star, \boldsymbol{b} \rangle_T$.

2.4.2 Mixed Integer Conic Programming

We focus on conic optimization problems where the decision variables are real numbers and also some of them could be integers. Opening the door to a class of optimization problems known as *mixed integer conic programming* (MICP).

Definition 2.28 (Mixed integer conic programs (MICP)). *Let $K \subseteq \mathbb{R}^n$ be a proper cone, $N = \{1, \ldots, n\}$, $Z \subseteq N$, $A \in \mathbb{R}^{m \times n}$, $\boldsymbol{b} \in \mathbb{R}^m$, and $\boldsymbol{c} \in \mathbb{R}^n$. The standard form* mixed integer conic programming (MICP) problem *is*

$$\begin{aligned} \textit{minimize} \quad & \boldsymbol{c}^T \boldsymbol{x} \\ \textit{subject to} \quad & A\boldsymbol{x} = \boldsymbol{b} \\ & \boldsymbol{x} \in K, \\ & x_i \in \mathbb{Z}, \quad \forall i \in Z. \end{aligned} \tag{MICP}$$

When $K = \mathbb{R}^n_+$ is the nonnegative orthant (MICP) becomes a mixed integer linear program (MILP), if $K = \mathcal{K}_2^{n-1,1}$ is the second–order cone or a cartesian product of them (MICP) is a *mixed integer second–order cone program* (MISOCP). If instead of the Lorentz cone is the p–order cone then (MICP) is a *mixed integer p–order cone program* (MIpOCP). Eventually, if the vector of decision variables is a real symmetric matrix in $\mathcal{S}^n$ and $K = \mathcal{S}^n_+$ is the PSD then (MICP) is a *mixed integer semidefinite program* (MISDP).

Location Theory: A Significant Application

One of the branches of operations research that has seen significant development since the 1960s is *location theory* (see Nickel and Puerto, 2006). Due to its growing importance, it has been recognized by the American Mathematical Society with the code 90B85.

A *location problem* arises whenever a decision-maker needs to determine the placement of a facility or resource, taking into account a given set of users. Although the development of location analysis dates back to the 1960s, its origins are much older, tracing back to the time of the Ancient Greeks. Wesolowsky (1993) states that Greek geometers had already provided at least three solutions to the location problem that is now known as the Weber problem. More recently, according to Kuhn (1967), it has been argued that location analysis originated in the 17th century with the *Fermat's problem*: given three points in the plane, find a fourth point that minimizes the sum of its distances to the three given points.

During the 17th century, various solutions were proposed to solve this problem. Evangelista Torricelli was the first to introduce a geometric approach to finding this fourth point, now known as the *Fermat–Torricelli point* (see, e.g., Laporte et al., 2019). However, in the last century, the *Weber problem*, introduced by Weber (1909), is considered to mark the beginning of modern location analysis (Smith et al., 2009). This foundational problem consists of finding a point in the plane that minimizes the sum of weighted Euclidean distances to a set of fixed demand points.

As the Weber problem as many other folkloristic location problems such as *p–median problem* (Cooper, 1963); *Euclidean minimax problem* (Hakimi, 1964), *set covering location problem* (Toregas et al., 1971); *maximal covering location problem* (Church and ReVelle, 1974); and *ordered median problem* (Blanco et al., 2014, 2016; Puerto, 2020); admits a formulation as mixed integer conic programming problem (MICP).

2.5 Graph Theory

Here, we summarize some standard definitions and properties of graph theory and combinatorial optimization. For more background and in-depth details, the reader is referred to Bondy and Murty (1976).

Many real-world situations can conveniently be described using a diagram consisting of a set of points along with lines joining certain pairs of these points. For example, the points could represent people, with lines joining pairs of friends; or the points might be communication centres, with lines representing communication links. Notice that in such diagrams one is mainly interested in whether or not two given points are joined by a line; the manner in which they are joined is immaterial. A mathematical abstraction of situations of this type gives rise to the concept of a graph. *Graph theory* is fundamental in understanding the structure and interrelationships within complex systems and has been proven to be a very powerful tool to analyze social or telecommunication networks (see, e.g., Barnes, 1969; Ramírez-Arroyo et al., 2020). Nevertheless, graph theory holds fundamental importance beyond its practical applications, as its ability to translate abstract mathematical ideas into concrete visual forms provides a rich framework for exploring deep mathematical concepts related to structure, symmetry, and connectivity, offering insights in different more theoretical disciplines. For instance, graph-theoretic approaches are used to explore knot theory (Murasugi, 1989), the study of surfaces (Boykov and Kolmogorov, 2003), knowledge bases (Basu and Blanning, 1997), or probabilistic methods (Erdős and Rényi, 1960; Gilbert, 1959).

A *graph* G is an ordered triple $G = (V, E, \psi)$ consisting of a nonempty set V of *vertices*, a set E, of *edges*, and an *incidence map* $\psi : E \to \mathcal{P}_2(V)$ that associates each edge of G with an unordered pair of (not necessarily distinct) vertices of G (here, $\mathcal{P}_2(V)$ stands for the set of all subsets of V with cardinality at most 2). If $e \in E$ is an edge and $u, v \in V$ are vertices such that $\psi(e) = \{u, v\}$, then e is said to *join* u and v; the vertices u and v are called the *ends* of the edge e.

Graphs are so named because they can be represented graphically, and it is this graphical representation which helps us understand many of their properties. Each vertex is indicated by a point, and each edge by a line joining the points which represent its ends. Most of the definitions and concepts in graph theory are suggested by the graphical representation. The ends of an edge are said to be *incident* with the edge, and vice versa. Two vertices which are incident with a common edge are *adjacent*, as are two edges which are incident with a common vertex. An edge with identical ends is called a *loop*, and an edge with distinct ends a *link*. A graph $H = (V', E', \psi')$ is a *subgraph* of G (written $H \subseteq G$) if $V' \subseteq V$, $E' \subseteq E$, and ψ' is the restriction of ψ to E'. Suppose that V' is a nonempty subset of V. The subgraph of G whose vertex set is V' and whose edge set is the set of those edges of G that have both ends in V' is called the subgraph of G *induced* by V' and is denoted by $G[V']$; we say that $G[V']$ is an *induced subgraph* of G.

A graph is *finite* if both its vertex set and edge set are finite, and is *simple* if it has no loops and no two of its links join the same pair of vertices. Hereinafter, we study only simple finite graphs, and so the term "graph" always means "simple finite graph". Notice that if the graph is simple then ψ is injective so we can identify E with the image of $\psi(E) \subseteq \mathcal{P}_2(V)$ hence in this work a graph is completely determined by the ordered pair (V, E). A *walk* in G is a finite nonnull sequence $W = w_0 w_1 \cdots w_k$, whose terms fulfill there is an edge $\{w_{i-1}, w_i\} \in E$ for $i = 1, \dots, k$. We say that W is a walk from w_0 to w_k, or a (w_0, w_k)*–walk*. If, in addition, the vertices $w_0 \cdots w_k$ are distinct, W is called a *path*. Two vertices u and v of G are said to be *connected* if there is a (u, v)–path in G. Connection is an equivalence relation on the vertex set V. Thus there is a partition of V into nonempty subsets $V_1, \dots, V_\omega$ such that two vertices u and v are connected if and only if both u and v belong to the same set V_i. The subgraphs $G[V_1], \dots, G[V_\omega]$ are called the *components* of G. If G has exactly one component, G is *connected*; otherwise G is *disconnected*.

If instead of having the edges in $\mathcal{P}_2(V)$ they belong to $V \times V$, i.e., they are ordered couples; then the graph is called *directed* and the edges are called *arcs*. Let $G = (V, A)$ be a directed graph or *digraph*, where V is the vertex set and $A \subset V \times V$ is the arc set of G. For each $v \in V$, we denote by $\delta^+(v) := \{w \in V : (v, w) \in A\}$ the set of its outgoing arcs, and $\deg^+(v) := |\delta^+(v)|$ is the outdegree. Analogously, $\delta^-(v) := \{w \in V : (w, v) \in A\}$ denotes the set of ingoing arcs of $\boldsymbol{v}$, and $\deg^-(v) := |\delta^-(v)|$ its indegree. Any directed graph has associated three matrices that allow to characterize the graph, namely the adjacency, the degree, and the laplacian matrix. The *adjacency matrix* of G is defined as $\mathrm{Adj}(G) := (a_{vw})_{v,w \in V}$, where $a_{vw} = 1$ if $(v, w) \in A$, and zero otherwise. The *degree matrix* of G is the diagonal matrix of order $|V| \times |V|$ defined as $D^+(G) := (d_{vw})_{v,w \in V}$, where $d_{vv} = \deg^+(v)$. Finally The *Laplacian matrix* of G is defined as $L^+(G) := D^+(G) - \mathrm{Adj}(G)$.

With each digraph D we can associate an (*undirected*) graph G on the same vertex set. Corresponding to each arc of D there is an edge of G with the same ends. This graph is the *underlying graph* of D. Conversely, given any graph G, we can obtain a digraph from G by specifying, for each link, an order on its ends. Such a digraph is called an orientation of G. A directed graph is *weakly connected* if the underlying graph is a connected graph. A directed graph is *strongly connected* if it contains a *directed path* (a path which respects the orientation) from u to v for every pair of vertices (u, v).

Besides, if one assigns weights to the edges of the graph we obtain a network. A *network* G is an ordered triple $G = (V, E; \Omega)$ such that (V, E) is a graph and $\Omega : E \to \mathbb{R}_+$ is the *edge-weight map* $e \mapsto \omega_e \in \mathbb{R}_+$ which assign a nonnegative weight to each edge in the graph.

Given a subset $\mathbb{M} \subseteq \mathbb{R}^n$, we say that $G = (V, A)$ is an $\mathbb{M}$-geometric graph (same for digraph or network) if its vertex set, V, is embedded in $\mathbb{M}$, i.e., $V \subset \mathbb{M}$; and each edge $e = \{\boldsymbol{o}_e, \boldsymbol{f}_e\} \in E$ can be identified with the segment in $\mathbb{R}^n$, with extremes $\boldsymbol{o}_e$ and $\boldsymbol{f}_e$ in V or with the vector of $\mathbb{R}^n$ associated with them, i.e., $\boldsymbol{f}_e - \boldsymbol{o}_e$.

2.5.1 Combinatorial Optimization

In *combinatorial optimization*, the goal is to find the best solution from a finite set of possible solutions, often structured as graphs. Some of the most popular and used optimization problems belong to this family, as the shortest path problems, minimum cost spanning trees, traveling salesperson problem, or maximum flow. Algorithms proposed to efficiently solve these problems (see, e.g., Dijkstra, 1959; Prim, 1957; Kruskal, 1956; Ford and Fulkerson, 1956) are based on exploiting the properties of the graph structures behind them. In more complex combinatorial problems, with tons of vertices or edges, sophisticated interconnections, multilayered, etc., it is even more crucial to understand the structures of the graphs to be constructed as a solution of a decision problem.

Conic optimization plays a fundamental role in combinatorial optimization and graph theory, where conic structures have been used to formulate stronger relaxations (Bie and Cristianini, 2006; Chuong, 2022); construct new supervised classification tools (Blanco et al., 2020b; Wang et al., 2018); derive efficient algorithms for challenging combinatorial problems (Alizadeh, 1995; Blanco and Puerto, 2022; Blanco and Martínez-Antón, 2024b; Dhyani Bhatt et al., 2021); or detect graph properties or invariants, as those induced by semidefinite programming (SDP) for problems such as the maximum stable set problem (Gaar et al., 2022); graph partitioning (Orecchia and Vishnoi, 2011); and the max-cut problem (Gaar and Rendl, 2020; Goemans and Williamson, 1995). Beyond SDP, second–order cone programming (SOCP) and p–order cone formulations (pOCP) have also been leveraged to strengthen or find good quality bounds for classical combinatorial optimization problems or to model robust versions of these problems (see, e.g., Ben-Tal and Nemirovski, 2001b; Buchheim and Kurtz, 2018; Burer and Chen, 2009; Liu et al., 2022; Muramatsu and Suzuki, 2003, among many others). Conic duality has been instrumental in identifying hidden combinatorial structures, such as exploiting Laplacian eigenvalues in spectral graph theory to design more efficient clustering and community detection algorithms (Qing and Wang, 2020).

Chapter III

Mediated graphs

Ich will neue Dinge sehen und sie erforschen. Ich will dunkles Wasser probieren, sprühende Bäume und wilde Winde sehen.
Quiero ver cosas nuevas e investigarlas. Quiero probar agua oscura y ver árboles chispeantes y vientos salvajes.
— Egon Schiele

In this chapter, we provide a new link between conic optimization and graph theory by introducing and analyzing a new family of geometric graphs. Despite its impact in the computation of explicit SOS decomposition of non-negative polynomials or SOC representation of general p–order and power cones, it has not been previously formally introduced, the so-called family of *mediated graphs*.

We formally analyze the family of mediated graphs, which will be defined as geometric directed graphs embedded in abelian groups, where almost all its vertices (*tails*) are the midpoint of two other vertices (*heads*) in the graph, and an arc joins each tail with its heads.

Literature Review

The underlying structure of these graphs is closely related to the concept of mediated set that was introduced by Reznick (1989) as a tool to provide a necessary and sufficient condition for an AGI-form to be decomposed as a sum of squares of polynomials. Since then, the notion of mediated set has been modified to be adapted to different problems (see, e.g., Hartzer et al. (2022); Magron and Wang (2023); Wang (2024)). Magron and Wang (2023) also exploit this structure to provide an SOC representation of sums of nonnegative circuits cones (SONC). Dressler et al. (2017) and Wang (2022) propose the use of mediated sets to represent convex semialgebraic sets using SONC. Sum of squares (SOS) decompositions were addressed by Reznick (1989); Iliman and De Wolff (2016a,b) using also mediated sets. Recently, in Wang (2024), these sets have been applied to provide optimal SOC representations of weighted geometric mean inequalities. The usefulness of the graph structure of a mediated set was already observed by Blanco and Martínez-Antón (2024a) for the same problem, where the authors provide explicit minimal SOC extended representations of *generalized power cones* (GPC). It allows us to formulate, exactly and efficiently, a *generalized power cone programming* (GPCP) problem as an SOCP with a direct impact in solving optimization problems involving these cones. Another recent contribution on mediated sets can be found in Powers and Reznick (2021).

The remainder of this chapter is organized as follows. In Section 3.1, we formally introduce the concept of mediated graphs and establish some fundamental geometric and algebraic properties derived from their definition. Section 3.2 is dedicated to studying optimal (extremal) graphs within the class of mediated graphs under a partial order that we define, based on the cardinality of the vertex set. The identification and computation of these optimal graphs form the core of this work. We motivate the need for their efficient computation by highlighting their connection to the existence of SOS decompositions of circuit polynomials and minimal SOC representations of more complex conic structures. In Sections 3.2.1 and 3.2.2, we introduce and analyze minimal and maximal mediated graphs, respectively. These sections present the main contributions of this work: the development of integer linear programming (ILP) formulations to compute these graphs. Besides, in Chapter VII, Section 7.1, we report the results of an extensive set of experiments demonstrating the validity and practical utility of our approaches. For maximal mediated graphs, we compare our optimization-based method with the enumerative approach proposed in Hartzer et al. (2022). For minimal mediated graphs, we analyze the performance of different domain formulations for which we derive integer linear optimization models. Finally, we draw some conclusions and indicate some potential future research on the topic in the last chapter.

3.1 Definition and Properties

We start by introducing the main definition in this work.

Definition 3.1 (Mediated graph). *Let $\mathbb{M} \subseteq \mathbb{R}^n$ and $\mathcal{A} \subset \mathbb{M}$ be a finite set. An $\mathbb{M}$-geometric digraph $G = (V, A)$ is said an $\mathcal{A}$-*mediated graph *if $\mathcal{A} \subset V$, $\delta^+(\boldsymbol{v}) \neq \emptyset$, and if $\boldsymbol{w} \in \delta^+(\boldsymbol{v})$, then $2\boldsymbol{v} - \boldsymbol{w} \in \delta^+(\boldsymbol{v})$, for all $\boldsymbol{v} \in V \backslash \mathcal{A}$.*

The family of $\mathcal{A}$-mediated graphs on $\mathbb{M}$ will be denoted as $\mathcal{M}_{\mathcal{A}}^{\mathbb{M}}$. The mention of the domain $\mathbb{M}$ will be omitted in the notation unless it is necessary to avoid confusion.

The definition of mediated graph implies that every vertex in V, except those in $\mathcal{A}$, is the midpoint of two of its out-adjacent vertices. Every point in $V \backslash \mathcal{A}$ is said to be a *mediated vertex*.

Remark 3.2. *Note that every nonempty mediated graph $G = (V, A)$ can be reduced to a graph $G' = (V, A')$, whose outdegree $\deg^+(\boldsymbol{v}) = 2$ for all $\boldsymbol{v} \in V \backslash \mathcal{A}$ and $\deg^+(\boldsymbol{a}) = 0$ for all $\boldsymbol{a} \in \mathcal{A}$ which is also a mediated graph. Thus, hereinafter, we assume without loss of generality, that, in every $\mathcal{A}$-mediated graph, each vertex has outdegree 2, except for those in $\mathcal{A}$ which have outdegree 0. Moreover, we assume $\mathcal{A} \neq \emptyset$, since the only $\emptyset$-mediated graph is the empty graph.*

Remark 3.3. *The domain where the vertex set of a mediated graph is defined has been taken as a subset of $\mathbb{R}^n$, but note that the only condition we need to define a mediated graph is $2\boldsymbol{v} - \boldsymbol{w} \in \mathbb{M}$ for any $\boldsymbol{v}, \boldsymbol{w} \in \mathbb{M}$. Hence, in a more general and abstract way, we can define a mediated graph in any domain $\mathbb{M}$, being $\mathbb{M}$ a $\mathbb{Z}$–module (i.e., and abelian group).*

In the following example, we illustrate the geometrical shapes of some mediated graphs.

Example 3.4. *Let $\mathcal{A} = \{(0,0), (7,0), (0,7)\}$ (red dots) in Figure 3.1 we show two different $\mathcal{A}$-mediated graphs in two different domains. In the left picture, we show a $\mathcal{A}$-mediated graph constructed on $\mathbb{M} = \mathbb{R}^2$. Note that, apart from the points in $\mathcal{A}$, four more vertices appear in the graph (blue dots), namely $(0.5, 0.5), (1, 1), (2, 2)$, and $(3.5, 3.5)$, all of them midpoints of two other vertices in the graph. The arrows indicate the arcs in the graph, each of them directed from the vertex to the two other vertices for which it is a midpoint. In the right picture, we show an example of a $\mathcal{A}$-mediated graph with domain $\mathbb{M} = \mathbb{Z}^2$. In this case, the graph consists of 10 vertices (3 of them those in $\mathcal{A}$), but the coordinates of the points are now integer numbers.*

In this case, the vertices not in $\mathcal{A}$ are: $(1,0)$, $(1,1)$, $(1,2)$, $(2,0)$, $(2,4)$, $(4,0)$, *and* $(4,1)$.

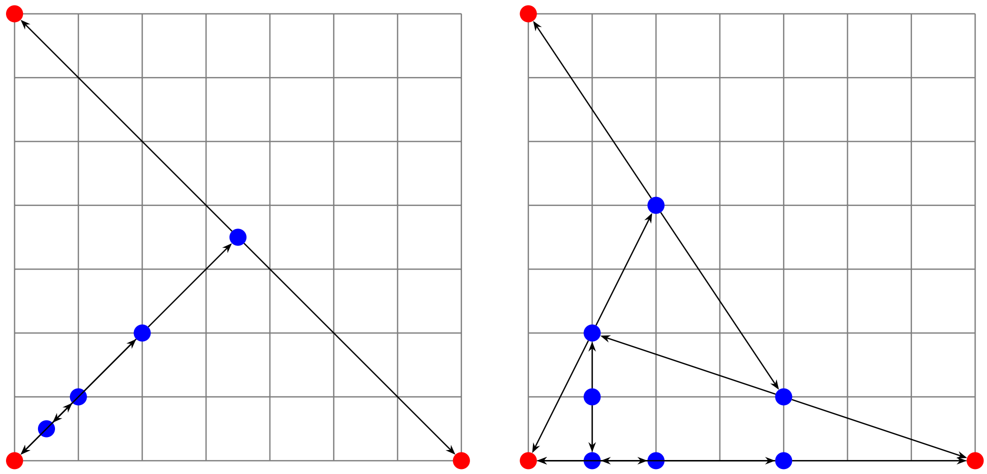

FIGURE 3.1: Two versions of $\mathcal{A}$-mediated graphs but with different vertex domains: $\mathbb{R}^2$ (left) and $\mathbb{Z}^2$ (right).

Although mediated graphs have been proven to be useful in different fields, in this chapter we provide a general framework for them, as well as explore some of their properties.

First, we derive some geometric and algebraic properties of a mediated graph, whose proof is straightforward, but allows us to understand the closeness properties of the family $\mathcal{M}_{\mathcal{A}}$.

Proposition 3.5. *Let $\mathcal{A} \subset \mathbb{M}$ be a finite set of points in $\mathbb{M}$, and $G = (V, A) \in \mathcal{M}_{\mathcal{A}}$. Then, the following properties are verified:*

1. *$G \in \mathcal{M}_{\mathcal{A}}^{\mathbb{M}'}$ for any $\mathbb{M} \subseteq \mathbb{M}'$.*
2. *$G \in \mathcal{M}_{\mathcal{A}'}$ for all $\mathcal{A} \subseteq \mathcal{A}' \subset \mathbb{M}$.*[1]
3. *$\mathcal{M}_{\emptyset} = \{(\emptyset, \emptyset)\}$.*
4. *If $\mathcal{A}' \subset \mathbb{M}$ and $(V', A') \in \mathcal{M}_{\mathcal{A}'}$, then $(V \cup V', A \cup A') \in \mathcal{M}_{\mathcal{A} \cup \mathcal{A}'}$.*
5. *$V \subset \mathrm{Conv}(\mathcal{A})$.*
6. *If $\mathcal{A}$ is affinely independent and $V \cap \mathrm{Conv}(\mathcal{A})^{\circ} \neq \emptyset$, then $\deg^{-}(\boldsymbol{a}) \geq 1$ for all $\boldsymbol{a} \in \mathcal{A}$.*
7. *The submatrix $L^{+}(G)_{V \setminus \mathcal{A}}$ of the Laplacian matrix of G is invertible, and the entries of its inverse are nonnegative.*

[1]without considering the isolated vertices in $\mathcal{A}' \setminus \mathcal{A}$

Proof. Since 1-6 are straightforward, we will only prove 7. It is just needed to see if the matrix satisfies the hypothesis of (Reznick, 1989, Lemma 4.3). Since, for all $\boldsymbol{v} \in V \backslash \mathcal{A}$, $\deg^+(\boldsymbol{v}) = 2$, thus the entries of the main diagonal of the matrix are equal to two; and it is clear that the entries out of the main diagonal only take values in $\{0, -1\}$. Each row is in the shape $(c_{\boldsymbol{vw}})_{\boldsymbol{w} \in V \backslash \mathcal{A}}$ with $\boldsymbol{v} \in V \backslash \mathcal{A}$, therefore it has as -1's as heads of $\boldsymbol{v}$ in $V \backslash \mathcal{A}$ so at most two. Eventually, assume that there exists a principal submatrix in which each row has exactly two -1's. This implies that there exists $U \subseteq V \backslash \mathcal{A}$ such that for all $\boldsymbol{v} \in U$ its two heads belong to U. So, the graph $(U, A \cap (U \times U))$ is an $\emptyset$-mediated graph, then $U = \emptyset$ by statement 3. □

In the family of mediated graphs $\mathcal{M}_{\mathcal{A}}$, we will analyze those graphs whose vertex set contains a finite set $\mathcal{B} \subset \mathbb{M}$. These subsets play a main role in this work.

$$\mathcal{M}_{\mathcal{A}}(\mathcal{B}) := \{(V, A) \in \mathcal{M}_{\mathcal{A}} : \mathcal{B} \subset V\}. \tag{3.1}$$

When $\mathcal{B}$ be a singleton, i.e., $\mathcal{B} = \{\boldsymbol{b}\}$ for some $\boldsymbol{b} \in \mathbb{M}$, $\mathcal{M}_{\mathcal{A}}(\boldsymbol{b}) := \mathcal{M}_{\mathcal{A}}(\{\boldsymbol{b}\})$.

In what follows, we analyze under which conditions the family $\mathcal{M}_{\mathcal{A}}(\mathcal{B})$ is not empty.

Definition 3.6 (Binary support). *Let n be a nonnegative integer number. We denote by $\Omega(n)$ the set of strictly positive coefficients in the binary decomposition of n, namely, if $n = \sum_{i=0}^{\lfloor \log_2(n) \rfloor} b_i 2^i$, then*

$$\Omega(n) := \{i \in \{0, \ldots, \lfloor \log_2(n) \rfloor\} : b_i = 1\}.$$

We adopt (Wang, 2024, Corollary 28) for mediated graphs to provide a first nonemptyness sufficient condition for $\mathcal{M}_{\mathcal{A}}(\boldsymbol{b})$.

Lemma 3.7. *Let $\mathcal{A} \subset \mathbb{R}^n$ be an affine independent set and $\boldsymbol{b} \in \mathrm{Conv}(\mathcal{A})^\circ$. Then, there exists nonempty graph $G = (V, A)$ in $\mathcal{M}_{\mathcal{A}}(\boldsymbol{b})$ with*

$$|V| = \sum_{\boldsymbol{a} \in \mathcal{A}} |\Omega(s_{\boldsymbol{a}})| + |\mathcal{A}| - 1,$$

where $\boldsymbol{s} = (s_{\boldsymbol{a}})_{\boldsymbol{a} \in \mathcal{A}} \in \mathbb{N}^{\mathcal{A}}$, $\gcd(\boldsymbol{s}) = 1$, and $\frac{1}{\|\boldsymbol{s}\|_1} \boldsymbol{s}$ are the barycentric coordinates of $\boldsymbol{b}$ with respect to $\mathcal{A}$.

In the following result, we generalize the previous result for any set $\mathcal{A}$ and any set $\mathcal{B}$ (not necessarily singleton). Notice that, by Carathéodory's theorem 2.8, for every point $\boldsymbol{b} \in \mathrm{Conv}(\mathcal{A})$, there is at least one subset $\mathcal{C} \subseteq \mathcal{A}$

affinely independent (a.i.), strictly containing the point $\boldsymbol{b}$. Hence, we can define

$$\mathcal{A}(\boldsymbol{b}) := \arg \min_{\mathcal{C} \subseteq \mathcal{A} \text{ a.i.}} \Bigg\{ \sum_{\boldsymbol{c} \in \mathcal{C}} |\Omega(s_{\boldsymbol{c}})| + |\mathcal{C}| : \\ \boldsymbol{s} = (s_{\boldsymbol{c}})_{\boldsymbol{c} \in \mathcal{C}} \in \mathbb{N}^{\mathcal{C}}, \quad \gcd(\boldsymbol{s}) = 1, \quad \boldsymbol{b} = \frac{1}{\|\boldsymbol{s}\|_1} \sum_{\boldsymbol{c} \in \mathcal{C}} s_{\boldsymbol{c}} \boldsymbol{c} \Bigg\}. \quad (3.2)$$

We denote by $\boldsymbol{s}^{\boldsymbol{b}} := (s_{\boldsymbol{a}}^{\boldsymbol{b}})_{\boldsymbol{a} \in \mathcal{A}(\boldsymbol{b})} \in \mathbb{N}^{\mathcal{A}(\boldsymbol{b})}$, where $\gcd(\boldsymbol{s}^{\boldsymbol{b}}) = 1$ and $\frac{1}{\|\boldsymbol{s}^{\boldsymbol{b}}\|_1} \boldsymbol{s}^{\boldsymbol{b}}$ are the barycentric coordinates of $\boldsymbol{b}$ with respect to $\mathcal{A}(\boldsymbol{b})$.

Theorem 3.8. *Let $\mathcal{A}, \mathcal{B} \subset \mathbb{R}^n$ be finite subsets and $\mathcal{B} \subset \operatorname{Conv}(\mathcal{A})$. Then, there exists a nonempty graph $G = (V, A) \in \mathcal{M}_{\mathcal{A}}(\mathcal{B})$ such that:*

$$|V| \leq \nu_{\mathcal{A}}(\mathcal{B}) := \sum_{\boldsymbol{b} \in \mathcal{B}} \left[\sum_{\boldsymbol{a} \in \mathcal{A}(\boldsymbol{b})} |\Omega(s_{\boldsymbol{a}}^{\boldsymbol{b}})| + |\mathcal{A}(\boldsymbol{b})| \right] - |\mathcal{B}|. \quad (3.3)$$

Proof. By Lemma 3.7, there exists $G_{\mathcal{A}(\boldsymbol{b})} = (V_{\mathcal{A}(\boldsymbol{b})}, A_{\mathcal{A}(\boldsymbol{b})})$ in $\mathcal{M}_{\mathcal{A}(\boldsymbol{b})}(\boldsymbol{b}) \subseteq \mathcal{M}_{\mathcal{A}}(\boldsymbol{b})$ (the inclusion is obtained from Proposition 3.5.2) with

$$|V_{\mathcal{A}(\boldsymbol{b})}| = \sum_{\boldsymbol{a} \in \mathcal{A}(\boldsymbol{b})} |\Omega(s_{\boldsymbol{a}}^{\boldsymbol{b}})| + |\mathcal{A}(\boldsymbol{b})| - 1.$$

By Proposition 3.5.4, there must be a graph $G = (V, A) \in \mathcal{M}_{\mathcal{A}}(\mathcal{B})$ where $V = \bigcup_{\boldsymbol{b} \in \mathcal{B}} V_{\mathcal{A}(\boldsymbol{b})}$, thus $|V| \leq \sum_{\boldsymbol{b} \in \mathcal{B}} |V_{\mathcal{A}(\boldsymbol{b})}|$. □

Note that the nonemptyness of $\mathcal{M}_{\mathcal{A}}(\mathcal{B})$ is not assured in general, even if $\mathcal{B} \subset \operatorname{Conv}(\mathcal{A}) \cap \mathbb{M}$. In the following result, we show a counterexample of this situation.

Example 3.9. *Let us consider $\mathbb{M} = (2\mathbb{Z})^2$, $\mathcal{A} = \{(0,0), (4,2), (2,4)\}$ and $\boldsymbol{b} = (2,2) \in \operatorname{Conv}(\mathcal{A}) \cap (2\mathbb{Z})^2$. Note that there is no choice to construct a $\mathcal{A}$-mediated graph that contains $\boldsymbol{b}$, and then $\mathcal{M}_{\mathcal{A}}(\boldsymbol{b}) = \emptyset$.*

In view of the possible nonexistence of mediated graphs, Powers and Reznick (2021) provide a lower bound for the *dilation* constant $k \in \mathbb{N}$ such that $\mathcal{M}_{k\mathcal{A}}(\mathcal{B})$ is nonempty for all $\mathcal{A} \subset \mathbb{M}$, where $k\mathcal{A} := \{k\boldsymbol{a} \in (2\mathbb{Z})^n : \boldsymbol{a} \in \mathcal{A}\}$ and $\mathcal{B} \subset \operatorname{Conv}(k\mathcal{A}) \cap \mathbb{Z}^n$ in the case $\mathbb{M} = (2\mathbb{Z})^n$.

Theorem 3.10. *Let $\mathcal{A} \subset (2\mathbb{Z})^n$ be an affine independent set. Then, for every integer $k \geq \{2, |\mathcal{A}| - 2\}$, there exists a $(k\mathcal{A})$-mediated graph, $G = (\mathrm{Conv}(k\mathcal{A}) \cap \mathbb{Z}^n, A)$ such that $\delta^+(\boldsymbol{v}) \subset (2\mathbb{Z})^n$ for every vertex $\boldsymbol{v} \in \mathrm{Conv}(k\mathcal{A}) \cap \mathbb{Z}^n$.*

3.2 Optimal Mediated Graphs

The family of $\mathcal{A}$-mediated graphs can be endowed with a partial order induced by the cardinality of their vertex sets. Specifically, given $G = (V, A)$, $G' = (V', A') \in \mathcal{M}_{\mathcal{A}}$:

$$G \preceq G' \text{ if and only if either } |V| < |V'| \text{ or } G = G'. \tag{3.4}$$

Based on this partial order, the family of $\mathcal{A}$-mediated graphs for a given finite set $\mathcal{A} \subset \mathbb{M}$ has two distinguished elements that arise when minimizing and maximizing the number of vertices in the graph. Since the enumeration of this family of graphs can be, in general, cumbersome, we develop approaches to construct these *optimal* graphs using mathematical optimization tools. The study and construction of these so-called minimal and maximal mediated graphs are motivated by their implications in different problems in convex algebraic geometry and then, in its application to efficiently represent useful convex optimization problems.

We separately analyze minimal and maximal mediated graphs for different reasons. On the one hand, minimal mediated graphs (MinMG, for short) have already been proven to be useful structures to derive the most efficient and simple SOC or SOS decompositions of other more complex convex sets, with a high impact in practical conic optimization problems (see, e.g., Blanco et al., 2014; Blanco and Martínez-Antón, 2024a; Magron and Wang, 2023; Wang, 2024). Furthermore, MinMG can be analyzed in *discrete* and *continuous* domains referring to the cardinality of $\mathrm{Conv}(\mathcal{A}) \cap \mathbb{M}$, finite and infinite, respectively. On the other hand, the known applications of maximal mediated graphs (MaxMG, for short) are related to the existence of SOS decomposition of circuit polynomials (Hartzer et al., 2022; Iliman and De Wolff, 2016a; Reznick, 1989). Clearly, the construction of MaxMG is only possible in discrete domains.

In this section, we analyze some properties of MinMG and MaxMG and propose different approaches for their construction.

3.2.1 Minimal Mediated Graphs

Note that the unique minimal mediated graph of $\mathcal{M}_{\mathcal{A}}$ is the edgeless graph with vertex set $\mathcal{A}$. Thus, we analyze here MinMG restricted to the family $\mathcal{M}_{\mathcal{A}}(\mathcal{B})$ for a nonempty set $\mathcal{B} \subset \mathrm{Conv}(\mathcal{A}) \cap \mathbb{M}$ (see (3.1)). In what follows, we formally introduce this subgraph.

Definition 3.11 (Minimal mediated graph)**.** *Let $\mathcal{A}, \mathcal{B} \subset \mathbb{M}$ be finite sets. We say that $G = (V, A) \in \mathcal{M}_{\mathcal{A}}(\mathcal{B})$, is a* minimal $\mathcal{A}$–mediated graph *for $\mathcal{B}$ if there not exists $G' = (V', A') \in \mathcal{M}_{\mathcal{A}}(\mathcal{B})$ such that $|V'| < |V|$.*

We denote by $\mathrm{MinMG}_{\mathcal{A}}(\mathcal{B})$ the family of minimal $\mathcal{A}$-mediated graphs for $\mathcal{B}$. Notice that a minimal mediated graph is a minimal element in the poset $(\mathcal{M}_{\mathcal{A}}(\mathcal{B}), \preceq)$. Some properties can be derived for this family of mediated graphs

Theorem 3.12. *Let $\mathcal{A} \subset \mathbb{M}$ and $\mathcal{B} \subset \mathbb{M}$. Then, any minimal mediated graph $G \in \mathcal{M}_{\mathcal{A}}(\mathcal{B})$ has at most $|\mathcal{B}|$ weak connected components.*

Proof. Let us first analyze the case when $\mathcal{B} = \{\boldsymbol{b}\}$. In case $\mathcal{M}_{\mathcal{A}}(\boldsymbol{b}) = \emptyset$ is clear. We prove the lemma by contraposition for nonempty $\mathcal{M}_{\mathcal{A}}(\boldsymbol{b})$. Suppose the graph $G = (V, A) \in \mathcal{M}_{\mathcal{A}}(\boldsymbol{b})$ is not weakly connected. Thus, one can construct the graph, $G' = (V', A')$ where:

$$V' := \{\boldsymbol{v} \in V : \text{ there exists a path from } \boldsymbol{b} \text{ to } \boldsymbol{v}\}$$
$$A' := A \cap (V' \times V').$$

Note that G' is an $\mathcal{A}$–mediated graph with $\boldsymbol{b} \in V'$. Given $\boldsymbol{v} \in V' \backslash \mathcal{A}$, by definition, there exists a path in G from $\boldsymbol{b}$ to $\boldsymbol{v}$. If $\boldsymbol{w}$ and $2\boldsymbol{v} - \boldsymbol{w}$ are the heads of $\boldsymbol{v}$ in G, then $\boldsymbol{w}, \boldsymbol{v} - \boldsymbol{w} \in V'$, and then $(\boldsymbol{v}, \boldsymbol{w}), (\boldsymbol{v}, 2\boldsymbol{v} - \boldsymbol{w}) \in A'$. Since, clearly, $\boldsymbol{b} \in V'$, $G' \in \mathcal{M}_{\mathcal{A}}(\boldsymbol{b})$. As G is not weakly connected, $V' \subsetneq V$, then $|V'| < |V|$, contradicting the minimality of G.

Let us now analyze the general case. If $G = (V, A) \in \mathcal{M}_{\mathcal{A}}(\mathcal{B})$ which is not weakly connected, it is enough to consider the graph $G'' = (V'', A'')$ defined by

$$V'' := \{\boldsymbol{v} \in V : \text{ there exists a path from } \mathcal{B} \text{ to } \boldsymbol{v}\}, \tag{3.5}$$
$$A'' := A \cap (V'' \times V'')$$

which, analogously to the singleton case, is $\mathcal{M}_{\mathcal{A}}(\boldsymbol{b})$, with $|V''| < |V|$, contradicting the minimality of G. □

The following result is straightforward from the construction in the previous result and provides us information about the indegrees of the vertices in a minimal mediated graph.

Corollary 3.13. *If $G \in \mathcal{M}_{\mathcal{A}}(\mathcal{B})$ is a minimal mediated graph, then* $\deg^-(v) \geq 1$ *for all $v \in V \backslash \mathcal{B}$.*

The following result is a straightforward consequence of Theorem 3.8 giving us an upper bound for the cardinality of a minimal mediated graph.

Corollary 3.14. *Let $\mathcal{A}, \mathcal{B} \subset \mathbb{R}^n$ and $G = (V, A) \in \mathrm{MinMG}_{\mathcal{A}}(\mathcal{B})$. Then,*

$$|V| \leq \nu_{\mathcal{A}}(\mathcal{B}).$$

Computing $\mathrm{MinMG}_{\mathcal{A}}(\mathcal{B})$ requires determining both the vertices in $\mathrm{Conv}(\mathcal{A})$ and the arcs that verify the *mediated* condition at minimum cardinality. For particularly structured sets $\mathcal{A}$, and singleton sets $\mathcal{B}$, Wang (2024) propose a brute-force algorithm and heuristic approaches to compute $\mathrm{MinMG}_{\mathcal{A}}(\mathcal{B})$ focused on deriving minimal SOC representations of weighted geometric mean inequalities. Blanco and Martínez-Antón (2024a) provide a mixed integer linear programming model (MILP) to compute this set. In both cases, $\mathbb{M} = \mathbb{R}^n$ for a given dimension $n \geq 1$. This framework will be named the *continuous domain* minimal mediated graph since the vertices are to be found in the continuous region $\mathrm{Conv}(\mathcal{A})$. On the other hand, in case $\mathbb{M}$ is a *lattice* (as $\mathbb{Z}^n$ or $(2\mathbb{Z})^n$), we call this framework the *discrete domain* minimal mediated set. The main difference stems in that the search of the vertices and links in the continuous domain case is to be done among infinitely many vectors, whereas in the discrete domain case, the search is done in a finite set of points. By analogy with facility location theory, this is exactly the same difference between the family of continuous location problems and discrete location problems.

In what follows, we analyze minimal mediated sets for these two families of domains and derive mathematical optimization models that allow us to compute the minimal mediated graphs, avoiding, in general, the enumeration of all potential minimal subgraphs.

Minimal Mediated Graphs in $\mathbb{R}^n$

The problem of deriving mathematical optimization models for the continuous case was already addressed by Blanco and Martínez-Antón (2024a) for the vertex sets of dilations of the standard simplex and a single interior lattice point. Below we state the result for the general continuous domain case, which is a straightforward extension of the formulation provided in the mentioned paper.

Theorem 3.15. *Let $\mathcal{A} \subset \mathbb{R}^n$ be a finite set of points, and $\mathcal{B} \subset \mathrm{Conv}(\mathcal{A})$. The following mixed integer linear programming model allows to compute $\mathrm{MinMG}_{\mathcal{A}}(\mathcal{B})$ for $\mathbb{M} = \mathbb{R}^n$.*

(C-MinMGP)

$$\begin{aligned}
\textit{Minimize} \quad & |\mathcal{A}| + |\mathcal{B}| + \sum_{v \in \mathcal{V} \setminus (\mathcal{A} \cup \mathcal{B})} z_v && && (3.6)\\
\textit{subject to} \quad & y_{vw} \le z_v, && \forall v \in \mathcal{V} \setminus \mathcal{A}, w \in \mathcal{V}, && (3.7)\\
& y_{vw} \le z_w, && \forall v \in \mathcal{V} \setminus \mathcal{A}, w \in \mathcal{V}, && (3.8)\\
& 2x_v \ge x_w + x_u - \Delta(2 - y_{vw} - y_{vu}), && \forall v \in \mathcal{V} \setminus \mathcal{A}, w \ne u \in \mathcal{V}, && (3.9)\\
& 2x_v \le x_w + x_u + \Delta(2 - y_{vw} - y_{vu}), && \forall v \in \mathcal{V} \setminus \mathcal{A}, w \ne u \in \mathcal{V}, && (3.10)\\
& \|x_v - x_w\|_1 \ge \varepsilon(z_v + z_w - 1), && \forall v \ne w \in \mathcal{V}, && (3.11)\\
& \sum_{w \in \mathcal{V}} y_{vw} = 2z_v, && \forall v \in \mathcal{V} \setminus \mathcal{A}, && (3.12)\\
& x_v = v, \quad z_v = 1 && \forall v \in \mathcal{A} \cup \mathcal{B}, && (3.13)\\
& y_{vw} \in \{0, 1\}, && \forall v \in \mathcal{V} \setminus \mathcal{A}, w \in \mathcal{V}, && \\
& z_v \in \{0, 1\}, && \forall v \in \mathcal{V}, && \\
& x_v \in \mathbb{R}^n, && \forall v \in \mathcal{V}, &&
\end{aligned}$$

where $\mathcal{V}$ is any index set satisfying: $\mathcal{A}, \mathcal{B} \subset \mathcal{V}$, and $|\mathcal{V}| = \nu_{\mathcal{A}}(\mathcal{B})$. The parameters $\Delta := \max\{\|a\|_\infty : a \in \mathcal{A}\}$, and ε is a small enough tolerance value.

Proof. In the above formulation, the following variables are used:

$$z_v = \begin{cases} 1 & \text{if } v \text{ is a vertex of the minimal mediated graph,} \\ 0 & \text{otherwise;} \end{cases}$$

$$y_{vw} = \begin{cases} 1 & \text{if } (v, w) \text{ is an arc of the minimal mediated graph,} \\ 0 & \text{otherwise;} \end{cases}$$

$x_v \in \mathbb{R}^n$: Coordinates of the vertices in the MinMG in case $z_v = 1, \forall v \in \mathcal{V}$.

Constrains (3.7) and (3.8) determines that an arc in the mediated graph is possible just in case the two extremes are vertices of the graph. Constraints (3.9) and (3.10) assures the correct construction of a mediated graph, that is, if

$(v, w), (v, u)$ are arcs in the mediated graph, then, v is the midpoint of w and u. Constraints (3.11) assures that each vertex, seen as a embedded coordinate in $\mathbb{R}^n$, is activated only once. Constraint (3.12) is derived from Remark 3.2 where mediated graph is simplified to one with exactly two outgoing arcs from each *proper* mediated vertex. Finally, Constraints (3.13) set as vertices of the mediated graph those in $\mathcal{A} \cup \mathcal{B}$. The minimality is assured by the minimization criterion on the number of mediated vertices (3.6). □

Note that the ℓ_1 or Manhattan norm constraints are nonlinear but they can be standardly rewritten as linear constraints. Thus, the model (C-MinMGP) results in a MILP.

Minimal Mediated Graphs in Discrete Domains

The computation of discrete domain minimal mediated set, as far as we know, has not been previously addressed, and although the above model could be adapted (by enforcing that the x-variables can only take feasible values in the finite set of points inside $\mathrm{Conv}(\mathcal{A}) \cap \mathbb{Z}^n$ or $\mathrm{Conv}(\mathcal{A}) \cap (2\mathbb{Z})^n$, it would not exploit the discrete nature of the problem, and will result in an inefficient approach to compute MinMG. In what follows, we describe an alternative integer linear programming model (ILP) that we propose for the problem.

Theorem 3.16. *Let $\mathcal{A}, \mathcal{B} \subset \mathbb{Z}^n$ be two finite sets points with $\mathcal{B} \subset \mathrm{Conv}(\mathcal{A})$. The following integer linear programming model allows to compute a mediated graph in $\mathrm{MinMG}_{\mathcal{A}}(\mathcal{B})$.*

$$\text{(D-MinMGP)}$$

$$\begin{aligned}
\textit{Minimize}\quad & |\mathcal{A}| + |\mathcal{B}| + \sum_{v \in \mathcal{V}\setminus(\mathcal{A}\cup\mathcal{B})} x_v && && (3.14)\\
\textit{subject to}\quad & y_{vw} \le x_v, && \forall v, w \in \mathcal{V}, && (3.15)\\
& y_{vw} \le x_w, && \forall v, w \in \mathcal{V}, && (3.16)\\
& y_{v(2v-w)} \ge y_{vw}, && \forall v \neq w \in \mathcal{V} \text{ if } 2v - w \in \mathcal{V}, && (3.17)\\
& y_{vw} = 0, && \forall v \neq w \in \mathcal{V} \text{ if } 2v - w \notin \mathcal{V}, && (3.18)\\
& \sum_{w \in V} y_{vw} = 2x_v, && \forall v \in \mathcal{V}\setminus\mathcal{A}, && (3.19)\\
& x_v = 1, && \forall v \in \mathcal{A}\cup\mathcal{B}, && (3.20)\\
& x_v \in \{0,1\}, && \forall v \in \mathcal{V}, && (3.21)\\
& y_{vw} \in \{0,1\}, && \forall v, w \in \mathcal{V}. && (3.22)
\end{aligned}$$

where $\mathcal{V}$ is the (finite) set of potential positions for the mediated vertices.

Proof. Defining the binary variables that completely identify a mediated graph in $\mathcal{M}_{\mathcal{A}}(\mathcal{B})$:

$$x_v = \begin{cases} 1 & \text{if } v \text{ is a mediated vertex in } \mathrm{MinMG}_{\mathcal{A}}(\mathcal{B}), \\ 0 & \text{otherwise;} \end{cases}$$

$$y_{vw} = \begin{cases} 1 & \text{if } (v, w) \text{ is an arc in } \mathrm{MinMG}_{\mathcal{A}}(\mathcal{B}), \\ 0 & \text{otherwise.} \end{cases}$$

These variables are adequately defined by constraints (3.15)-(3.22). Constraints (3.15) and (3.16) ensure that no arcs are possible unless the extreme vertices are part of the graph. Constraints (3.17) and (3.18) imply the verification of the *mediated* condition: if (v, w) is an arc in the mediated graph, then, $(v, 2v - w)$ is also an arc in case all the extreme are feasible vertices. Constraint (3.18) states that all the mediated vertices (except those in $\mathcal{A}$) must have exactly two ongoing arcs. Constraints (3.20). The domain of the variables are given in Constraints (3.21) and (3.22). The minimality is assured by the minimization criterion on the number of mediated vertices (3.14). Note that the elements in $\mathcal{A}$ are excluded from the sum of the variables since they are always in the mediated graph, and then, its size is incorporated into the objective function as a constant (that can be avoided when solving the model). □

Remark 3.17. *The ILP model (D-MinMGP) has $O(|\mathcal{V}|^2)$ variables and $O(|\mathcal{V}|^2)$ linear constraints. For large sizes of $\mathcal{V}$ the problem can be computationally costly. Some strategies can be applied to the model in order to facilitate the solution procedure:*

- *Constraints (3.15) are not necessary. They are already induced by Constraints (3.19). Note that in case $x_v = 0$, all the outgoing arcs from v are not allowed in the solution.*

- *Constraints (3.16) can be strengthened by aggregating all the constraints for a given w, i.e., one can replace Constraints (3.16) by*

$$\sum_{v \in \mathcal{V}} y_{vw} \leq |\mathcal{V}| x_w, \quad \forall w \in \mathcal{V}.$$

- *The y-variables are not required to be defined for the case y_{vv} for $v \in \mathcal{V}$. Note that loops are not allowed in a mediated graph. The same applies for the x-variables for $v \in \mathcal{A} \cup \mathcal{B}$, that are already fixed to one in our model.*

Remark 3.18. *Note that the ILP (D-MinMGP) allows to compute a single minimal mediated graph in the discrete domain case. It might be possible that more than one mediated graph achieves this minimum cardinality. One could obtain the whole list of mediated graphs in* $\mathrm{MinMG}_{\mathcal{A}}(\mathcal{B})$ *by iteratively solving the problem and adding constraints to filter the previously obtained mediated graphs until the optimal solution achieves an objective value strictly larger than the minimum cardinal. Specifically, if solving for the first time the problem we obtain a minimum cardinality of ν, with sets of arcs (provided by the solutions in the y-variables) $A_{(1)}$, one can add the constraints:*

$$|\mathcal{A}| + |\mathcal{B}| + \sum_{v \in \mathcal{V} \setminus (\mathcal{A} \cup \mathcal{B})} x_v \leq \nu,$$
$$\sum_{v,w \in \mathcal{V}} y_{vw} \leq |A_{(1)}| - 1$$

and solve the problem again. Thus, in the kth iteration, when the set of arcs $A_{(k)}$ is obtained, we would add the constraint:

$$\sum_{v,w \in \mathcal{V}} y_{vw} \leq |A_{(k)}| - 1$$

In case the problem is infeasible, then the list of elements in $\mathrm{MinMG}_{\mathcal{A}}(\mathcal{B})$ *is already obtained, otherwise, a new constraint is incorporated, and the problem is solved again.*

Example 3.19. *Let us consider the set $\mathcal{A} = \{(0,0),(7,0),(0,7)\}$ and $\mathcal{B} = \{(1,1)\}$. In Figure 3.2 we show the five elements in* $\mathrm{MinMG}_{\mathcal{A}}(\mathcal{B})$ *in case $\mathbb{M} = \mathbb{Z}^2$. They were obtained in the same order as they as plotted by cutting off the solutions previously obtained. All of them have ten vertices. Observe that although the first and the second; and the third and the fourth mediated graphs are symmetric with respect to the line $\{x_1 = x_2\}$, the three obtained* proper *mediated graphs have a very different combinatorial structure.*

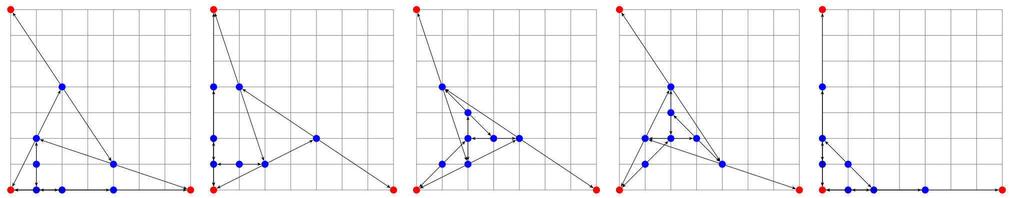

FIGURE 3.2: The entire set $\mathrm{MinMG}_{\mathcal{A}}(\mathcal{B})$ of Example 3.19.

3.2.2 Maximal Mediated Graphs

In what follows, we analyze maximal mediated graphs, i.e., those mediated graphs for $\mathcal{A}$ that have maximum vertex cardinality. Note that in the *continuous* case, the set of potential vertices for the mediated graph is not finite. Thus, in this section, we focus on maximal mediated graphs for discrete domains. Note that in discrete domains, the number of vertices of any $\mathcal{A}$-mediated graph can be at most $|\mathrm{Conv}(\mathcal{A}) \cap \mathbb{M}| < \infty$ ensuring the existence of maximal elements.

Definition 3.20 (Maximal mediated graph)**.** *Let $\mathcal{A} \subset \mathbb{M}$ be a finite set of points. $G = (V, A) \in \mathcal{M}_{\mathcal{A}}$, is a* maximal $\mathcal{A}$–mediated graph, *if there not exists $G' = (V', A') \in \mathcal{M}_{\mathcal{A}}$ such that $|V'| > |V|$.*

We denote by $\mathrm{MaxMG}_{\mathcal{A}}$ the family of maximal $\mathcal{A}$–mediated graphs. Notice that a maximal mediated set is a maximal element in the poset $(\mathcal{M}_{\mathcal{A}}, \preceq)$.

The first observation that we address is the unification of notation of maximal mediated sets. The maximal $\mathcal{A}$–mediated set was defined as the $\mathcal{A}$–mediated set that contains every $\mathcal{A}$–mediated set (Hartzer et al., 2022; Iliman and De Wolff, 2016a; Reznick, 1989), i.e., maximality understood by the order induced by the set inclusion. Indeed, this kind of set are maximum for this order in the set of all $\mathcal{A}$–mediated sets. In what follows we state the equivalence between our definition of maximal mediated graph and those of maximal mediated sets in the literature.

Theorem 3.21. *$G = (V, A) \in \mathcal{M}_{\mathcal{A}}$ is a maximal mediated graph if and only if V is the maximal mediated set. Furthermore, if $G = (V, A)$ and $G' = (V', A')$ are maximal, then $V = V'$.*

Proof. Let G be a maximal mediated graph. If there is an $\mathcal{A}$–mediated set V' such that $V' \not\subseteq V$, then $V \subset V \cup V'$. Since, $V \cup V'$ is an $\mathcal{A}$–mediated set there is an $\mathcal{A}$–mediated graph $G' = (V \cup V', A')$. However, $G' \succ G$ and that is not possible by the maximality of G. So, V is the maximal mediated set.

On the other hand, let V be the maximal $\mathcal{A}$–mediated set. Assume there is $G' = (V', A') \succeq G$, that implies either $|V'| > |V|$ or $G' = G$. However, the first condition cannot be true for the maximality of V so $G' = G$. Hence, G is maximal. $\square$

In what follows, we provide our mathematical optimization formulation that we propose to compute the maximal mediated graph for a set $\mathcal{A}$.

Theorem 3.22. *Let $\mathcal{A} \subset \mathbb{Z}^n$ be a finite set of points. The following integer linear programming model allows to compute a mediated graph in* $\mathrm{MaxMG}_{\mathcal{A}}$.

(D-MaxMGP)

$$
\begin{aligned}
&\textit{Maximize} && |\mathcal{A}| + \sum_{v \in \mathcal{V}\setminus\mathcal{A})} x_v && && (3.23)\\
&\textit{subject to} && \sum_{v \in \mathcal{V}} y_{vw} \le |\mathcal{V}| x_v, && \forall w \in \mathcal{V}, && (3.24)\\
& && \sum_{w \in \mathcal{V}} y_{vw} \le |\mathcal{V}| x_v, && \forall v \in \mathcal{A}, && (3.25)\\
& && y_{v(2v-w)} \ge y_{vw}, && \forall v \neq w \in \mathcal{V} \textit{ if } 2v - w \in \mathcal{V}, && (3.26)\\
& && y_{vw} = 0, && \forall v \neq w \in \mathcal{V} \textit{ if } 2v - w \notin \mathcal{V}, && (3.27)\\
& && \sum_{w \in V} y_{vw} = 2x_v, && \forall v \in \mathcal{V}\setminus\mathcal{A}, && (3.28)\\
& && x_v = 1, && \forall v \in \mathcal{A} \cup \mathcal{B}, && (3.29)\\
& && x_v \in \{0,1\}, && \forall v \in \mathcal{V}, && (3.30)\\
& && y_{vw} \in \{0,1\}, && \forall v, w \in \mathcal{V}. && (3.31)
\end{aligned}
$$

where $\mathcal{V} = \mathrm{Conv}(\mathcal{A}) \cap \mathbb{Z}^d$.

Proof. Note that the formulation is similar to the one provided in Theorem 3.16. Instead of maximizing the number of vertices in the obtained mediated graph, this cardinality is maximized. $\square$

Chapter IV

Conic Algebraic Geometry

Dime: ¿no ves aquel caballero que hacia nosotros viene sobre un caballo rucio rodado, que trae puesto en la cabeza un yelmo de oro?
—Lo que yo veo y columbro —respondió Sancho— no es sino un hombre sobre un asno pardo como el mío, que trae sobre la cabeza una cosa que relumbra.
—Pues ese es el yelmo de Mambrino —dijo don Quijote—.

— Miguel de Cervantes. *El ingenioso hidalgo don Quijote de La Mancha*, Capítulo 21

The use of conic structures in mathematical optimization problems has been widely extended within the last few years. The development of interior point methods with specialized barriers has given room to efficiently solve problems involving cones with high practical interest. The incorporation of exact techniques to solve conic optimization problems in different off-the-shelf optimization solvers has allowed practitioners to use these tools to make decisions in different fields. This is the case of facility location (Blanco, 2019; Blanco and Gázquez, 2023; Blanco et al., 2014, 2016; Xue and Ye, 2000); supervised classification (Blanco et al., 2020a,b); network covering (Blanco and Martínez-Antón, 2024b); power control (Chiang et al., 2007); portfolio selection (Krokhmal and Soberanis, 2010; Lu, 2006; Vinel and Krokhmal, 2014); geometric programming (Avriel and Williams, 1971; Nestorenko et al., 2022; Ota et al., 2019), among many others. Thus, a lot of theoretical results have emerged to understand the geometry of cones (Hien, 2015; Kian et al., 2019; Lu et al., 2020; Roy and Xiao, 2022). In terms of efficiency of optimization problems involving cones, different polyhedral approximations have been proposed (Ben-Tal and Nemirovski, 2001b; Lubin et al., 2018; Krokhmal and Soberanis, 2010; Vinel and Krokhmal, 2014) to take advantage of linear programming solvers to compute approximate solutions to conic optimization problems. Nevertheless, in the early 2000s, Glineur et al. (2000) states that interior points approaches have a better performance than the linear programming approximations proposed by Ben-Tal and Nemirovski (2001b). More recently, in view of the impressive developments of integer programming solvers, in Vielma et al. (2008); Vinel and Krokhmal (2014), linear approximations are recommended for both conic programs with continuous and/or integer variables.

In practice, among the vast variety of cones, some of them have been extensively analyzed since most of the cones can be *rewritten* in terms of these basic cones (Lu et al., 2020). These cones are the power cone and the exponential cone, whose efficient representation and incorporation also allow the incorporation of many other cones such as the second–order cone, the p–order cone, and PSD, etc. As already stated by one of the most popular conic optimization solvers, Mosek.

4.1 Minimal Representations of Generalized Power Cones

Second–order cones (SOC) are fundamental structures in conic optimization, that have been proven to be useful in different applied disciplines such as engineering design (Blanco and Martínez-Antón, 2024b; Góez and Anjos, 2019; Mohammadisiahroudi et al., 2024); robust optimization (Zhen et al., 2022); financial modeling (Brar and Hare, 2020; Lu, 2006); or machine learning (Kucukyavuz et al., 2023; López and Maldonado, 2016; Maldonado and López, 2014), among many others (see, e.g., Lobo et al., 1998; Alizadeh and Goldfarb, 2003). Recently, an SOC representation of a specific cone of sparse nonnegative polynomials has been proposed by Averkov (2019) and Magron and Wang (2023). The SOC (also known as the Lorentz cone) in $\mathbb{R}^{n+1}$ is defined as $\mathcal{K}_2^{n,1} = \{(x,z) \in \mathbb{R}^{n+1} : \|x\|_2 \leq z\}$. The natural extension of these cones are the p–order cones, where the Euclidean norm is replaced by the ℓ_p or Hölder norm. These cones have been recommended in different applications where measuring with non-Euclidean-based distances is recommended. For instance, in Blanco et al. (2020b), support vector machines with ℓ_p–norm-based margins are analyzed. In their computational experiments, the authors conclude that some datasets obtain the benefit of these norms with respect to the classical (Euclidean) classifiers in terms of the obtained accuracies and the number of nonzero features used for the classification. In multiple criteria and combinatorial optimization, ℓ_p–based aggregation of the objectives has been beneficial in terms of fairness (Bektaş and Letchford, 2020; Blanco and Gázquez, 2023; Kostreva et al., 2004). The incorporation of p–order cones into any of these optimization problems is performed, for practical purposes, by *rewriting* these cones as a finite set of SOCs (Alizadeh and Goldfarb, 2003; Blanco and Martínez-Antón, 2024a), which are the cones that the available optimization solvers allow.

In this section, we analyze a general type of power cone, the $(p, \boldsymbol{\alpha})$ *or generalized power cone* (GPC), which, given $1 \leq p \leq \infty$, $\boldsymbol{\alpha} \in \Delta_d$, is defined as

$$\mathcal{K}_p^{n,d}(\boldsymbol{\alpha}) := \{(\boldsymbol{x}, \boldsymbol{z}) \in \mathbb{R}^n \times \mathbb{R}_+^d : \|\boldsymbol{x}\|_p \leq \boldsymbol{z}^{\boldsymbol{\alpha}}\},$$

where $\|\cdot\|_p$ denotes the ℓ_p–norm in $\mathbb{R}^n$, Δ_d is the standard simplex, and for any $\boldsymbol{z} \in \mathbb{R}_+^d$ and $\boldsymbol{\alpha} \in \Delta_d$, $\boldsymbol{z}^{\boldsymbol{\alpha}}$ is the weighted geometric mean of $\boldsymbol{z}$ with weights $\boldsymbol{\alpha}$ (see Definition 2.20). This cone has, in particular cases, the p–order cone and the power cone, and its efficient representation would allow us to solve optimization problems that naturally appear in different fields.

An extended representation of a cone (or any set, in general) involves reformulating the set equivalently by lifting it onto a higher-dimensional space and identifying it with a product of simpler sets. Different representations may be valid for the same set, and thus, a natural measure of the quality of a representation is its complexity, which includes the dimension of the embedding space and the number of factor sets in the representation. In this section, we derive different extended representations of the $(p, \boldsymbol{\alpha})$–power cone by means of simpler power cones and study its complexity. In case p and $\boldsymbol{\alpha}$ are rational, we provide extended representations of the cone as three-dimensional rotated quadratic cones. The main advantage of these simpler cones is that they are efficiently handled by most off-the-shelf optimization solvers such as Gurobi, CPLEX, or FICO. We deal with the problem of constructing optimal representations by solving a mathematical optimization problem.

Literature Review

Different authors have already addressed the analysis of representations for particular cases of these cones. The general case of p–order cones, $\mathcal{K}_p^{n,1}$, has been studied in Krokhmal and Soberanis (2010); Vinel and Krokhmal (2014) where the authors use the so-called *tower of variables* technique to represent these cones through three-dimensional p–order cones, $\mathcal{K}_p^{2,1}$. In these papers, the authors provide different polyhedral approximations for solving p–order cone programs (pOCP) and their mixed-integer extensions (MIpOCP). In case p and $\boldsymbol{\alpha}$ have rational entries, the cones can be adequately represented through three-dimensional rotated quadratic cone, $\mathcal{K}^{1,2}\left(\frac{1}{2}\right)$. Second–order cone representation with $\boldsymbol{\alpha} = (\frac{s}{r}, \frac{r-s}{r})$ has been already analyzed in Krokhmal and Soberanis (2010); Blanco et al. (2014) using either tower of variables or tree-based representations derived from the binary decomposition of r and s, with a cardinality of representation of $O(\log_2(r))$. In Morenko et al. (2013), an algorithm is proposed to represent cones where $\boldsymbol{\alpha} = \left(\frac{r_1}{2^k}, \frac{r_2}{2^k}, \frac{r_3}{2^k}\right)$ with cardinality of k. This construction generalizes and improves the previous representations, where $\boldsymbol{\alpha} = (\frac{s}{r}, \frac{r-s}{r})$, since this case is equivalent to choose $\boldsymbol{\alpha} = (\frac{s}{2^k}, \frac{r-s}{2^k}, \frac{2^k-r}{2^k})$ in this construction. The general multidimensional version of this cone, i.e., $\boldsymbol{\alpha} = \left(\frac{r_1}{2^k}, \dots, \frac{r_d}{2^k}\right)$ was analyzed in Kian et al. (2019) with a similar strategy, obtaining a representation with cardinality $O(k)$. As far as we know, the general rational case, $\boldsymbol{\alpha} = (\frac{s_1}{\hat{s}}, \dots, \frac{s_d}{\hat{s}})$, has been only previously analyzed in Wang (2024) where the author proposes a brute-force enumeration approach as well as some heuristic algorithms for the computation of a minimal representation of the cone by second–order cones. The authors of this dissertation note that the tower of variables method Ben-Tal and Nemirovski (2001b) can be generalized to the general rational case to derive a naive representation with cardinality $O(\hat{s})$. In contrast to that approach, we compute the minimal representation of the general rational case by means of solving a novel mixed integer linear optimization problem (MILP). The previous approaches analyzing rational cones and the obtained cardinalities are summarized in Table 4.1.

It should be made clear that, in Table 4.1, the term *cardinality* is identified with the number of rotated quadratic cones $\mathcal{K}^{1,2}\left(\frac{1}{2}\right)$ involved in the representations.

Apart from the particular simplifications, this type of generalized power

Ref.	Cone	Methodology	Cardinality
Krokhmal and Soberanis (2010)	$\mathcal{K}^{1,2}\left(\frac{s}{r}, \frac{r-s}{r}\right)$	Tower of variables	$O(\log_2(r))$
Blanco et al. (2014)	$\mathcal{K}^{1,2}\left(\frac{s}{r}, \frac{r-s}{r}\right)$	Binary decomposition	$O(\log_2(r))$
Morenko et al. (2013)	$\mathcal{K}^{1,3}\left(\frac{r_1}{2^k}, \frac{r_2}{2^k}, \frac{r_3}{2^k}\right)$	A successive algorithm	$O(k)$
Kian et al. (2019)	$\mathcal{K}^{1,d}\left(\frac{r_1}{2^k}, \dots, \frac{r_d}{2^k}\right)$	IP model and heuristic	$O(k)$
Ben-Tal and Nemirovski (2001b)	$\mathcal{K}^{1,d}\left(\frac{s_1}{\hat{s}}, \dots, \frac{s_d}{\hat{s}}\right)$	Tower of variables	$O(\hat{s})$
Wang (2024)	$\mathcal{K}^{1,d}\left(\frac{s_1}{\hat{s}}, \dots, \frac{s_d}{\hat{s}}\right)$	A brute force and heuristics algorithms	$O(\max\{\log_2(\hat{s}), d-1\})$
Blanco and Martínez-Antón (2024a)	$\mathcal{K}^{1,d}\left(\frac{s_1}{\hat{s}}, \dots, \frac{s_d}{\hat{s}}\right)$	Math-optimization based approach	$O(\max\{\log_2(\hat{s}), d-1\})$

TABLE 4.1: Summary of state-of-the-art for SOC representations of rational cones.

cone appears, for instance, when modeling attraction between different bodies. According to the law of universal gravitation by Newton (1687), the attraction of two objects can be obtained as

$$F = \frac{G m_1 m_2}{\|\boldsymbol{x}_1 - \boldsymbol{x}_2\|_2^2}$$

where G is the gravity constant, m_1 and m_2 are the masses of the two bodies, and $\boldsymbol{x}_1$ and $\boldsymbol{x}_2$ their positions in the space. Thus, given a minimum threshold for the attraction between the two objects, T, the inequality modeling all the masses and positions with such a minimum attraction can be written as $\frac{G m_1 m_2}{\|\boldsymbol{x}_1 - \boldsymbol{x}_2\|_2^2} \geq T$, or equivalently,

$$\|\boldsymbol{x}\|_2^2 \leq \frac{G}{T} m_1 m_2, \quad \boldsymbol{x} \in \mathbb{R}^3, \quad m_1, m_2 \in \mathbb{R}_+,$$

where $\boldsymbol{x} = \boldsymbol{x}_1 - \boldsymbol{x}_2$. Thus, the region defined by the inequality above is exactly one of the cones in our family of generalized power cones, specifically $\mathcal{K}_2^{3,2}\left(\frac{1}{2}\right)$. The cones that we analyze here generalize the inequalities described above. First, by representing objects in higher-dimensional spaces ($\mathbb{R}^n$) instead of $\mathbb{R}^3$. Second, by using different distance measures to the Euclidean norm in $\mathbb{R}^n$. And third, by extending the product of two masses to the weighted geometric mean of d different factors that affect the attraction between the bodies. In Chapter VI, Section 6.2 we provide more details on this generalization and its incorporation to a facility location problem.

In this section, we analyze this general cone, and apart from providing constructive approaches to simply represent the cones, we derive a novel approach to construct minimal representations of the cone as simpler second–order cones. The main structures that we use for this construction are the mediated graphs (see Chapter III).

The rest of this section is organized as follows. Section 4.1.1 is devoted to set the notation and the definition of the main concepts; and seeing possible extensions of the general $(p, \boldsymbol{\alpha})$–power cone by means of simpler $\boldsymbol{\beta}$–power cones and analyzing the complexity between them. In Section 4.1.2, we will show the optimal extended representation of rational $\boldsymbol{\alpha}$–power cone using second–order cones, for this purpose we will introduce the idea of $\boldsymbol{\alpha}$–mediated graph as a special kind of mediated graph, its relationship with these extended representations and address the problem of finding minimal $\boldsymbol{\alpha}$–mediated graphs (M$\boldsymbol{\alpha}$MGP) via combinatorial programming. In Chapter VII, Section 7.1.3, we show the computational performance of our mathematical programming model of M$\boldsymbol{\alpha}$MGP.

4.1.1 Extended Representations of Generalized Power Cones

In this section, we provide valid extended representations of the $(p, \boldsymbol{\alpha})$–power cone by means of simpler power cones. We analyze the features of the different representations. First of all, we need to know what an extended representation is. The formal definition of this representation is stated as follows.

Definition 4.1 (Extended representation). *Given a set $Q \subseteq \mathbb{R}^n$, we say that a finite family $\mathcal{E} = \{Q_\ell\}_{\ell=1}^{\mathcal{L}_\mathcal{E}}$ with $Q_\ell \subseteq \mathbb{R}^{n_\ell}$, for $\ell = 1, \dots, \mathcal{L}_\mathcal{E}$ is an* extended representation *of Q if there exist $m_\mathcal{E} \in \mathbb{Z}_+$ and projections $\pi_\ell : \mathbb{R}^n \times \mathbb{R}^{m_\mathcal{E}} \to \mathbb{R}^{n_\ell}$, for $\ell = 1, \dots, \mathcal{L}_\mathcal{E}$, such that:*

$$\boldsymbol{x} \in Q \text{ if and only if } \exists \boldsymbol{w} \in \mathbb{R}^{m_\mathcal{E}} \text{such that } \pi_\ell(\boldsymbol{x}, \boldsymbol{w}) \in Q_\ell \ \forall \ell = 1, \dots, \mathcal{L}_\mathcal{E}.$$

We denote by $\mathrm{Ext}(Q)$ *the class of families that are extended representations of Q.*

For any extended representation $\mathcal{E}$ of the set Q, the integer $m_\mathcal{E}$ in the above definition will be denoted as the *extended dimension* of $\mathcal{E}$ to represent Q and the integer $\mathcal{L}_\mathcal{E}$ will be called the *cardinality of representation*.

Note that this definition differs slightly from the notion of *extended formulation* of a polytope that has been widely studied in combinatorial optimization (see, e.g., Kaibel and Walter, 2015). The key idea of our notion of

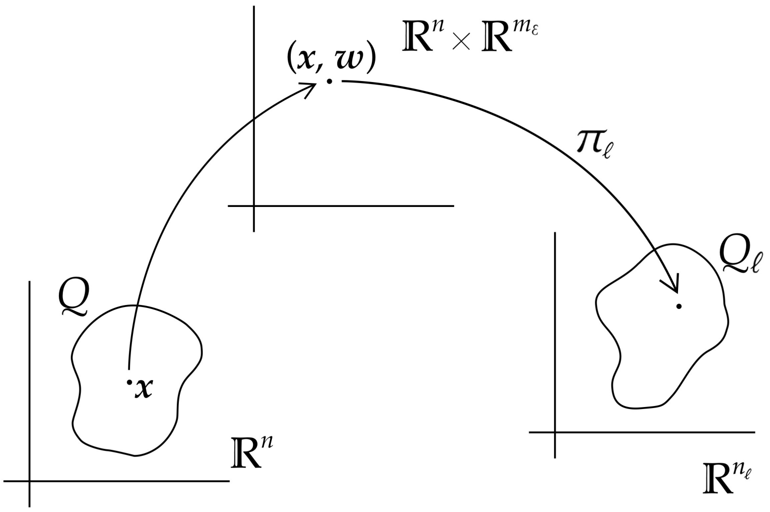

FIGURE 4.1: Illustrative diagram about extended representation concept.

extended representation is to lift the original set Q onto a higher-dimensional space, keeping the components of the original set Q, but allowing a simpler and more suitable representation at the price of adding some new variables and constraints. A clear illustration of this type of extension is the one commonly used to reformulate disjunctive linear programming problems. Let $Q := \text{Conv}(\bigcup_{i=1}^{k} P_i)$ the convex hull of the union of k polytopes $P_1, \ldots, P_k \subset \mathbb{R}^n$, each of them defined by means of linear inequalities, $P_i = \{\boldsymbol{x} \in \mathbb{R}^n : A_i\boldsymbol{x} \leq \boldsymbol{b}_i\}$ with $A_i \in \mathbb{R}^{m_i \times n}$, $\boldsymbol{b}_i \in \mathbb{R}^{m_i}$ for $i = 1, \ldots, k$. While Q is difficult to be represented as a set of inequalities in $\mathbb{R}^n$, it can be represented by the set

$$
\begin{aligned}
Q' = \{(\boldsymbol{x}, \boldsymbol{x}_1, \ldots, \boldsymbol{x}_k, \lambda_1, \ldots, \lambda_k) \in \mathbb{R}^n \times \mathbb{R}^{nk} \times \mathbb{R}^k \mid \\
& \boldsymbol{x} - \sum_{i=1}^{k} \boldsymbol{x}_i = \boldsymbol{0}, \\
& A_i\boldsymbol{x}_i - \boldsymbol{b}_i\lambda_i \leq \boldsymbol{0}, \quad \forall i = 1, \ldots, k, \\
& \sum_{i=1}^{k} \lambda_i = 1, \\
& \lambda_i \geq 0, \forall i = 1, \ldots, k\}
\end{aligned}
$$

(see, e.g., Balas, 1998). Hence, taking the projections

$$(\boldsymbol{x}, \boldsymbol{x}_1, \ldots, \boldsymbol{x}_k, \lambda_1, \ldots, \lambda_k) \longmapsto (\boldsymbol{x}, \boldsymbol{x}_1, \ldots, \boldsymbol{x}_k),$$
$$(\boldsymbol{x}, \boldsymbol{x}_1, \ldots, \boldsymbol{x}_k, \lambda_1, \ldots, \lambda_k) \longmapsto (\boldsymbol{x}_i, \lambda_i) \text{ for } i = 1, \ldots, k \text{ and}$$
$$(\boldsymbol{x}, \boldsymbol{x}_1, \ldots, \boldsymbol{x}_k, \lambda_1, \ldots, \lambda_k) \longmapsto (\lambda_1, \ldots, \lambda_k).$$

Then $\mathcal{E} := \{H_0, H_1, \ldots, H_k, \Delta_k\}$ is an extended representation of Q where $\mathcal{L}_{\mathcal{E}} = k+2$, $m_{\mathcal{E}} = nk + k$, H_0 is the affine subspace of $\mathbb{R}^{n+nk}$ defined by $\boldsymbol{x} = \sum_{i=1}^{k} \boldsymbol{x}_i$, H_i is the polyhedron of $\mathbb{R}^{n+1}$ defined by $([A_i; -\boldsymbol{b}_i], \boldsymbol{0})$ for $i = 1, \ldots, k$; and Δ_k is the standard simplex.

An extended representation can be seen as a generalized intersection of the sets that are part of the extension, as stated in the following result, whose proof is straightforward from the definition.

Proposition 4.2. *Let $Q \subseteq \mathbb{R}^n$ and $\mathcal{E} = \{Q_\ell\}_{\ell=1}^{\mathcal{L}_{\mathcal{E}}}$ with $Q_\ell \subset \mathbb{R}^{n_\ell}$, for $\ell = 1, \ldots, \mathcal{L}_{\mathcal{E}}$. Then, $\mathcal{E} \in \mathrm{Ext}(Q)$ if and only if there exist $m_{\mathcal{E}} \in \mathbb{Z}_+$ and projections $\pi_\ell : \mathbb{R}^n \times \mathbb{R}^{m_{\mathcal{E}}} \to \mathbb{R}^{n_\ell}$, for $\ell = 1, \ldots, \mathcal{L}_{\mathcal{E}}$, such that*

$$Q = \mathrm{proj}_n \left(\boldsymbol{\pi}^{-1} \left(\prod_{\ell=1}^{\mathcal{L}_{\mathcal{E}}} Q_\ell \right) \right) = \mathrm{proj}_n \left(\bigcap_{\ell=1}^{\mathcal{L}_{\mathcal{E}}} \left(\pi_\ell^{-1}(Q_\ell) \right) \right) \cong \mathrm{proj}_n \left(\bigcap_{\ell=1}^{\mathcal{L}_{\mathcal{E}}} \left(Q_\ell \times \mathbb{R}^{m_{\mathcal{E}} - d_\ell} \right) \right),$$

where $\mathrm{proj}_n : \mathbb{R}^n \times \mathbb{R}^{m_{\mathcal{E}}} \to \mathbb{R}^n$ is the canonical projection over $\mathbb{R}^n$ and $\boldsymbol{\pi} = (\pi_1 \times \cdots \times \pi_{\mathcal{L}_{\mathcal{E}}})$.

The constructions derived in this section will be based on nesting sequential representations. The correctness of the global extended representation of this construction is based on the following result.

Proposition 4.3. *Let $\mathcal{E} = \{Q_1, \ldots, Q_{\mathcal{L}_{\mathcal{E}}}\} \in \mathrm{Ext}(Q)$ and $\mathcal{E}_\ell = \{Q_{\ell 1}, \ldots, Q_{\ell \mathcal{L}_{\mathcal{E}_\ell}}\} \in \mathrm{Ext}(Q_\ell)$, for all $\ell = 1, \ldots, \mathcal{L}_{\mathcal{E}}$. Then,*

$$\mathcal{E}' := \bigcup_{\ell=1}^{\mathcal{L}_{\mathcal{E}}} \mathcal{E}_\ell \in \mathrm{Ext}(Q).$$

Proof. Let us define $m_{\mathcal{E}'} := m_{\mathcal{E}} + \sum_{\ell=1}^{\mathcal{L}_{\mathcal{E}}} m_{\mathcal{E}_\ell}$. For each $\ell = 1, \ldots, \mathcal{L}_{\mathcal{K}}$ and $s = 1, \ldots, \mathcal{L}_{\mathcal{E}_\ell}$, and define $\pi'_{\ell s} : \mathbb{R}^n \times \mathbb{R}^{m_{\mathcal{E}'}} \to \mathbb{R}^{n_{\ell s}}$ as

$$\pi'_{\ell s} := \pi_{\ell s} \circ \left(\pi_\ell \times id_{m_{\mathcal{E}_\ell}} \right) \circ \left(id_{n+m_{\mathcal{K}}} \times \mathrm{proj}_{m_{\mathcal{E}_\ell}} \right)$$

where π_ℓ is the projection of the extended representation $\mathcal{E}$ for the set Q_ℓ, and $\pi_{\ell s}$ the projection of the extended representation $\mathcal{E}_\ell$ for the set $Q_{\ell s}$. There we denote by $\text{proj}_{m_{\mathcal{E}_\ell}}$ the projection from $\mathbb{R}^{\sum_{\ell=1}^{\mathcal{L}_\mathcal{E}} m_{\mathcal{E}_\ell}}$ onto the coordinates in $\mathbb{R}^{m_{\mathcal{E}_\ell}}$. The commutative diagram of the constructed projection is as follows:

$$\begin{tikzcd}
\mathbb{R}^n \times \mathbb{R}^{m_{\mathcal{E}'}} \arrow[r, "(id_{d+m_\mathcal{E}} \times \text{proj}_{m_{\mathcal{E}_\ell}})"] \arrow[d, "\pi'_{\ell s}"'] & \mathbb{R}^n \times \mathbb{R}^{m_\mathcal{E}} \times \mathbb{R}^{m_{\mathcal{E}_\ell}} \arrow[d, "(\pi_\ell \times id_{m_{\mathcal{E}_\ell}})"] \\
\mathbb{R}^{n_{\ell s}} & \mathbb{R}^{n_\ell} \times \mathbb{R}^{m_{\mathcal{E}_\ell}} \arrow[l, "\pi_{\ell s}"']
\end{tikzcd}$$

Thus, with the above definitions, it only remains to prove that

$$x \in Q \text{ if and only if } \exists w \in \mathbb{R}^{m_{\mathcal{E}'}} \text{such that } \pi'_{\ell s}(x, w) \in Q_{\ell s}$$

for every $\ell = 1, \ldots, \mathcal{L}_\mathcal{E}$ and $s = 1, \ldots, \mathcal{L}_{\mathcal{E}_\ell}$ is true.

Considering that $\mathcal{E} \in \text{Ext}(Q)$, it implies that

$$x \in Q \text{ if and only if there exists } w_0 \in \mathbb{R}^{m_\mathcal{E}} \text{ verifying } \pi_\ell(x, w_0) \in Q_\ell$$

for every $\ell = 1, \ldots, \mathcal{L}_\mathcal{E}$. Therefore, since $\mathcal{E}_\ell \in \text{Ext}(Q_\ell)$ for every $\ell = 1, \ldots, \mathcal{L}_\mathcal{E}$, there must then exist $w_\ell \in \mathbb{R}^{m_{\mathcal{E}_\ell}}$ with $\ell = 1, \ldots, \mathcal{L}_\mathcal{E}$ satisfying

$$\pi_{\ell s}(\pi_\ell(x, w_0), w_\ell) \in Q_{\ell s}$$

for all $s = 1, \ldots, \mathcal{L}_{\mathcal{K}_\ell}$.

In sum, taking $w := (w_0, w_1, \ldots, w_{\mathcal{L}_\mathcal{E}}) \in \mathbb{R}^{m_{\mathcal{E}'}}$, by definition of $\pi'_{\ell s}$, we get that $x \in Q$ if and only if $\pi'_{\ell s}(x, w) = \pi_{\ell s}(\pi_\ell(x, w_0), w_\ell) \in Q_{\ell s}$ for every $\ell = 1, \ldots, \mathcal{L}_\mathcal{E}$ and $s = 1, \ldots, \mathcal{L}_{\mathcal{E}_\ell}$. □

Next, we will study different extended representations of the generalized power cone. The first result is based on splitting the constraint defining the (p, α)–power cone in two simple constraints (with a single linking variable), being the obtained constraints of simpler cones, in this case, a p–order cone and an α–power cone. As a consequence, being able to represent the original power cone stems from adequately representing (separately) each of these two cones.

Lemma 4.4. *Given* $1 \leq p \leq \infty$, $\alpha \in \Delta_d$. *Then,* $\mathcal{E} := \{\mathcal{K}_p^{n,1}, \mathcal{K}^{1,d}(\alpha)\} \in \text{Ext}(\mathcal{K}_p^{n,d}(\alpha))$ *with* $m_\mathcal{E} = 1$ *and* $\mathcal{L}_\mathcal{E} = 2$.

Proof. The proof is straightforward. □

In what follows, we provide extended representations of p–order cones and $\boldsymbol{\alpha}$–power cones.

The first result is a generalized version of the so-called *tower of variables*, originally proposed by Ben-Tal and Nemirovski (2001b) for $n = 2^k$. The general case has been already proven in Krokhmal and Soberanis (2010), and an alternative notation/representation of this result can be found in Vinel and Krokhmal (2014). This allows one to derive a reformulation of a p–order cone in dimension $n+1$ as $n-1$ p–order cones in dimension 3 using $n-2$ new variables.

Hereinafter, given $n \in \mathbb{N}$ and a set X, n copies of X are denoted by $X, \overset{n)}{\ldots}, X$.

Lemma 4.5. *Given* $1 \leq p \leq \infty$. *Then,* $\mathcal{E} := \{\mathcal{K}_p^{2,1}, \overset{n-1)}{\ldots}, \mathcal{K}_p^{2,1}\} \in \operatorname{Ext}(\mathcal{K}_p^{n,1})$ *with* $m_{\mathcal{E}} = n-2$ *and* $\mathcal{L}_{\mathcal{E}} = n-1$.

Proof. The construction of the three-dimensional cones to represent the p–order cone can be done using a tree-shaped structure. Recall that the cone $\mathcal{K}_p^{n,1}$ is defined by an inequality $\|(x_1, \ldots, x_n)\|_p \leq w$, or equivalently,

$$\sum_{j=1}^{n} x_j^p \leq w^p.$$

Let T be binary a tree with vertices indexed by the subsets of $\{1, \ldots, n\}$, $2^{\{1,\ldots,n\}}$, and being the root vertex $R_0 = \{1, \ldots, n\}$ and its leaves $\{1\}, \ldots, \{n\}$. At each level of the tree, the parent index set is partitioned into two disjoint sets until the singleton vertices are reached.

For each nonleave vertex, $v \in 2^{\{1,\ldots,n\}}$, in the tree we denote by $c_1(v)$ and $c_2(v)$ its unique children vertices. Then, the following constraints equivalently represent the constraint defining the cone:

$$w_v \geq \|(w_{c_1(v)}, w_{c_2(v)})\|_p, \quad \forall v \in T \text{ (nonleave vertices)}$$

where vertex $w_{\{i\}}$ is identified with the original variable x_i, and the root vertex variable $w_{\{1,\ldots,n\}}$ is identified with the variable w. Thus, there are as many constraints as nonleave vertices in the tree $(n-1)$ and as many variables as nonroot and nonleave vertices in the tree $(n-2)$. □

The proof of the above result is constructive and allows an easy representation of the p–order cone by means of a binary tree. In Figure 4.2 we show a tree for $n = 7$, which results in the following representation of the p–order cone $\mathcal{K}_p^{7,1}$:

$$\begin{aligned}
w &\geq \|(w_{\{1,2,3\}}, w_{\{4,5,6,7\}})\|_p,\\
w_{\{1,2,3\}} &\geq \|(w_{\{1,2\}}, x_3)\|_p,\\
w_{\{1,2\}} &\geq \|(x_1, x_2)\|_p,\\
w_{\{4,5,6,7\}} &\geq \|(w_{\{4,5,6\}}, x_7)\|_p,\\
w_{\{4,5,6\}} &\geq \|(w_{\{4,5\}}, x_6)\|_p,\\
w_{\{4,5\}} &\geq \|(x_4, x_5)\|_p
\end{aligned}$$

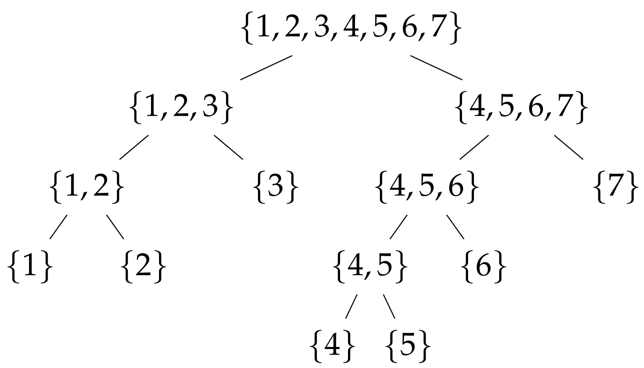

FIGURE 4.2: Tree for the tower of variables construction of Lemma 4.5 for $n = 7$.

In the next result, we show that each of the three-dimensional cones that are part of the extended representation of the p–order cone can be represented as a family of $\frac{1}{p}$–power cones and a half-space.

We denote by $\mathcal{H}^{n+1} := \left\{(\boldsymbol{x}, w) \in \mathbb{R}^n \times \mathbb{R} : \displaystyle\sum_{i=1}^{n} x_i \leq w\right\}$.

Lemma 4.6. *Given* $1 \leq p \leq \infty$. *Then,* $\mathcal{E} := \left\{\mathcal{K}^{1,2}\left(\frac{1}{p}\right), \overset{n)}{\ldots}, \mathcal{K}^{1,2}\left(\frac{1}{p}\right), \mathcal{H}^{n+1}\right\} \in \mathrm{Ext}(\mathcal{K}_p^{n,1})$ *with* $m_{\mathcal{E}} = n$ *and* $\mathcal{L}_{\mathcal{E}} = n + 1$.

Proof. The proof is based on that, for $w > 0$, the inequality defining the cone $\mathcal{K}_p^{n,1}$, $\|\boldsymbol{x}\|_p \leq w$ is equivalent to:

$$\sum_{j=1}^{n} \frac{x_j^p}{w^{p-1}} \leq w$$

Let q be the conjugate of p, i.e., $\frac{1}{p}+\frac{1}{q}=1$. Since $p-1=\frac{p}{q}$, we get that be above equation is equivalent to:

$$\sum_{j=1}^{n}\frac{x_j^p}{w^{\frac{p}{q}}}\leq w,$$

which can be split into the following inequalities by adding auxiliary variables $t_1,\ldots,t_n\geq 0$:

$$\sum_{j=1}^{n} t_j \leq w, \tag{4.1}$$

$$x_j^p \leq t_j w^{\frac{p}{q}}, \quad \forall j=1,\ldots,n; \tag{4.2}$$

where (4.1) define the half-space $\mathcal{H}^{n+1}$. Constraints (4.2) can be rewritten as:

$$x_j \leq t_j^{\frac{1}{p}} w^{\frac{1}{q}}.$$

Thus, $(x_j,(t_j,w)) \in \mathcal{K}^{1,2}\left(\frac{1}{p}\right)$, for $j=1,\ldots,n$.

In case $w=0$, the proof is straightforward. □

Finally, by Proposition 4.3, and the previous lemmas 4.4, 4.5, and 4.6 we get that one can construct an extended representation of the $(n+d)$-dimensional $(p,\boldsymbol{\alpha})$–power cone by means of power cones and half-spaces.

Corollary 4.7. *Given* $1\leq p\leq\infty$, $\boldsymbol{\alpha}\in\Delta_d$. *Then,*

$$\mathcal{E}:=\left\{\mathcal{K}^{1,2}\left(\frac{1}{p}\right),\overset{2(n-1)}{\ldots},\mathcal{K}^{1,2}\left(\frac{1}{p}\right),\mathcal{H}^{2+1},\overset{n-1)}{\ldots},\mathcal{H}^{2+1},\mathcal{K}^{1,d}(\boldsymbol{\alpha})\right\}\in \mathrm{Ext}(\mathcal{K}_p^{n,d}(\boldsymbol{\alpha}))$$

with $m_{\mathcal{E}}=3n-3$ *and* $\mathcal{L}_{\mathcal{E}}=3n-2$.

Here, the original cone $\mathcal{K}_p^{n,d}(\boldsymbol{\alpha})$ is first represented by a p–order cone and a $\boldsymbol{\alpha}$–power cone. Then, the p–order cone is represented by $n-1$ three-dimensional p–order cones. Finally, each of these cones is represented as simpler three-dimensional $\frac{1}{p}$–power cones.

The above representation of the $(p,\boldsymbol{\alpha})$–power cone requires embedding the cone in a higher-dimensional space with $3n-3$ extra dimensions and using $3n-2$ sets in the representation (power cones and half-spaces). In the following results, we provide alternative representations reducing the cardinality of the representations.

Theorem 4.8. *Given* $1 \leq p \leq \infty$, $\boldsymbol{\alpha} \in \Delta_d$. *Then,*

$$\mathcal{E} := \left\{ \mathcal{K}^{1,d}(\boldsymbol{\alpha}), \mathcal{H}^{n+1}, \mathcal{K}^{1,d+1}\left(\frac{1}{p}, \frac{1}{q}\boldsymbol{\alpha}\right), \overset{n)}{\ldots}, \mathcal{K}^{1,d+1}\left(\frac{1}{p}, \frac{1}{q}\boldsymbol{\alpha}\right) \right\} \in \mathrm{Ext}(\mathcal{K}_p^{n,d}(\boldsymbol{\alpha}))$$

with $m_{\mathcal{E}} = n+1$ *and* $\mathcal{L}_{\mathcal{E}} = n+2$.

Proof. For the first extension, it is enough to apply Lemma 4.6 replacing w by $\boldsymbol{z}^{\boldsymbol{\alpha}}$ in the proof. Hence, we have that

$$\left\{ \mathcal{K}_1^{n,d}(\boldsymbol{\alpha}), \mathcal{K}^{1,d+1}\left(\frac{1}{p}, \frac{1}{q}\boldsymbol{\alpha}\right), \overset{n)}{\ldots}, \mathcal{K}^{1,d+1}\left(\frac{1}{p}, \frac{1}{q}\boldsymbol{\alpha}\right) \right\} \in \mathrm{Ext}(\mathcal{K}_p^{n,d}(\boldsymbol{\alpha})).$$

To represent the cones $\mathcal{K}_1^{n,d}(\boldsymbol{\alpha})$ in the extension, i.e., elements $(\boldsymbol{t}, \boldsymbol{z}) \in \mathbb{R}^n \times \mathbb{R}^d$ such that $\|\boldsymbol{t}\|_1 \leq \boldsymbol{z}^{\boldsymbol{\alpha}}$, we split the constraint as:

$$\|\boldsymbol{t}\|_1 \leq w, \tag{4.3}$$

$$w \leq \boldsymbol{z}^{\boldsymbol{\alpha}}. \tag{4.4}$$

where (4.3) define the half-space $\mathcal{H}^{n+1}$ and (4.4) the cone $\mathcal{K}^{1,d}(\boldsymbol{\alpha})$. Thus, $\{\mathcal{K}^{1,d}(\boldsymbol{\alpha}), \mathcal{H}^{n+1}\} \in \mathrm{Ext}(\mathcal{K}_1^{n,d}(\boldsymbol{\alpha}))$ with extended dimension 1 (a single extra variable to link the constraints).

Applying Proposition 4.3, we get the desired result. □

The above result provides an alternative extension requiring embedding the cone into a $n+1$ extra-dimensional space by means of $n+2$ sets (cones and half-spaces).

Finally, we provide the simplest extended representation of the cone.

Theorem 4.9. *Given* $1 \leq p \leq \infty$, $\boldsymbol{\alpha} \in \Delta_d$. *Then,*

$$\mathcal{E} := \left\{ \mathcal{K}^{1,2}\left(\frac{1}{p}\right), \overset{n)}{\ldots}, \mathcal{K}^{1,2}\left(\frac{1}{p}\right), \mathcal{H}^{n+1}, \mathcal{K}^{1,d}(\boldsymbol{\alpha}) \right\} \in \mathrm{Ext}(\mathcal{K}_p^{n,d}(\boldsymbol{\alpha}))$$

with $m_{\mathcal{E}} = n+1$ *and* $\mathcal{L}_{\mathcal{E}} = n+2$.

Proof. The proof is straightforward from Proposition 4.3, and lemmas 4.4 and 4.6. □

In Figure 4.3 we illustrate the extended representation of the cone derived from the above result. A summary of the results derived above is shown in

$$\mathcal{K}_p^{n,d}(\boldsymbol{\alpha}) \left[\begin{array}{l} m_{\mathcal{E}} = 1 \\ \mathcal{L}_{\mathcal{E}} = 2 \end{array}\right] \begin{cases} \mathcal{K}_p^{n,1} \left[\begin{array}{l} m_{\mathcal{E}_1} = n \\ \mathcal{L}_{\mathcal{E}_1} = n+1 \end{array}\right] \begin{cases} \mathcal{K}^{1,2}\left(\frac{1}{p}\right) \\ \cdot \\ \cdot \; n) \\ \cdot \\ \mathcal{K}^{1,2}\left(\frac{1}{p}\right) \\ \mathcal{H}^{n+1} \end{cases} \\ \\ \mathcal{K}^{1,d}(\boldsymbol{\alpha}) \end{cases}$$

FIGURE 4.3: Extended representation of Theorem 4.9.

Table 4.2. Note that unless $n = 1$, the representation in Theorem 4.9 is strictly stronger than the one in Corollary 4.7.

Result	$m_{\mathcal{E}}$	$\mathcal{L}_{\mathcal{E}}$	$\mathcal{K}^{1,d}(\boldsymbol{\alpha})$	$\mathcal{K}^{1,d+1}\left(\frac{1}{p}, \frac{1}{q}\boldsymbol{\alpha}\right)$	$\mathcal{K}^{1,2}(\frac{1}{p})$	$\mathcal{H}^{n+1}$	$\mathcal{H}^{2+1}$
Corollary 4.7	$3n-3$	$3n-2$	1	–	$2(n-1)$	–	$n-1$
Theorem 4.8	$n+1$	$n+2$	1	n	–	1	–
Theorem 4.9	$n+1$	$n+2$	1	–	n	1	–

TABLE 4.2: Summary of main results from Section 4.1.1.

Remark 4.10. *Note that one can analogously represent more general cones in the form:*

$$\mathcal{K}_p(\boldsymbol{\alpha})[f,g,h] := \left\{(\boldsymbol{x},\boldsymbol{z},\boldsymbol{t}) \in \mathbb{R}^{n_1} \times \mathbb{R}^{n_2} \times \mathbb{R}^{n_3} : \|f(\boldsymbol{x})\|_p \leq h(\boldsymbol{z})^{\boldsymbol{\alpha}} + g(\boldsymbol{t})\right\}$$

where $f : \mathbb{R}^{n_1} \to \mathbb{R}^n$, $g : \mathbb{R}^{n_3} \to \mathbb{R}$, *and* $h : \mathbb{R}^{n_2} \to \mathbb{R}^d_+$ *are linear functions, by adding to the representations above* $n + d + 1$ *extra variables and linear equations (hyperplanes).*

4.1.2 Optimal SOC Representations

The extended representations derived in the previous section allow one to reduce the representation of the complex cone $\mathcal{K}_p^{n,d}(\boldsymbol{\alpha})$ by means of simpler power cones $\mathcal{K}^{1,d'}(\boldsymbol{\beta})$ for $\boldsymbol{\beta} \in \Delta_{d'}$. For the sake of simplification, in the rest of the section, we denote $d' = d$, and $\boldsymbol{\beta} = \boldsymbol{\alpha}$. The main implications of these representations come from the fact that one can restrict the variables of an optimization problem to belong to a $(p, \boldsymbol{\alpha})$–power cone, but formulate the constraints as constraints in the form $x \leq \boldsymbol{z}^{\boldsymbol{\alpha}}$ for some $\boldsymbol{\alpha} \in \Delta_d$. In case the components of $\boldsymbol{\alpha}$ are rational, i.e., $\boldsymbol{\alpha} \in \mathbb{Q}^d$, or equivalently, $\boldsymbol{\alpha} = (\frac{s_1}{\hat{s}}, \ldots, \frac{s_d}{\hat{s}}) \in \Delta_d$ with $s_1, \ldots, s_d \in \mathbb{Z}_+$, $\gcd(s_1, \ldots, s_d) = 1$, and $\hat{s} = \sum_{j=1}^d s_j$; one can go further and derive representations by means of second–order cones. In this section, we present a mathematical optimization-based approach to construct a minimal SOC extended representation of rational power cones (in terms of the cardinality of representation and extended dimension). The mathematical optimization model that we propose to construct a minimal SOC extended representation of the cone is based on mediated graphs. In this case, we are interested in a kind of mediated graphs entire determined by $\boldsymbol{\alpha}$.

Definition 4.11 ($\boldsymbol{\alpha}$–mediated graph)**.** *Let $\boldsymbol{\alpha} = \frac{1}{\hat{s}}(s_1, \ldots, s_d) \in \Delta_d$ be a vector, $\mathcal{A}_{\boldsymbol{\alpha}} := \{\hat{s}\boldsymbol{e}_j : j = 1, \ldots, d-1\} \cup \{\boldsymbol{0}\} \subset \mathbb{R}^{d-1}$, and $\boldsymbol{b}_{\boldsymbol{\alpha}} := (s_1, \ldots, s_{d-1}) \in \mathbb{R}^{d-1}$. An $\boldsymbol{\alpha}$–*mediated graph *is an $\mathcal{A}_{\boldsymbol{\alpha}}$–mediated graph $G = (V, A) \in \mathcal{M}_{\mathcal{A}_{\boldsymbol{\alpha}}}(\boldsymbol{b}_{\boldsymbol{\alpha}})$.*

We denote by $\mathcal{M}_{\boldsymbol{\alpha}} := \mathcal{M}_{\mathcal{A}_{\boldsymbol{\alpha}}}(\boldsymbol{b}_{\boldsymbol{\alpha}})$ the set of all $\boldsymbol{\alpha}$–mediated graphs.

In Figure 4.4 we show a toy example of $\boldsymbol{\alpha}$–mediated graph for $\boldsymbol{\alpha} = (\frac{1}{6}, \frac{2}{6}, \frac{3}{6})$. In this case, $\mathcal{A}_{\boldsymbol{\alpha}} = \{(6,0), (0,6), (0,0)\}$ (red dots) and $\boldsymbol{b}_{\boldsymbol{\alpha}} = (1,2)$ (green dot). The set of mediated vertices in the plot is $V \backslash \mathcal{A}_{\boldsymbol{\alpha}} = \{(1,2), (2,4), (4,2)\}$ (blue dots). Note that $\boldsymbol{b}_{\boldsymbol{\alpha}} = (1,2) \in V$ and for each of the elements $\boldsymbol{v}$ in $V \backslash \mathcal{A}_{\boldsymbol{\alpha}}$ there exist two different points in V (the arrows in the plot from each of the elements in $V \backslash \mathcal{A}_{\boldsymbol{\alpha}}$) such that $\boldsymbol{v}$ is the average of those vectors. For instance $(1,2) = \frac{1}{2}((0,0) + (2,4))$; $(2,4) = \frac{1}{2}((0,6) + (0,0))$; and $(3,2) = \frac{1}{2}((0,4) + (6,0))$.

$$\boldsymbol{\alpha} = (1,2,3)/6$$

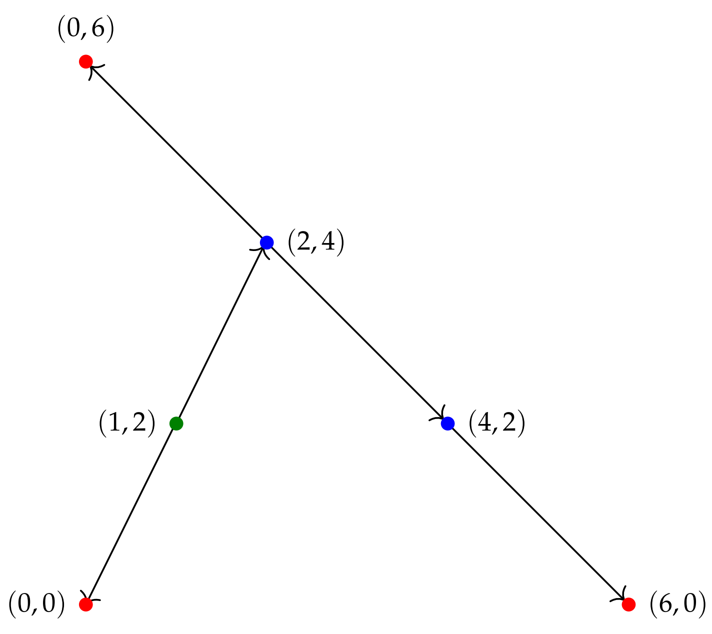

FIGURE 4.4: An $(\frac{1}{6}, \frac{2}{6}, \frac{3}{6})$–mediated graph.

Given an $\boldsymbol{\alpha}$–mediated graph, $G = (V, A)$, we know all the vertices belong to the convex hull, $\mathrm{Conv}(\mathcal{A}_{\boldsymbol{\alpha}})$, of $\mathcal{A}_{\boldsymbol{\alpha}}$. Furthermore, by definition, if $(\boldsymbol{v}, \boldsymbol{u}), (\boldsymbol{v}, \boldsymbol{w})$ are arcs in G, then $\boldsymbol{\mu}^{\boldsymbol{v}} = \frac{1}{2}(\boldsymbol{\mu}^{\boldsymbol{u}} + \boldsymbol{\mu}^{\boldsymbol{w}})$, where $\boldsymbol{\mu}^{\boldsymbol{v}} \in \Delta_d$ are the barycentric coordinates of $\boldsymbol{v}$ with respect to $\mathcal{A}_{\boldsymbol{\alpha}}$.

The following result states the correspondence between the SOC extended representations and the mediated graphs.

Theorem 4.12. *There exists a* one-to-one *correspondence between $\mathcal{M}_{\boldsymbol{\alpha}}$ and the set of extended representations by second–order cones of $\mathcal{K}^{1,d}(\boldsymbol{\alpha})$.*

Proof. Let us first prove any $\boldsymbol{\alpha}$–mediated graph $G = (V, A)$ induces an extended representation of $\mathcal{K}^{1,d}(\boldsymbol{\alpha}) = \{x \le \boldsymbol{z}^{\boldsymbol{\alpha}}\}$ using (rotated) second–order cones $\mathcal{K}^{1,2}(\frac{1}{2})$. Let us consider the vector of variables $\boldsymbol{w} = (w_{\boldsymbol{v}})_{\boldsymbol{v} \in V} \in \mathbb{R}^V_+$ indexed in V where $w_{\boldsymbol{b}_{\boldsymbol{\alpha}}} := x$, $w_{\hat{s}\boldsymbol{e}_i} := z_i$ for $i = 1, \dots, d-1$, and $w_{\boldsymbol{0}} := z_d$. Now, we will see the following projections $\pi_j : \mathbb{R}^V \to \mathbb{R}^3$

$$\pi_{\boldsymbol{v}}(\boldsymbol{w}) := \Big(w_{\boldsymbol{v}}, \boldsymbol{w}_{\delta^+(\boldsymbol{v})}\Big) \in \mathbb{R}^3, \quad \forall \boldsymbol{v} \in V \backslash \mathcal{A}_{\boldsymbol{\alpha}}$$

where $\delta^+(\boldsymbol{v})$ is the set of outgoing arcs of $\boldsymbol{v}$ in G, define an SOC extended representation of the cone $\mathcal{K}^{1,d}(\boldsymbol{\alpha})$.

Let us consider $(x, \boldsymbol{z}) \in \mathcal{K}^{1,d}(\boldsymbol{\alpha})$, that is, $x \le \boldsymbol{z}^{\boldsymbol{\alpha}}$. As already mentioned, there always exists $w_{\boldsymbol{v}} \in \mathbb{R}_+$ verifying $w_{\boldsymbol{v}} \le \boldsymbol{z}^{\boldsymbol{\mu}^{\boldsymbol{v}}}$ for $\boldsymbol{v} \in V \backslash \mathcal{A}_{\boldsymbol{\alpha}} \backslash \{\boldsymbol{b}_{\boldsymbol{\alpha}}\}$, and

$$w_{\boldsymbol{v}} \le \prod_{\boldsymbol{u} \in \delta^+(\boldsymbol{v})} w_{\boldsymbol{u}}^{\frac{1}{2}}.$$

On the other hand, if $\pi_{\boldsymbol{v}}(\boldsymbol{w}) = \Big(w_{\boldsymbol{v}}, \boldsymbol{w}_{\delta^+(\boldsymbol{v})}\Big) \in \mathcal{K}^{1,2}\left(\frac{1}{2}\right), \forall \boldsymbol{v} \in V \backslash \mathcal{A}_{\boldsymbol{\alpha}}$. In particular, $\pi_{\boldsymbol{b}_{\boldsymbol{\alpha}}}(\boldsymbol{w}) = \Big(x, \boldsymbol{w}_{\delta^+(\boldsymbol{b}_{\boldsymbol{\alpha}})}\Big) \in \mathcal{K}^{1,2}\left(\frac{1}{2}\right)$ and then,

$$\prod_{\boldsymbol{u} \in \delta^+(\boldsymbol{b}_{\boldsymbol{\alpha}})} w_{\boldsymbol{u}}^{\frac{1}{2}} \le \prod_{\boldsymbol{u} \in \delta^+(\boldsymbol{b}_{\boldsymbol{\alpha}})} \boldsymbol{z}^{\frac{1}{2}\boldsymbol{\mu}^{\boldsymbol{u}}} = \boldsymbol{z}^{\frac{1}{2} \sum\limits_{\boldsymbol{u} \in \delta^+(\boldsymbol{b}_{\boldsymbol{\alpha}})} \boldsymbol{\mu}^{\boldsymbol{u}}} = \boldsymbol{z}^{\boldsymbol{\alpha}}.$$

Thus, $(x, \boldsymbol{z}) \in \mathcal{K}^{1,d}(\boldsymbol{\alpha})$.

Note that the above proof is fully reversible, so any second–order cone extended representation for $\mathcal{K}^{1,d}(\boldsymbol{\alpha})$ can be identified with an element in $\mathcal{M}_{\boldsymbol{\alpha}}$. $\square$

The above result does not just relate mediated graphs with SOC representations of $\mathcal{K}^{1,d}(\boldsymbol{\alpha})$, this makes the problem of finding a minimal $\boldsymbol{\alpha}$–mediated graph equivalent to the problem of finding a minimal SOC representation. Moreover, the cardinality of representation is the cardinality, $|V \backslash \mathcal{A}_{\boldsymbol{\alpha}}| = |V| - d$, of the set of mediated vertices $V \backslash \mathcal{A}_{\boldsymbol{\alpha}}$.

Remark 4.13 (Bounds for the cardinality of an $\boldsymbol{\alpha}$–mediated graph)**.** *Wang (2024) proves two lower bounds for the number of vertices in a minimal $\boldsymbol{\alpha}$–mediated graph, one based on the dimension of the vertices (d) and other in the sum of the elements $s_1, \ldots, s_d$, i.e., $\hat{s}$. Being this way, the maximum of both values, $\max\{d - 1, \lceil \log_2(\hat{s}) \rceil\}$, a suitable lower bound for the number of mediated vertices.*

On the other hand, as $\mathcal{A}_{\boldsymbol{\alpha}}$ is affinely independent and $\boldsymbol{b}_{\boldsymbol{\alpha}} \in \mathrm{Conv}(\mathcal{A}_{\boldsymbol{\alpha}})$ we are in conditions to use Lemma 3.7. Thus, we can overestimate the size of the representation for the cone by using the binary decomposition of the elements $s_1, \ldots, s_d$. Then, an upper bound for the minimum size of an $\boldsymbol{\alpha}$–mediated graph is $\sum_{i=1}^{d} |\Omega(s_i)| + |\Omega(2^{\lceil \log_2(\hat{s}) \rceil} - \hat{s})| + d - 1$. The representations which reach this upper bound are the most common when p–order cones are reformulated in several applications in the literature (see, e.g., Blanco and Gázquez, 2023; Blanco and Martínez-Antón, 2024b; Blanco et al., 2014).

Now we can apply directly Theorem 3.15 and (C-MinMGP) to solve both problems, finding a minimal $\boldsymbol{\alpha}$–mediated graph and finding a minimal SOC extended representation of $\mathcal{K}^{1,d}(\boldsymbol{\alpha})$. Nevertheless, (C-MinMGP) is too generic to deal with the now-called *minimal $\boldsymbol{\alpha}$–mediated graph problem* (M$\boldsymbol{\alpha}$MGP in short). Hence, we present a concrete mathematical optimization model to construct minimal $\boldsymbol{\alpha}$–mediated graphs, and then also to obtain minimal SOC representations of power cones.

Given $\boldsymbol{\alpha} \in \Delta_d$, the goal of the M$\boldsymbol{\alpha}$MGP is to construct a minimal $\boldsymbol{\alpha}$–mediated graph. The M$\boldsymbol{\alpha}$MGP has the flavor of a continuous location problem, where a set of services (the mediated vertices) is to be located in a given space, taking into account a given set of *users* (the elements in $\mathcal{A}_{\boldsymbol{\alpha}}$) located at certain coordinates in the space.

We would like first to highlight that the minimal $\boldsymbol{\alpha}$–mediated graph may not be unique; that is, it may exist different $\boldsymbol{\alpha}$–mediated graphs with minimum cardinality. A counterexample is shown in the following example.

Example 4.14. *Let us consider $\boldsymbol{\alpha} = \frac{1}{74}(13, 17, 44) \in \Delta_3$. In Figure 4.5 we plot three different minimal $\boldsymbol{\alpha}$–mediated graphs with the same cardinality (10). The three* *mediated graphs provide different extended representations of the cone with the same cardinality. Specifically:*

$$
\begin{array}{lll}
x^2 \leq w_1 z_3 & x^2 \leq w_1 z_3 & x^2 \leq w_1 z_3 \\
w_1^2 \leq w_2 w_3 & w_1^2 \leq w_2 w_3 & w_1^2 \leq w_2 w_3 \\
w_2^2 \leq w_4 w_5 & w_2^2 \leq x w_4 & w_2^2 \leq x w_4 \\
w_3^2 \leq w_5 z_2 & w_3^2 \leq w_5 z_2 & w_3^2 \leq z_1 z_2 \\
w_4^2 \leq w_3 w_6 & w_4^2 \leq w_5 z_1 & w_4^2 \leq w_1 w_5 \\
w_5^2 \leq x w_6 & w_5^2 \leq w_4 w_6 & w_5^2 \leq w_6 z_2 \\
w_6^2 \leq w_4 z_1 & w_6^2 \leq w_2 z_2 & w_6^2 \leq w_2 w_4
\end{array}
$$

Observe that the three minimal representations are different and nonequivalent, in the sense that there are no possible permutations in the indices of the w-variables that transform one representation in another.

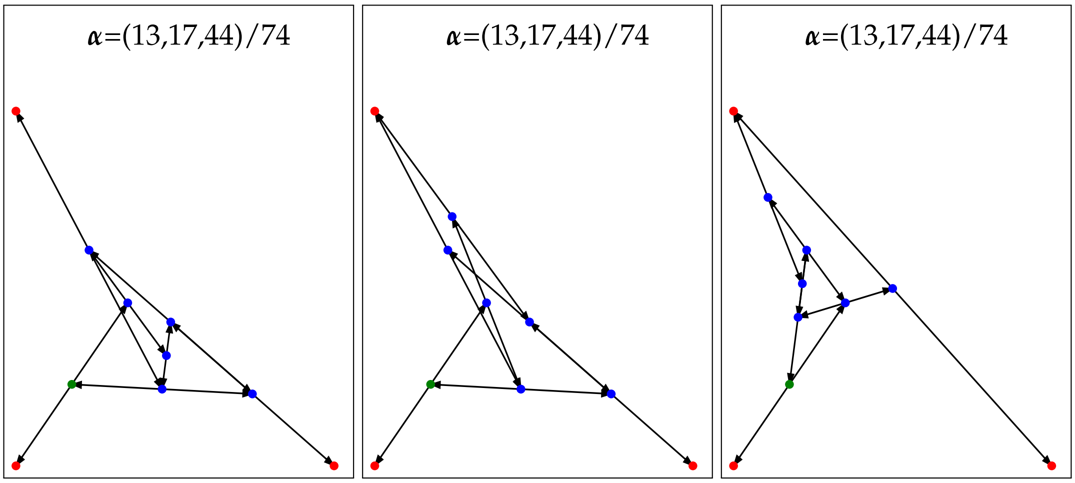

FIGURE 4.5: Counterexample on the uniqueness of minimal $\boldsymbol{\alpha}$-mediated graph, $\boldsymbol{\alpha} = \frac{1}{74}(13, 17, 44)$.

For the sake of describing the problem, we denote by $I_A = \{0, 1, \ldots, d\}$ the index sets for the elements in $\mathcal{A}_{\boldsymbol{\alpha}} \cup \{\boldsymbol{b}_{\boldsymbol{\alpha}}\}$, where 0 is assumed to be the index associated to $\boldsymbol{b}_{\boldsymbol{\alpha}}$. Observe that the size of the mediated graph is unknown and to be determined by our model. Thus, unlike what happens in other location problems, the problem not only consists of *filling* the coordinates of a given number of vectors adequately, but this number is to be decided. Then, we overestimate the size of the mediated graph by $d + \Lambda_{\boldsymbol{\alpha}}$ (where $\Lambda_{\boldsymbol{\alpha}}$ is the upper bound described in Remark 4.13 minus d), and denote by $I_M = \{d+1, \ldots, d + \Lambda_{\boldsymbol{\alpha}}\}$ the index set for the *enlarged* mediated graph. Once, all these $\Lambda_{\boldsymbol{\alpha}}$ coordinates are decided, and in order to account for a minimal size set of coordinates, we will group in a single element each of the equal-coordinates vectors, transforming the set of $\Lambda_{\boldsymbol{\alpha}}$ coordinates into one that formally represents the unknown vertices of the $\boldsymbol{\alpha}$–mediated graph. That is, if $\boldsymbol{v}_{d+1}, \ldots, \boldsymbol{v}_{d+\Lambda_{\boldsymbol{\alpha}}}$ are the coordinates of the enlarged mediated vertices, we compute the effective vertex set, V, by removing repeated elements from the multiset. Additionally, for the sake of simplification, we denote by $I = I_A \cup I_M = \{0, \ldots, d + \Lambda_{\boldsymbol{\alpha}}\}$, the whole sets of coordinates involved in the problem.

We use the following set of variables in our model:

- To assure the correct construction of the mediated graph $G = (V, A)$, we consider the following binary variables that account for the active arcs in the graph:
$$y_{ij} = \begin{cases} 1 & \text{if } (\boldsymbol{v}_i, \boldsymbol{v}_j) \in A, \\ 0 & \text{otherwise,} \end{cases}$$
for all $i \in I_M \cup \{0\}, j \in I, i \neq j$.

- In order to account for the number of effective mediated elements in the overestimated set, we use the standard variables in facility location to activate vertices:
$$z_j = \begin{cases} 1 & \text{if vertex } \boldsymbol{v}_j \text{ is an active vertex in the mediated graph,} \\ 0 & \text{otherwise} \end{cases}$$
for all $j \in I$.

  Note that the amount $\sum_{j \in I_M} z_j$ provides the number of different mediated vertices, and then, its cardinality.

  Since all the elements in $\mathcal{A}_{\boldsymbol{\alpha}} \cup \{\boldsymbol{b}_{\boldsymbol{\alpha}}\}$ must be vertices of the graph, we fix $z_0 = \cdots = z_d = 1$ in our model.

- We consider continuous variables in $[0, \hat{s}]$ to model the coordinates of the vertices in the mediated graph:
$$v_{jk} \in [0, \hat{s}] : k\text{th coordinate of the } j\text{th vertex in the mediated graph.}$$
for $j \in I$, $k = 1, \ldots, d-1$. The first d vertices have fixed coordinates to the elements in $\mathcal{A}_{\boldsymbol{\alpha}} \cup \{\boldsymbol{b}_{\boldsymbol{\alpha}}\}$ that must be part of the mediated graph. Thus, we fix their values to $\boldsymbol{v}_0 = \boldsymbol{b}_{\boldsymbol{\alpha}}$, $\boldsymbol{v}_j = \hat{s}\boldsymbol{e}_j$ (for $j = 1, \ldots, d-1$), and $\boldsymbol{v}_d = \mathbf{0}$.

With the above variables, the mixed integer linear program (MILP) that we propose to find a minimal $\boldsymbol{\alpha}$–mediated graph, and furthermore, a minimal extended representation of the cone, is the following:

$$
\begin{aligned}
& & & \text{(M}\boldsymbol{\alpha}\text{MGP)} \\
\text{minimize} \quad & \sum_{j \in I_M \cup \{0\}} z_j & & (4.5) \\
\text{subject to} \quad & \sum_{j \in I} y_{ij} = 2z_i, \forall i \in I_M \cup \{0\}, & & (4.6) \\
& y_{ij} \leq z_j, \forall i \in I_M \cup \{0\}, j \in I, & & (4.7) \\
& \boldsymbol{v}_i \geq \frac{1}{2}(\boldsymbol{v}_j + \boldsymbol{v}_k) - \hat{s}(2 - y_{ij} - y_{ik}), \forall i \in I_M \cup \{0\}, j \neq k \in I, & & (4.8) \\
& \boldsymbol{v}_i \leq \frac{1}{2}(\boldsymbol{v}_j + \boldsymbol{v}_k) + \hat{s}(2 - y_{ij} - y_{ik}), \forall i \in I_M \cup \{0\}, j \neq k \in I, & & (4.9) \\
& \|\boldsymbol{v}_i - \boldsymbol{v}_j\|_1 \geq \varepsilon(z_i + z_j - 1), \forall i, j \in I (i \neq j), & & (4.10) \\
& \boldsymbol{v}_0 = \boldsymbol{b}_{\boldsymbol{\alpha}}, \\
& \boldsymbol{v}_i = \hat{s}\boldsymbol{e}_i, \forall i \in I_A \setminus \{0, d\}, \\
& \boldsymbol{v}_d = \boldsymbol{0}, \\
& z_0 = \cdots = z_d = 1, \\
& y_{ij} \in \{0, 1\}, \forall i \in I_M \cup \{0\}, j \in I, i \neq j, \\
& z_j \in \{0, 1\}, \forall j \in I, \\
& \boldsymbol{v}_i \in \mathbb{R}^{d-1}, \forall i \in I_M.
\end{aligned}
$$

The objective function (4.5) in the above problem accounts for the number of (active) vertices in the mediated set of the $\boldsymbol{\alpha}$–mediated graph. Constraints (4.6) ensures that there are exactly two outgoing arcs from each active vertex in the mediated graph. Constraints (4.7) ensure that only active vertices can be chosen to construct arcs in the mediated graph. Constraints (4.8) and (4.9) are the requirements for the mediated graph, i.e., the arcs are constructed as averages of the end vertex coordinates. With Constraints (4.10) we assure that in case two mediated vertices are active, then their coordinates must be different (since their ℓ_1 distance between them must be greater than ε, and zero otherwise). The rest of the constraints are the variable fixing equations and the domains for each of the variables.

The above formulation is an MILP, which can be hard to solve for general instances of the problem since the number of binary variables to decide is $\Lambda_{\boldsymbol{\alpha}} + (\Lambda_{\boldsymbol{\alpha}} + d - 1)\Lambda_{\boldsymbol{\alpha}}$. We incorporate different valid inequalities that strengthen the linear relaxation and break symmetries of the problem.

Specifically, in case $\boldsymbol{v}_j$ is not an active vertex, we fix its coordinates to the arbitrary vector $(\hat{s}, \overset{d-1}{\ldots}, \hat{s})$, by adding the following constraints:

$$\hat{s}(1 - z_j) \leq v_{jk} \leq \hat{s}(1 + z_j), \quad \forall j \in I, k = 1, \ldots, d-1. \tag{4.11}$$

Note that in case $z_j = 0$, these constraints enforce that $\boldsymbol{v}_j = (\hat{s}, \overset{d-1}{\ldots}, \hat{s})$, otherwise, the constraint is redundant ($0 \leq v_{jk} \leq 2\hat{s}$, which is always satisfied). Observe that in case the vertex is not activated, the assignment of coordinates to the vertex is not relevant, and any value is possible. Thus, fixing it to a given value allows to reduce the exploration of the branch-and-bound tree.

The second set of valid inequalities that we consider are the following:

$$z_j \leq z_{j-1}, \quad \forall j \in I \backslash \{0\}$$

These constraints force the non-activated vertices to be assigned to the last indices in I. Thus, given $\kappa = \sum_{j \in I} z_j$, the vertices in the mediated graph have coordinates $\boldsymbol{v}_0, \ldots, \boldsymbol{v}_{d+\kappa}$, being the remainder, $\boldsymbol{v}_{d+\kappa+1} = \cdots = \boldsymbol{v}_{d+\Lambda_{\boldsymbol{\alpha}}} = (\hat{s}, \overset{d-1}{\ldots}, \hat{s})$ by constraints (4.11).

Observe that there are still a lot of symmetries in the problem since any permutation of the coordinates of the active mediated vertices is an alternative solution with the same objective value. We break symmetries in our model by enforcing the active vertices to be sorted in nondecreasing order with the following valid inequalities:

$$v_{jk} \geq v_{(j-1)k}, \quad \forall j \in I_M \backslash \{d\}.$$

where $k \in \{1, \ldots, d-1\}$ is a chosen coordinate to sort the elements in the mediated set.

Example 4.15. *Taking $\boldsymbol{\alpha} = \frac{1}{6}(1, 2, 3)$, the minimal $\boldsymbol{\alpha}$–mediated graph that we obtained solving the optimization problem above is the one drawn in Figure 4.4. Note that this graph induces a minimal SOC extended representation of the power cone $\mathcal{K}^{1,3}(\boldsymbol{\alpha}) = \{x^6 \leq z_1 z_2^2 z_3^3\}$ with cardinality* 3 *(the number of extra mediated vertices* *in the graph). The constraints induced by the graph are:*

$$x^2 \leq w_1 z_3 \tag{4.12}$$

$$w_1^2 \leq w_2 z_2 \tag{4.13}$$

$$w_2^2 \leq w_1 z_1 \tag{4.14}$$

One can easily check that the obtained representation is valid by combining the above constraints:

$$\begin{aligned} x^6 w_2 &\overset{(4.12)}{\leq} w_1^3 z_3^3 w_2 \overset{(4.13)}{\leq} z_2 z_3^3 w_1 w_2^2 \\ &\overset{(4.14)}{\leq} z_2 z_3^3 w_1^2 z_1 \overset{(4.13)}{\leq} z_1 z_2^2 z_3^3 w_2 \Rightarrow x^6 \leq z_1 z_2^2 z_3^3 \end{aligned}$$

Remark 4.16. *The representations that have been already applied in the literature, specially in the representation of p–order cones, and that allow us to derive an upper bound for the cardinality of the optimal mediated graphs (Remark 4.13) can be easily constructed using binary decomposition (see Blanco et al. (2014) for further details). The special mediated graphs obtained in such are characterized by verifying that each mediated vertex is linked in the mediated graph with at most one other mediated vertex. This condition can be easily enforced in our model with the linear constraints:*

$$\sum_{i \in I_M} y_{ij} \leq z_j, \quad \forall j \in I_M.$$

4.1.3 Optimization over Generalized Power Cones

Minimal representations of generalized power cones and minimal mediated graphs in $\mathbb{R}^n$ have a direct impact on the solution of conic optimization problems. More specifically, *generalized power cone programming* (GPCP).

Definition 4.17 (Generalized power cone program)**.** *Given* $1 \leq p \leq \infty$, $\boldsymbol{\alpha} \in \Delta_d$, $F \in \mathbb{R}^{m \times n}$, $G \in \mathbb{R}^{m \times d}$, $\boldsymbol{h} \in \mathbb{R}^m$, $\boldsymbol{c} \in \mathbb{R}^n$, *and* $\boldsymbol{d} \in \mathbb{R}^d$*. The standard form* generalized power cone programming (GPCP) problem *is*

$$\begin{aligned} \textit{minimize} \quad & \boldsymbol{c}^T \boldsymbol{x} + \boldsymbol{d}^T \boldsymbol{z} \\ \textit{subject to} \quad & F\boldsymbol{x} + G\boldsymbol{z} = \boldsymbol{h}, \\ & \|\boldsymbol{x}\|_p \leq \boldsymbol{z}^{\boldsymbol{\alpha}}, \\ & \boldsymbol{x} \in \mathbb{R}^n, \\ & \boldsymbol{z} \in \mathbb{R}^d_+. \end{aligned} \tag{GPCP}$$

The above problem, although it belongs to the family of conic problems, requires to be equivalently reformulated as a second–order cone (or even semidefinite) program to be numerically solved in practice (e.g., using the available off-the-shelf solvers). With solutions of (C-MinMGP) or (MαMGP), one can build a minimal extended reformulation of an GPCP into an SOCP. On the one hand, let $\boldsymbol{\alpha} = \frac{1}{\hat{s}}(s_1, \ldots, s_d) \in \Delta_d$, $\mathcal{A}_{\boldsymbol{\alpha}} = \{\hat{s}\boldsymbol{e}_j : j = 1, \ldots, d-1\} \cup \{\mathbf{0}\} \subset \mathbb{R}^{d-1}$, and $\boldsymbol{b}_{\boldsymbol{\alpha}} := (s_1, \ldots, s_{d-1}) \in \mathbb{R}^{d-1}$. On the other hand, let $1 < p = \frac{r}{s} < \infty$, and $\mathcal{A}_p = \{0, r\}$. Then, each couple of mediated graphs $G_p = (V_p, A_p) \in \mathcal{M}_{\mathcal{A}_p}(s)$ and $G_{\boldsymbol{\alpha}} = (V_{\boldsymbol{\alpha}}, A_{\boldsymbol{\alpha}}) \in \mathcal{M}_{\mathcal{A}_{\boldsymbol{\alpha}}}(\boldsymbol{b}_{\boldsymbol{\alpha}})$ are in one-to-one correspondence to the following SOCP extended reformulation of (GPCP):

$$
\begin{array}{lll}
\text{minimize} & \boldsymbol{c}^T\boldsymbol{x} + \boldsymbol{d}^T\boldsymbol{z} & \\
\text{subject to} & F\boldsymbol{x} + G\boldsymbol{z} = \boldsymbol{h}, & \\
& \displaystyle\sum_{j=1}^{d} t_j \leq \eta_{\boldsymbol{b}_{\boldsymbol{\alpha}}}, & \\
& \xi_{js} = x_j, \quad \xi_{jr} = t_j, \quad \xi_{j0} = \eta_{\boldsymbol{b}_{\boldsymbol{\alpha}}}, & j = 1, \ldots, n, \\
& \eta_{\hat{s}\boldsymbol{e}_i} = z_i, \quad \eta_{\mathbf{0}} = z_d, & i = 1, \ldots, d-1 \\
& \xi_{jv}^2 \leq \displaystyle\prod_{u \in \delta_p^+(v)} \xi_{ju} & j = 1, \ldots, n; \quad v \in V_p \setminus \mathcal{A}_p \\
& \eta_{\boldsymbol{v}}^2 \leq \displaystyle\prod_{\boldsymbol{u} \in \delta_{\boldsymbol{\alpha}}^+(\boldsymbol{v})} \eta_{\boldsymbol{u}}, & \boldsymbol{v} \in V_{\boldsymbol{\alpha}} \setminus \mathcal{A}_{\boldsymbol{\alpha}}, \\
& \boldsymbol{t}, \boldsymbol{z}, \boldsymbol{\xi}, \boldsymbol{\eta} \geq 0. &
\end{array}
$$

The number of SOC constraints in the reformulation is $n(|V_p| - 2) + |V_{\boldsymbol{\alpha}}| - d$, the number of variables is $n|V_p| + |V_{\boldsymbol{\alpha}}|$, and the number of linear constraints is $O(m + n|V_p| + |V_{\boldsymbol{\alpha}}|)$ taking into account the ones hiding in the SOC constraints. According with Blanco et al. (2025), assuming that the coefficients of the input data $(F, G, \boldsymbol{h}, \boldsymbol{c}, \boldsymbol{d})$ have bit size at most τ, then the feasibility of (GPCP) can be tested in $m(n|V_p| + |V_{\boldsymbol{\alpha}}|)^{O(n|V_p| + |V_{\boldsymbol{\alpha}}|)}$ arithmetic operations over $\tau(n|V_p| + |V_{\boldsymbol{\alpha}}|)^{O(n|V_p| + |V_{\boldsymbol{\alpha}}|)}$-bit numbers. An ε-optimal solution of (GPCP) can be obtained through binary search in $(\tau + N)m(n|V_p| + |V_{\boldsymbol{\alpha}}|)^{O(n|V_p| + |V_{\boldsymbol{\alpha}}|)}$ arithmetic operations, where $N = 2^{-\varepsilon} \in \mathbb{Z}_+$. So finding minimal mediated graphs is highly recommended to reduce the computational complexity of (GPCP).

On the other hand, note that the solution of (MαMGP) allows to construct the minimal mediated graph, and then, the explicit SOCP representation of the problem. Specifically, let $(\boldsymbol{v}_p^\star, \boldsymbol{z}_p^\star, \boldsymbol{y}_p^\star)$ be the solution of (MαMGP) for $(\frac{s}{r}, \frac{r-s}{r})$, defining $V_p^\star := \{v_{pj}^\star \in \mathbb{R} : z_{pj}^\star = 1\}$ and $A_p^\star := \{(v_{pi}^\star, v_{pj}^\star) \in \mathbb{R}^2 : y_{pij}^\star = 1\}$, then the mediated graph $G_p^\star := (V_p^\star, A_p^\star) \in \mathrm{MinMG}_{\mathcal{A}_p}(s)$. Likewise, let $(\boldsymbol{v}_{\boldsymbol{\alpha}}^\star, \boldsymbol{z}_{\boldsymbol{\alpha}}^\star, \boldsymbol{y}_{\boldsymbol{\alpha}}^\star)$ be the solution of (M$\boldsymbol{\alpha}$MGP) for $\boldsymbol{\alpha}$, defining $V_{\boldsymbol{\alpha}}^\star := \{\boldsymbol{v}_{\boldsymbol{\alpha}j}^\star \in \mathbb{R}^{d-1} : z_{\boldsymbol{\alpha}j}^\star = 1\}$ and $A_{\boldsymbol{\alpha}}^\star := \{(\boldsymbol{x}_{\boldsymbol{\alpha}i}^\star, \boldsymbol{x}_{\boldsymbol{\alpha}j}^\star) \in \mathbb{R}^{d-1} \times \mathbb{R}^{d-1} : y_{\boldsymbol{\alpha}ij}^\star = 1\}$, then the mediated graph $G_{\boldsymbol{\alpha}}^\star := (V_{\boldsymbol{\alpha}}^\star, A_{\boldsymbol{\alpha}}^\star) \in \mathrm{MinMG}_{\mathcal{A}_{\boldsymbol{\alpha}}}(\boldsymbol{b}_{\boldsymbol{\alpha}})$. Hence, the SOCP defined by $G_p^\star$ and $G_{\boldsymbol{\alpha}}^\star$ is a minimal SOCP (also SDP) extended reformulation of (GPCP).

4.2 Polynomial Optimization

Needless to say, conic optimization provides by itself a fundamental framework for addressing a broad class of convex optimization problems, and that is particularly useful, through convenient relaxations via the Moment-SOS hierarchy (Lasserre, 2001), to optimize multivariate polynomials restricted on feasible regions defined by semialgebraic sets. At the core of this methodology lies the ability to certify polynomial nonnegativity using SOS decompositions, which translates nonnegativity conditions into semidefinite constraints. This approach is particularly powerful in several applications, as optimal control, probability, or dynamical systems where ensuring stability, safety, and optimality often relies on verifying polynomial inequalities (Henrion et al., 2020; Parrilo, 2003; Parrilo and Lall, 2003; Pauwels et al., 2017).

4.2.1 Optimization over SONC Cones

The following result is a rewriting of a lemma in Magron and Wang (2023).

Lemma 4.18. *For an affine independent set $\mathcal{A} \subset \mathbb{R}^n$ and a lattice point $\boldsymbol{\beta} \in \mathrm{Conv}(\mathcal{A})^\circ \cap \mathbb{Z}^n$, there exists an $\mathcal{A}$–mediated graph $G_{\mathcal{A}}^{\boldsymbol{\beta}} = (V_{\mathcal{A}}^{\boldsymbol{\beta}}, A_{\mathcal{A}}^{\boldsymbol{\beta}}) \in \mathcal{M}_{\mathcal{A}}(\boldsymbol{\beta})$ such that the denominators of coordinates of points in $V_{\mathcal{A}}^{\boldsymbol{\beta}}$ are odd numbers and the numerators of coordinates of points in $V_{\mathcal{A}}^{\boldsymbol{\beta}} \backslash \{\boldsymbol{\beta}\}$ are even numbers.*

Proof. The proof is straightforward from (Magron and Wang, 2023, Lemma 8) and Definition 3.1. □

Because of the above lemma and Remark 3.3, in this section, we consider the abelian group

$$\mathbb{M} = \left\{ \left(\frac{r_1}{s_1}, \dots, \frac{r_n}{s_n} \right) \in \mathbb{Q}^n \mid r_i \in (2\mathbb{Z}), s_i \in \mathbb{Z}\backslash(2\mathbb{Z}), i = 1, \dots, n \right\}.$$

For a polynomial $p = \sum_{\alpha \in \mathcal{A}} p_\alpha x^\alpha$, let $\Lambda(p) := \{\alpha \in \mathcal{A} : \alpha \in (2\mathbb{Z})^n \text{ and } p_\alpha > 0\}$ and $\Gamma(p) := \mathrm{Supp}(p) \backslash \Lambda(p)$. Then, we can write p as $p = \sum_{\alpha \in \Lambda(p)} c_\alpha x^\alpha + \sum_{\beta \in \Gamma(p)} d_\beta x^\beta$. For each $\beta \in \Gamma(p)$, let

$$\mathcal{C}_p(\beta) := \{\mathcal{T} \subseteq \Lambda(p) : (\mathcal{T}, \beta) \text{ is a circuit}\}. \tag{4.15}$$

Specially, if p is SONC, then it has a decomposition

$$p = \sum_{\beta \in \Gamma(p)} \sum_{\mathcal{T} \in \mathcal{C}_p(\beta)} f_{\mathcal{T}}^{\beta} + \sum_{\alpha \in \tilde{A}} c_\alpha x^\alpha, \tag{4.16}$$

where $p_{\mathcal{T}}^{\beta}$ is a nonnegative polynomial supported on $\mathcal{T} \cup \{\beta\}$ and

$$\tilde{A} := \left\{ \alpha \in \Lambda(p) : \alpha \notin \bigcup_{\beta \in \Gamma(p)} \bigcup_{\mathcal{T} \in \mathcal{C}_p(\beta)} \mathcal{T} \right\}.$$

Theorem 4.19. *Let $p = \sum_{\alpha \in \Lambda(p)} c_\alpha x^\alpha + \sum_{\beta \in \Gamma(f)} d_\beta x^\beta \in \mathbb{R}[x]$. For every $\beta \in \Gamma(p)$ and for every subset $\mathcal{T} \in \mathcal{C}_p(\beta)$, let $G_{\mathcal{T}}^{\beta} = (V_{\mathcal{T}}^{\beta}, A_{\mathcal{T}}^{\beta}) \in \mathcal{M}_{\mathcal{T}}^{\mathbb{M}}(\beta)$. Let $V := \cup_{\beta \in \Gamma(p)} \cup_{\mathcal{T} \in \mathcal{C}_p(\beta)} V_{\mathcal{T}}^{\beta}$ and $G = (V, A) \in \mathcal{M}_{\Lambda(p)}(\Gamma(p))$. Then, p is* SONC *if and only if p can be written as $p = \sum_{v \in V \backslash \Lambda(p)} (a_v x^{u_v} - b_v x^{w_v})^2 + \sum_{\alpha \in \tilde{A}} c_\alpha x^\alpha$, with $2u_v, 2w_v \in \delta^+(v)$, and $a_v, b_v \in \mathbb{R}$.*

Proof. The proof follows from Lemma 4.18, Proposition 3.5, and (Magron and Wang, 2023, Theorem 12). □

A convex cone $K \subseteq \mathbb{R}^n$ has a Q–lift of size k if it can be written as the projection of a slice of Q^k, that is, there is L being the intersection of an affine subspace and Q^k and a linear map $\pi : Q^k \to \mathbb{R}^d$ such that $K = \pi(L)$.

Given sets of lattice points $\mathcal{A} \subseteq (2\mathbb{Z})^n$ and $\mathcal{B} \subset \mathrm{Conv}(\mathcal{A}) \cap \mathbb{Z}^n$ such that $\mathcal{A} \cap \mathcal{B} = \emptyset$, define the SONC cone supported on $\mathcal{A}, \mathcal{B}$ as

$$\mathrm{SONC}_{\mathcal{AB}} := \left\{ (c, d) \in \mathbb{R}_+^{\mathcal{A}} \times \mathbb{R}^{\mathcal{B}} : \sum_{\alpha \in \mathcal{A}} c_\alpha x^\alpha + \sum_{\beta \in \mathcal{B}} d_\beta x^\beta \in \mathrm{SONC} \right\}. \tag{4.17}$$

The following theorem was proved in Magron and Wang (2023).

Theorem 4.20. *Let $\mathcal{A} \subseteq (2\mathbb{Z})^n$ and $\mathcal{B} \subset \mathrm{Conv}(\mathcal{A}) \cap \mathbb{Z}^n$ such that $\mathcal{A} \cap \mathcal{B} = \emptyset$. Then, the convex cone $\mathrm{SONC}_{\mathcal{AB}}$ has an $(\mathcal{S}_+^2)^k$-lift for some $k \in \mathbb{N}$.*

The map $\pi : (\mathcal{S}_+^2)^k \to \mathbb{R}_+^{\mathcal{A}} \times \mathbb{R}^{\mathcal{B}}$ is given in terms of the sum of signomial squares decomposition of Theorem 4.19. A polynomial p is a SONC supported on $\mathcal{A} \cup \mathcal{B}$ if and only if for some $G = (V, A) \in \mathcal{M}_{\mathcal{A}}(\mathcal{B})$,$p$ can be written as $p = \sum_{v \in V \setminus \mathcal{A}} (a_v \boldsymbol{x}^{\boldsymbol{u}_v} - b_v \boldsymbol{x}^{\boldsymbol{w}_v})^2 + \sum_{\boldsymbol{\alpha} \in \tilde{A}} c_{\boldsymbol{\alpha}} \boldsymbol{x}^{\boldsymbol{\alpha}}$, with $2\boldsymbol{u}_v, 2\boldsymbol{w}_v \in \delta^+(\boldsymbol{v})$, and $a_v, b_v \in \mathbb{R}$. This is equivalent to the existence of PSD matrices $Q_v, Q_{\boldsymbol{\alpha}} \in \mathcal{S}_+^2$ for $\boldsymbol{v} \in V \setminus \mathcal{A}$, and $\boldsymbol{\alpha} \in \tilde{A}$ such that

$$p = \sum_{v \in V \setminus \mathcal{A}} [\boldsymbol{x}^{\boldsymbol{u}_v}, \boldsymbol{x}^{\boldsymbol{w}_v}] Q_v \begin{bmatrix} \boldsymbol{x}^{\boldsymbol{u}_v} \\ \boldsymbol{x}^{\boldsymbol{w}_v} \end{bmatrix} + \sum_{\boldsymbol{\alpha} \in \tilde{A}} [\boldsymbol{x}^{\frac{1}{2}\boldsymbol{\alpha}}, 0] Q_{\boldsymbol{\alpha}} \begin{bmatrix} \boldsymbol{x}^{\frac{1}{2}\boldsymbol{\alpha}} \\ 0 \end{bmatrix}. \tag{4.18}$$

Hence, let $k = |V \setminus \mathcal{A}| + |\tilde{A}|$, the linear map $\pi : (\mathcal{S}_+^2)^k \to \mathbb{R}_+^{\mathcal{A}} \times \mathbb{R}^{\mathcal{B}}$ that maps an element $(Q_1, \ldots, Q_k) \in (\mathcal{S}_+^2)^k$ to the the coefficient vector of p via the equality (4.18) yields an $(\mathcal{S}_+^2)^k$-lift for $\mathrm{SONC}_{\mathcal{AB}}$.

The above lifting allows to tackle the following unconstrained polynomial optimization problem for a given polynomial $p \in \mathbb{R}[\boldsymbol{x}]$:

$$\inf\{p(\boldsymbol{x}) : \boldsymbol{x} \in \mathbb{R}^n\} = \sup\{\xi : p(\boldsymbol{x}) - \xi \geq 0, \boldsymbol{x} \in \mathbb{R}^n\} \tag{4.19}$$

via SOCP, based on the minimal mediated graph defined by the support of the polynomial p. One can replace the nonnegativity constraint in (4.19) by the following one to obtain a SONC relaxation with optimal value denoted by ξ_{SONC}:

$$\sup\{\xi : p(\boldsymbol{x}) - \xi \in \mathrm{SONC}\} \tag{4.20}$$

This is a conic optimization problem over the SONC cone and yields a lower bound for the optimal value $\xi^\star$ of (4.19), i.e., $\xi_{\mathrm{SONC}} \leq \xi^\star$. By Theorem 4.20, the SONC optimization problem (4.20) can be formulated as an SOCP where the number of linear constraints is in the order of the dimension of $\mathbb{R}_d[\boldsymbol{x}]$ where d is the degree of p, i.e., $\binom{n+d}{n}$; and the number of SOC constraints is in the order of the objective value of (C-MinMGP) for $\mathcal{A} = \Lambda(p)$ and $\mathcal{B} = \Gamma(p)$.

4.2.2 SOS decomposition of Nonnegative Circuits

Given a mediated graph $G = (V, A) \in \mathcal{M}_{\mathcal{A}}(\mathcal{B})$, the construction of a sum of squares (SOS) decomposition —in fact, Sum of Binomial Squares (SOBS)— is based on mediated graphs in the intersection of $\mathcal{M}_{\mathcal{A}}(\boldsymbol{\beta})$ and the set of sub-mediated graphs of G for each $\boldsymbol{\beta} \in \mathcal{B}$. In this shape each range of mediated graphs $G_{\boldsymbol{\beta}} = (V_{\boldsymbol{\beta}}, A_{\boldsymbol{\beta}}) \in \mathcal{M}_{\mathcal{A}}(\boldsymbol{\beta})$ that is subgraph of G for $\boldsymbol{\beta} \in \mathcal{B}$ defines an SOS decomposition of $p = \sum\limits_{\boldsymbol{\beta} \in \mathcal{B}} p_{\boldsymbol{\beta}}$ as $p = \sum\limits_{\boldsymbol{\beta} \in \mathcal{B}} \sigma_{\boldsymbol{\beta}}$ where $p_{\boldsymbol{\beta}} = \sigma_{\boldsymbol{\beta}}$ is an SOS decomposition of $p_{\boldsymbol{\beta}}$ whose number of squares is $|V_{\boldsymbol{\beta}}| - (d+1)$.

However, the author of the present thesis realize this claim on the number of squares just follows directly from (Iliman and De Wolff, 2016a, Theorem 5.2) in the extremal case, when the coefficient of $\boldsymbol{\beta}$ in $p_{\boldsymbol{\beta}}$ is $\pm\Theta_{p_{\boldsymbol{\beta}}}$, because of the interior case is derived from a convexity argument from the extremal cases. Whereas the theoretical result of the characterization of the intersection of SONC and SOS by means of the combinatorial structure of the Newton polytope is correct, we consider it necessary to demonstrate an explicit SOS decomposition of SONC polynomials that use the original support and coefficients of the polynomial.

First, we define the global minimizer of a nonnegative circuit $\boldsymbol{s}_p^\star \in \mathbb{R}^n$ as the unique vector satisfying

$$\prod_{k=1}^{n} \left(e^{s_{pk}^\star}\right)^{\alpha(j))_k - \alpha(0)_k} = e^{\langle \boldsymbol{s}_p^\star, \overrightarrow{\boldsymbol{\alpha}(0)\boldsymbol{\alpha}(j)} \rangle} = \frac{\lambda_j c_0}{\lambda_0 c_j} \tag{4.21}$$

for all $j = 1, \ldots, n$, where $\mathcal{A} = \{\boldsymbol{\alpha}(0), \ldots, \boldsymbol{\alpha}(n)\}$.

Theorem 4.21. *Let $\mathcal{A} = \{\boldsymbol{\alpha}(0), \ldots, \boldsymbol{\alpha}(n)\}$, and $p(\boldsymbol{x}) = \sum\limits_{j=0}^{n} c_j \boldsymbol{x}^{\boldsymbol{\alpha}(j)} + c\boldsymbol{x}^{\boldsymbol{\beta}}$ be a nonnegative circuit polynomial and $G = (V, A) \in \mathcal{M}_{\mathcal{A}}(\boldsymbol{\beta})$ be a mediated graph. Then,*

1. *if $\boldsymbol{\beta} \notin (2\mathbb{Z})^n$,*

$$p(\boldsymbol{x}) = c_{\boldsymbol{\beta}\boldsymbol{\beta}} \frac{c_0}{\lambda_0} e^{\langle \boldsymbol{s}_p^\star, \boldsymbol{\alpha}(0) \rangle} \sum_{m=0}^{1} \frac{\Theta_p + (-1)^m c}{2\Theta_p} \left(\frac{\boldsymbol{x}^{\frac{\boldsymbol{\beta}'}{2}}}{\sqrt{e^{\langle \boldsymbol{s}_p^\star, \boldsymbol{\beta}' \rangle}}} + (-1)^m \frac{\boldsymbol{x}^{\frac{\boldsymbol{\beta}''}{2}}}{\sqrt{e^{\langle \boldsymbol{s}_p^\star, \boldsymbol{\beta}'' \rangle}}} \right)^2$$
$$+ \frac{c_0}{\lambda_0} e^{\langle \boldsymbol{s}_p^\star, \boldsymbol{\alpha}(0) \rangle} \sum_{\boldsymbol{\gamma} \in V \setminus (\mathcal{A} \cup \{\boldsymbol{\beta}\})} c_{\boldsymbol{\beta}\boldsymbol{\gamma}} \left(\frac{\boldsymbol{x}^{\frac{\boldsymbol{\gamma}'}{2}}}{\sqrt{e^{\langle \boldsymbol{s}_p^\star, \boldsymbol{\gamma}' \rangle}}} - \frac{\boldsymbol{x}^{\frac{\boldsymbol{\gamma}''}{2}}}{\sqrt{e^{\langle \boldsymbol{s}_p^\star, \boldsymbol{\gamma}'' \rangle}}} \right)^2;$$

2. *if* $\boldsymbol{\beta} \in (2\mathbb{Z})^n$ *and* $c < 0$,

$$p(\boldsymbol{x}) = (\Theta_p + c)\left(\boldsymbol{x}^{\frac{\beta}{2}}\right)^2 + \frac{c_0}{\lambda_0} e^{\langle \boldsymbol{s}_p^\star, \boldsymbol{\alpha}(0)\rangle} \sum_{\gamma \in V \backslash \mathcal{A}} c_{\beta\gamma} \left(\frac{\boldsymbol{x}^{\frac{\gamma'}{2}}}{\sqrt{e^{\langle \boldsymbol{s}_p^\star, \gamma' \rangle}}} - \frac{\boldsymbol{x}^{\frac{\gamma''}{2}}}{\sqrt{e^{\langle \boldsymbol{s}_p^\star, \gamma'' \rangle}}} \right)^2;$$

where $\gamma', \gamma'' \in \delta^+(\gamma)$, $c_{\beta\gamma} \geq 0$ *is the entry* $(\boldsymbol{\beta}, \gamma)$ *in* $(L^+(G)_{V\backslash\mathcal{A}})^{-1}$ *for every* $\gamma \in V \backslash \mathcal{A}$.

Proof. For the first part, notice that the polynomial p can be written as a convex combination of the extremal nonnegative circuit with its support

$$p(\boldsymbol{x}) = \sum_{m=0}^{1} \frac{\Theta_p + (-1)^m c}{2\Theta_p} \left[\sum_{j=0}^{n} c_j \boldsymbol{x}^{\boldsymbol{\alpha}(j)} + (-1)^m \Theta_p \boldsymbol{x}^{\boldsymbol{\beta}} \right] \tag{4.22}$$

Now, note $\boldsymbol{s}_p^\star$ is the solution of

$$\begin{bmatrix} \boldsymbol{\alpha}(1) - \boldsymbol{\alpha}(0) \\ \vdots \\ \boldsymbol{\alpha}(n) - \boldsymbol{\alpha}(0) \end{bmatrix} \boldsymbol{s}_p^\star = \begin{bmatrix} \log\left(\frac{\lambda_1 c_0}{\lambda_0 c_1}\right) \\ \vdots \\ \log\left(\frac{\lambda_d c_0}{\lambda_0 c_n}\right). \end{bmatrix} \tag{4.23}$$

This linear system has a unique solution by affine independence of $\boldsymbol{\alpha}(0), \boldsymbol{\alpha}(1), \ldots, \boldsymbol{\alpha}(n)$. In this way, we have the extremal case $p_m^*(\boldsymbol{x}) = \sum_{j=0}^{n} c_j \boldsymbol{x}^{\boldsymbol{\alpha}(j)} + (-1)^m \Theta_p \boldsymbol{x}^{\boldsymbol{\beta}}$ for $m = 0, 1$. Evaluating in $\left(e^{\boldsymbol{s}_p^\star} \circ \boldsymbol{x}\right)$, where $\circ$ stands for the Hadamard product, it becomes

$$p_m^*\left(e^{\boldsymbol{s}_p^\star} \circ \boldsymbol{x}\right) = \frac{c_0}{\lambda_0} e^{\langle \boldsymbol{s}_p^\star, \boldsymbol{\alpha}(0)\rangle} \left[\sum_{j=0}^{n} \lambda_j \boldsymbol{x}^{\boldsymbol{\alpha}(j)} + (-1)^m \boldsymbol{x}^{\boldsymbol{\beta}} \right]. \tag{4.24}$$

Now, $p_1^*\left(e^{\boldsymbol{s}_p^\star} \circ \boldsymbol{x}\right)$ is a positive multiple of a simplicial AGI-form so by Reznick's SOS decomposition of AGI-forms Reznick (1989) and the fact of $\boldsymbol{\beta} \notin (2\mathbb{Z})$ it easy to see that

$$p_m^*\left(e^{s_p^\star}\circ x\right) = \frac{c_0}{\lambda_0}e^{\langle s_p^\star,\alpha(0)\rangle}\left[c_{\beta\beta}\left(x^{\frac{\beta'}{2}}+(-1)^m x^{\frac{\beta''}{2}}\right)^2+\sum_{\gamma\in V\setminus(\mathcal{A}\cup\{\beta\})}c_{\beta\gamma}\left(x^{\frac{\gamma'}{2}}-x^{\frac{\gamma''}{2}}\right)^2\right]. \tag{4.25}$$

where $c_{\beta\gamma}\geq$ is the entry (β,γ) of $(L^+(G)_{V\setminus\mathcal{A}})^{-1}$ for every $\gamma\in V\setminus\mathcal{A}$ (Properties 3.5.7). So, gathering the terms

$$\begin{aligned} p(e^{s_p^\star}\circ x) = \frac{c_0}{\lambda_0}e^{\langle s_p^\star,\alpha(0)\rangle}\sum_{m=0}^{1}\frac{\Theta_p+(-1)^m c}{2\Theta_p}\left[c_{\beta\beta}\left(x^{\frac{\beta'}{2}}+(-1)^m x^{\frac{\beta''}{2}}\right)^2\right] \\ +\frac{c_0}{\lambda_0}e^{\langle s_p^\star,\alpha(0)\rangle}\sum_{\gamma\in V\setminus(\mathcal{A}\cup\{\beta\})}c_{\beta\gamma}\left(x^{\frac{\gamma'}{2}}-x^{\frac{\gamma''}{2}}\right)^2, \end{aligned} \tag{4.26}$$

it just remains to undo the transformation to achieve the desired result.

To prove the second part, notice that the polynomial p can be written as

$$p(x)=\sum_{j=0}^{n}c_j x^{\alpha(j)}-\Theta_p x^{\beta}+(\Theta_p+c)x^{\beta}=p_1^*(x)+(\Theta_p+c)\left(x^{\frac{\beta}{2}}\right)^2. \tag{4.27}$$

Now, use the same argument for $p_1^*(x)$ in the proof of the first part and yield the result. □

In both cases, the number of squares is $|V|-n$. Then, let $\mathcal{A}\subset(2\mathbb{Z})^n$ be an affine independent set, $\mathcal{B}\subset\mathbb{Z}^n\cap\mathrm{Conv}(\mathcal{A})^\circ$ be a finite set, and let $p\in\mathbb{R}[x]$ be a SONC supported on $\mathcal{A}\cup\mathcal{B}$. Given a mediated graph $G=(V,A)\in\mathcal{M}_{\mathcal{A}}(\mathcal{B})$, the construction and a range of mediated graphs $G_\beta=(V_\beta,A_\beta)\in\mathcal{M}_{\mathcal{A}}(\beta)$ that are subgraphs of G for $\beta\in\mathcal{B}$ then $p=\sum_{\beta\in\mathcal{B}}p_\beta$ where p_β nonnegative circuit polynomial supported on $\mathcal{A}\cup\{\beta\}$ can be written as $p=\sum_{\beta\in\mathcal{B}}\sigma_\beta$ where $p_\beta=\sigma_\beta$ is the SOS decomposition of Theorem 4.21. Notice that the involved binomials can be $\left(s_\gamma x^{\frac{\gamma'}{2}}-t_\gamma x^{\frac{\gamma''}{2}}\right)$ and $\left(s_\beta x^{\frac{\beta'}{2}}+t_\beta x^{\frac{\beta'}{2}}\right)$ for $\gamma\in V\setminus\mathcal{A}$, $\gamma',\gamma''\in\delta^+(\gamma)$, $s_\gamma,t_\gamma\in\mathbb{R}_+$ if $\beta\notin(2\mathbb{Z})^n$; and $\left(x^{\frac{\beta}{2}}\right)$ if $\beta\in(2\mathbb{Z})^n$ so the number of squares of the decomposition is less or equal to $|V|+|\mathcal{B}|-n-1$, being equality if the coefficient of β in p_β is different from $\pm\Theta_{p_\beta}$ for every $\beta\in\mathcal{B}$. The number of squares decreases in one unit for each $\boldsymbol{\beta} \in \mathcal{B}$ that satisfies the equality. Hence, let $(\boldsymbol{x}_p^\star, \boldsymbol{y}_p^\star)$ be the solution of (D-MinMGP) for $\mathcal{A}$ and $\mathcal{B}$, defining $V_p^\star := \{\gamma \in \mathbb{Z}^n : x_{p\gamma}^\star = 1\}$ and $A_p^\star := \{(\gamma, \gamma') \in \mathbb{Z}^n \times (2\mathbb{Z})^n : y_{p\gamma,\gamma'}^\star = 1\}$, then by Theorem 3.16, the mediated graph $G_p^\star := (V_p^\star, A_p^\star) \in \mathrm{MinMG}_{\mathcal{A}}(\mathcal{B})$. Thus, we can apply Theorem 4.21 to each $p_{\boldsymbol{\beta}}$ with $G_p^\star$ providing an SOS decomposition of p which reduces the number of squares and the support of the decomposition, expanding the sparsity and reducing the rank of the associated positive semidefinite Gram matrix of p.

Intersection of SONC and SOS Cones

The main application of maximal mediated graphs is the certification of a SONC (sums of nonnegative circuit) polynomial to be sum of squares (SOS) decomposable. In case the polynomial is SOS, one can incorporate the constraints induced by such a polynomial as SDP constraints in a nonlinear optimization problem, and then, efficiently handle by the available solvers. Nevertheless, certifying the SOS condition is known to be NP-hard (Iliman and De Wolff, 2016a). Our approach allows for an efficient and automated methodology to check, in practice this condition. In what follows, we provide further details about the application of our methodology to this problem.

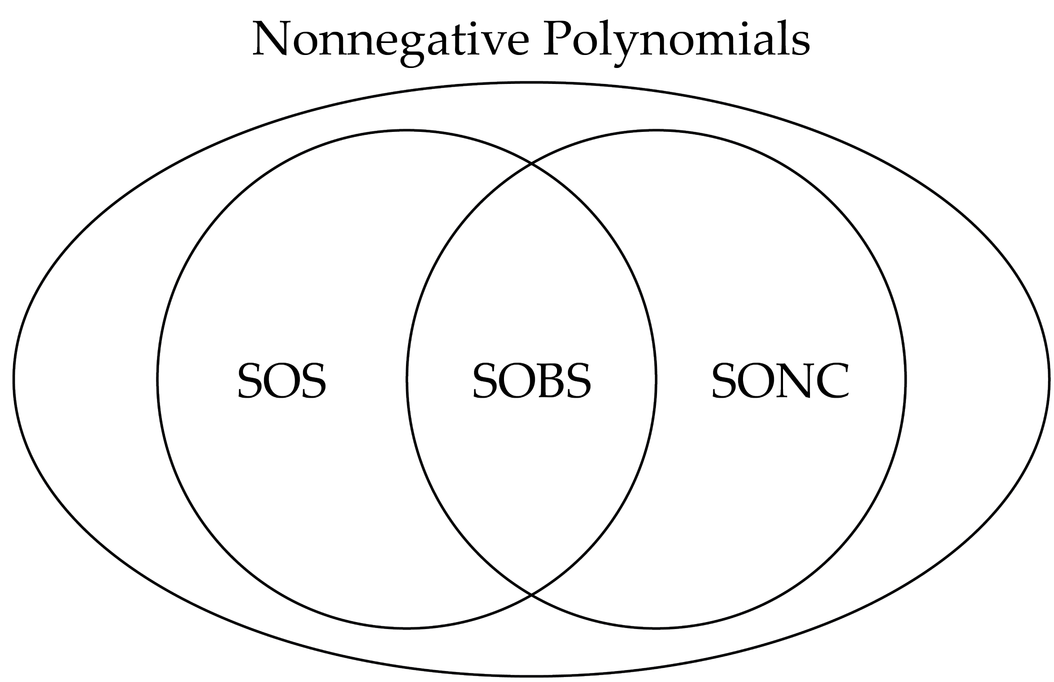

FIGURE 4.6: Nonnegative, SOS, SOBS, and SONC polynomials. A characterization of the intersections between them.

Let $\mathcal{A} \subset (2\mathbb{Z})^n$ be a finite affine independent set, and $\mathcal{B} \subset \mathbb{Z}^n \cap \mathrm{Conv}(\mathcal{A})^\circ$ be a finite set. Hartzer et al. (2022) showed a complete characterization of the polynomials supported on $\mathcal{A} \cup \mathcal{B}$ that lie in the intersection of SONC and SOS cones. That result can be adapted in terms of the solution of (D-MaxMGP).

Corollary 4.22. *Let $p \in \mathbb{R}[\boldsymbol{x}]$ be a* SONC *supported on $\mathcal{A} \cup \mathcal{B}$ and $\boldsymbol{x}^\star$ the solution of* (D-MaxMGP) *for $\mathcal{A}$. Then, p is* SOS *if and only if either $\boldsymbol{x}^\star_{\boldsymbol{\beta}} = 1$ or $\boldsymbol{\beta} \in (2\mathbb{Z})^n$ and its coefficient is positive for every $\boldsymbol{\beta} \in \mathcal{B}$.*

Proof. The result is straightforward from (Hartzer et al., 2022, Theorem 3.9) and Theorem 3.22. □

Figure 4.6 summarizes the interactions between these four fundamental cones of polynomials.

Chapter V

Complexity

VLADIMIR. — Tu aurais dû être poète.
ESTRAGON. — Je l'ai été. (*Geste vers ses haillons.*) Ça ne se voit pas?

Silence.

— Samuel Beckett. *En attendant Godot*

In this chapter, we derive different complexity results for the p–order feasibility problem by means of the required number of arithmetic operations and on which numbers (in bits). In Table 5.1 we summarize the main results derived in this chapter, indicating the numbered Lemma or Theorem where the result is stated and proved. In the first part of the chapter we derive the complexity results by *rewriting* the problem equivalently as an SDP feasibility problem, and then, applying the complexity result in Porkolab and Khachiyan (1997) (Theorem 2.26). Nevertheless, in this chapter we explicitly exploit the structure of the cone $\mathcal{K}_p^{n,1}$, avoiding the rewriting of this cone as a subset of the semidefinite cone, but still following the same paradigm of Porkolab and Khachiyan (1997). Thus, we get improved complexity bounds for the general case (Theorem 5.14), but, additionally, we analyze particular cases for the value of p, where the complexity can be further improved, as the case when p is even (Theorem 5.13), when p is in the form $\frac{r}{r-1}$ with r even (Corollary 5.15), or the very special case of the SOCP (Theorem 5.11).

Additionally, we use the geometric and algebraic structure of p–order cone to derive bounds on either the log–modulus of feasible solutions, or the discrepancy otherwise, and bounds on the number of arithmetic operations and bit size of the involved numbers for the feasibility problem. In case the p–order cone problem is feasible we derive bounds for Euclidean norm of a solution $(\boldsymbol{x}, z)$ to the system. In case the problem is infeasible, we compute

	p	No. arithmetic operations
Theorem 5.2	$\frac{r}{s} \in \mathbb{Q}_{>1}$	$m(n \log r)^{O((n \log r)^2)}$
Theorem 5.14	$\frac{r}{s} \in \mathbb{Q}_{>1}$	$\min\{[r(m+n)]^{O(n)}, m(rn)^{O(n^2)}\}$
Theorem 5.13	$r \in 2\mathbb{N}$	$m(r \min\{m,n\})^{O(n)}$
Corollary 5.15	$\frac{r}{r-1}, r \in 2\mathbb{N}$	$m(r \min\{m,n\})^{O(\min\{m,n^2\})}$
Theorem 5.11	2 (SOCP)	$m \min\{m,n\}^{O(\min\{m,n\})}$

TABLE 5.1: Summary of our complexity results for the p–order feasibility problem

bounds for the minimal violation of the linear system involved in the feasibility problem. Table 5.2 summarizes the results we obtained in this line. In the first part we detail the logarithmic upper bound for a feasible solution to the problem. In the second part, we detail the logarithm of the bound for the logarithm of the minimal violation (the so-called log–discrepancy).

	p	log–modulus
Lemma 5.5	$r \in 2\mathbb{N}$	$\tau(\min\{m,n\}r)^{O(n)}$
Theorem 5.6	$\frac{r}{s} \in \mathbb{Q}_{>1}$	$\tau(nr)^{O(n \min\{m,n\})}$
Theorem 5.7	$\frac{r}{r-1}, r \in 2\mathbb{N}$	$\tau(r \min\{m,n\})^{O(\min\{m,n\})}$
	p	log–discrepancy
Theorem 5.8	$\frac{r}{s} \in \mathbb{Q}_{>1}$	$-\tau(rn)^{O(n \min\{m,n\})}$
Theorem 5.8	$\frac{r}{r-1}, r \in 2\mathbb{N}$	$-\tau(r \min\{m,n\})^{O(\min\{m,n\})}$

TABLE 5.2: Summary of the bounds on feasible solutions and discrepancies for p–order cone feasibility problems.

The complexity results obtained in this chapter have a direct impact in the complexity of solving p–order cone optimization problems, i.e., minimizing a linear function subject to some linear constraints and the requirements that some of the variables belong to $\mathcal{K}_p^{n,1}$. Using the feasibility algorithm as an oracle, one can apply any binary search technique to derive, up to some tolerance $\varepsilon > 0$, the optimal value for the optimization problems. Some complexity results in this line will be derived for some interesting families of optimization problems involving ℓ_p–norms, as the norm minimization problem, support vector machines, continuous location problems, robust least squares, or robust linear optimization.

The rest of the chapter is organized as follows. In Section 5.1, we state the notation and main results use to derive the complexity results in this chapter. In this section we also prove the complexity results that can be derived for the problem by rewriting the problem as a semidefinite programming problem. In Section 5.2, we provide the upper bounds for the feasible solutions and the discrepancy for the p–order feasibility problem. Section 5.3 is devoted to prove the complexity bounds for the p–order feasibility problem. Exploiting the geometry of p–order cones we apply a similar strategy as the one by Porkolab and Khachiyan (1997) to derive new complexity bounds for the problem. We also analyze some particular cases for the value of p, namely, $p = 2$, p nonnegative even integer, and p of the form $\frac{r}{r-1}$ with r nonnegative integer. In Section 5.4, we extend our complexity results to problems involving several p–order cone constraints. Finally, in Chapter VI, Section 6.1 we emphasize how the complexity bounds are applied to optimization problems that involve p–order cones.

5.1 p–Order Feasibility Problem

The main question that we address in this chapter is on the complexity of the p–order feasibility problem which is defined as follows.

Definition 5.1 (p–order feasibility problem)**.** *The* p–order feasibility problem *consists of determining whether there exists a real vector* $(\boldsymbol{x}, z) \in \mathbb{R}^{n+1}$ *such that*

$$\begin{aligned} F\boldsymbol{x} + Gz &\leq H, \\ (\boldsymbol{x}, z) &\in \mathcal{K}_p^{n,1}. \end{aligned} \tag{$\mathbf{F}_p$}$$

where $F \in \mathbb{Z}^{m\times n}, G, H \in \mathbb{Z}^m$ *for* $m \in \mathbb{N}$.

We will denote by $\boldsymbol{f}_i^T$ the ith row of matrix F, for $i = 1, \dots, m$, and $G = (g_1, \dots, g_m)$, and $H = (h_1, \dots, h_m)$.

Note that when $n = 1$ the ℓ_p–norm becomes $|\cdot|$ and the feasibility problem ($\mathbf{F}_p$) is trivial. Therefore we assume throughout the chapter that $n \geq 2$.

The special case of the SOCP ($p = 2$) can be seen as a particular case of the *semidefinite feasibility problem* by a direct identification of the Lorentz cone with a subcone of the SDP cone using the Schur complement. Thus, the complexity of the 2–order feasibility problem can be analyzed using the results in Porkolab and Khachiyan (1997) (Theorem 2.26) for the semidefinite feasibility problem ($\mathbf{F}_{\text{SDP}}$)

On the other hand, in Section 4.1, we derived minimal SOC reformulations of the p–order cone. Thus, combining these results and those for the SDP feasiblility problem, the complexity results obtained for the SOCP can be extended to any $p \in \mathbb{Q}_{>1}$ by applying an explicit and minimal semidefinite extended representation of ($\mathbf{F}_p$), and then use Theorem 2.26, as we prove in the following result.

Theorem 5.2. *Let $p = \frac{r}{s} \in \mathbb{Q}$, with $r > s \in \mathbb{N}$ and $\gcd(r,s) = 1$. Then ($\mathbf{F}_p$) can be tested in $m(n\log r)^{O((n\log r)^2)}$ arithmetic operations over $\tau(n\log r)^{O((n\log r)^2)}$–bit numbers.*

Proof. Let us first analyze the case $p = 2$, and then we extend the result for any p. Recall by the Schur complement, $(\boldsymbol{x}, z) \in \mathcal{K}_2^{n,1}$ if and only if $\text{Arw}(\boldsymbol{x}, z) \succeq 0$. Thus, ($\mathbf{F}_p$), with $p = 2$, is equivalent to

$$\left\langle \text{Arw}\left(\frac{1}{2}\boldsymbol{f}_i, \frac{g_i}{n+1}\right), \text{Arw}(\boldsymbol{x}, z)\right\rangle \le h_i \quad i = 1, \dots, m, \quad \text{Arw}(\boldsymbol{x}, z) \succeq 0. \tag{5.1}$$

Based on the identification of ($\mathbf{F}_2$) as (5.1), to rewrite this feasibility problem as ($\mathbf{F}_{\text{SDP}}$) one must note that in the condition $\text{Arw}(\boldsymbol{x}, z) \succeq 0$ are hidden $\frac{1}{2}n(n+1)$ extra linear constraints. Hence, by Theorem 2.26, if the integer coefficients of ($\mathbf{F}_p$) have at most bit size τ, its feasibility can be tested in $mn^{O(n^2)}$ arithmetic operations over $\tau n^{O(n^2)}$–bit numbers. Continuing with the general case. Recall $(x, y, z) \in \mathcal{K}^{1,2}\left(\frac{1}{2}\right)$ if and only if $(2x, y - z, y + z) \in \mathcal{K}_2^{2,1}$. As we already mentioned $\mathcal{K}_2^{2,1}$ is a subset of $\mathcal{S}_+^3$. But, if we consider the three-dimensional rotated second order cone it is easy to see that $\mathcal{K}^{1,2}\left(\frac{1}{2}\right) = \mathcal{S}_+^2$.

In Blanco and Martínez-Antón (2024a) (Section 4.1), the authors derived a minimal three-dimensional rotated second order cone ($\mathcal{S}_+^2$) extended representation based on a minimal mediated graphs. In the case of the p–order cone with $p = \frac{r}{s}$, $r > s$, and $\gcd(r,s) = 1$ this graph $G = (V \cup \{0, r\}, A)$ satisfies $V \subset (0, r)$, $|V| = \lceil \log r \rceil$, $s \in V$, and it is defined by the sets of outgoing arcs $\delta^+(v) = \{u, 2v - u\} \subset V \cup \{0, r\}$ for all $v \in V$. With all of this, ($\mathbf{F}_p$) is equivalent to

$$\begin{aligned}
&F\boldsymbol{x} + Gz \leq H, \\
&\sum_{j=1}^{d} t_j - z \leq 0, \\
&\mathrm{BlockDiag}\left(W_{jv}\right)_{\substack{j=1,\dots,n \\ v\in V}} \succeq 0,
\end{aligned}$$

where $W_{jv} = \begin{bmatrix} w_{ju} & w_{jv} \\ w_{jv} & w_{j,2v-u} \end{bmatrix} \in \mathcal{S}^2$, with $j = 1, \dots, n$; $v \in V$, and $u, 2v - u \in \delta^+(v)$; and $w_{j0} = z$, $w_{js} = x_j$, and $w_{jr} = t_j$. Again, in the semidefinite constraint are hidden $O((n \log r)^2)$ affine constraints thus, by Porkolab and Khachiyan (1997), its feasibility can be tested in $m(n \log r)^{O((n \log r)^2)}$ arithmetic operations over $\tau(n \log r)^{O((n \log r)^2)}$–bit numbers. □

In the previous result, the complexity of ($\mathbf{F}_p$) is obtained by rewriting the problem as a particular case of ($\mathbf{F}_{\mathrm{SDP}}$) and then apply the results for the general case. As already announced, better complexity bounds can be obtained by explicitly exploiting the structure of $\mathcal{K}_p^{n,1}$.

5.2 Bounding Solutions and Discrepancies

In this section, we derive some results related to the known answer to ($\mathbf{F}_p$). Specifically, in case the problem is certified to be feasible we derive upper bounds on the log–modulus of at least one feasible solution. In case the problem is infeasible, we analyze its discrepancy, that is the minimum violation of the feasibility. We also derive lower bounds to this value in case the system is infeasible.

The first result that we address is the one of representing ℓ_p–norm based constraints in the first order formula language.

Lemma 5.3. *Let $p = \frac{r}{s}$ with $r > s \in \mathbb{N}$ and $\gcd(r, s) = 1$. Then, the following statements are equivalent:*

1. $\|\boldsymbol{x}\|_p = z$,

2. $(\boldsymbol{x}, z)$ *satisfies the following first order formula:*

$$\exists \boldsymbol{t} \in \mathbb{R}^n \left\{ \bigwedge_{j=1}^{n} \left[(x_j^r = z^{r-s} t_j^s) \vee (-x_j^r = z^{r-s} t_j^s) \right], \sum_{j=1}^{n} t_j = z, t_1 \geq 0, \dots, t_n \geq 0 \right\}. \tag{5.2}$$

And also the following statements:

1. $\|\boldsymbol{x}\|_p \leq z$,
2. $(\boldsymbol{x}, z)$ *satisfies the following first order formula:*

$$\exists \boldsymbol{t} \in \mathbb{R}^n \left\{ \bigwedge_{j=1}^{n} \left[(x_j^r \leq z^{r-s} t_j^s) \wedge (-x_j^r \leq z^{r-s} t_j^s) \right], \sum_{j=1}^{n} t_j \leq z, t_1 \geq 0, \dots, t_n \geq 0 \right\}. \tag{5.3}$$

Proof. The proof follows by rewriting equivalently the inequality/equation $\|\boldsymbol{x}\|_p \lhd z$ as a standard formula (SF) as detailed in Lemma 4.6. □

Lemma 5.4. *Given a positive $p \in \mathbb{Q}$ with conjugate q one has*

$$\min_{(\boldsymbol{x},z) \in \mathcal{K}_p^{n,1}} \{\boldsymbol{f}^T \boldsymbol{x} + gz : z = R\} = R(g - \|\boldsymbol{f}\|_q), \tag{5.4}$$

$$\min_{(\boldsymbol{x},z) \in \mathcal{K}_p^{n,1}} \{\boldsymbol{f}^T \boldsymbol{x} + gz : z \leq R\} = \min\{0, R(g - \|\boldsymbol{f}\|_q)\}. \tag{5.5}$$

Proof. To show the first identity, observe that

$$\begin{aligned}\min_{(\boldsymbol{x},z) \in \mathcal{K}_p^{n,1}} \{\boldsymbol{f}^T \boldsymbol{x} + gz : z = R\} &= R(g - \|\boldsymbol{f}\|_q) + \min_{(\boldsymbol{x},z) \in \mathcal{K}_p^{n,1}} \{\boldsymbol{f}^T \boldsymbol{x} + \|\boldsymbol{f}\|_q z : z = R\} \\ &= R(g - \|\boldsymbol{f}\|_q),\end{aligned}$$

where the last equality follows from the fact that $(\boldsymbol{f}, \|\boldsymbol{f}\|_q)$ belongs to the boundary of $\mathcal{K}_q^{n,1} = (\mathcal{K}_p^{n,1})^*$.
For the second identity, note that if $(\boldsymbol{f}, g) \in \mathcal{K}_q^{n,1}$, then $\min_{(\boldsymbol{x},z) \in \mathcal{K}_p^{n,1}} \{\boldsymbol{f}^T \boldsymbol{x} + gz : z \leq R\} = 0$. Otherwise $g - \|\boldsymbol{f}\|_q < 0$, which means that the minimum on the left-hand side of (5.5) is negative and hence it is attained at a vector $(\boldsymbol{x}, R)$. Then (5.5) becomes a consequence of (5.4). □

In what follows, we analyze the bounds on the feasible solutions of ($\mathbf{F}_p$). We first analyze the case $p = r \in 2\mathbb{N}$.

Lemma 5.5. *Let $p = r \in 2\mathbb{N}$. Then, there exists a feasible solution (x, z) of ($\mathbf{F}_p$) such that $\|(x, z)\|_2 \leq R$, where $\log R = \tau(\min\{m, n\}r)^{O(n)}$.*

Proof. In this case the problem ($\mathbf{F}_p$) is equivalent to the quantifier free formula:

$$\{f_1^T x + g_1 z - h_1 \leq 0, \dots, f^T x_m + g_m z - h_m \leq 0,$$
$$x_1^r + \cdots + x_n^r \leq z^r, z \geq 0\}. \quad (5.6)$$

Observe that this formula consists of $m + 2$ polynomial inequalities of degree at most r in $(n + 1)$ free variables. If the integer coefficients appearing in (5.6) have height at most 2^τ, then Proposition 2.3 implies that any feasible solution satisfies $\|(x, z)\|_2 \leq R$, where $\log R \leq \tau(mr)^{O(n)}$.

By Proposition 2.9, there is a set $I \subseteq M$ of size at most $\min\{m, n + 1\}$ such that the system

$$f_i^T x + g_i z = h_i, \quad i \in I, \quad \|x\|_p \leq z,$$

is feasible, and any of its solutions solve the original problem ($\mathbf{F}_p$). For this reason, we can obtain a better bound by replacing m with $\min\{m, n + 1\}$, namely $\log R \leq \tau(\min\{m, n\}r)^{O(n)}$. □

The next result that we prove is the general case, which is the analog of (Porkolab and Khachiyan, 1997, Theorem 3.1) for ($\mathbf{F}_{\text{SDP}}$).

Theorem 5.6. *Let $p = \frac{r}{s} \in \mathbb{Q}$, with $r > s \in \mathbb{N}$ and $\gcd(r, s) = 1$. Then:*

1. *There exists a feasible solution (x, z) of ($\mathbf{F}_p$) such that $\|(x, z)\|_2 \leq R$, where $\log R = \tau(nr)^{O(n \min\{m,n\})}$.*
2. *Moreover, if the feasible set of ($\mathbf{F}_p$) is bounded, then the above bound holds for any feasible solution of ($\mathbf{F}_p$).*

Proof. Suppose that the problem ($\mathbf{F}_p$) is feasible, and let us define:

$$\Omega_R := \{(x, z) \in \mathcal{K}_p^{n,1} : z = R\},$$
$$\Theta(R) := \min_{(x,z) \in \Omega_R} \max\{f_1^T x + g_1 z - h_1, \dots, f_m^T x + g_m z - h_m\}.$$

For any $R \geq 0$ and considering Δ_m as in (2.3),

$$\begin{aligned}\Theta(R) &= \min_{(\boldsymbol{x},z)\in\Omega_R} \max_{\boldsymbol{\lambda}\in\Delta_m} \sum_{i=1}^{m} \lambda_i(\boldsymbol{f}_i^T\boldsymbol{x} + g_i z - h_i) \\ &= \max_{\boldsymbol{\lambda}\in\Delta_m} \min_{(\boldsymbol{x},z)\in\Omega_R} \left[\left(\sum_{i=1}^{m}\lambda_i\boldsymbol{f}_i^T\right)\boldsymbol{x} + \left(\sum_{i=1}^{m}\lambda_i g_i\right) z - \sum_{i=1}^{m}\lambda_i h_i\right] \\ &= \max_{\boldsymbol{\lambda}\in\Delta_m} \left[R\left(\sum_{i=1}^{m}\lambda_i g_i - \left\|\sum_{i=1}^{m}\lambda_i\boldsymbol{f}_i\right\|_q\right) - \sum_{i=1}^{m}\lambda_i h_i\right].\end{aligned}$$

The second equality follows from von Neumann's minimax theorem 2.12 and the last one follows the first identity (5.4) from Lemma 5.4.

Now, consider the formula

$$\Phi(R) := \forall\boldsymbol{\lambda}\in\Delta_m \left\{R\left(\sum_{i=1}^{m}\lambda_i g_i - \left\|\sum_{i=1}^{m}\lambda_i\boldsymbol{f}_i\right\|_q\right) - \sum_{i=1}^{m}\lambda_i h_i \leq 0 \wedge R \geq 0\right\}.$$

By Theorem 5.3, $\Phi(R)$ can be rewritten in the standard form (SF) as follows

$$\begin{aligned}&\forall\boldsymbol{\lambda}\in\mathbb{R}^m \quad \exists(\boldsymbol{t},w)\in\mathbb{R}^{n+1}\left\{\left\{\left[\lambda_1\geq 0,\dots,\lambda_m\geq 0,\quad \sum_{i=1}^{m}\lambda_i = 1\right] \implies\right.\right. \\ &\left[\sum_{j=1}^{n} t_j = w, \bigwedge_{j=1}^{n}\left[\left[\left(\sum_{i=1}^{m}\lambda_i f_{ij}\right)^r = w^s t_j^{r-s}\right] \vee \left[-\left(\sum_{i=1}^{m}\lambda_i f_{ij}\right)^r = w^s t_j^{r-s}\right]\right],\right. \\ &\left.\left.\left. R\left(\sum_{i=1}^{m}\lambda_i g_i - w\right) - \sum_{i=1}^{m}\lambda_i h_i \leq 0, t_1\geq 0,\dots,t_n\geq 0\right]\right\} \wedge (R\geq 0)\right\}.\end{aligned}$$

Then, for any $R \in \mathbb{R}$, the following statements are equivalent:

- (**F**$_p$) has a feasible solution in Ω_R,
- $\Theta(R) \leq 0$,
- R satisfies $\Phi(R)$.

By our original assumption, (**F**$_p$) is feasible, and hence there is a nonnegative R that satisfies $\Phi(R)$. Next, $\Phi(R)$ is a standard formula (SF) of degree at most r with $k = 1$ free variable and $\omega = 2$ quantifiers. Furthermore, $\Phi(R)$ consists of $O(m+n)$ atomic polynomials inequalities in $O(m+n)$ variables. The expression $\left(\sum_{i=1}^{m}\lambda_i f_{ij}\right)^r$ involves integer coefficients of height at most 2^τ, thus the expansion yields coefficients with bit size at most $B = r(\tau + \log(m))$.

Now from Proposition 2.3 it follows that $\Phi(R)$ can be satisfied by a positive number R such that

$$\log R = r(\tau + \log(m))(O(m+n)r)^{O(mn)} = \tau((m+n)r)^{O(mn)}. \tag{5.7}$$

By Proposition 2.9, there is a set $I \subseteq M$ of size at most $\min\{m, n+1\}$ such that the system

$$\boldsymbol{f}_i^T \boldsymbol{x} + g_i z = h_i, \quad i \in I, \quad \|\boldsymbol{x}\|_p \leq z,$$

is feasible, and any solution solves the original problem ($\mathbf{F}_p$). For this reason, we can obtain a better bound by replacing m with $\min\{m, n+1\}$. Since $\|(\boldsymbol{x}, z)\|_2 \leq \sqrt{n+1}\,\|(\boldsymbol{x}, z)\|_\infty \leq \sqrt{n+1}R$, part 1 of the theorem follows.

To show part 2, consider the formula $\Phi'(R) := \forall R' \in \mathbb{R}\{\Phi(R') \implies (R' \leq R)\}$. Note that $\Phi'(R)$ can be written in prenex form as

$$\forall R' \in \mathbb{R}, \exists \boldsymbol{\lambda} \in \mathbb{R}^m, \forall (\boldsymbol{t}, w) \in \mathbb{R}^{n+1} \Bigg\{ \Bigg\{ \left[\lambda_1 \geq 0, \ldots, \lambda_m \geq 0, \quad \sum_{i=1}^m \lambda_i = 1 \right] \wedge$$
$$\left[\left(\bigvee_{j=1}^n (t_j < 0) \right) \vee (w < 0) \vee \left(\sum_{j=1}^n t_j \neq w \right) \right.$$
$$\bigvee_{j=1}^n \left[\left[\left(\sum_{i=1}^m \lambda_i f_{ij} \right)^r \neq w^s t_j^{r-s} \right] \wedge \left[- \left(\sum_{i=1}^m \lambda_i f_{ij} \right)^r \neq w^s t_j^{r-s} \right] \right]$$
$$\left. \vee \left(R' \left(\sum_{i=1}^m \lambda_i g_i - w \right) - \sum_{i=1}^m \lambda_i h_i > 0 \right) \right] \Bigg\} \vee (0 \leq R' \leq R) \Bigg\}.$$

It is easy to see that $\Phi'(R)$ is satisfied if and only if

$$R \geq \max\{z : (\boldsymbol{x}, z) \text{ feasible for } (\mathbf{F}_p)\}.$$

Hence, we can apply Proposition 2.3 to $\Phi'(R)$ to conclude that, similarly to (5.7), $\log R = \tau((m+n)r)^{O(mn)}$. It remains to show that m can be replaced by $\min\{m, n+1\}$. To this end, note that if the solution set of ($\mathbf{F}_p$) is bounded, then there exists a system $\boldsymbol{f}_i^T \boldsymbol{x} + g_i z \leq h_i, \quad i \in I, \quad \|\boldsymbol{x}\|_p \leq z$ with at most $n+1$ inequalities whose solution is still bounded. This is because the solution of problem ($\mathbf{F}_p$) is bounded if and only if the recession cone of ($\mathbf{F}_p$) is trivial, namely —see (2.4)—,

$$\mathcal{K}_p^{n,1} \cap \bigcap_{i=1}^m H_i = \{\mathbf{0}\}, \tag{5.8}$$

where H_i is the halfspace $\{(\boldsymbol{x}, z) \in \mathbb{R}^{n+1} : \boldsymbol{f}_i^T \boldsymbol{x} + g_i z \leq 0\}$. With $\Omega_1 = \{(\boldsymbol{x}, z) \in \mathcal{K}_p^{n,1} : z = 1\}$, (5.8) is equivalent to the emptiness of the intersection of the $(m+1)$ convex sets $\Omega_1, H_1, \ldots, H_m \subset \mathbb{R}^{n+1}$. By Helly's theorem 2.11 there exists at most $(n+2)$ sets among $\Omega_1, H_1, \ldots, H_m \subset \mathbb{R}^{n+1}$ whose intersection is still empty. The claim follows since Ω_1 must be one of these sets. □

If the conjugate q of p is an even integer, for instance when $q = p = 2$, the bound of Theorem 5.6 can be improved as stated in the following result.

Theorem 5.7. *Let $r \in 2\mathbb{N}$ and $p = \frac{r}{r-1}$. Then*

1. *Any solution $(\boldsymbol{x}, z)$ of ($\mathbf{F}_p$) satisfies $\|(\boldsymbol{x}, z)\|_2 \leq R$, where*

$$\log R = \tau (r \min\{m, n\})^{O(\min\{m,n\})}.$$

2. *Moreover, if the feasible set of ($\mathbf{F}_p$) is bounded, then the above bound holds for any feasible solution of ($\mathbf{F}_p$).*

Proof. First let us notice that $q = (1 - \frac{1}{p})^{-1} = (\frac{r}{r} - \frac{r-1}{r})^{-1} = r \in 2\mathbb{N}$. The idea is then to adapt the proof of Theorem 5.6 by considering the formula $\Phi(R)$ in the following standard form (SF):

$$\forall \boldsymbol{\lambda} \in \mathbb{R}^m \quad \exists w \in \mathbb{R} \left\{ \left\{ \left[\lambda_1 \geq 0, \ldots, \lambda_m \geq 0, \quad \sum_{i=1}^m \lambda_i = 1 \right] \implies \right.\right.$$
$$\left.\left. \left[\sum_{j=1}^n \left(\sum_{i=1}^m \lambda_i f_{ij} \right)^r = w^r, R \left(\sum_{i=1}^m \lambda_i g_i - w \right) - \sum_{i=1}^m \lambda_i h_i \leq 0, w \geq 0 \right] \right\} \wedge (R \geq 0) \right\}.$$

One advantage given by the assumption on p is that the variable $\boldsymbol{t}$ is not needed anymore, so $\Phi(R)$ is a standard formula (SF) of degree at most r with $k = 1$ free variable and $\omega = 2$ quantifiers. Furthermore, $\Phi(R)$ consists of $O(m)$ atomic polynomials inequalities in $O(m)$ variables. The expansion of $\left(\sum_{i=1}^m \lambda_i f_{ij}\right)^r$ with integer coefficients of height at most 2^τ yields coefficients with bit size at most $B = r(\tau + \log(m))$.

From Proposition 2.3 it follows that $\Phi(R)$ can be satisfied by a positive number R such that

$$\log R = r(\tau + \log(m))(O(m)r)^{O(m)} = \tau (mr)^{O(m)}. \tag{5.9}$$

In the two parts of Theorem 5.6 we can replace m with $\min\{m, n+1\}$, yielding the desired result. $\square$

Let R be the bound defined as

$$R(p,n,m,\tau) := \begin{cases} \tau(r\min\{m,n\})^{O(n)} & \text{if } p = r \in 2\mathbb{N}, \\ \tau(r\min\{m,n\})^{O(\min\{m,n\})} & \text{if } p = \frac{r}{r-1}, \quad r \in 2\mathbb{N}, \\ \tau(rn)^{O(n\min\{m,n\})} & \text{otherwise,} \end{cases} \tag{5.10}$$

and let $\mathcal{K}_p^{n,1}(R) = \{(\boldsymbol{x}, z) \in \mathcal{K}_p^{n,1} : z \leq R\}$. The *discrepancy* of ($\mathbf{F}_p$) is the optimal value of the following optimization problem:

$$\theta^* := \min\{\theta : \boldsymbol{f}_i^T\boldsymbol{x} + g_i z \leq h_i + \theta, \quad i \in M, \quad (\boldsymbol{x}, z) \in \mathcal{K}_p^{n,1}(R)\}. \tag{5.11}$$

Since $\mathcal{K}_p^{n,1}(R)$ is compact, the minimum in (5.11) is always attained. In addition $\theta^* \leq 0$ if and only if ($\mathbf{F}_p$) is feasible.

The result below is the analog of (Porkolab and Khachiyan, 1997, Theorem 4.2).

Theorem 5.8. *Let $p = \frac{r}{s} \in \mathbb{Q}$, with $r > s \in \mathbb{N}$ and $\gcd(r,s) = 1$. Assume that ($\mathbf{F}_p$) is infeasible. Then $-\log\theta^* = \tau(rn)^{O(n\min\{m,n\})}$. If $r \in 2\mathbb{N}$ and $s = r-1$ then $-\log\theta^* = \tau(r\min\{m,n\})^{O(\min\{m,n\})}$.*

The proof of Theorem 5.8 is postponed at the end of Section 5.3.2.

5.3 On the Complexity of the p–Order Feasibility Problem

The result below is the analog of (Porkolab and Khachiyan, 1997, Lemma 5.2).

Theorem 5.9. *If $p = \frac{r}{s} \in \mathbb{Q}$, with $r > s \in \mathbb{N}$ and $\gcd(r,s) = 1$, then the feasibility of ($\mathbf{F}_p$) can be tested in $((m+n)r)^{O(n)}$ arithmetic operations over $\tau((m+n)r)^{O(n)}$–bit numbers.*
If $p = r \in 2\mathbb{N}$ then the feasibility of ($\mathbf{F}_p$) can be tested in $(mr)^{O(n)}$ arithmetic operations over $\tau(mr)^{O(n)}$–bit numbers.
If $p = \frac{r}{r-1}$ with $r \in 2\mathbb{N}$ then the feasibility of ($\mathbf{F}_p$) can be tested in $(mr)^{O(m)}$ arithmetic operations over $\tau(mr)^{O(m)}$–bit numbers.

Proof. By Theorem 5.3, the sentence

$$\exists (\boldsymbol{x}, z, \boldsymbol{t}) \in \mathbb{R}^{2n+1} \left\{ \bigwedge_{i=1}^{m} (\boldsymbol{f}_i^T \boldsymbol{x} + g_i z \leq h_i), t_1 \geq 0, \dots, t_n \geq 0, \right.$$
$$\left. \bigwedge_{j=1}^{n} \left[(x_j^r \leq z^{r-s} t_j^s) \wedge (-x_j^r \leq z^{r-s} t_j^s) \right], \sum_{j=1}^{n} t_j \leq z \right\} \tag{5.12}$$

states that ($\mathbf{F}_p$) is feasible. From Theorem 2.5 it follows that the validity of the above sentence can be determined in $((m+n)r)^{O(n)}$ operations over $\tau((m+n)r)^{O(n)}$-bit numbers.

If $p = r \in 2\mathbb{N}$ the formula becomes

$$\exists (\boldsymbol{x}, z) \in \mathbb{R}^{n+1} \left\{ \bigwedge_{i=1}^{m} (\boldsymbol{f}_i^T \boldsymbol{x} + g_i z \leq h_i), \sum_{j=1}^{n} x_j^r \leq z^r, z \geq 0 \right\}. \tag{5.13}$$

From Theorem 2.5 it follows that the validity of the above sentence can be determined in $(mr)^{O(n)}$ operations over $\tau(mr)^{O(n)}$-bit numbers.

Eventually, if $p = \frac{r}{r-1}$ with $r \in 2\mathbb{N}$, consider the sentence

$$\exists R \in \mathbb{R} \quad \Phi(R), \tag{5.14}$$

where $\Phi(R)$ is the formula defined in the proof of Theorem 5.7. This sentence also states that ($\mathbf{F}_p$) is feasible. Observe that (5.14) consists of $O(m)$ polynomial inequalities of degree at most r in $O(m)$ variables and has integer coefficients of bit size at most $B = r(\tau + \log(rm))$. The last part of the lemma follows again from Theorem 2.5. □

For $r = p = q = 2$, Theorem 5.9 directly implies the following corollary when considering the self-dual second–order cone.

Corollary 5.10. *The feasibility of an* SOCP *can be tested in* $m^{O(\min\{m,n\})}$ *arithmetic operations over* $\tau m^{O(\min\{m,n\})}$.

As we will see in the next section, the bound of Corollary 5.10 can be improved even further.

5.3.1 Complexity Bounds on SOCP

The result below is the analog of (Porkolab and Khachiyan, 1997, Theorem 5.1).

Theorem 5.11. *The feasibility of an* SOCP *can be tested in* $m \min\{m,n\}^{O(\min\{m,n\})}$ *arithmetic operations over* $\tau \min\{m,n\}^{O(\min\{m,n\})}$*–bit numbers.*

Proof. If $m \le n$ then the result follows directly from Corollary 5.10. Let us assume that $m \ge n$.

Given a set $I \subset M = \{1,\dots,m\}$, let us consider the following optimization problem

$$\theta(I) := \min\{\theta : \boldsymbol{f}_i^T \boldsymbol{x} + g_i z \le h_i + \theta, \quad i \in I, \quad (\boldsymbol{x}, z) \in \mathcal{K}_2^{n,1}(R)\}, \tag{5.15}$$

where $R = R(2,n,m,\tau)$ (5.10). In particular, we have $\theta(M) = \theta^*$, the latter quantity has been defined in (5.11). Denote by $(\boldsymbol{x}(I), z(I))$ the unique least norm solution of the system $\boldsymbol{f}_i^T \boldsymbol{x} + g_i z \le h_i + \theta(I), i \in I, (\boldsymbol{x}, z) \in \mathcal{K}_2^{n,1}(R)$, and let $V(I) = \{i \in I : \boldsymbol{f}_i^T \boldsymbol{x}(I) + g_i z(I) > h_i + \theta(I)\}$ the index set of constraints violated by $(\boldsymbol{x}(I), z(I))$. A set I is called a basis, if $V(J) \ne V(I)$ for any proper subset $J \subset I$. A basis J is a basis for I, if $J \subseteq I$ and $V(J) = V(I)$. Any basis for M is called optimal. In particular, if S is an optimal basis, then

$$V(S) = V(M) = \emptyset, \text{ and consequently, } \theta(S) = \theta(M) = \theta^*. \tag{5.16}$$

From Helly's theorem, it follows that $D := \max\{|I| : I \text{ is a basis}\} \le n+1$. Given an optimal basis S, we can apply Corollary 5.10 to $\boldsymbol{f}_i^T \boldsymbol{x} + g_i z \le h_i, i \in S, (\boldsymbol{x}, z) \in \mathcal{K}_p^{n,1}$ and determine the feasibility of the original system that define the SOCP in $n^{O(n)}$ operations over $\tau n^{O(n)}$-bit numbers. Clarkson (1995)'s algorithm finds an optimal basis by performing expected $N = O(Dm + D^3 \sqrt{m \log m} \log m) \le m\mathrm{poly(n)}$ violation tests. Each of these checks whether $j \in V(I)$ for a sample set I of cardinality $O(D^2 \log D)$ and an index $j \in M \backslash I$. Note that the inclusion $j \in V(I)$ can be written as the sentence

$$\begin{aligned} V_I^j := \forall (\boldsymbol{x}, z), (\boldsymbol{y}, w) \in \mathbb{R}^{n+1} \quad \forall \theta, \rho \in \mathbb{R} \\ \{\{(\boldsymbol{x}^T \boldsymbol{x} \le z^2, z \ge 0) \wedge (\boldsymbol{y}^T \boldsymbol{y} \le w^2, w \ge 0) \wedge S_I(\boldsymbol{x}, z, \theta) \\ \wedge [S_I(\boldsymbol{y}, w, \rho) \implies (\theta \le \rho)] \wedge [S_I(\boldsymbol{y}, w, \theta) \implies (\|(\boldsymbol{x}, z)\|_2^2 \le \|(\boldsymbol{y}, w)\|_2^2)]\} \\ \implies (\boldsymbol{f}_j^T \boldsymbol{x} + g_j z > h_j + \theta)\}, \end{aligned} \tag{5.17}$$

where $S_I(\boldsymbol{x}, z, \theta)$ is the quantifier free formula

$$\left\{ \bigwedge_{i \in I} (\boldsymbol{f}_i^T \boldsymbol{x} + g_i z \le h_i + \theta) \wedge (\|(\boldsymbol{x}, z)\|_2^2 \le R^2) \right\}.$$

Each violation test can thus be represented by a sentence in prenex form with $O(|I|) \leq O(n)$ polynomial inequalities of degree 2 in $O(n)$ variables. Note also that the coefficient of these polynomial inequalities are integers of bit size $B \leq \max\{\tau, \log R\} = \tau \min\{m,n\}^{O(\min\{m,n\})}$. Now from Theorem 2.5 it follows that each violation test can be accomplished in $n^{O(n)}$ operations over $\tau n^{O(n)}$-bit numbers. But the expected number of violation tests is bounded in $m\mathrm{poly}(\mathrm{n})$. Hence, we conclude that for all n and m, testing the feasibility of a SOCP requires expected $mn^{O(n)}$ operations over $\tau n^{O(n)}$-bit numbers. □

Remark 5.12. *Our complexity bound from Theorem 5.11 heavily relies on the result by Renegar (1992a) (Theorem 2.5). This latter result has been previously improved, e.g., in (Basu et al., 2007, Theorem 14.14), where the authors obtain a similar algebraic complexity but a slight improvement in terms of bit size for the output and integers appearing in the intermediate computations. In particular the intermediate integers have bit sizes that are linear in the input bit size but does not depend on the number of polynomial (in)equalities. However in our case this does not yield any improvements because* $\log R$ *still depends polynomially on the number of (in)equalities.*

In what follows we analyze the complexity bounds for other special cases for the values of p in ($\mathbf{F}_p$).

Theorem 5.13. *The feasibility of* ($\mathbf{F}_p$) *where* $p = r \in 2\mathbb{N}$ *is a positive even number can be tested in* $m(r\min\{m,n\})^{O(n)}$ *arithmetic operations over* $\tau(r\min\{m,n\})^{O(n)}$*-bit numbers.*

Proof. It is enough to follow the proof of Theorem 5.11, while relying on Corollary 5.10 instead of Theorem 5.9, selecting $R = R(p,n,m,\tau)$ (5.10), and replacing the sentence (5.17) by the following one

$$
\begin{aligned}
V_I^j := \forall (\boldsymbol{x},z),(\boldsymbol{y},w) \in \mathbb{R}^{n+1} \quad \forall \theta,\rho \in \mathbb{R} \\
\Bigg\{\Bigg\{ \left(\sum_{k=1}^n x_k^r \leq z^r, z \geq 0 \right) \wedge \left(\sum_{k=1}^n y_k^r \leq w^r, w \geq 0 \right) \wedge S_I(\boldsymbol{x},z,\theta) \\
\wedge\, [S_I(\boldsymbol{y},w,\rho) \implies (\theta \leq \rho)] \wedge [S_I(\boldsymbol{y},w,\theta) \implies (\|(\boldsymbol{x},z)\|_2^2 \leq \|(\boldsymbol{y},w)\|_2^2)] \Bigg\} \\
\implies (\boldsymbol{f}_j^T \boldsymbol{x} + g_j z > h_j + \theta) \Bigg\}.
\end{aligned}
$$

□

5.3.2 Complexity Bounds on General ($\mathbf{F}_p$)

Once it is shown the complexity of SOCP, the proof can be modified to derive the complexities of more general cases.

Theorem 5.14. *Let $p = \frac{r}{s} \in \mathbb{Q}$, with $r > s \in \mathbb{N}$ and $\gcd(r, s) = 1$. The feasibility of ($\mathbf{F}_p$) can be tested in $\min\{[r(m+n)]^{O(n)}, m(rn)^{O(n^2)}\}$ arithmetic operations over $\tau \min\{[r(m+n)]^{O(n)}, (rn)^{O(n^2)}\}$–bit numbers.*

Proof. It is enough to follow the proof of Theorem 5.11, while relying on Corollary 5.10 instead of Theorem 5.9, selecting $R = R(p, n, m, \tau)$ (5.10), and replacing the sentence (5.17) by

$$\begin{aligned} V_I^j := \forall (\boldsymbol{x}, z), (\boldsymbol{y}, w) \in \mathbb{R}^{n+1}, \forall \theta, \rho \in \mathbb{R}\{\{(\|\boldsymbol{x}\|_p \le z, \|\boldsymbol{y}\|_p \le w) \wedge S_I(\boldsymbol{x}, z, \theta) \\ \wedge [S_I(\boldsymbol{y}, w, \rho) \implies (\theta \le \rho)] \wedge [S_I(\boldsymbol{y}, w, \theta) \implies (\|(\boldsymbol{x}, z)\|_2^2 \le \|(\boldsymbol{y}, w)\|_2^2)]\} \\ \implies (\boldsymbol{f}_j^T \boldsymbol{x} + g_j z > h_j + \theta)\}. \end{aligned}$$

By Theorem 5.3 the membership of $(\boldsymbol{x}, z)$ in $\mathcal{K}_p^{n,1}$ can be expressed by the formula (5.3) where $\lhd$ stands for $\le$. Then V_I^j is a sentence involving 2 quantifiers, $O(n)$ polynomial inequalities of degree at most r in $O(n^2)$ variables. The value of B remains unchanged. So for fixed dimension, Clarkson (1995)'s algorithm yields a better bound. □

The result below is the analog of (Porkolab and Khachiyan, 1997, Theorem 5.4).

Corollary 5.15. *Given $r \in 2\mathbb{N}$, the feasibility of ($\mathbf{F}_p$) with $p = \frac{r}{r-1}$ can be tested in $m(r \min\{m, n\})^{O(\min\{m, n^2\})}$ arithmetic operations over $\tau(r \min\{m, n\})^{O(\min\{m, n^2\})}$-bit numbers.*

Proof. This is a direct consequence of Theorem 5.14 and Theorem 5.9. □

Theorem 5.16. *Given an optimal basis S of (5.11), in $(rn)^{O(n \min\{m,n\})}$ operations over $\tau(rn)^{O(n \min\{m,n\})}$-bit numbers we can find a system of univariate polynomial inequalities with integer coefficients such that θ^* is the only real solution of the system. In particular, θ^* is a root of a nontrivial polynomial $p(\theta) \in \mathbb{Z}[\theta]$ such that $\log \mathrm{height}(p) = \tau(rn)^{O(n \min\{m,n\})}$.*

Proof. Assume without loss of generality that the given basis S coincides with M. In particular, $m \le n + 1$. From von Neumman's minimax theorem and

(5.5), it follows that for $R \geq 0$

$$
\begin{aligned}
\theta^* &= \min_{(\boldsymbol{x},z)\in\mathcal{K}_p^{n,1}(R)} \max_{\boldsymbol{\lambda}\in\Delta_m} \sum_{i=1}^m \lambda_i(\boldsymbol{f}_i^T\boldsymbol{x} + g_i z - h_i) \\
&= \max_{\boldsymbol{\lambda}\in\Delta_m} \min_{(\boldsymbol{x},z)\in\mathcal{K}_p^{n,1}(R)} \left\{ \left(\sum_{i=1}^m \lambda_i \boldsymbol{f}_i^T\right)\boldsymbol{x} + \left(\sum_{i=1}^m \lambda_i g_i\right) z - \sum_{i=1}^m \lambda_i h_i \right\} \\
&= \max_{\boldsymbol{\lambda}\in\Delta_m} \left\{ \min\left[0, R\left(\sum_{i=1}^m \lambda_i g_i - \left\|\sum_{i=1}^m \lambda_i \boldsymbol{f}_i\right\|_q\right)\right] - \sum_{i=1}^m \lambda_i h_i \right\}.
\end{aligned}
$$

Consider the formula $\Lambda(\theta)$ defined as

$$
\forall \boldsymbol{\lambda} \in \Delta_m \left\{ \min\left[0, R\left(\sum_{i=1}^m \lambda_i g_i - \left\|\sum_{i=1}^m \lambda_i \boldsymbol{f}_i\right\|_q\right)\right] - \sum_{i=1}^m \lambda_i (h_i + \theta) \leq 0 \right\},
$$

where $R = R(p, n, m, \tau)$ (5.10). This formula states that $\theta \geq \theta^*$, and it can be written as follows

$$
\begin{aligned}
&\forall \boldsymbol{\lambda} \in \mathbb{R}^m \quad \exists (\boldsymbol{t}, w) \in \mathbb{R}^{n+1} \Bigg\{ \left[\lambda_1 \geq 0, \ldots, \lambda_m \geq 0, \quad \sum_{i=1}^m \lambda_i = 1 \right] \implies \\
&\qquad \Bigg\{ \Bigg[t_1 \geq 0, \ldots, t_n \geq 0, \sum_{j=1}^n t_j = w, \\
&\qquad \bigwedge_{j=1}^n \left[\left[\left(\sum_{i=1}^m \lambda_i f_{ij} \right)^r = w^s t_j^{r-s} \right] \vee \left[-\left(\sum_{i=1}^m \lambda_i f_{ij} \right)^r = w^s t_j^{r-s} \right] \right] \Bigg] \\
&\wedge \left[\left(\sum_{i=1}^m \lambda_i (h_i + \theta) \geq 0 \right) \vee \left(R\left(\sum_{i=1}^m \lambda_i g_i - w \right) - \sum_{i=1}^m \lambda_i (h_i + \theta) \leq 0 \right) \right] \Bigg\} \Bigg\}.
\end{aligned}
$$

Now θ^* is the only real solution of $\Lambda^*(\theta) := \forall \theta' \in \mathbb{R}\{\Lambda(\theta) \wedge [\Lambda(\theta') \implies (\theta \leq \theta^*)]\}$. By consecutively applying Theorem 2.4 to $\Lambda(\theta)$ and $\Lambda^*(\theta)$, the latter formula can be transformed into a quantifier free formula $\Lambda^{**}(\theta)$. This requires $[r(m+n)]^{O(mn)} \leq (rn)^{O(n\min\{m,n\})}$ operations with $\max\{\tau, \log R\}[r(m+n)]^{O(mn)} \leq \tau(rn)^{O(n\min\{m,n\})}$-bit numbers. The formula $\Lambda^{**}(\theta)$ is composed of univariate polynomial relations $p(\theta) \lhd 0$, where $\lhd \in \{\leq, <, =, \neq, >, \geq\}$. Since θ^* is the only real solution of $\Lambda^{**}(\theta)$, this formula can be transformed into an equivalent system of polynomial inequalities, which must contain a polynomial p such that $p(\theta^*) = 0$. □

Theorem 5.17. *Given $r \in 2\mathbb{N}$, let $p = \frac{r}{r-1}$. Then we can replace the bounds of Theorem 5.16 by $(r\min\{m,n\})^{O(\min\{m,n\})}$ and $\tau(r\min\{m,n\})^{O(\min\{m,n\})}$.*

Proof. It is enough to follow the proof of Theorem 5.16 by relying on Theorem 5.7 instead of Theorem 5.6, and writing the formula $\Lambda(\theta)$ as

$$\forall \boldsymbol{\lambda} \in \mathbb{R}^m \quad \exists w \in \mathbb{R} \Bigg\{ \left[\lambda_1 \geq 0, \ldots, \lambda_m \geq 0, \quad \sum_{i=1}^{m} \lambda_i = 1 \right] \implies \Bigg\{ \left[\sum_{j=1}^{n} \left(\sum_{i=1}^{m} \lambda_i f_{ij} \right)^r = w^r, w \geq 0 \right] \wedge \left[\left(\sum_{i=1}^{m} \lambda_i (h_i + \theta) \geq 0 \right) \vee \left(R \left(\sum_{i=1}^{m} \lambda_i g_i - w \right) - \sum_{i=1}^{m} \lambda_i (h_i + \theta) \leq 0 \right) \right] \Bigg\} \Bigg\}.$$

□

Remark 5.18. *The minimal polynomial of an algebraic number α is the primitive irreducible polynomial $p \in \mathbb{Z}[x]$ such that $p(\alpha) = 0$ and the leading coefficient of p is positive. The* height *of α is the height of its minimal polynomial. Theorem 5.17 and the well-known Mignotte's inequality recalled in Proposition 2.6 show that* $\log \mathrm{height}(\theta^*) = \tau(r\min\{m,n\})^{O(\min\{m,n\})}$.

Theorem 5.16 and Theorem 5.17 immediately imply Theorem 5.8.

Proof of Theorem 5.8. Since the problem (**F**$_p$) is infeasible, one has $\theta^* > 0$. Theorem 5.16 and Theorem 5.17 imply that the positive algebraic number θ^* is a root of a nontrivial polynomial $p \in \mathbb{Z}[x]$ with integer coefficients of bit sizes $\tau(rn)^{O(n\min\{m,n\})}$ and $\tau(r\min\{m,n\})^{O(\min\{m,n\})}$, respectively. Proposition 2.6 implies that $\theta^* \geq \frac{1}{1+\mathrm{height}(p)}$, yielding the desired result. □

Remark 5.19. *If $p = r \in 2\mathbb{N}$, then one can write the formula $\Lambda(\theta)$ from the proof of Theorem 5.16 as*

$$\forall (\boldsymbol{x}, z) \in \mathbb{R}^{n+1} \Bigg\{ \bigwedge_{i \in M} [\boldsymbol{f}_i^T \boldsymbol{x} + g_i z - (h_i + \theta) \leq 0], \quad \sum_{j=1}^{b} x_j^r \leq z^r, z \geq 0, \|(\boldsymbol{x}, z)\|_2^2 \leq R^2 \Bigg\}, \tag{5.18}$$

with $\log R \leq \tau(\min\{m,n\}r)^{O(n)}$. The bounds of Theorems 5.8 and 5.16 become $(\min\{m,n\}r)^{O(n)}$ and $\tau(\min\{m,n\}r)^{O(n)}$.

5.4 Generalization to Several p–Order Cone Constraints

In this section, we generalize our results to the case of more than one p–order cone constraints. Namely, given $d \in \mathbb{N}$ and $n_1, \ldots, n_d \in \mathbb{N}$, we consider the norm constraints $(\boldsymbol{x}_k, z_k) \in \mathcal{K}_p^{n_k,1}, k = 1, \ldots, d$. With $n := n_1 + \cdots + n_d$, let $(\boldsymbol{x}, \boldsymbol{z}) := (\boldsymbol{x}_1; \ldots; \boldsymbol{x}_d; z_1; \ldots; z_d) \in \mathbb{R}^{n+d}$ be the full vector of variables. Given $p = \frac{r}{s} \in \mathbb{Q}$, with $r > s \in \mathbb{N}$ and $\gcd(r,s) = 1$, we consider the p–order feasibility problem that consists of determining whether there exists a real vector $(\boldsymbol{x}, \boldsymbol{z}) \in \mathbb{R}^{n+d}$ such that

$$\begin{aligned} F_1\boldsymbol{x}_1 + G_1 z_1 + \cdots + F_d\boldsymbol{x}_d + G_d z_d &\leq H, \\ (\boldsymbol{x}_k, z_k) \in \mathcal{K}_p^{n_k,1}, \quad k &= 1, \ldots, d, \end{aligned} \tag{5.19}$$

where $F_k \in \mathbb{Z}^{m \times n_k}, G_k, H \in \mathbb{Z}^m$ for $m \in \mathbb{N}^*$. We assume that all tuples $(\boldsymbol{x}_k, z_k)$ are independent. The above problem involves $n + d$ variables and $m + d$ constraints. If this independence assumption does not hold then one can always introduce additional variables satisfying it and encode the dependencies via linear equality constraints.

The result of Theorem 5.9 can be generalized as follows.

Theorem 5.20. *Let us consider (5.19) and assume that all tuples $(\boldsymbol{x}_k, z_k)$ are independent.*
If $p = \frac{r}{s} \in \mathbb{Q}$, with $r > s \in \mathbb{N}$ and $\gcd(r,s) = 1$, then the feasibility of (5.19) can be tested in $[(m + n + d)r]^{O(n+d)}$ arithmetic operations over $\tau[(m + n + d)r]^{O(n+d)}$–bit numbers.
If $p = r \in 2\mathbb{N}$ then the feasibility of (5.19) can be tested in $[(m + d)r]^{O(n+d)}$ arithmetic operations over $\tau[(m + d)r]^{O(n+d)}$–bit numbers.
If $p = \frac{r}{r-1}$ with $r \in 2\mathbb{N}$ then the feasibility of (5.19) can be tested in $[(m + d)r]^{O(md^2)}$ arithmetic operations over $\tau[(m + d)r]^{O(md^2)}$–bit numbers.

Proof. We sketch the proof by emphasizing the main differences with respect to the single constraint case.

- Thanks to the independence assumption, Equation (5.4) in Lemma 5.4 can be generalized as follows:

$$\min_{\substack{(\boldsymbol{x}_k, z_k) \in \mathcal{K}_p^{n_k,1}: \\ k=1,\ldots,d}} \left\{ \sum_{k=1}^{d} (\boldsymbol{f}_k^T \boldsymbol{x}_k + g_k z_k) : z_1 = R_1, \ldots, z_d = R_d \right\} = \sum_{k=1}^{d} R_k (g_k - \|\boldsymbol{f}_k\|_q),$$

where $\|\cdot\|_q$ is the dual of the $\|\cdot\|_p$ norm, i.e., q is such that $\frac{1}{p}+\frac{1}{q}=1$.

- Lemma 5.5 becomes $\|(\boldsymbol{x},\boldsymbol{z})\|_2 \leq R$, where $\log R = \tau[(\min\{m,n\}+d)r]^{O(n+d)}$.
- In Theorem 5.6, $\Theta(R)$ is replaced by $\Theta(R_1,\ldots,R_d)$ defined as

$$\min_{\substack{(x_k,z_k)\in\Omega_{R_k}:\\ k=1,\ldots,d}} \max\left\{\sum_{k=1}^{d}\left(\boldsymbol{f}_{1k}^T\boldsymbol{x}_k+g_{1k}z_k\right)-h_1,\ldots,\sum_{k=1}^{d}\left(\boldsymbol{f}_{mk}^T\boldsymbol{x}_k+g_{mk}z_k\right)-h_m\right\},$$

where $\Omega_{R_k}=\{(\boldsymbol{x},z)\in\mathcal{K}_p^{n_k,1}: z=R_k\}$.

For any $R_1,\ldots,R_d\geq 0$ and considering Δ_m as in (2.3),

$$\begin{aligned}
\Theta(R_1,\ldots,R_d) &= \min_{\substack{(x_k,z_k)\in\Omega_{R_k}:\\ k=1,\ldots,d}} \max_{\boldsymbol{\lambda}\in\Delta_m}\sum_{i=1}^{m}\lambda_i\left(\sum_{k=1}^{d}\left(\boldsymbol{f}_{ik}^T\boldsymbol{x}_k+g_{ik}z_k\right)-h_i\right)\\
&= \max_{\boldsymbol{\lambda}\in\Delta_m}\min_{\substack{(x_k,z_k)\in\Omega_{R_k}:\\ k=1,\ldots,d}}\left[\sum_{k=1}^{d}\left(\left(\sum_{i=1}^{m}\lambda_i\boldsymbol{f}_{ik}^T\right)\boldsymbol{x}_k+\left(\sum_{i=1}^{m}\lambda_i g_{ik}\right)z_k\right)-\sum_{i=1}^{m}\lambda_i h_i\right]\\
&= \max_{\boldsymbol{\lambda}\in\Delta_m}\left[\sum_{k=1}^{d}R_k\left(\sum_{i=1}^{m}\lambda_i g_{ik}-\left\|\sum_{i=1}^{m}\lambda_i\boldsymbol{f}_{ik}\right\|_q\right)-\sum_{i=1}^{m}\lambda_i h_i\right].
\end{aligned}$$

Then $\Phi(R)$ is replaced by $\Phi(R_1,\ldots,R_d)$ defined as

$$\forall\boldsymbol{\lambda}\in\Delta_m\left\{\sum_{k=1}^{d}R_k\left(\sum_{i=1}^{m}\lambda_i g_{ik}-\left\|\sum_{i=1}^{m}\lambda_i\boldsymbol{f}_{ik}\right\|_q\right)-\sum_{i=1}^{m}\lambda_i h_i\leq 0 \right.$$
$$\left.\wedge\,(R_1\geq 0,\ldots,R_d\geq 0)\right\}.$$

By Theorem 5.3, $\Phi(R)$ can be rewritten in the standard form (SF) as follows

$$\forall \boldsymbol{\lambda} \in \mathbb{R}^m, \exists (\boldsymbol{t}_k, w_k)_{k=1}^d \in \mathbb{R}^{n+d} \Bigg\{ \Bigg\{ \left[\wedge_{i=1}^m \lambda_i \geq 0, \quad \sum_{i=1}^m \lambda_i = 1 \right] \implies$$
$$\left[\sum_{j=1}^{n_1} t_{1j} = w_1, \ldots, \sum_{j=1}^{n_d} t_{dj} = w_d, \bigwedge_{k=1}^d \bigwedge_{j=1}^{n_k} t_{kj} \geq 0, \right.$$
$$\left. \bigwedge_{k=1}^d \bigwedge_{j=1}^{n_k} \left[\left[\left(\sum_{i=1}^m \lambda_i f_{ikj} \right)^r = w_k^s t_{kj}^{r-s} \right] \vee \left[- \left(\sum_{i=1}^m \lambda_i f_{ikj} \right)^r = w_k^s t_{kj}^{r-s} \right] \right] \right],$$
$$\left. \sum_{k=1}^d R_k \left(\sum_{i=1}^m \lambda_i g_{ik} - w_k \right) - \sum_{i=1}^m \lambda_i h_i \leq 0 \right] \Bigg\} \wedge (R_1 \geq 0, \ldots, R_d \geq 0) \Bigg\}.$$

yielding $\|(\boldsymbol{x}, \boldsymbol{z})\|_2 \leq R$, with $\log R = \tau[(n+d)r]^{O(\min\{m,n+d\}(n+d)d)}$.

- As in Theorem 5.7, $\Phi(R)$ can be rewritten in the standard form

$$\forall \boldsymbol{\lambda} \in \mathbb{R}^m \quad \exists \boldsymbol{w} \in \mathbb{R}^d \Bigg\{ \Bigg\{ \left[\lambda_1 \geq 0, \ldots, \lambda_m \geq 0, \quad \sum_{i=1}^m \lambda_i = 1 \right] \implies$$
$$\left[\bigwedge_{k=1}^d \sum_{j=1}^n \left(\sum_{i=1}^m \lambda_i f_{ikj} \right)^r = w_k^r, w_1, \ldots, w_d \geq 0 \right.$$
$$\left. \sum_{k=1}^d R_k \left(\sum_{i=1}^m \lambda_i g_{ik} - w_k \right) - \sum_{i=1}^m \lambda_i h_i \leq 0 \right] \Bigg\} \wedge (R_1 \geq 0, \ldots, R_d \geq 0) \Bigg\},$$

yielding $\|(\boldsymbol{x}, \boldsymbol{z})\|_2 \leq R$, with $\log R = \tau[(\min\{m,n\}+d)r]^{O(\min\{m,n+d\}d^2)}$.

□

Similarly, we can extend the results of Theorem 5.11, Theorem 5.13, Corollary 5.15 and Theorem 5.14, respectively.

Theorem 5.21. *Let us consider (5.19) and assume that all tuples $(\boldsymbol{x}_k, z_k)$ are independent.*
If $p = 2$, the feasibility of (5.19) can be tested in $m[\min\{m,n\}+d]^{O(\min\{n+d,md^2\})}$ arithmetic operations over $\tau[\min\{m,n\}+d]^{O(\min\{n+d,md^2\})}$–bit numbers.
If $p = r \in 2\mathbb{N}$, the feasibility of (5.19) can be tested in $m[r\min\{m,n\}+d]^{O(n+d)}$ arithmetic operations over $\tau[r\min\{m,n\}+d]^{O(n+d)}$–bit numbers.
If $r \in 2\mathbb{N}$ and $p = \frac{r}{r-1}$, the feasibility of (5.19) can be tested in either $[r(m+d)]^{O(md^2)}$ arithmetic operations over $\tau[r(m+d)]^{O(md^2)}$-bit numbers or $m[r(n+$

$d)]^{O((n+d)n)}$ *arithmetic operations over* $\tau[r(n+d)]^{O(\min\{m,n+d\}d^2+(n+d)n)}$*–bit numbers.*

If $p = \frac{r}{s} \in \mathbb{Q}$, *with* $r > s \in \mathbb{N}$ *and* $\gcd(r,s) = 1$, *the feasibility of* (5.19) *can be tested in either* $[r(m+n+d)]^{O(n+d)}$ *arithmetic operations over* $\tau[r(m+n+d)]^{O(n+d)}$*-bit numbers or* $m[r(n+d)]^{O((n+d)n)}$ *arithmetic operations over* $\tau[r(n+d)]^{O((\min\{m,d\}+n)(n+d)d)}$*–bit numbers.*

We also emphasize that in the case of considering several cone constraints with distinct values of $p_i = \frac{r_i}{s_i} \in \mathbb{Q}$, with $r_i > s_i \in \mathbb{N}$ and $\gcd(r_i, s_i) = 1$, complexity estimates are obtained in a similar way as above, by simply replacing r by $\max\{r_1, \ldots, r_d\}$.

Chapter VI

Applications

Prometeo robó el fuego a los Dioses y se lo dio a los hombres.
Por ello, fue encadenado a una roca y torturado por toda la eternidad.
— Apolodoro, *Biblioteca*, libro I, 7

This chapter is the end of the road from theory to practice. It is divided in sections according to the nature of how the theory is applied in each case.

In Section 6.1, we emphasize how the complexity bounds are applied to optimization problems that involve p–order cones.

The goal of Section 6.2 is propose a novel location problem to optimally locate a given number of facilities in the Euclidean space, and decide their coverage radii based on different features to maximize the overall coverage of a given set of users. The radii will represent an attraction measure based on Newton's law of universal gravitation. We propose a generalized power cone program to solve it.

Eventually, Section 6.3 yields a mathematical optimization-based framework to determine the location of leak detection devices along a network. Assuming that the devices are endowed with a known coverage area.

6.1 Complexity Bounds for Some Significant p–Order Cone Programs

The complexity of the feasibility problem studied in Chapter V has a direct impact in the complexity of solving, with some tolerance $\varepsilon > 0$, optimization problems involving p–order cones. For instance, if the objective function of the problem ranges in $[\texttt{lb}, \texttt{ub}]$, by binary search approaches, the complexity of solving the optimization problem equals $\log_2(\frac{\texttt{ub}-\texttt{lb}}{\varepsilon})$ times the complexity of the feasibility oracle. In what follows, we provide detailed complexity results for some optimization problems of interest in different fields.

6.1.1 Norm Minimization

We start with the classical application, *ℓ_p–norm minimization problem* (p-NMP), that is defined in standard form as

$$\begin{aligned} &\text{minimize } \|\boldsymbol{x}\|_p \\ &\text{subject to } A\boldsymbol{x} \le \boldsymbol{b}, \end{aligned} \tag{p-NMP}$$

where $A \in \mathbb{Z}^{m\times n}$ and $\boldsymbol{b} \in \mathbb{Z}^m$. Geometrically, this program stands for the vector closest to zero ($\mathbf{0}$) in the half-space of the normed space $(\mathbb{R}^n, \|\cdot\|_p)$ defined by $A\boldsymbol{x} \le \boldsymbol{b}$. This problem has an extended representation to a p–order cone program by means of an auxiliary variable $z \in \mathbb{R}$ as below:

$$\begin{aligned} \text{minimize} \quad & z \\ \text{subject to} \quad & A\boldsymbol{x} \le \boldsymbol{b}, \\ & (\boldsymbol{x}, z) \in \mathcal{K}_p^{n,1}. \end{aligned} \tag{6.1}$$

The feasibility problem associated to (6.1) corresponds to an instance of ($\mathbf{F}_p$), with $\boldsymbol{f}_i = \boldsymbol{a}_i$ being the ith column of A, $i = 1, \dots, m$; $g_1 = \dots = g_m = 0$, and $h_1 = b_1, \dots, h_m = b_m$.

Corollary 6.1. *Let us assume that the coefficients of the input data A, b have bit size at most τ, and let $N \in \mathbb{Z}_+, \varepsilon = 2^{-N}$.*

If $p = \frac{r}{s} \in \mathbb{Q}$ with $r > s \in \mathbb{N}$ and $\gcd(r,s) = 1$, the feasibility of (6.1) can be tested in $\min\{[r(m+n)]^{O(n)}, m(rn)^{O(n^2)}\}$ arithmetic operations over $\tau\min\{[r(m+n)]^{O(n)}, (rn)^{O(n^2)}\}$–bit numbers. If the problem is feasible, then according to the proof of Theorem 5.6, there exists a solution $(\boldsymbol{x}, z)$ satisfying $z \le R$, with $\log R \le \tau(rn)^{O(n\min\{m,n\})}$, yielding an upper bound for (p-NMP).
An ε–optimal solution of (p-NMP) can be obtained through binary search in $(\tau + N)\min\{[r(m+n)]^{O(n)}, m(rn)^{O(n^2)}\}$ arithmetic operations.

For the Euclidean norm minimization (2-NMP), feasibility can be tested in $m\min\{m,n\}^{O(\min\{m,n\})}$ arithmetic operations over $\tau\min\{m,n\}^{O(\min\{m,n\})}$ bit-numbers, and we get an upper bound of bit size $\tau\min\{m,n\}^{O(\min\{m,n\})}$ for the *problem* (2-NMP)*. An ε–optimal solution of* (2-NMP) *can be obtained through binary search in* $(\tau + N)m \min\{m, n\}^{O(\min\{m,n\})}$ *arithmetic operations.*

Proof. The two feasibility estimates follow directly from Theorem 5.14 and Theorem 5.11, respectively. As mentioned at the beginning of this section, the optimization cost of the binary search procedure depends on the available lower and upper bounds on the minimum. In the case of norm minimization, we can obviously select 0 as a lower bound, and an upper bound bit size according to the one involved in the proof of Theorem 5.6. □

Our complexity results can be similarly applied to minimize sum or maximum of norms, see § 2.2 from Alizadeh and Goldfarb (2003) for the corresponding formulations as SOCPs in the case of Euclidean norms.

6.1.2 Support Vector Machines

A slightly different version of the norm minimization problem appears in supervised classification problems, in the so-called ℓ_p*–Support Vector Machines* (see, e.g., Blanco et al., 2020b). Given a training sample

$$\{(x_1, y_1), \ldots, (x_m, y_m)\} \subseteq \mathbb{Q}^m \times \{-1, +1\},$$

the goal is to construct an hyperplane-based classifier separating the two classes (-1 and 1) by maximizing the ℓ_p–norm separation between them. The problem is stated as:

$$\begin{aligned} \text{minimize} \quad & \|\omega\|_p + C\sum_{i=1}^m \xi_i \\ \text{subject to} \quad & y_i(\omega^T x_i + b) \geq 1 - \xi_i, \quad \forall i = 1, \ldots, m, \\ & \omega \in \mathbb{R}^n, b \in \mathbb{R}, \\ & \xi \geq 0. \end{aligned} \tag{ℓ_p-SVM}$$

where ω and b are the coefficients of the separating hyperplane ($H = \{\omega^T z + b : z \in \mathbb{R}^n\}$), and ξ are the missclassification errors. The parameter $C > 0$ allows one to find a trade-off between the margin separation and the missclassification.

Note that this problem can be rewritten in the shape of the above norm minimization problem problem as follows:

$$\begin{array}{ll} \text{minimize} & z + C\sum_{i=1}^{m} \xi_i \\ \text{subject to} & y_i(\boldsymbol{\omega}^T x_i + b) + \xi_i \geq 1, \quad \forall i = 1, \ldots, m, \\ & \boldsymbol{\omega} \in \mathbb{R}^n, b \in \mathbb{R}, \\ & \boldsymbol{\xi} \geq 0, \\ & (\boldsymbol{\omega}, z) \in \mathcal{K}_p^{n,1} \end{array}$$

The complexity of testing feasibility of the above problem is very similarly to the case of norm minimization, stated in Corollary 6.1.

Corollary 6.2. *Assume that the coefficients of the input data $(C, \boldsymbol{x}_i)$ are rational numbers with bit size at most τ, and let $N \in \mathbb{Z}_+, \varepsilon = 2^{-N}$.*
If $p = \frac{r}{s} \in \mathbb{Q}$ with $r > s \in \mathbb{N}$ and $\gcd(r,s) = 1$, then the feasibility of problem (ℓ_p-SVM) can be tested in $\min\{[r(m+n)]^{O(n)}, m(rn)^{O(n^2)}\}$ arithmetic operations over $\tau \min\{[r(m+n)]^{O(n)}, (rn)^{O(n^2)}\}$-bit numbers. An ε–optimal solution of (ℓ_p-SVM) can be obtained through binary search in $(\tau + N)\min\{[r(m+n)]^{O(n)}, m(rn)^{O(n^2)}\}$ arithmetic operations.
If $p = 2$, it can be tested in $m \min\{m,n\}^{O(\min\{m,n\})}$ arithmetic operations over $\tau \min\{m,n\}^{O(\min\{m,n\})}$-bit numbers.
An ε–optimal solution of (ℓ_p-SVM) can be obtained through binary search in $(\tau + N)m \min\{m,n\}^{O(\min\{m,n\})}$ arithmetic operations.

6.1.3 Robust Least Squares

Least squares problems consist of finding the coefficient of a linear hyperplane that minimize the sum of the squares differences between the *predicted* and the *observed* values. Then, given a dataset $\{(\boldsymbol{x}_1, y_1), \ldots, (\boldsymbol{x}_k, y_k)\} \in \mathbb{R}^n \times \mathbb{R}$, with input data X and response data $\boldsymbol{y}$, a least square problem can be formulated as:

$$\min_{\boldsymbol{\omega} \in \mathbb{R}^n} \|X\boldsymbol{\omega} - \boldsymbol{y}\|_2^2$$

In case the data are uncertain, in robust least squares (Bertsimas and Copenhaver, 2018; El Ghaoui and Lebret, 1996) allows to derive solutions to the system by incorporating uncertainty sets for the parameters X and $\boldsymbol{y}$ in the above problem. Specifically, assuming that

$$\mathcal{U}_X = \{\widetilde{X} \in \mathbb{R}^{n\times k} : \|\widetilde{X}\|_p \leq \nu_X\}$$
$$\mathcal{U}_y = \{\widetilde{\boldsymbol{y}} \in \mathbb{R}^{k} : \|\widetilde{\boldsymbol{y}}\|_p \leq \nu_{\boldsymbol{y}}\}$$

the *robust least squares* method is stated as the following problem:

$$\min_{\substack{\boldsymbol{\omega}\in\mathbb{R}^n\\ \widetilde{X}\in\mathcal{U}_X,\widetilde{\boldsymbol{y}}\in\mathcal{U}_y}} \|(X+\widetilde{X})\boldsymbol{\omega} - (\boldsymbol{y}+\widetilde{\boldsymbol{y}})\|_2^2$$

Bertsimas and Copenhaver (2018) proved that the above problem can be reformulated as follows:

$$\min_{\boldsymbol{\omega}\in\mathbb{R}^n} \|X\boldsymbol{\omega} - \boldsymbol{y}\|_2^2 + \nu_X\|\boldsymbol{\omega}\|_q + \nu_{\boldsymbol{y}}$$

where $\|\cdot\|_q$ is the dual of the $\|\cdot\|_p$ norm, i.e., q is such that $\frac{1}{p}+\frac{1}{q}=1$. Thus, the above problem can be reformulated as a p–OCP:

$$\begin{array}{ll} \text{minimize} & \|X\boldsymbol{\omega} - \boldsymbol{y}\|_2^2 + \nu_X z + \nu_{\boldsymbol{y}} \\ \text{subject to} & \boldsymbol{\omega} \in \mathbb{R}^n, \\ & z \in \mathbb{R}, \\ & (\boldsymbol{\omega}, z) \in \mathcal{K}_q^{n,1}, \end{array}$$

which can be solved with a similar complexity as the one in Corollary 6.2 from the previous subsection.

6.1.4 Continuous Locations Problems

One of the foundational problems in facility location is the Weber problem (Weber, 1909; Fekete et al., 2005). Given a set of points $\mathcal{X} = \{\boldsymbol{x}_1, \ldots, \boldsymbol{x}_d\} \subset \mathbb{R}^n$, the goal is to find a point $\boldsymbol{x} \in \mathbb{R}^n$ minimizing the sum of the (λ-weighted) distances to the points in $\mathcal{X}$. Using ℓ_p–norms, the problem is stated as:

$$\min_{\boldsymbol{x}\in\mathbb{R}^n} \sum_{i=1}^{d} \lambda_i \|\boldsymbol{x} - \boldsymbol{x}_i\|_p \tag{Weber}$$

which can be equivalently rewritten as a standard conic pOCP as follows:

$$\begin{array}{ll}\text{minimize} & \displaystyle\sum_{i=1}^{d} \lambda_i z_i \\ \text{subject to} & \boldsymbol{w}_i = \boldsymbol{x}_i - \boldsymbol{x}, \quad \forall i = 1, \ldots, d, \\ & \boldsymbol{w}_i \in \mathbb{R}^n, \quad \forall i = 1, \ldots, d, \\ & \boldsymbol{x} \in \mathbb{R}^n, \\ & (\boldsymbol{w}_i, z_i) \in \mathcal{K}_p^{n,1}, \quad \forall i = 1, \ldots, d.\end{array}$$

A generalized version of the Weber problem is the *continuous ordered median location problem* (COMP). Given weights $\omega_1, \ldots, \omega_d$ —one can assume without loss of generality that they are in $[-1, 1]$—; in the COMP, the distances from the points to the new points are sorted in nondecreasing order, and the $\boldsymbol{\omega}$-weights are assigned to the sorted sequence of distances, i.e., the COMP can be formulated as:

$$\min_{\boldsymbol{x} \in \mathbb{R}^n} \sum_{i=1}^{d} \omega_i \lambda_{(i)} \|\boldsymbol{x} - \boldsymbol{x}_{(i)}\|_p \tag{COMP}$$

where $\boldsymbol{x}_{(i)} \in \{\boldsymbol{x}_1, \ldots, \boldsymbol{x}_d\}$ such that

$$\|\boldsymbol{x} - \boldsymbol{x}_{(1)}\| \geq \|\boldsymbol{x} - \boldsymbol{x}_{(2)}\| \geq \cdots \geq \|\boldsymbol{x} - \boldsymbol{x}_{(d)}\|.$$

This unified framework allows, by adequately choosing the $\boldsymbol{\omega}$-weights, to model different problem of interest, as constructing the point minimizing the maximum of the distances from $\mathcal{X}$ to the new point —$\boldsymbol{\omega} = (1, 0, \ldots, 0)$, the sum of the m largest distances ($\boldsymbol{\omega} = (1, \overset{m}{\ldots}, 1, 0, \ldots, 0)$—; and many other measures. In case $\omega_1 \geq \ldots \geq \omega_d \geq \omega_{d+1} := 0$, it is known (Blanco et al., 2014) that this problem is convex and it can be rewritten as

$$
\begin{array}{ll}
\text{minimize} & \displaystyle\sum_{i=1}^{d}(u_i + v_i) \\
\text{subject to} & \boldsymbol{w}_i = \boldsymbol{x}_i - \boldsymbol{x}, \quad \forall i = 1, \ldots, d, \\
& u_i + v_k \geq \omega_i \lambda_k z_k, \quad \forall i, k = 1, \ldots, d, \\
& \boldsymbol{w}_i \in \mathbb{R}^n, \quad \forall i = 1, \ldots, d, \\
& \boldsymbol{x} \in \mathbb{R}^n, \\
& \boldsymbol{u}, \boldsymbol{v} \in \mathbb{R}^n, \\
& (\boldsymbol{w}_i, z_i) \in \mathcal{K}_p^{n,1}, \quad \forall i = 1, \ldots, d.
\end{array}
$$

As a straightforward consequence of Theorem 5.21, we obtain the following result.

Corollary 6.3. *Let* $p = \frac{r}{s} \in \mathbb{Q}$*, with* $r > s \in \mathbb{N}$*,* $\gcd(r, s) = 1$*, and let* $N \in \mathbb{Z}_+, \varepsilon = 2^{-N}$*. Assuming that the coefficients of the input data* $(\boldsymbol{x}_i, \lambda_i)$ *have bit size at most* τ*, then the feasibility of* (COMP) *can be tested in* $(r(d^2 + nd))^{O(nd)}$ *arithmetic operations over* $\tau(r(d^2 + nd))^{O(nd)}$*–bit numbers. An* ε*–optimal solution of* (COMP) *can be obtained through binary search in* $(\tau + N)(r(d^2 + nd))^{O(nd)}$ *arithmetic operations. If* $p = 2$*, it can be tested in* $(nd)^{O(nd)}$ *arithmetic operations over* $\tau(nd)^{O(nd)}$*–bit numbers, furthermore a* ε*–optimal solution of* (COMP) *can be obtained by binary search in* $(\tau + N)(nd)^{O(nd)}$ *arithmetic operations.*

Note that this complexity can be directly extended to mixed-norm continuous location problems where the distance to each of the points is measured with a different ℓ_p–norm. In this case, we can obtain complexity estimates by considering the worse case scenario, as mentioned at the end of Section 5.4. Similar results can also be obtained for the multiple-allocation multiple-facility counterpart of the above problem that is described in (Blanco et al., 2016).

6.1.5 Robust Linear Optimization

It has been shown by Ben-Tal and Nemirovski (1999) that the robust counterpart of a linear program with ellipsoidal uncertainties can be formulated as an SOCP. We use the notation from § 3.2 in Alizadeh and Goldfarb (2003).

Let us consider the *robust linear optimization problem*:

$$\begin{aligned} \text{minimize} \quad & \hat{\boldsymbol{c}}^T \hat{\boldsymbol{x}} \\ \text{subject to} \quad & \hat{A}\hat{\boldsymbol{x}} \leq \boldsymbol{b}, \\ & \boldsymbol{x} \in \mathbb{R}^n, \end{aligned} \tag{Robust-LP}$$

where the constraint data $\hat{A} \in \mathbb{R}^{m\times n}$ and $\boldsymbol{b} \in \mathbb{Z}^m$ are not known exactly. To ease the presentation, the above problem can be rewritten as

$$\begin{aligned} \text{minimize} \quad & \boldsymbol{c}^T \boldsymbol{x} \\ \text{subject to} \quad & A\boldsymbol{x} \leq \boldsymbol{0}, \\ & x_{n+1} = -1, \\ & \boldsymbol{x} \in \mathbb{R}^{n+1}, \end{aligned} \tag{6.2}$$

where $A = [\hat{A}, \boldsymbol{b}]$, $\boldsymbol{c} = (\hat{\boldsymbol{c}}, 0)$, $\boldsymbol{x} = (\hat{\boldsymbol{x}}, x_{n+1})$.

In Ben-Tal and Nemirovski (1999), the authors consider the case where the uncertainty set is the Cartesian product of ellipsoidal regions, one for each row $\boldsymbol{a}_i^T$ of A centered at some given row vector $\overline{\boldsymbol{a}}_i^T \in \mathbb{Z}^{n+1}$, namely in the set $\{\boldsymbol{a}_i \in \mathbb{R}^{n+1} : \boldsymbol{a}_i = \overline{\boldsymbol{a}}_i + B_i\boldsymbol{u}, \|\boldsymbol{u}\|_2 \leq 1\}$, where B_i is a positive semidefinite matrix. Then they show that the robust counterpart of (6.2) is

$$\begin{aligned} & \text{minimize } \boldsymbol{c}^T\boldsymbol{x} \\ & \text{subject to } \|B_i\boldsymbol{x}\|_2 \leq -\overline{\boldsymbol{a}}_i^T\boldsymbol{x}, \quad i = 1, \dots, m, \\ & \qquad x_{n+1} = -1, \\ & \qquad \boldsymbol{x} \in \mathbb{R}^{n+1}. \end{aligned} \tag{6.3}$$

Thanks to Theorem 5.21, the complexity of testing feasibility of (6.3) (resp. optimizing) can be readily estimated, yielding the following result.

Corollary 6.4. *Assume that $B_i \in \mathbb{Z}^{(n+1)\times(n+1)}$ is positive definite for each $i = 1, \dots, m$. Let τ be the maximal bit size of the input data $(\boldsymbol{c}, B_i^{-1}, \overline{\boldsymbol{a}}_i)$, and let $N \in \mathbb{Z}_+, \varepsilon = 2^{-N}$. The feasibility of* (Robust-LP) *can be tested in $(mn)^{O(mn)}$ arithmetic operations over $\tau(mn)^{O(mn)}$–bit numbers. An ε–optimal solution of* (Robust-LP) *can be obtained through binary search in $(\tau + N)(mn)^{O(mn)}$ arithmetic operations.*

Proof. For each $i = 1, \dots, m$, let us introduce auxiliary variable $\boldsymbol{y}^{(i)} := B_i\boldsymbol{x}$, so that $\boldsymbol{x} = B_i^{-1}\boldsymbol{y}^{(i)}$, and $z_i := -\overline{\boldsymbol{a}}_i^T B_i^{-1}\boldsymbol{y}^{(i)}$. Then each inequality constraint $\|B_i\boldsymbol{x}\|_2 \leq -\overline{\boldsymbol{a}}_i^T\boldsymbol{x}$ is equivalent to $\|\boldsymbol{y}^{(i)}\|_2 \leq z_i$. We have to consider the

$(m-1)n$ linear equality constraints $B_i^{-1}\boldsymbol{y}^{(i)} = B_j^{-1}\boldsymbol{y}^{(j)}$, for all $i \neq j$. The corresponding SOCP involves $n_{\text{socp}} = nm$ variables $(\boldsymbol{y}^{(1)}, \ldots, \boldsymbol{y}^{(m)})$ and $m_{\text{socp}} = m + (m-1)n$ linear equality constraints. The number d of cone constraints is equal to m. By Theorem 5.21, the feasibility of the resulting SOCP can be tested in $m_{\text{socp}}[\min\{m_{\text{socp}}, n_{\text{socp}}\} + m]^{O(\min\{n_{\text{socp}}+m, m_{\text{socp}}m^2\})}$ arithmetic operations over $\tau[\min\{m_{\text{socp}}, n_{\text{socp}}\} + m]^{O(\min\{n_{\text{socp}}+m, m_{\text{socp}}m^2\})}$-bit numbers. The desired result follows after noticing that $\min\{m_{\text{socp}}, n_{\text{socp}}\} + m = mn + m + \min\{0, m-n\} = O(mn)$ and $n_{\text{socp}} + m = mn + m \leq m_{\text{socp}}m^2$. $\square$

A similar complexity estimate can be obtained if some B_i is not invertible. In this case, for any $\boldsymbol{x}$ in the kernel of B_i, the corresponding cone constraint is replaced by a linear inequality constraint $0 \leq -\overline{\boldsymbol{a}}_i^T\boldsymbol{x}$. In the worse case scenario, the whole feasible set is the union of 2^m feasible regions obtained by splitting the ambient space into the range and kernel of the matrices $B_1, \ldots, B_m$. For the sake of simplicity, we restrict ourselves to the case of ellipsoidal uncertainties but the extension to ℓ_p–ball based uncertainties might be derived similarly using the robust reformulations in Bertsimas et al. (2004).

6.2 Gravitational Covering Location Problem

The goal of the problem that we propose is to optimally locate a given number of facilities in $\mathbb{R}^n$, and decide their coverage radii based on different features to maximize the overall coverage of a given set of users.

This problem belongs to the family of covering location problems, that arise whenever a decision-maker aims to cover a given demand in case the facilities have a limited coverage area. In several practical situations, the services to be located are unable to satisfy the demand outside their coverage area but the demand covered by the services wants to be maximized. Church and ReVelle (1974) introduce the maximal covering location problem (MCLP) as the problem of finding the positions of k services on a given space, each of them endowed with a given coverage area, maximizing the covered demand of the users. The MCLP has attracted significant attention from both researchers and practitioners (Wei and Murray, 2015). Specifically, this type of problem has been applied in different fields, such as in the location of emergency services (Toregas et al., 1971), leak detection (Blanco and Martínez-Antón, 2024b), mail advertising (Dwyer and Evans, 1981), archaeology (Bell and Church, 1985), among many others. The interested reader is referred to García and Marín (2019) for further details and recent advances in covering location.

To formulate the problem we first describe the parameters and decision variables that we use in our mathematical optimization model.

We are given a set of demand points $\{\boldsymbol{a}_i\}_{i\in I} \subset \mathbb{R}^n$ indexed by the set I. We assume that $|J|$ facilities are to be located in $\mathbb{R}^n$, indexed by the set J.

We assume that each demand point is allowed to be serviced by a facility if it belongs to a coverage area induced by a ℓ_p–norm ball centered at the facility's coordinates. The radius of each facility has to be determined based on different features, such as the capacity of the facility, the satisfaction level, or the distance to certain points of interest. In particular, a demand point located at $\boldsymbol{a} \in \mathbb{R}^n$ can be covered by a facility located at $\boldsymbol{x} \in \mathbb{R}^n$ only if $\|\boldsymbol{x} - \boldsymbol{a}\|_p \leq G m_1^{\alpha_1} \cdots m_d^{\alpha_d}$, where $m_1, \ldots, m_d$ are the different features affecting the coverage radius, and $G \in \mathbb{R}_+, \boldsymbol{\alpha} = (\alpha_1, \ldots, \alpha_d) \in \Delta_d$ are the aggregation parameters for these values. Note that the shape of this coverage area extends the notion of attraction between two bodies (in this case the demand points and the facilities) stated in the law of universal gravitation by Newton (1687), where the attraction of two objects can be obtained as:

$$\frac{G m_1 m_2}{\|\boldsymbol{x}_1 - \boldsymbol{x}_2\|_2^2}$$

where G is the gravity constant, m_1 and m_2 are the masses of the two bodies, and $\boldsymbol{x}_1$ and $\boldsymbol{x}_2$ their positions in the space.

Observe that the assumption of the dependence of the coverage radii with different features has a practical interest in real-world situations where the decision-makers may decide to give a different service to the users based on their characteristics (certain profile of users of interest, preferred communities, serve minorities instead of just those closer to the facility, etc). Thus, the consideration of attraction-function measures, as the one generalizing Newton's law, would provide insights into the convenience of locating the service in different places, as well as which users are more favorable to the coverage. Specifically, one facility may sacrifice to cover certain users which are closer at the price of covering others that are further but provide better coverage.

The values of the features for the coverage radius could depend only on the demand point (i.e., certain characteristics of the specific demand point) or only on the facility (as the capacity level), or both (as the interest of a demand point for a given facility or vice versa). The values of these features are unknown, and determining their values informs the decision-maker about the importance that should be given to each of them in the coverage of demand points. A budget B is available to invest in the features.

In addition, each demand point $i \in I$ is endowed with a weight $\omega_i \in \mathbb{R}_+$, which models the population of the region identified with the demand point or the profit for covering it.

The goal of the *gravitational maximal covering location problem* is to determine the optimal positions of the facilities indexed in J that maximize the overall profit for covering the demand I such that the cost for the values of the different features does not exceed the given budget.

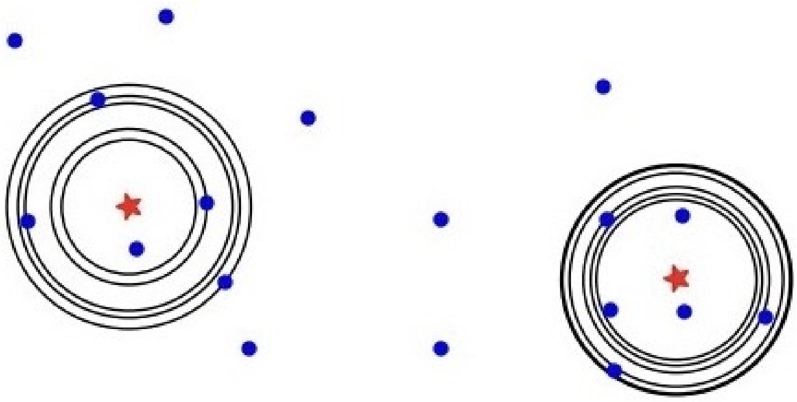

FIGURE 6.1: Solution of gravitational covering location problem for two facilities with three features in the Euclidean plane. Each radii is different for each pair demand-facility and is determined by the solution following the Newton's law of universal gravitation.

To derive our mathematical programming formulation for the problem, we use the following sets of decision variables:

$$y_{ij} = \begin{cases} 1 & \text{if demand point } i \text{ is accounted as covered by facility } j, \\ 0 & \text{otherwise} \end{cases}$$

for all $i \in I, j \in J$.

$$\boldsymbol{x}_j \in \mathbb{R}^n: \text{ Coordinates of the placement of the facilities}, \quad \forall j \in J.$$

$m_{ijk} \in \mathbb{R}_+$: Value of feature k affecting the coverage of demand point i by facility j for $i \in I, j \in J$, and $k = 1, \ldots, d$.

The gravitational covering location problem can be formulated as the following GPCP:

$$
\begin{aligned}
\text{maximize} \quad & \sum_{i \in I} \sum_{j \in J} \omega_i y_{ij} && (6.4)\\
\text{subject to} \quad & \|\boldsymbol{x}_j - \boldsymbol{a}_i\|_p \leq G_{ij} m_{ij1}^{\alpha_1} \cdots m_{ijd}^{\alpha_d} + M(1 - y_{ij}), \forall i \in I, j \in J, && (6.5)\\
& \sum_{j \in J} y_{ij} \leq 1, \forall i \in I, && (6.6)\\
& \sum_{i \in I} \sum_{j \in P} \sum_{k=1}^{d} m_{ijk} \leq B, && (6.7)\\
& \boldsymbol{x}_j \in \mathbb{R}^n, \forall j \in J,\\
& y_{ij} \in \{0, 1\}, \forall i \in I, j \in J,\\
& m_{ijk} \in \mathbb{R}_+, \forall i \in I, j \in J, k = 1, \ldots, d.
\end{aligned}
$$

The objective function (6.4) in the above model is the overall weighted coverage of the solution. Constraints (6.5) enforce that in case the demand point i is covered by facility j, $\boldsymbol{a}_i$ must belong to the coverage area determined by the different features. Otherwise, the value of the parameter $M > \max_{i,i' \in I} \|\boldsymbol{a}_i - \boldsymbol{a}_{i'}\|_p$ makes this constraint redundant. Constraints (6.6) state that each demand point can be accounted as covered by at most one facility. Constraint (6.7) is the budget constraint. Finally, the domains of the variables are detailed.

Observe that constraints (6.5) can be written as conic constraints in the shape of those in Remark 4.10, i.e., Constraints (6.5) are equivalent to:

$$(\boldsymbol{x}, \boldsymbol{y}, \mathbf{m}) \in \mathcal{K}_p(\boldsymbol{\alpha})[f_{ij}, g_{ij}, h_{ij}], \quad \forall i \in I, j \in J,$$

where $f_{ij}(\boldsymbol{x}) = \boldsymbol{x}_j - \boldsymbol{a}_i$, $h_{ij}(\mathbf{m}) = G_{ij} \cdot (m_{ij1}, \ldots, m_{ijd})$, and $g_{ij}(\boldsymbol{y}) = M(1 - y_{ij})$

Note that one can incorporate more sophisticated expressions for the m-variables in the form of linear or conic constraints keeping a similar structured problem.

6.3 Network Covering: A Leak Detection Problem

The design of leak detection systems on water supply networks has attracted great interest due to the economic and environmental impact associated with the systematic loss of this resource. Needless to say, the important role water plays in our social and economic life system, such as in agriculture, manufacturing, the production of electricity, and sustaining human health.

In urban networks, where the supply pipelines network is buried, an average of 20% to 30% of the supply water is periodically lost (El-Zahab and Zayed, 2019). This average exceeds 50% in places with less technological development where poor maintenance makes the system more vulnerable. It is also known (El-Zahab and Zayed, 2019) that ∼70% of the amount of wasted water is provoked by losses caused by leaks in modern networks. Pipe internal roughness or friction factors are the main causes of leakage of a water pipeline network (Walski, 1987; El-Abbasy et al., 2014), and as the pipelines get older, they become more susceptible to damage. In developed countries, it is expected that the annual disbursements for water leaks in their supply networks would be close to 10 billion USD, of which 2 billion would go to costs for damages due to water loss and 8 billion to social effects costs. Additionally, the International Institute of Water Management forecasts that 33% of the world's population will experience water scarcity by 2025 (Seckler et al., 1998). Thus, the efficient management of water supplies is and will be one of the main concerns of water authorities throughout the world.

Most of the efforts related to the management of water supply networks have focused on the detection of leaks once they occur. Rapid detection of the leak location is then crucial to minimize the impact of the leaks. Hamilton and Charalambous (2013) suggests three different phases in the leak detection problem: *localization*, *location* and *pinpointing*. In the *localization* phase, the goal is to detect if a leak has occurred within a certain network segment after a suspected leak. There are several proposed machine learning based methodologies to estimate leak probabilities or to classify the event leak/no leak based on historic leakage datasets (El-Abbasy et al., 2016; Li et al., 2011). In the *location* phase, the uncertain area where the leak is localized is narrowed to ∼ 30cm. Finally, in the *pinpointing* phase, the exact position of the leak is to be determined with a pre-specified accuracy of ∼ 20cm by using hydrophones and/or geophones (Fantozzi et al., 2009; Royal et al., 2011). Previously to the determination of the position of the leak, a vast amount of literature have being devoted to modeling the determination of false/true leak alarms by the different available devices (Cody et al., 2020a,b).

Another line of research on this topic is the design of control devices and methods for the accurate and quick detection of leakages. This is the case of the design of devices that accurately detect the leak within a restricted area (Khulief et al., 2012). Nevertheless, these devices are expensive and the adequate placement of the limited units must be strategically determined. One of the most popular approaches is by partitioning the network in *district-metered areas* where the flow and the pressure are monitored (leaks can be detected by a decrease of flow and pressure) by means of leak-detection devices at each of this areas (see, e.g., Puust et al., 2010). However, one still has to decide the number of devices and their exact locations in each of the district-metered areas.

There are different types of devices designed to help in the different leak detection phases which are classified into static and dynamic devices. Static devices, such as sensors or data loggers, are usually located on the network, at utility holes, or directly on the ground, attached to the network. They keep a data transmission flow with a central server to detect and localize leaks. In contrast, dynamic devices are portable and used in the location and pinpointing phases on more specific areas where the leak was suspected to occur. Whereas static devices can be automated, dynamic ones must be controlled on-site by humans. Different technologies have been designed for the two different types of devices (see, e.g., Li et al., 2015, for further details).

Most of the research on static leak detection systems is focused on the adequate estimation of the signals transmitted from the devices to the central server to detect an actual leak (Mohamed et al., 2012; Tijani et al., 2022). A few works analyze the optimal placement of a given number of static devices on a finite number of potential placements based on the capability of each of the potential places to detect a leak (Venkateswaran et al., 2018), or in the use of historic data to place the devices at the more convenient places (Casillas et al., 2013).

The models that we propose belong to the family of continuous covering location problems. In this type of problem, the goal is to find the position of one or more services (in this case, the leak detection devices), each of them endowed with a *coverage area*, i.e., a limited region where the service/signal can be provided. Covering Location Problems are usually classified into *(partial) set covering location problems*, (P)SCLP, and *maximal covering location problems*, MCLP. The goal of the (P)SCLP is to determine the minimum number of services (or equivalently the minimum set-up cost for them) to cover (part of) a given demand. In MCLP the number of services is known and the goal is to place them to cover as much demand as possible. These problems have been widely studied in the literature in case the given demand points to cover are finite and planar, and the coverage areas are Euclidean disks (see García and Marín, 2019; Murray and Tong, 2007; Murray, 2021; Pelegrín and Xu, 2023, for further information on this problems). Several extensions of these problems have been studied, by imposing connectivity between the services in higher dimensional spaces and different coverage areas (Blanco and Gázquez, 2021), multiple types of services (Blanco et al., 2023a), under uncertainty (Hosseininezhad et al., 2013), regional demand (Blanquero et al., 2016), or with ellipsoidal coverage areas (Tedeschi and Andretta, 2021).

We provide versions of the PSCLP and the MCLP, where instead of covering demand points, the goal is to cover lengths/volumes of the water supply pipeline networks, and the services to be located are the devices to detect leaks. The goal is either to find the number of devices and their optimal placement to fully or partially cover the whole length of the network (in the case of the PSCLP) or to find the placements of a given number of devices to maximize the length of the network which is covered by the devices. We assume that the coverage areas of the devices are ℓ_p–norm based balls and that covering a part of the network with these shapes implies that the device is able to detect a leak there. As far as we know, this problem has never been investigated before despite its practical applications. Murray and Tong (2007) analyze planar covering problems with generalized types of demand, as line segments or polygons, but where partial coverage is not allowed. In our approach, a part of the different elements taking part of the network is allowed to be covered, being the overall coverage maximized or lower bounded in our models.

We derive mathematical programming formulations for our model. First, we analyze the simple case when a single device is to be located. Next, we extend the model to the case of the simultaneous location of more than one device. We propose MINLP formulations for the problems, that are reformulated as MISOCP. We analyze some properties of the model that allow us to develop a strategy to construct initial solutions by solving an ILP. We also design a math-heuristic approach to approximately the problem by solving, sequentially, the single-device versions of the problem. We have tested all our approaches in real-world urban water networks. In addition to analyzing the computational performance of our algorithms, we provide managerial insights about the locations obtained with our approaches, compared to the application of the classical algorithms in the literature, namely vertex and edge-restricted covering problems. mathematical optimization, the cornerstone of the developments in this section, has been already recognized as a very powerful tool to analyze real-world pipeline networks (see, e.g., Blanco et al., 2022, 2023b).

The rest of the section is organized as follows. In Section 6.3.1, we introduce the problem under analysis and illustrate some of the solutions that can be obtained. Section 6.3.2 is devoted to analyzing the problem of locating a single device, which will be helpful in the development of approximation algorithms for the multi-device case. In Section 6.3.3, the general case is analyzed. We provide mixed integer conic programming formulations for the maximal and partial set covering location problems and a deep study of them. We also provide a method to construct initial solutions for the problem based on the geometric properties of the solutions and a math-heuristic approach based on solving, iteratively, single-device instances. The results of our computational experiments on real-world urban pipeline networks are reported in Chapter VII, Section 7.2.2.

6.3.1 Length-Coverage Location of Devices

In this section, we introduce the problem under study and fix the notation for the rest of the subsections.

Let $G = (V, E; \Omega)$ be an undirected geometric network with a set of vertices V, a set of edges E, and nonnegative edge weights Ω. The graph represents an urban water pipeline network, where the weights are the diameter or roughness of each of the pipelines in the network, which together with its length will allow us to compute the covered volume of the network. We assume that the geometric graph is embedded in $\mathbb{R}^n$, i.e., $V \subseteq \mathbb{R}^n$ and each (undirected) edge $e = \{\boldsymbol{o}_e, \boldsymbol{f}_e\} \in E$ is identified with a segment in $\mathbb{R}^n$, with ends $\boldsymbol{o}_e$ and $\boldsymbol{f}_e$ in V. Abusing notation, we identify edge $e \in E$ either with the segment induced by its ends, i.e., $e \equiv [\boldsymbol{o}_e, \boldsymbol{f}_e]$ or with the vector of $\mathbb{R}^n$ associated with them, i.e., $e \equiv \boldsymbol{f}_e - \boldsymbol{o}_e$.

A device located at $\boldsymbol{x} \in \mathbb{R}^n$ is endowed with a ℓ_p–ball coverage area in the form:

$$\mathbb{B}_R(\boldsymbol{x}) = \{\boldsymbol{y} \in \mathbb{R}^n : \|\boldsymbol{x} - \boldsymbol{y}\|_p \leq R\}$$

where $R \in \mathbb{R}_+$ is the given coverage radius, and $1 \leq p \leq \infty$. Note that each of the devices can be endowed with a different radius and a different norm, based on their technical specifications.

For each edge $e \in E$, and a finite set of positions for the devices $\mathcal{X} \subset \mathbb{R}^n$, we denote by $\text{CovWLength}_G(e, \mathcal{X})$ the weighted length of the edge covered by the devices. Let us denote by $\text{TotWLength}_\text{G}$ the total weighted length of the network, i.e., $\text{TotWLength}_\text{G} = \sum\limits_{e \in E} \omega_e \|\boldsymbol{o}_e - \boldsymbol{f}_e\|_p$ with $\omega_e \in \Omega$.

We analyze in this section two covering location problems to determine the position of the leak detection devices, namely the *partial set network length covering location problem* (PSNLCLP) and the *maximal network length covering location problem* (MNLCLP). In both cases, the goal is to place the different types of devices in the space to accurately detect a leak on the network.

Partial Set Network Length Covering Location Problem (PSNLCLP)

The goal of this problem is to determine the minimum number of devices and their positions in $\mathbb{R}^n$ in order to cover at least $100\gamma\%$ of the weighted length of the network, for a given $\gamma \in (0, 1]$.

The PSNLCLP can be mathematically stated as:

$$\min_{\substack{\mathcal{X} \subseteq \mathbb{R}^n: \\ \sum_{e \in E} \text{CovWLength}_G(e, \mathcal{X}) \geq \gamma \text{TotWLength}_\text{G}}} |\mathcal{X}|$$

The number of devices in the objective function can be replaced by the overall set-up costs for them, in whose case, the model read:

$$\min_{\substack{\mathcal{X} \subseteq \mathbb{R}^n: \\ \sum_{e \in E} \text{CovWLength}_G(e, \mathcal{X}) \geq \gamma \text{TotWLength}_\text{G}}} \sum_{X \in \mathcal{X}} f_X$$

being f_X a given set-up cost for the device $X \in \mathcal{X}$.

For the sake of simplicity, in this section, we analyze the first model, although all the results are also valid for the second one.

Maximal Network Length Covering Location Problem (MNLCLP)

In this problem the number of devices to locate is given, an integer $k \geq 1$, and the goal is to find their positions to maximize the weighted-covered length of the network. While the MNLCLP consists of solving

$$\max_{\substack{\mathcal{X}\subseteq\mathbb{R}^n:\\|\mathcal{X}|=k}} \sum_{e\in E} \mathrm{CovWLength}_G(e,\mathcal{X})$$

Both in the PSNLCLP and the MNLCLP, one can provide different coverage for the different devices that want to be located. In the PSNLCLP, it is assumed that the number of available devices is unlimited (although minimized), but one can assume that different types of devices with different specifications are available. In the MNLCLP, since exactly k of them are to be located, different radii can be specified for each of them.

In the following example, we illustrate the two problems described above analyzed in a real network (see Section 7.2.2).

Example 6.5. *Let us consider the network drawn in Figure 6.2. There, each edge has a different weight indicating the diameter of the pipeline (as larger the weight thicker the line in the plot). Devices with identical Euclidean disk coverage areas of radius* 0.5 *are to be located (the network has been scaled to fit in a disk of radius* 5*). In Figure 6.3 we show the solutions of the PSNLCLP for* $\gamma = 0.75$ *(right) and the solution of MNLCLP for* $k = 5$ *(left). There, the centers are highlighted as red stars, the covered segments of the network are colored in blue, and the coverage of the devices are the red disks.*

Note that the flexible approach that we propose does not force the devices to be located at the vertices or edges of the network, being able to cover a larger amount of the volume of the network with a smaller number of devices.

Example 6.6. *The two problems that we introduce here are defined in a very general framework (n-dimensional spaces, networks with no further assumptions, and general coverage shapes). In Figure 6.4 we show solutions for the MNLCLP for the same instance that in Example 6.5, with* $k = 5$ *but in case the coverage areas are induced by* ℓ_1*–norm (left) and* ℓ_∞*–norm (right) balls.*

Remark 6.7. *As already mentioned, most covering location problems on networks assume that the centers must be located either on the edges or the vertices of the network (see, e.g., Berman and Wang, 2011; Berman et al., 2016). Here, this condition is no longer assumed, allowing the centers to be located at any place in the space*

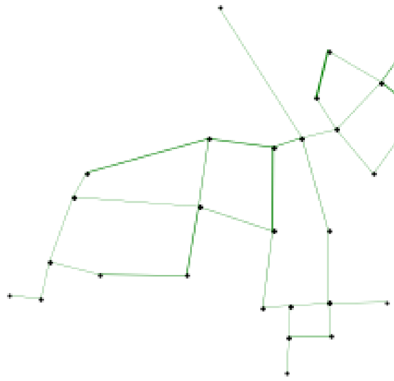

FIGURE 6.2: Pipeline urban network of Example 6.5.

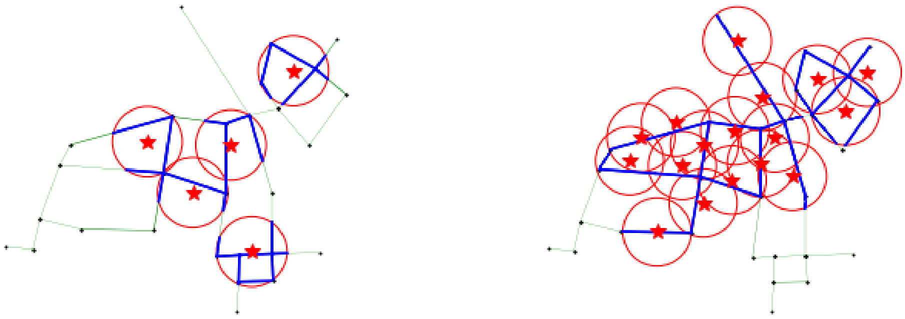

FIGURE 6.3: Solutions of MNLCLP ($k = 5$) and PSNLCLP ($\gamma = 0.75$) of the network of Example 6.5.

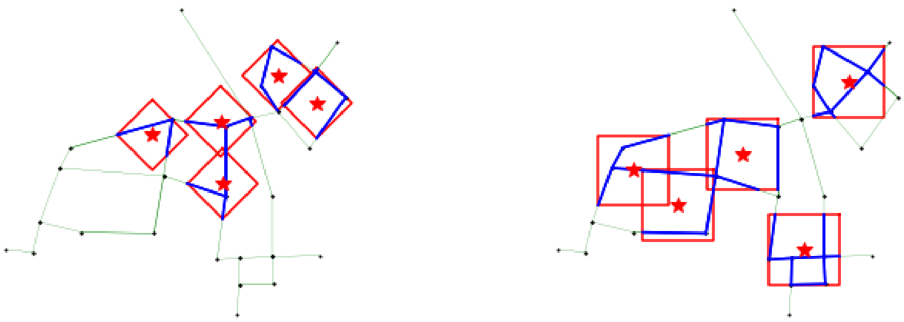

FIGURE 6.4: Solutions of MNLCLP with $k = 5$ for coverage areas defined by ℓ_1–norm (left) and ℓ_∞–norm (right) balls.

where the network lives. This flexibility allows positions for the devices providing a larger coverage of the network. In Figure 6.5 we show the solutions of the edge-restricted (left) and vertex-restricted (right) versions of the MNLCLP, where one can observe that the optimal positions of the devices are different from those obtained for the MNLCLP.

We have compared the covered lengths of the three problems (MNLCLP, edge-restricted

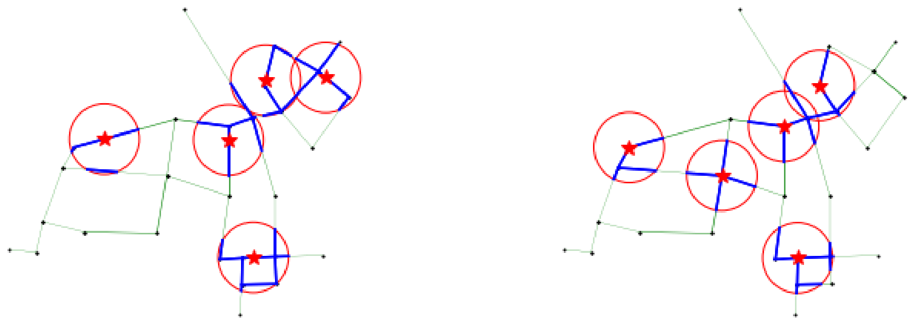

FIGURE 6.5: Solutions of the edge-restricted and vertex-restricted versions of MNLCLP for $k = 5$ for the network of Example 6.5.

MNLCLP, and vertex-restricted MNLCLP) for different values of k (2, 5, and 8), and different radii R (0.1, 0.25, and 0.5). In Figure 6.6 we show a bar diagram with the average deviations (for each k) of the two restricted versions with respect to the covered length of the general approach that we propose. As can be observed, the solutions of the unrestricted MNLCLP are able to cover more than 6% than the edge-restricted problem and more than 20% than the vertex-restricted problem. Since undetected leaks may produce fatal consequences in an urban area and leak detection devices are expensive, the use of the solutions of our models is advisable in this situation.

6.3.2 The Single-Device Maximal Network Length Covering Location Problem

In this section, we first analyze the MNLCLP in case $k = 1$ (a single device). We provide a mathematical programming model for the problem that will be useful for the general construction of the multi-device instances of MNLCLP and PSNLCLP derived in this section.

Let $e \in E$ be an edge in the network and $\boldsymbol{x} \in \mathbb{R}^n$ a given location for a device. In case the coverage area of the device in $\boldsymbol{x}$, $\mathbb{B}_R(\boldsymbol{x})$, does not *touch* the edge, then the covered length is clearly zero. Otherwise, since $\mathbb{B}_R(\boldsymbol{x})$ is a compact and convex body in $\mathbb{R}^n$, $\partial\mathbb{B}_R(\boldsymbol{x})$, the boundary of the ball, will touch the segment in two points (that may coincide in case the segment belong to a tangent hyperplane of the ball). These points belong to the segment $[\boldsymbol{o}_e, \boldsymbol{f}_e]$, that can be parameterized as:

$$\boldsymbol{y}_e^0 = \lambda_e^0 \boldsymbol{o}_e + (1 - \lambda_e^0)\boldsymbol{f}_e \quad \text{and} \quad \boldsymbol{y}_e^1 = \lambda_e^1 \boldsymbol{o}_e + (1 - \lambda_e^1)\boldsymbol{f}_e$$

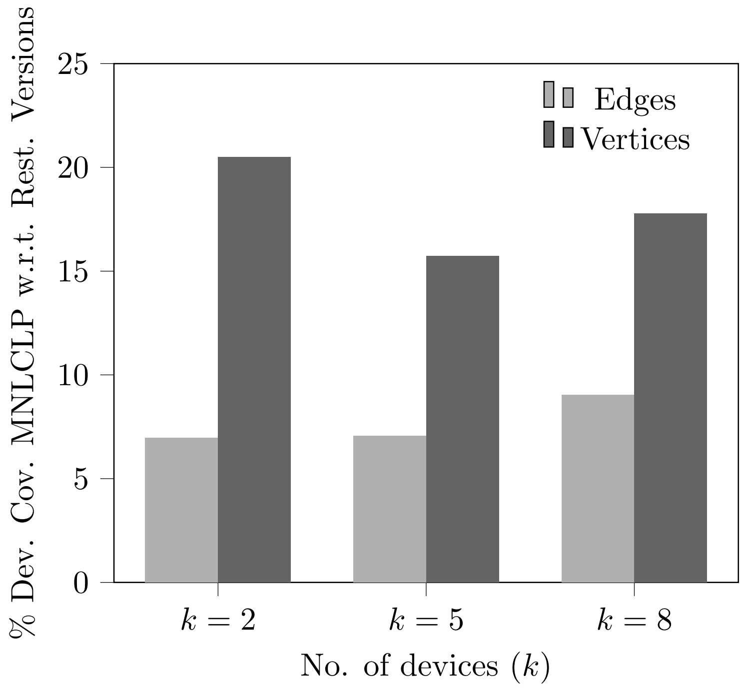

FIGURE 6.6: Average length coverage deviations between the solutions of MNLCLP and the edges/vertices-restricted versions of the problem.

for some $\lambda_e^0, \lambda_e^1 \in [0, 1]$. We can assume without loss of generality that $\boldsymbol{y}_e^0$ is closer to $\boldsymbol{o}_e$ than $\boldsymbol{y}_e^1$, so we restrict the λ-values to $\lambda_e^0 \leq \lambda_e^1$.

With the above parameterization, the length of the edge covered by $\boldsymbol{x}$ is $(\lambda_e^1 - \lambda_e^0)L_e$ (here, L_e stands for the length of the edge e).

To derive our mathematical programming formulation for the problem, we use the following sets of decision variables:

$$z_e = \begin{cases} 1 & \text{if edge } e \text{ intersects the device's coverage area,} \\ 0 & \text{otherwise} \end{cases}$$

$\boldsymbol{x}$: Coordinates of the placement of the device.

$\boldsymbol{y}_e^0, \boldsymbol{y}_e^1$: Intersections points of $\partial \mathbb{B}_R(\boldsymbol{x})$ with the edge e

λ_e^0, λ_e^1: Parameterization values in the segment of intersection points $\boldsymbol{y}_e^0$ and $\boldsymbol{y}_e^1$, respectively.

The single-device MNLCLP can be formulated as the following mathematical programming model, that we denote as (1-MNLCLP):

$$\begin{aligned}
\text{maximize} \quad & \sum_{e\in E} \omega_e L_e(\lambda_e^1 - \lambda_e^0) && && (6.8)\\
\text{subject to} \quad & \|\boldsymbol{x} - \boldsymbol{y}_e^s\|_p z_e \leq R, && \forall e \in E, s \in \{0,1\}, && (6.9)\\
& \boldsymbol{y}_e^s = \lambda_e^s \boldsymbol{o}_e + (1-\lambda_e^s)\boldsymbol{f}_e, && \forall e \in E, s \in \{0,1\}, && (6.10)\\
& \lambda_e^0 \leq \lambda_e^1, && \forall e \in E, && (6.11)\\
& \lambda_e^1 \leq z_e, && \forall e \in E, && (6.12)\\
& \lambda_e^0, \lambda_e^1 \geq 0, && \forall e \in E, && (6.13)\\
& z_e \in \{0,1\}, && \forall e \in E, && (6.14)\\
& \boldsymbol{x} \in \mathbb{R}^n. && && (6.15)
\end{aligned}$$

Constraints 6.9 enforce that in case the device coverage area intersects the edge, the intersection points must be in the coverage area of $\boldsymbol{x}$. This constraint can be equivalently rewritten as:

$$\|\boldsymbol{x} - \boldsymbol{y}_e^s\|_p \leq R + \Delta(1 - z_e), \quad \forall e \in E, s \in \{0,1\}$$

where Δ a big enough constant with $\Delta > \max\Big\{\|\boldsymbol{z}_1 - \boldsymbol{z}_2\|_p : \boldsymbol{z}_1, \boldsymbol{z}_2 \in \{\boldsymbol{o}_e, \boldsymbol{f}_e : e \in E\}\Big\}$. Constraints (6.10) are the parameterizations of the intersection points. Constraints (6.11) force that $\boldsymbol{y}_e^0$ is closer to $\boldsymbol{o}_e$ than $\boldsymbol{y}_e^1$. In case the device does not intersect an edge, by Constraints (6.12) fix to zero the coefficients of the parameterization, adding a value of zero to the covered lengths in the objective function. (6.13)-(6.15) are the domains of the variables.

(1-MNLCLP) is a MIpOCP problem because of the discrete variables z and the p–order cone constraints (6.9). These can be efficiently reformulate as a MISOCP that can be solved using the off-the-shelf software (Blanco and Martínez-Antón, 2024a).

Generating Feasible Solutions of MNLCLP

The single-device version of the MNLCLP is already a challenging combinatorial problem since it requires computing a *feasible* group of edges which is able to be covered by the device (in addition to the computation of the covered volume). In what follows, we analyze some geometric properties and algorithmic strategies for this problem, that will result in an ILP formulation to generate good quality initial feasible solutions to this problem. The same ideas will be extended to generate solutions also for the multi-device problem.

The following result, whose proof is straightforward from Constraints (6.9) provides a geometric characterization of the potential position for the device to be located given that the *touched* set of edges is known.

Lemma 6.8. *Let $\bar{z} \in \{0,1\}^E$ be a feasible solution for* 1-MNLCLP*. Denote by $C := \{e \in E : \bar{z}_e = 1\}$, the edges (total or partially) covered by the device. Then, we get that*

$$\boldsymbol{x} \in \bigcap_{e \in C} (e \oplus \mathbb{B}_R(\mathbf{0})), \tag{Cov}$$

The above result states that the position of the device, $\boldsymbol{x}$, must belong to the intersection of the extended segments induced by the edges in the cluster C. In Figure 6.7 (left picture) we illustrate the shape of $e \oplus \mathbb{B}_R(\mathbf{0})$ for a given edge $e \in E$. In Figure 6.7 (right picture) we show the intersection of three of these types of sets, where a device covering the three segments is allowed to be located.

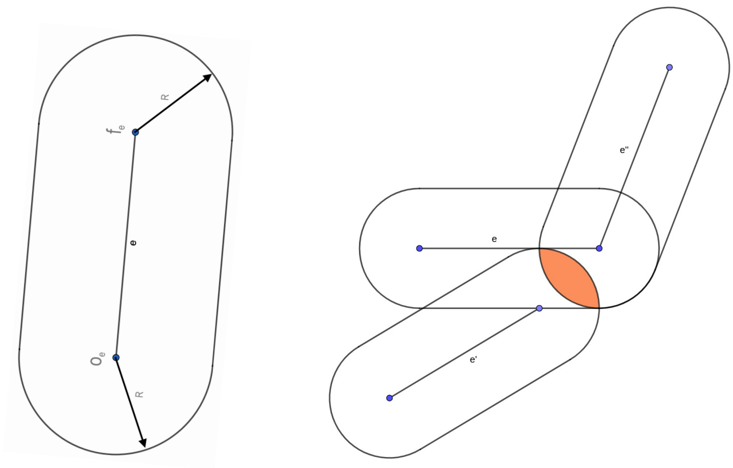

FIGURE 6.7: Shape of extended edges (left) and the intersection of three of these *compatible* shapes (right).

As already mentioned, the main combinatorial decision of our models is to determine the sets of edges that are allowed to be *touched* by the same device, i.e., $S \subset E$, such that $\bigcap_{e \in S} (e \oplus \mathbb{B}_R(\mathbf{0})) \neq \emptyset$. Defining the set $\mathcal{C}$ as

$$\mathcal{C} := \left\{ S \subset E : \bigcap_{e \in S} (e \oplus \mathbb{B}_R(\mathbf{0})) \neq \emptyset \right\}$$

each element $S \in \mathcal{C}$ will be called a *compatible subset* for the device. In general, unless the radius is big enough, not all the subsets of E belong to $\mathcal{C}$.

In the following result, we describe a polynomial set (in $|E|$) of valid inequalities for our model that avoid those noncompatible sets in our models.

Lemma 6.9. *The following inequalities are valid for the* 1*-MNLCLP:*

$$\sum_{e \in S} z_e \leq n, \quad \forall S \subset E \text{ with } |S| = n+1 \text{ and } \bigcap_{e \in S} (e \oplus \mathbb{B}_R(\mathbf{0})) = \emptyset \tag{6.16}$$

Proof. It is straightforward to see, by Constraints (6.9), that the following condition is verified by any solution of (6.8)-(6.15):

$$\sum_{e \in S} z_e \leq |S| - 1, \quad \forall S \subset E : \bigcap_{e \in S} (e \oplus \mathbb{B}_R(\mathbf{0})) = \emptyset,$$

Thus, by Helly's theorem 2.11, since the sets taking part of the intersections above, $(e \oplus \mathbb{B}_R(\mathbf{0}))$, are compact and convex for any $e \in E$, the result follows. ☐

Corollary 6.10. *Let $\bar{z} \in \{0,1\}^E$ be a solution of the system of Diophantine inequalities* (6.16)*. Then, $\bar{z}$ is a feasible solution for the* 1*-MNLCLP.*

In the classical MCLP, the above observation allows us to replace the nonlinear covering constraints —in the shape of (6.9)— with inequalities in the shape of (6.16), and the continuous variables which are involved in these constraints can be forgotten (see, e.g., Blanco and Gázquez, 2021; Blanco et al., 2023a). In our model, the latter is no longer possible as in classic MCLP since the λ-values are also needed to compute the covered volume of the network.

Thus, we propose the following integer linear programming formulation to obtain valid compatible subsets for the models,

$$\begin{aligned}
\text{maximize} \quad & \sum_{e \in E} \omega_e L_e z_e && (6.17)\\
\text{subject to} \quad & \sum_{e \in S} z_e \leq n, \quad \forall S \subset E(|S| = n+1) : \bigcap_{e \in S} (e \oplus \mathbb{B}_R(\mathbf{0})) = \emptyset, && (6.18)\\
& z_e \in \{0,1\}, \qquad \forall e \in E. && (6.19)
\end{aligned}$$

The above mathematical programming model is an edge-based version of the classical 1-MCLP, which is known to be NP-hard. The main advantage of this representation is that one can use techniques from integer linear programming to strengthen or solve it, using the available off-the-shelf solvers.

The main bottleneck of this formulation is the computation of the intersections of $n+1$ sets in the form $e \oplus \mathbb{B}_R(\mathbf{0})$ which are empty, in whose case the corresponding inequality is added to the pool of constraints. The general methodology that can be applied for any dimension and any ℓ_p–norm, is by applying a relax-and-cut approach based on solving the problems above by removing Constraints (6.18), separating the violated constraints and incorporating them on-the-fly in an embedded branch-and-cut algorithm.

In what follows, we focus on the planar Euclidean case, which is the most useful case in practice, and for which the formulations can be further simplified.

Observe that for $n = 2$, Constraints (6.16) are equivalent to:

$$\begin{aligned} z_e + z_{e'} &\leq 1, \forall e, e' \in E : (e \oplus \mathbb{B}_R(\mathbf{0})) \cap (e' \oplus \mathbb{B}_R(\mathbf{0})) = \emptyset, \\ z_e + z_{e'} + z_{e''} &\leq 2, \forall e, e', e'' \in E : (e \oplus \mathbb{B}_R(\mathbf{0})) \cap (e' \oplus \mathbb{B}_R(\mathbf{0})) \cap (e'' \oplus \mathbb{B}_R(\mathbf{0})) = \emptyset, \\ z_e &\in \{0,1\}, \forall e \in E. \end{aligned}$$

Thus, in order to incorporate these types of constraints one needs to check two and three-wise intersections of objects in the form $e \oplus \mathbb{B}_R(\mathbf{0})$. Although these shapes can be difficult to handle in general, the planar Euclidean case can be efficiently handled by analyzing the geometry of these bodies like Minkowski sums of segments and disks.

The following results are instrumental for the development of the algorithm that we propose to generate the above sets of constraints. From now on, $\|\cdot\|$ denotes the Euclidean norm in $\mathbb{R}^2$.

Lemma 6.11. *Let e, e' be two segments in $\mathbb{R}^2$ and $\delta(e, e') := \min\{\|\boldsymbol{x} - \boldsymbol{x}'\| : \boldsymbol{x} \in e, \boldsymbol{x}' \in e'\}$. Then, if $\delta(e, e') > 0$, there exist $\boldsymbol{x} \in e$ and $\boldsymbol{x}' \in e'$ with $\delta(e, e') = \|\boldsymbol{x} - \boldsymbol{x}'\|$ such that either $\boldsymbol{x} \in \{\boldsymbol{o}_e, \boldsymbol{f}_e\}$ or $\boldsymbol{x}' \in \{\boldsymbol{o}_{e'}, \boldsymbol{f}_{e'}\}$.*

Proof. The result follows by observing that the minimum distance between two segments is always achieved by choosing one of the extremes of the segments. □

Lemma 6.12. *Let e be a segment in $\mathbb{R}^2$ and $\boldsymbol{y} \in \mathbb{R}^2$ be a point. Let $\boldsymbol{z}$ be the intersection point between the line, r, induced by e and its orthogonal line passing* *through the point $\boldsymbol{y}$. Then, $\delta(e, \boldsymbol{y}) := \min\{\|\boldsymbol{x} - \boldsymbol{y}\| : \boldsymbol{x} \in e\}$ can be computed as:*

$$\delta(e, \boldsymbol{y}) = \|\boldsymbol{y} - (\min\{\max\{0, \mu\}, 1\}(\boldsymbol{f}_e - \boldsymbol{o}_e) + \boldsymbol{o}_e)\|,$$

where μ denotes the parameterization value of $\boldsymbol{z}$ in r pointed at $\boldsymbol{o}_e$.

Proof. Let $\boldsymbol{z}$ be the intersection point between the line, r, induced by e and its orthogonal line passing through the point $\boldsymbol{y}$. We denote by μ the parameterization of $\boldsymbol{z}$ in the ray induced by the segment pointed at $\boldsymbol{o}_e$. Thus, $\|\boldsymbol{y} - \boldsymbol{z}\| = \min\{\|\boldsymbol{y} - \boldsymbol{w}\| : \boldsymbol{w} \in r\}$. Since $\boldsymbol{z} \in r$, one can parameterize $\boldsymbol{z}$ as $\boldsymbol{z} = (1 - \mu)\boldsymbol{o}_e + \mu \boldsymbol{f}_e$ for some $\mu \in \mathbb{R}$. Let us analyze the different possible values for μ:

- If $\mu \in [0, 1]$, one gets that:

$$\begin{aligned}\|\boldsymbol{y} - (\mu(\boldsymbol{f}_e - \boldsymbol{o}_e) + \boldsymbol{o}_e)\| = \|\boldsymbol{y} - \boldsymbol{z}\| &= \min\{\|\boldsymbol{y} - \boldsymbol{w}\| : \boldsymbol{w} \in r\} \\ &\leq \min\{\|\boldsymbol{y} - \boldsymbol{w}\| : \boldsymbol{w} \in e\} = \delta(e, \boldsymbol{y}).\end{aligned}$$

- If $\mu < 0$, will show that $\delta(e, \boldsymbol{y}) = \|\boldsymbol{y} - \boldsymbol{o}_e\|$. Let $\lambda \in [0, 1]$ and $\boldsymbol{x} = (1 - \lambda)\boldsymbol{o}_e + \lambda \boldsymbol{f}_e \in e$. Then:

$$\begin{aligned}\|\boldsymbol{y} - \boldsymbol{o}_e\|^2 &= \|\boldsymbol{y} - \boldsymbol{z}\|^2 + \|\boldsymbol{z} - \boldsymbol{o}_e\|^2 \\ &= \|\boldsymbol{y} - \boldsymbol{z}\|^2 + \|\mu(\boldsymbol{f}_e - \boldsymbol{o}_e) + \boldsymbol{o}_e - \boldsymbol{o}_e\|^2 \\ &= \|\boldsymbol{y} - \boldsymbol{z}\|^2 + |\mu|^2\|(\boldsymbol{f}_e - \boldsymbol{o}_e)\|^2 \\ &\leq \|\boldsymbol{y} - \boldsymbol{z}\|^2 + |(\mu - \lambda)|^2\|(\boldsymbol{f}_e - \boldsymbol{o}_e)\|^2 \\ &= \|\boldsymbol{y} - \boldsymbol{z}\|^2 + \|\mu(\boldsymbol{f}_e - \boldsymbol{o}_e) + \boldsymbol{o}_e - (\lambda(\boldsymbol{f}_e - \boldsymbol{o}_e) + \boldsymbol{o}_e)\|^2 \\ &= \|\boldsymbol{y} - \boldsymbol{z}\|^2 + \|\boldsymbol{z} - \boldsymbol{x}\|^2 \\ &= \|\boldsymbol{y} - \boldsymbol{x}\|^2.\end{aligned}$$

- In case $\mu > 1$, let us see that $\delta(e, \boldsymbol{y}) = \|\boldsymbol{y} - \boldsymbol{f}_e\|$. Let $\lambda \in [0,1]$ and $\boldsymbol{x} = \lambda(\boldsymbol{f}_e - \boldsymbol{o}_e) + \boldsymbol{o}_e$ be in e:

$$\begin{aligned}
\|\boldsymbol{y} - \boldsymbol{f}_e\|^2 &= \|\boldsymbol{y} - \boldsymbol{z}\|^2 + \|\boldsymbol{z} - \boldsymbol{f}_e\|^2 \\
&= \|\boldsymbol{y} - \boldsymbol{z}\|^2 + \|\mu(\boldsymbol{f}_e - \boldsymbol{o}_e) + \boldsymbol{o}_e - \boldsymbol{f}_e\|^2 \\
&= \|\boldsymbol{y} - \boldsymbol{z}\|^2 + \|\mu(\boldsymbol{f}_e - \boldsymbol{o}_e) + \boldsymbol{o}_e - \boldsymbol{f}_e + \boldsymbol{o}_e - \boldsymbol{o}_e\|^2 \\
&= \|\boldsymbol{y} - \boldsymbol{z}\|^2 + |\mu - 1|^2\|(\boldsymbol{f}_e - \boldsymbol{o}_e)\|^2 \\
&\leq \|\boldsymbol{y} - \boldsymbol{z}\|^2 + |(\mu - \lambda)|^2\|(\boldsymbol{f}_e - \boldsymbol{o}_e)\|^2 \\
&= \|\boldsymbol{y} - \boldsymbol{z}\|^2 + \|\mu(\boldsymbol{f}_e - \boldsymbol{o}_e) + \boldsymbol{o}_e - (\lambda(\boldsymbol{f}_e - \boldsymbol{o}_e) + \boldsymbol{o}_e)\|^2 \\
&= \|\boldsymbol{y} - \boldsymbol{z}\|^2 + \|\boldsymbol{z} - \boldsymbol{x}\|^2 \\
&= \|\boldsymbol{y} - \boldsymbol{x}\|^2.
\end{aligned}$$

Summarizing, we get that the point in e closest to $\boldsymbol{y}$ is in the form $(1-\lambda)\boldsymbol{o}_e + \lambda \boldsymbol{f}_e$ with

$$\lambda = \begin{cases} 0 & \text{if } \mu < 0, \\ \mu & \text{if } 0 \leq \mu \leq 1, \\ 1 & \text{if } \mu > 1. \end{cases}$$

that is, $\lambda = \min\{\max\{0, \mu\}, 1\}$, being then

$$\delta(e, \boldsymbol{y}) = \|\boldsymbol{y} - (\min\{\max\{0, \mu\}, 1\}(\boldsymbol{f}_e - \boldsymbol{o}_e) + \boldsymbol{o}_e)\|.$$

□

Given a set of edges, E, and a radius R, using the above results, we develop algorithms to compute the two and three-wise intersections of sets in the form $e \oplus \mathbb{B}_R(\boldsymbol{0})$, for $e \in E$. The pseudocodes are shown in Algorithms 1 and 2. The set M, which is initialized to the empty set, will contain, the pairs (e, e') of $E \times E$ with $(e \oplus \mathbb{B}_R(\boldsymbol{0})) \cap (e' \oplus \mathbb{B}_R(\boldsymbol{0})) = \emptyset$ by checking the distance between the segments, $\delta(e, e')$. On the one hand, in case, $\delta(e, e') = 0$, both segments intersect so also their Minkowski sums. On the other hand, if $\delta(e, e') \neq 0$, we denote by r_e and $r_{e'}$ the lines containing the segments e and e', respectively, and by $\boldsymbol{y}_0$ their intersection point. By Lemma 6.11 there exist $\boldsymbol{x}, \boldsymbol{x}' \in \mathbb{R}^2$ with $\delta(e, e') = \|\boldsymbol{x} - \boldsymbol{x}'\|$, being $\boldsymbol{x} \in \{\boldsymbol{o}_e, \boldsymbol{f}_e\}$ or $\boldsymbol{x}' \in \{\boldsymbol{o}_{e'}, \boldsymbol{f}_{e'}\}$. Thus, four distances are enough to compute $\delta(e, e')$, namely $\delta_1 := \delta(\boldsymbol{o}_{e'}, e)$, $\delta_2 := \delta(\boldsymbol{f}_{e'}, e)$, $\delta_3 := \delta(\boldsymbol{o}_e, e')$ and $\delta_4 := \delta(\boldsymbol{f}_e, e')$, being $\delta(e, e') = \min\{\delta_1, \delta_2, \delta_3, \delta_4\}$. In case $\delta(e, e') > 2R$, then $(e \oplus \mathbb{B}_R(\boldsymbol{0})) \cap (e' \oplus \mathbb{B}_R(\boldsymbol{0})) = \emptyset$, and the tuple (e, e') is added to M.

For the three-wise intersections, the set M is again initialized to the empty set. Then, for each triplet (e_1, e_2, e_3) whose pairwise intersection is nonempty (by Algorithm 1), we solve the following mathematical optimization problem:

$$
\begin{aligned}
\varepsilon^\star(e_1, e_2, e_3) := \min\ & \varepsilon && && (6.20)\\
\text{s.t. } & \boldsymbol{y}_i = (1-\lambda_i)\boldsymbol{o}_{e_i} + \lambda_i \boldsymbol{f}_{e_i}, && i = 1,2,3, && (6.21)\\
& \|\boldsymbol{x} - \boldsymbol{y}_i\| \leq R + \varepsilon, && i = 1,2,3, && (6.22)\\
& \boldsymbol{x} \in \mathbb{R}^2, && && (6.23)\\
& \lambda_1, \lambda_2, \lambda_3 \in [0,1], && && (6.24)\\
& \varepsilon \in \mathbb{R}. && && (6.25)
\end{aligned}
$$

The above problem is polynomial-time solvable since it is an SOCP. Furthermore, its objective value provides a way to check for the emptiness of the three-wise intersection problem.

Lemma 6.13. *Let $e_1, e_2, e_3 \in E$ with $(e_i \oplus \mathbb{B}_R(\mathbf{0})) \cap (e_j \oplus \mathbb{B}_R(\mathbf{0})) \neq \emptyset$ for all $i, j \in \{1,2,3\}$. Then, $(e_1 \oplus \mathbb{B}_R(\mathbf{0})) \cap (e_2 \oplus \mathbb{B}_R(\mathbf{0})) \cap (e_3 \oplus \mathbb{B}_R(\mathbf{0})) \neq \emptyset$ if and only if $\varepsilon^\star(e_1, e_2, e_3) \leq 0$.*

6.3.3 A General Model for PSNLCLP and MNLCLP

In this section, we provide a general methodology to deal with the optimal location of devices in both the PSNLCLP and the MNLCLP. In the single-device problem analyzed in the previous section, the coverage of an edge can be directly computed by parameterizing the intersection of the boundary of the ball with the edge. Nevertheless, in the multi-device problem, the covered length does not coincide with the sum of the coverages of every single device separately, since the same part of a segment may be covered by two or more devices, but the covered length must be accounted for only once (otherwise the optimal placement for a set of devices is the collocation of all of them in the more weighted edge).

We illustrate the situation in the following toy example.

Example 6.14. *Let us consider a planar network with a single edge e and four devices with Euclidean ball coverage areas as drawn in Figure 6.8. The four devices* touch *the edge. The covered length of the edge is highlighted with thicker segments in the picture. Clearly, this length cannot be computed by adding up separately each of the covered lengths of the devices.*

Algorithm 1: A complete set of 2-wise incompatible edges.

Data: Set of edges, E, and radius R.
$M = \emptyset$
for $(e, e') \in E \times E$ **do**
  Set: $\bar{e} = \boldsymbol{f}_e - \boldsymbol{o}_e$.
  Set: $\bar{e'} = \boldsymbol{f}_{e'} - \boldsymbol{o}_{e'}$.
  Compute the intersection point of the lines $\boldsymbol{o}_e + \langle \bar{e} \rangle$ and $\boldsymbol{o}_{e'} + \langle \bar{e'} \rangle$: $\boldsymbol{y}_0$.
  Calculate μ_0, μ'_0 such that $\boldsymbol{y}_0 = \mu_0 \bar{e} + \boldsymbol{o}_e$ and $\boldsymbol{y}_0 = \mu'_0 \bar{e'} + \boldsymbol{o}_{e'}$.
  if μ_0 *or* $\mu'_0 \notin [0, 1]$ **then**
    1. Compute the intersection point of the lines $\boldsymbol{o}_e + \langle \bar{e} \rangle$ and $\boldsymbol{o}_{e'} + \langle \bar{e}^{\perp} \rangle$: $\boldsymbol{y}_1$.
       Calculate μ_1 such that $\boldsymbol{y}_1 = \mu_1 \bar{e} + \boldsymbol{o}_e$.
       Set: $\delta_1 = \|\boldsymbol{o}_{e'} - (\min\{\max\{0, \mu_1\}, 1\}\bar{e} + \boldsymbol{o}_e)\|$.

    2. Compute the intersection point of the lines $\boldsymbol{o}_e + \langle \bar{e} \rangle$ and $\boldsymbol{f}_{e'} + \langle \bar{e}^{\perp} \rangle$: $\boldsymbol{y}_2$.
       Calculate μ_2 such that $\boldsymbol{y}_2 = \mu_2 \bar{e} + \boldsymbol{o}_e$.
       Set: $\delta_2 = \|\boldsymbol{f}_{e'} - (\min\{\max\{0, \mu_2\}, 1\}\bar{e} + \boldsymbol{o}_e)\|$.

    3. Compute the intersection point of the lines $\boldsymbol{o}_e + \langle \bar{e'}^{\perp} \rangle$ and $\boldsymbol{o}_{e'} + \langle \bar{e'} \rangle$: $\boldsymbol{y}_3$.
       Calculate μ_3 such that $\boldsymbol{y}_3 = \mu_3 \bar{e'} + \boldsymbol{o}_{e'}$.
       Set: $\delta_3 = \|\boldsymbol{o}_e - (\min\{\max\{0, \mu_3\}, 1\}\bar{e'} + \boldsymbol{o}_{e'})\|$.

    4. Compute the intersection point of the lines $\boldsymbol{f}_e + \langle \bar{e'}^{\perp} \rangle$ and $\boldsymbol{o}_{e'} + \langle \bar{e'} \rangle$: $\boldsymbol{y}_4$.
       Calculate μ_4 such that $\boldsymbol{y}_4 = \mu_4 \bar{e'} + \boldsymbol{o}_{e'}$.
       Set: $\delta_4 = \|\boldsymbol{f}_e - (\min\{\max\{0, \mu_4\}, 1\}\bar{e'} + \boldsymbol{o}_{e'})\|$.

    if $\min\{\delta_1, \delta_2, \delta_3, \delta_4\} > 2R$ **then**
      Add (e, e') to M.

Result: $M = \{(e, e') \in E \times E : (e \oplus \mathbb{B}_R(\mathbf{0})) \cap (e' \oplus \mathbb{B}_R(\mathbf{0})) = \emptyset\}$.

Algorithm 2: A complete set of 3-wise incompatible edges (which are pair-wise compatible).

Data: Set of edges, E, and radius R.
$L = \{(e_1, e_2, e_3) \in E \times E \times E : (e_1 \oplus \mathbb{B}_R(\mathbf{0})) \cap (e_2 \oplus \mathbb{B}_{\mathbb{R}}(\mathbf{0})) \neq \emptyset,$
$(e \oplus \mathbb{B}_R(\mathbf{0})) \cap (e_3 \oplus \mathbb{B}_R(\mathbf{0})) \neq \emptyset, (e_2 \oplus \mathbb{B}_R(\mathbf{0})) \cap (e_3 \oplus \mathbb{B}_R(\mathbf{0})) \neq \emptyset\}$.
$M = \emptyset$.
for $(e_1, e_2, e_3) \in L$ **do**
  Compute $\varepsilon^\star(e_1, e_2, e_3)$.
  if $\varepsilon^\star(e_1, e_2, e_3) > 0$ **then**
    Add (e_1, e_2, e_3) to M.

Result: $M =$
$$\{(e_1, e_2, e_3) \in E^3 : (e_1 \oplus \mathbb{B}_R(\mathbf{0})) \cap (e_2 \oplus \mathbb{B}_R(\mathbf{0})) \cap (e_3 \oplus \mathbb{B}_R(\mathbf{0})) = \emptyset\}.$$

In what follows, we derive a mathematical programming model that overcomes this situation.

Observe that the positions of the intersection points of the coverage areas of k devices with an edge (segment) e provide a partition of the edge in

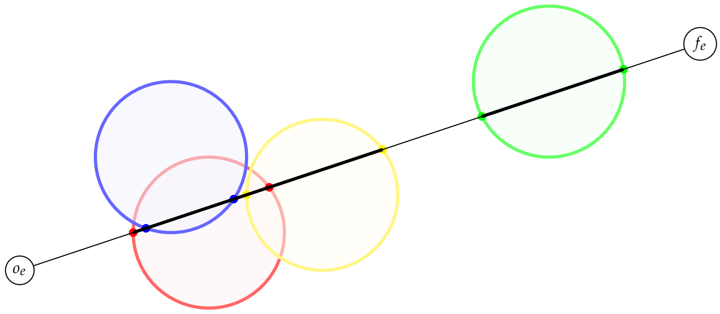

FIGURE 6.8: Example of interaction between the coverages of different devices.

at most $2k+1$ subsegments of e. Each of those subsegments is either fully covered or noncovered by the device. Let $\lambda_{1e}^0, \lambda_{1e}^1, \ldots, \lambda_{ke}^0, \lambda_{ke}^1$ the parameterizations of the intersection points of the k devices with respect to e (here λ_{je}^0 and λ_{je}^1 stand for the parameterizations of the intersection of the coverage area of jth device with segment induced by the edge e).

We assume that the devices not intersecting the edge have both lambda values equal to zero. Sorting the λ^0 and λ^1 values one gets two sorted sequences in the form:

$$\Lambda_e^0 := \lambda_{(1)e}^0 \leq \cdots \leq \lambda_{(k)e}^0$$
$$\Lambda_e^1 := \lambda_{(1)e}^1 \leq \cdots \leq \lambda_{(k)e}^1$$

Merging both lists one gets all the partitions of the segment e by the different intersection points:

$$\Lambda_e := \lambda_{(1)e}^{i_1} \leq \cdots \leq \lambda_{(2k)e}^{i_{2k}}$$

where $i_1, \ldots, i_{2k} \in \{0, 1\}$.

For each $\ell \in \{1, \ldots, 2k-1\}$, the intervals $[\lambda_{(\ell)e}^{i_\ell}, \lambda_{(\ell+1)e}^{i_{\ell+1}}]$ along with $[\boldsymbol{o}_e, \lambda_{(1)e}^{i_1}]$ and $[\lambda_{(2k)e}^{i_{2k}}, \boldsymbol{f}_e]$ induce a subdivision of the segment e into $2k+1$ pieces (some of them probably singletons). Furthermore, in case any of the extreme points, $\boldsymbol{o}_e$ and $\boldsymbol{f}_e$, are covered by a device, the corresponding subsegment will be a singleton ($[\boldsymbol{o}_e, \boldsymbol{o}_e] = \{\boldsymbol{o}_e\}$ or $[\boldsymbol{f}_e, \boldsymbol{f}_e] = \{\boldsymbol{f}_e\}$), whose length is zero. Otherwise, in case any extreme subsegment is not covered, still its contribution to the objective function is zero. Thus, in our formulation, it is enough considering the $2k-1$ intermediate subsegments in the subdivision.

Given the sequence Λ_e for the k given devices located at $\boldsymbol{x}_1, \ldots, \boldsymbol{x}_k$, one can easily determine which of the subsegments in the partitions are covered by the facilities as stated by the following straightforward observation.

Lemma 6.15. *A subsegment in the form* $s = [\lambda^{i_\ell}_{(\ell)e}, \lambda^{i_{\ell+1}}_{(\ell+1)e}]$ *is covered by a set of devices if and only if* $s \subseteq [\lambda^0_{je}, \lambda^1_{je}]$ *for some* $j = 1, \ldots, k$ *with* $\lambda^0_{je} < \lambda^1_{je}$.

With the above observations, we derive mathematical programming formulations for the multi-device versions of PSNLCLP and MNLCLP.

We denote by $K = \{1, \ldots, k\}$ the index set for the devices to locate and by $Q = \{1, \ldots, 2k-1\}$ the index sets for the intermediate subsegments in the partition induced by the Λ sequences. We assume that the jth device is endowed with a ℓ_p–norm-based coverage area with radius $R_j \in \mathbb{R}_+$.

We use the following decision variables in our models:

$$z_{je} = \begin{cases} 1 & \text{if edge } e \text{ intersect the } j\text{th device's coverage area,} \\ 0 & \text{otherwise} \end{cases} \quad \forall j \in K, \forall e \in E.$$

$$\boldsymbol{x}_{j1}, \ldots, \boldsymbol{x}_{jn} \in \mathbb{R}^n : \text{ Coordinates of the } j\text{th device,} \quad \forall j \in K.$$

$$\lambda^0_{je}, \lambda^1_{je} : \text{Parameterization in the segment of the two intersection points of } \partial\mathbb{B}_{R_j}(\boldsymbol{x}_j) \text{ with segment } e, \forall j \in K, \forall e \in E.$$

$$w_{e\ell} = \begin{cases} 1 & \text{if the } \ell\text{th subsegment of edge } e \text{ is covered by some device,} \\ 0 & \text{otherwise,} \end{cases}$$

for $\ell \in Q, \forall e \in E$.

$$\xi^s_{je\ell} = \begin{cases} 1 & \text{if } \lambda^s_{je} \text{ is sorted in } \ell\text{th position in the list of } \Lambda_e, \\ 0 & \text{otherwise,} \end{cases}$$

for $j \in K, \forall \ell \in Q \cup \{2k\}, \forall e \in E$.

With the above set of variables, the amount:

$$L_e \left[\sum_{j \in K} \sum_{s=0}^{1} \lambda^s_{je} \xi^s_{je(\ell+1)} - \sum_{j \in K} \sum_{s=0}^{1} \lambda^s_{je} \xi^s_{je\ell} \right]$$

determines the length of the ℓth subsegment in case it is covered by any of the devices in K. Note that in case such a subsegment is $[\lambda^s_{je}, \lambda^{s'}_{j'e}]$, the above expression becomes $L_e(\lambda^{s'}_{j'e} - \lambda^s_{je})$ which is the desired amount.

Thus, the overall volume coverage of the network can be computed as:

$$\sum_{e\in E}\sum_{\ell\in Q} \omega_e w_{e\ell} L_e \left[\sum_{j\in K}\sum_{s=0}^{1} \lambda^s_{je}\xi^s_{je(\ell+1)} - \sum_{j\in K}\sum_{s=0}^{1} \lambda^s_{je}\xi^s_{je\ell}\right]$$

In order to adequately represent the decision variables in our model, the following constraints are considered:

1. **Coverage constraints:**

$$\|(\lambda^s_{je} e + \boldsymbol{o}_e) - \boldsymbol{x}_j\|_p z_{je} \leq R_j, \quad \forall j \in K,\ \forall e \in E,\ s = 0,1 \tag{6.26}$$

These constraints enforce that in case an edge is accounted as *touched* by the jth device ($z_{je} = 1$), the two intersection points $(\lambda^0_{je} e + \boldsymbol{o}_e)$ and $(\lambda^1_{je} e + \boldsymbol{o}_e)$ belong to $\mathbb{B}_{R_j}(\boldsymbol{x}_j) \cap e$. This constraint can be reformulated as:

$$\|(\lambda^s_{je} e + \boldsymbol{o}_e) - \boldsymbol{x}_j\|_p z_{je} \leq R_j + \Delta(1 - z_{je}), \quad \forall j \in K, \forall e \in E,\ s = 0,1$$

where Δ a big enough constant with $\Delta > \max\Big\{\|\boldsymbol{z}_1 - \boldsymbol{z}_2\|_p : \boldsymbol{z}_1, \boldsymbol{z}_2 \in \{\boldsymbol{o}_e, \boldsymbol{f}_e : e \in E\}\Big\}$.

2. **Directed parameterization:**

$$\lambda^0_{je} \leq \lambda^1_{je}, \quad \forall j \in K,\ \forall e \in E. \tag{6.27}$$

In case the coverage area of a device j touches the segment e, the segment is oriented in the parameterization.

3. **Zero parameterizations for untouched edges:**

$$\lambda^1_{je} \leq z_{je}, \quad \forall j \in K,\ \forall e \in E. \tag{6.28}$$

In case the jth device does not touch the segment induced by an edge e, the covered length of such an edge by the device will be zero. By (6.26), in that case, the device is not restricted to touching the segment, but to assure that no length is accounted for, we fix both λ-values in the fictitious intersection to zero.

4. **Λ-sorting constraints:**

$$\sum_{j\in K}(\xi^0_{je\ell}+\xi^1_{je\ell})=1,\quad \forall e\in E,\ \forall \ell\in Q\cup\{2k\}, \tag{6.29}$$

$$\sum_{\ell\in Q\cup\{2k\}}\xi^s_{je\ell}=1,\quad \forall j\in K,\ \forall e\in E,\ s=0,1 \tag{6.30}$$

$$\sum_{j\in K}(\lambda^0_{je}\xi^0_{je\ell}+\lambda^1_{je}\xi^1_{je\ell})\leq \sum_{j\in K}(\lambda^0_{je}\xi^0_{je(\ell+1)}+\lambda^1_{je}\xi^1_{je(\ell+1)}), \forall e\in E,\ \forall \ell\in Q. \tag{6.31}$$

These constraints allow us to adequately define the variables ξ. Constraints (6.29) and (6.30) assure that for each e each λ_e-value is sorted in exactly a single position in Q and that each position is assigned to exactly one λ_e value. Constraint (6.31) enforces that the ξ-variables sort the λ-values in non-decreasing order.

5. **Coverage of subsegments:**

$$w_{e\ell}\leq \sum_{j\in K}\left(\sum_{i\leq\ell}\xi^0_{jei}+\sum_{i>\ell}\xi^1_{jei}-1\right),\quad \forall e\in E,\ \forall \ell\in Q, \tag{6.32}$$

The coverage of a subsegment $\ell\in Q$ is assured by the existence of a device j for which its λ^0_{je} is sorted in a position anterior to ℓ ($\sum_{i\leq\ell}\xi^0_{jei}=1$) and λ^1_{je} in a posterior position to ℓ ($\sum_{i>\ell}\xi^1_{jei}=1$). Thus, in case both values are 1, the conditions of Lemma 6.15 are verified, and the subsegment is covered. Otherwise, one of the above sums is zero, and the constraint is redundant. Indeed, if $\sum_{i\leq\ell}\xi^0_{jei}=0$, then, by (6.30), $\sum_{i>\ell}\xi^0_{jei}=1$. Thus, by (6.27) and (6.31), one has that $\sum_{i>\ell}\xi^1_{jei}=1$. Similarly, if $\sum_{i>\ell}\xi^1_{jei}=0$, one has that $\sum_{i\leq\ell}\xi^0_{jei}=1$. In both cases, $\sum_{i\leq\ell}\xi^0_{jei}+\sum_{i>\ell}\xi^1_{jei}-1$ takes value zero, implying that the jth device does not cover the subsegment.

Apart from the constraints above, we incorporate into our model the following valid inequalities that allow us to strengthen it:

1. **Touched segments and covered subsegments:**

$$\sum_{\ell\in Q}w_{e\ell}\leq 2\sum_{j\in K}z_{je},\quad \forall e\in E.$$

In case the whole segment is not touched by any device, non of the subsegments are covered.

2. **Symmetry breaking:**

$$\sum_{i=1}^{n} \boldsymbol{x}_{ji} \leq \sum_{i=1}^{n} \boldsymbol{x}_{(j+1)i}, \quad \forall j \in K, j < k.$$

   Since the devices to be located are indistinguishable, any permutation of the j-index will result in an alternative optimal solution, hindering the solution procedure based on a branch-and-bound tree. The above inequality prevents such an amount of alternative optima.

3. **Incompatible edges:**

$$z_{ej} + z_{e'j} \leq 1, \forall j \in K, \forall e, e' \in E,$$

   with $\min\{\|\boldsymbol{x} - \boldsymbol{x}'\|_p : \boldsymbol{x} \in e, \boldsymbol{x}' \in e'\} > 2R$.

   Edges, which are far enough, are not able to be simultaneously touched by the same device.

Conic Programming for MNLCLP

Using the variables and constraints previously described, the following conic programming formulation is valid for the MNLCLP:

$$\text{maximize} \quad \sum_{e \in E} \sum_{\ell \in Q} \omega_e w_{e\ell} L_e \left[\sum_{j \in K} \sum_{s=0}^{1} \lambda_{je}^s \xi_{je(\ell+1)}^s - \sum_{j \in K} \sum_{s=0}^{1} \lambda_{je}^s \xi_{je\ell}^s \right]$$

$$\begin{aligned}
\text{subject to} \quad & (6.26) - (6.32), & \\
& \lambda_{je}^s \in [0,1], & \forall j \in K, \forall e \in E, s = 0,1, \\
& \boldsymbol{x}_j \in \mathbb{R}^n, & \forall j \in K, \\
& z_{je} \in \{0,1\}, & \forall j \in K, \forall e \in E, \\
& \xi_{je\ell}^s \in \{0,1\}, & \forall j \in K, \forall e \in E, \forall \ell \in Q \cup \{2k\}, s = 0,1, \\
& w_{e\ell} \in \{0,1\}, & \forall e \in E, \forall \ell \in Q.
\end{aligned}$$

Conic Programming for PSNLCLP

PSNLCLP seeks to minimize the number of devices to cover at least a portion $\gamma \in (0,1]$ of the length of the network. Although the above variables and constraints can be used to derive similarly a model for this problem, the number of devices, k, to locate is unknown in this case. We estimate an upper bound for this parameter and consider the following binary variables to *activate/desactivate* them.

$$y_j = \begin{cases} 1 & \text{if device } j \text{ is activated,} \\ 0 & \text{otherwise.} \end{cases} \quad \forall j \in K.$$

Then, the PSNLCLP can be formulated as follows:

$$\begin{aligned}
\min \quad & \sum_{j\in K} y_j \\
\text{s.t. } & (6.26) - (6.32), && (6.33)\\
& \sum_{e\in E}\sum_{\ell\in Q} \omega_e w_{e\ell} L_e \left[\sum_{j\in K}\sum_{s=0}^{1} \lambda_{je}^s \xi_{je(\ell+1)}^s - \sum_{j\in K}\sum_{s=0}^{1} \lambda_{je}^s \xi_{je\ell}^s\right] \geq \gamma \sum_{e\in E} \omega_e L_e, && (6.34)\\
& z_{je} \leq y_j, \quad \forall j \in K, \forall e \in E; && (6.35)\\
& \lambda_{je}^s \in [0,1], \quad \forall j \in K, \forall e \in E, s = 0,1,\\
& \boldsymbol{x}_j \in \mathbb{R}^n, \quad \forall j \in K,\\
& z_{je} \in \{0,1\}, \quad \forall j \in K, \forall e \in E,\\
& \xi_{je\ell}^s \in \{0,1\}, \quad \forall j \in K, \forall e \in E, \forall \ell \in Q \cup \{2k\}, s = 0,1,\\
& w_{e\ell} \in \{0,1\}, \quad \forall e \in E, \forall \ell \in Q,\\
& y_j \in \{0,1\}, \quad \forall j \in K.
\end{aligned}$$

In this case, the objective function accounts for the number of activated devices, Constraint (6.34) assures that at least a portion of γ of the coverage volume is attained, and (6.35) prevents covering edges by devices that are not activated.

Instead of minimizing the number of devices one may also minimize the set-up costs by incorporating individual set-up costs for each of the available devices (f_j for $j \in K$) and replace the above objective function by $\sum_{j\in K} f_j y_j$.

To avoid multiple optimal solutions due to symmetry, we also incorporate into the model the following constraints that avoid activating the jth device in case the $(j-1)$th device is not activated in the solution.

$$y_{j-1} \geq y_j, \quad \forall j \in P, j > 1.$$

Remark 6.16. *The complexity of the PSNLCLP highly depends on the number of potential devices to locate (k), since the number of constraints and variables are affected by this parameter. We derive a method to compute a reasonable upper bound for that parameter which is based on computing the minimum number of devices necessary to cover each edge in $U_\gamma \subseteq E$ where U_γ is defined as a minimal set verifying that*

$$\sum_{e \in U_\gamma} \omega_e L_e \geq \gamma \sum_{e \in E} \omega_e L_e.$$

We initialize $U_\gamma = \emptyset$, and sort the sequence $\{\omega_e L_e\}_{e \in E}$ such that $\omega_{e_1} L_{e_1} \geq \omega_{e_2} L_{e_2} \geq \cdots \geq \omega_{e_i} L_{e_i} \geq \omega_{e_{i+1}} L_{e_{i+1}} \geq \cdots$. Then, we define $U_\gamma = \{e_1, \ldots, e_m\}$ such that:

$$\sum_{i=1}^{m} \omega_{e_i} L_{e_i} \geq \gamma \sum_{e \in E} \omega_e L_e > \sum_{i=1}^{m-1} \omega_{e_i} L_{e_i}.$$

Since the minimum number of devices necessary to cover a single edge e is $\left\lceil \frac{L_e}{2R} \right\rceil$, we can fix $k = \sum_{e \in U_\gamma} \left\lceil \frac{L_e}{2R} \right\rceil$.

The mixed integer conic programming (MICP) models that we develop for MNLCLP and PSNLCLP have $O(k^2|E|)$ variables, $O(k|E|)$ linear constraints, and $O(k|E|\log_2(r))$ second–order cone constraints (where $p = \frac{r}{s}$; see Section 4.1). Thus, it is advisable in these models to design alternative solution strategies for solving them or to provide initial solutions that alleviate the search for optimal solutions by providing lower bounds for our problem. In the following sections, we propose different alternatives taking advantage of the geometric properties of these problems.

Constructing Initial Feasible Solutions

The geometric properties that we derive in Section 6.3.2 for the single-device problem can be also extended to the k-device case. Specifically, one can construct solutions of MNLCLP by avoiding the computation of covered lengths in the models and assuming that once an edge of the network is touched by the coverage area of a device, the whole is accounted as covered. With these assumptions, we construct initial solutions to our problem by solving the following integer linear programs:

$$\max \quad \sum_{e\in E}\sum_{j\in K} \omega_e L_e z_{je} \tag{6.36}$$

$$\text{s.t.} \sum_{j\in K} z_{je} \leq 1, \quad \forall e \in E, \tag{6.37}$$

$$\sum_{e\in S} z_{je} \leq n, \forall S \subset E(|S| = n+1) : \bigcap_{e\in S}(e \oplus \mathbb{B}_R(\mathbf{0})) = \emptyset, \forall j \in K, \tag{6.38}$$

$$z_{je} \in \{0,1\}, \quad \forall e \in E, \forall j \in K. \tag{6.39}$$

In the problem above, the overall weighted length of the covered edges is to be maximized by restricting edges to be covered by the same device to those which are feasible for the MNLCLP. The edges are also enforced to be accounted for at most once in the solution.

The strategies for generating and separating the constraints of the above problem are identical to those detailed in Section 6.3.2.

As can be observed in our computational experience (Section 7.2.2), the incorporation of these initial solutions to the original formulation of MNLCLP is advisable to derive exact optimal solutions to the problem in less CPU time.

Math-heuristic Approach

In addition to the exact approaches provided by formulations MNLCLP or PSNLCLP and the generation of initial solutions in the previous section, we propose a math-heuristic procedure to obtain good quality approximated solutions for the problems for larger size instances, in less CPU time. The math-heuristic is based on solving, sequentially, the single-device location problem (6.8)-(6.15) that was described in Section 6.3.2.

We show in Algorithm 3 a pseudocode for this procedure. As already mentioned, the approach is based on solving, sequentially, a single-device location device problem until a certain termination criterion (which depends on the problem to solve, MNLCLP or PSNLCLP) is verified. In case the problem is the MNLCLP the algorithm ends when the number of devices in the pool reaches the value of k. Otherwise, for the PSNLCLP the algorithm ends when the covered weighted length reaches the desired value.

At each iteration, a device is located, and the network to be covered in the next iteration is updated from the previous iteration by removing the segments that have been covered.

Algorithm 3: Math-heuristic 2.

Data: Network $G = (V, E; \Omega)$, number of devices k, and radius R.
$V' = V, E' = E, \Omega' = \Omega$
$X = \emptyset$
while *Termination_Criterion* **do**
    Solve $\boldsymbol{x}, \lambda_e^0, \lambda_e^1, z_e = \arg$ (6.8)-(6.15) for $e \in E', \omega_e \in \Omega'$ and R.
    Update `Termination_Criterion` Add $\boldsymbol{x}$ to X.
    for $e \in E'$ **do**
        if $z_e = 1$ **then**
            if $\lambda_e^0 \in (0, 1)$ **then**
                Add $\boldsymbol{y}_e^0$ to V'.
                Add $\{\boldsymbol{o}_e, \boldsymbol{y}_e^0\}$ to E'.
                Add ω_e to Ω'.
            if $\lambda_e^1 \in (0, 1)$ **then**
                Add $\boldsymbol{y}_e^1$ to V'.
                Add $\{\boldsymbol{y}_e^1, \boldsymbol{f}_e\}$ to E'.
                Add ω_e to Ω'.
            Remove e from E'

Result: $X \in \mathbb{R}^{n \times k}$: Location of the devices.

Chapter VII

Computational Experience

Batter my heart, three-person'd God.
— John Donne. *Holy Sonnet* XIV

After all theoretical and practical development, in this chapter, we report the results of an extensive set of experiments demonstrating the validity and practical utility of our approaches.

They are divided in sections depending on the approach whose performance is tested. In Section 7.1, for maximal mediated graphs, we compare our optimization-based method with the enumerative approach proposed in Hartzer et al. (2022). For minimal mediated graphs, we analyze the performance of different domain formulations for which we derive integer linear optimization models. In Section 7.1.3, we show the computational performance of our specific mathematical programming model for compute minimal second–order cone representations. In Section 7.2.1, we have run a series of experiments to analyze the performance of solving the proposed gravitational covering location problem with an optimal second–order cone representation of the generalized power cone with respect to the usual naive representation. The results of our computational experiments on real-world urban pipeline networks are reported in Section 7.2.2.

7.1 Computing Optimal Mediated Graphs

In this section, we report the results of our computational experience, which we performed to validate the proposals and compare them with other approaches in the literature.

7.1.1 Data

We use the datasets provided by Hartzer et al. (2022) to analyze their proposed algorithm to compute maximal mediated sets and that the authors made publicly available at `https://polymake.org/downloads/MMS/csv/`. The dataset contains simplicial sets, $\mathcal{A} = \{v_0, v_1, \ldots, v_n\}$, in dimensions $n \in \{2,3,4,5,6,7,8,9\}$ of different sizes, measured by their degrees:

$$d(\mathcal{A}) := \min \left\{ \rho \in \mathbb{Z}_+ : \sum_{l=1}^{n} w_l \leq 2\rho \text{ for all } w \in \text{Conv}(\mathcal{A}) \cap (2\mathbb{Z})^n \right\}.$$

The authors generated all the simplicial sets and lattices for some of the dimensions and degrees and sampled these sets for the rest of the dimensions and higher degrees. In total, 8,941,852 maximal mediated sets were computed in Hartzer et al. (2022), distributed by dimension as shown in Table 7.1. We randomly select some of these instances to compute the minimal and the maximal mediated graph using our approach. In the third column of Table 7.1, we detail the number of random instances selected for each combination of n and d.

n	2	2	2	3	3	4	4	4	4	4	5	5	6	6	7	7	8	9
d	50	100	150	10	16	6	8	10	14	16	8	16	16	20	4	16	16	16
#	1000	1000	300	500	1000	150	1000	1000	1000	1000	1000	1000	1000	1000	15	1000	1000	300

TABLE 7.1: Size for the samples of the simplices from Hartzer et al. (2022).

We compute the maximal mediated graphs of the selected random sets $\mathcal{A}$, as detailed above. We also run the enumeration-and-filtering algorithm proposed in Hartzer et al. (2022) to compare the efficiency of our approach with respect to the only previous proposal for this task.

For the minimal mediated graphs, a set of interior points $\mathcal{B}$ is required to obtain *proper* subgraphs. We then run our model for a random selection of $s \in \{1,3,5\}$ integer points inside the convex hull of the points in $\mathcal{A}$ to analyze the performance on different numbers of points in $\mathcal{B}$.

The models were coded in `Python` and solved using the optimization solver `Gurobi 12.0` on an Apple M1 Max with 64 GB RAM.

7.1.2 Results on Maximal Mediated Graphs

We run our MILP model (D-MaxMGP) for all the samples of the instances provided in Table 7.1. In total 15110 problems were solved. We also run the algorithm proposed in (Hartzer et al., 2022, Algorithm 4.3).

In Figure 7.1 we show the performance profiles for obtaining the maximal mediated graph of both our mathematical optimization-based approach and the algorithm proposed in Hartzer et al. (2022) (named `BM` and `HRWY`, for the initials of the authors' last names). In the plots, we represent the percent of instances solved in less than each unit of CPU time (in log-scales to ease the distinction). For a fair comparison, we do not include in those times the time required to enumerate the points inside the given lattices. It is evident that the performance of our approach is superior to the one in Hartzer et al. (2022). Although solving a MILP may require, in the worst case, the enumeration of the whole set of integer feasible points, the solution methods for these problems are designed to avoid such an enumeration by branching, bounding, and reducing the feasible region by cutting off part of the space.

The summary of the obtained results is shown in Table 7.2, where we report, for each value of n and d, the average CPU times (in seconds) with both our methodology (`time_BM`) and the enumerative methodology (`time_HRWY`) only for those instances that were optimally solved with each procedure. The percent of instances in each row that were not optimally solved within one hour with the enumerative methodology is reported in column `unsolved_HRWY`. Our methodology was capable of solving optimally all the instances within the time limit.

In Figure 7.2 we show, for each dimension n, the average CPU times (log-scale) to compute the maximal mediated graph with the optimization-based methodology that we propose (`BM`) and with the enumerative strategy proposed in Hartzer et al. (2022) (`HRWY`). We also represent in the same plot, the average CPU times to enumerate the points inside the simplex, required to compute the optimal mediated graph with both methodologies.

In view of the results we conclude that the CPU time required by our optimization-based methodology to obtain the maximal mediated graphs is significantly smaller than the enumerative procedure proposed in Hartzer et al. (2022), and in some cases even able to construct the optimal solutions when the enumerative approach is not capable to do it.

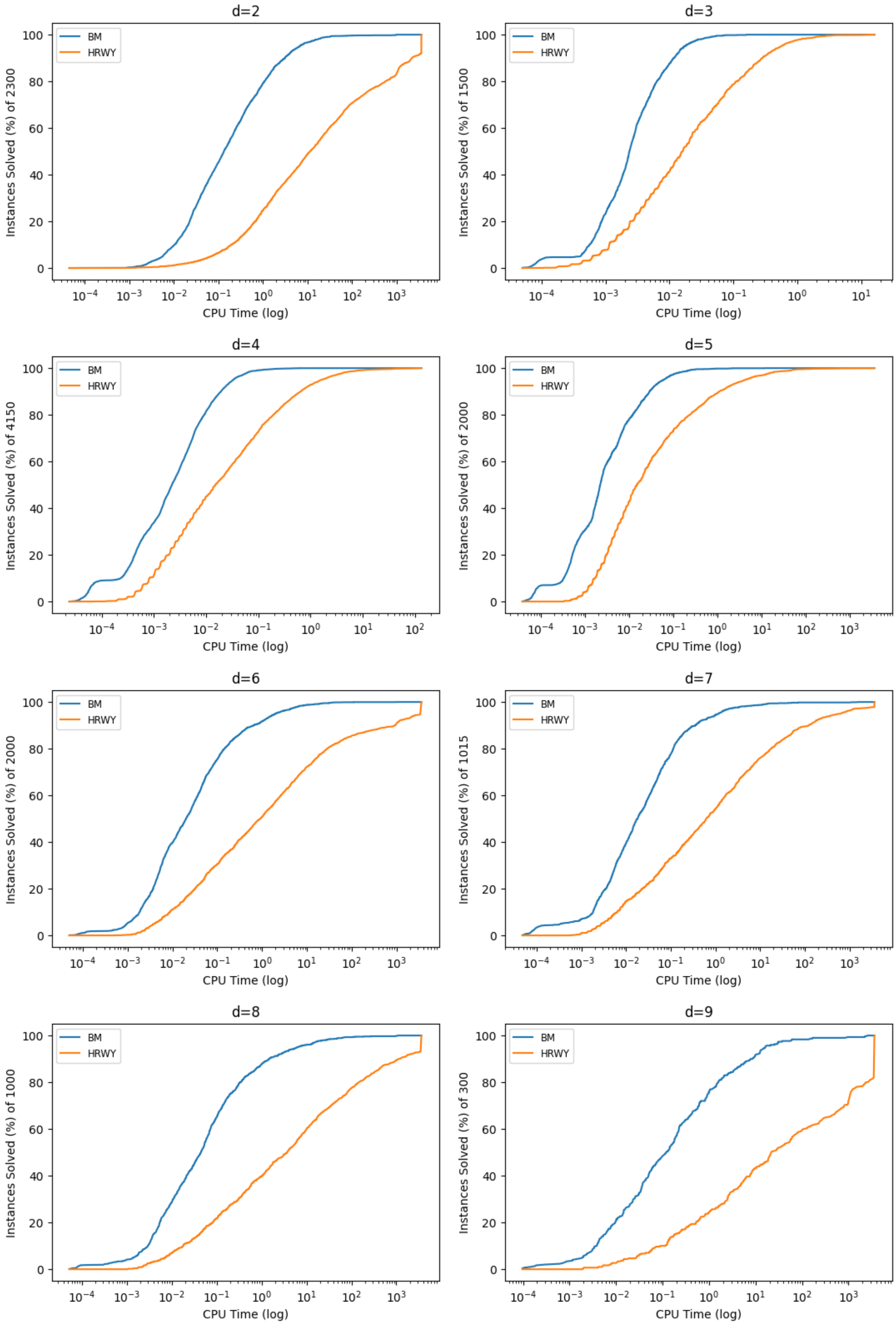

FIGURE 7.1: Performance profiles for our approach (orange) and the one in Hartzer et al. (2022) (blue).

n	d	time_BM	time_HRWY	unsolved_HRWY
	50	0.05	5.71	0%
2	**100**	1.97	373.61	4.30%
	150	23.91	818.49	46.67%
3	**10**	0.00	0.01	0%
	16	0.01	0.20	0%
	6	0.00	0.00	0%
	8	0.00	0.00	0%
4	**10**	0.00	0.04	0%
	14	0.01	0.83	0%
	16	0.02	1.63	0%
5	**8**	0.00	0.02	0%
	16	0.04	4.60	0.10%
6	**16**	0.09	32.05	0.30%
	20	2.09	197.51	9.90%
7	**4**	0.00	0.01	0%
	16	3.16	58.28	2.20%
8	**16**	5.04	130.39	6.80%
9	**16**	22.51	307.61	17.67%

TABLE 7.2: Summary of our computational experiments for the maximal mediated graph.

Although the construction involved in the enumerative approach can be useful for understanding the geometry of the mediated graphs, our approach has the advantage that it allows to solve then larger instances in reasonable CPU time. The combination of our approach and the reduction strategies in the enumerative approach by incorporating conditions in the form of linear inequalities in our model could result in a better approach, that will be explored in a forthcoming paper.

7.1.3 Results on Minimal Mediated Graphs

For the minimal mediated graphs, we randomly select 20 random instances from each row, i.e., or each dimension n. For each of them, we randomly select s interior points to the simplex $\mathcal{A}$, for $s \in \{1, 3, 5\}$. These points form the set $\mathcal{B}$. Then, we consider three different domains for the vertices in the minimal mediated graph $\mathbb{M} \in \{\mathbb{R}^n, \mathbb{Z}^n, (2\mathbb{Z})^n\}$. In total, we solve 270 instances with each of the three optimization models that we propose. We run the extended approach highlighted in Remark 3.18 to construct the whole set of minimal mediated graphs for given sets $\mathcal{A}$ and $\mathcal{B}$ on a specific domain $\mathbb{M}$.

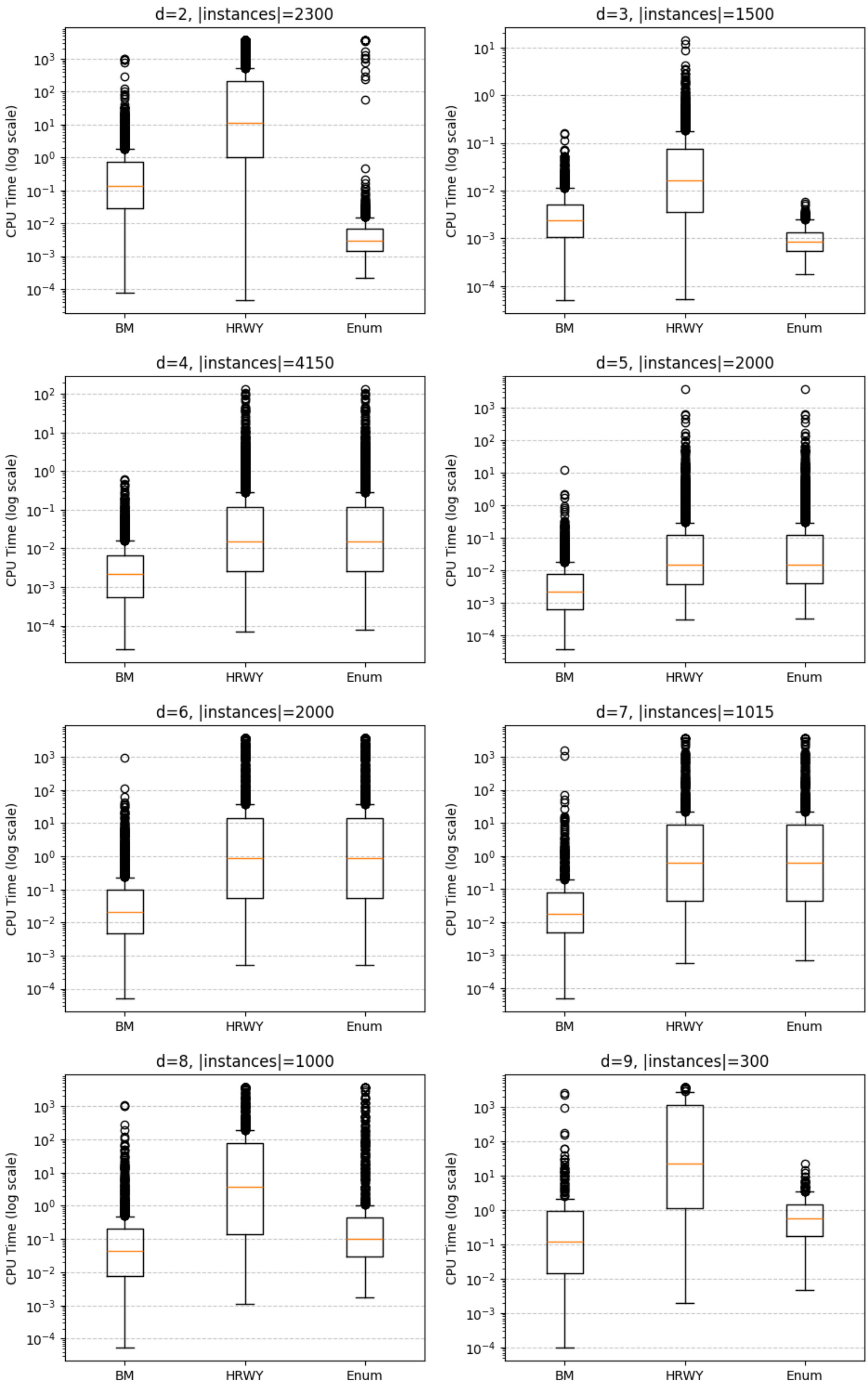

FIGURE 7.2: Boxplots for the CPU times (in log-scale) required to compute the maximal mediated graphs with our methodology (BM), the methodology in Hartzer et al. (2022), and the CPU time required to enumerate the required points.

For $\mathbb{M} = \mathbb{R}^n$ (continuous domain), since the mathematical optimization problem is affected by the number of potential mediated vertices in the graph (upper bounded by $\nu_{\mathcal{A}}(\mathcal{B})$ which can be large), following the suggestion in (Blanco and Martínez-Antón, 2024a), we solve the problems iteratively. Specifically, we start by taking $\mathcal{V}$ an index set with cardinal 1, and solve the problem. In case the problem is feasible, we are done, and the solution is a minimal mediated graph. Otherwise, we increase the cardinal of $\mathcal{V}$ and repeat the process until a feasible solution is found. In most of the cases, the cardinal of the minimal mediated graph is much smaller than the upper bound and we avoid solving huge integer linear problems. In general, we empirically tested that checking infeasibility requires much less time than solving a single but larger integer linear problem.

In Table 7.3 we summarize the results of our experiments. There, the first two columns indicate the dimension (n) and the number of random points chosen in the set $\mathcal{B}$. Then, for each domain $\mathbb{M} \in \{\mathbb{R}^n, \mathbb{Z}^n, (2\mathbb{Z})^n\}$, and then, different approaches we report the average sizes of the minimal mediated graph, the CPU time (in seconds) required to compute one minimal mediated graph, the average CPU time (in seconds) per extra minimal mediated graph computed, and the number of minimal mediated graphs obtained. For the domain $(2\mathbb{Z})^n$, either a single minimal mediated set was found or the problem was infeasible. Thus, we do not report the value *Av. Time Rest* for this domain since all the values are zero.

As expected, as the domain is larger, the problem becomes more challenging. Although one could also expect that al larger the size of $|\mathcal{B}|$ more difficult the problem, this is not always true, as can be seen for $n = 2$, where the problem for $s = 3$ is more time demanding than the others. The same happens for the computation of more than one minimal mediated graph in $\mathrm{MinMG}_{\mathcal{A}}(\mathcal{B})$.

Regarding the size of the obtained minimal mediated graph, the number of vertices is slightly larger for $(2\mathbb{Z})^n$ than for $\mathbb{Z}^n$, and the same happens for $\mathbb{Z}^n$ and $\mathbb{R}^n$. Note that although the approaches are different, they all solve the same problems but in different, but nested, feasible regions. In fact, feasible solutions in the domain $(2\mathbb{Z})^n$, are also feasible for $\mathbb{Z}^n$, and those for $\mathbb{Z}^n$ are feasible for $\mathbb{R}^n$. This observation also affects the number of graphs in $\mathrm{MinMG}_{\mathcal{A}}(\mathcal{B})$, where for the domain $\mathbb{R}^n$ larger numbers of minimal mediated graphs were found.

Note that the case $n = 2$ is particular, since in the dataset in Hartzer et al. (2022), the authors consider simplices with very large extremes compared to the other. Thus, the planar case can be more time-demanding than the higher dimensional, because of the degree of the simplices that have been tested.

n	$\|\mathcal{B}\|$	# Vertices $(2\mathbb{Z})^n$	$\mathbb{Z}^n$	$\mathbb{R}^n$	Time First Sol. $(2\mathbb{Z})^n$	$\mathbb{Z}^n$	$\mathbb{R}^n$	Av. Time Rest $\mathbb{Z}^n$	$\mathbb{R}^n$	$\|\text{MinMG}_{\mathcal{A}}(\mathcal{B})\|$ $(2\mathbb{Z})^n$	$\mathbb{Z}^n$	$\mathbb{R}^n$
	1	5.24	5.24	4.53	0.02	0.15	43.32	0.32	0.01	1.00	1.06	1.29
2	3	7.83	7.78	7.06	0.04	1.35	55.53	4.86	2.51	1.00	2.94	17.56
	5	10.39	10.11	8.94	0.07	0.91	9.78	1.91	0.30	1.00	6.44	17.28
	1	5.18	5.18	5.18	0.01	0.03	0.01	0.02	0.00	1.00	1.00	1.00
3	3	8.00	7.73	7.73	0.01	0.06	0.86	0.11	0.29	1.00	1.45	2.64
	5	10.55	10.45	10.45	0.01	0.11	16.10	0.07	3.62	1.00	3.36	10.73
	1	6.00	6.00	5.40	0.01	0.18	13.83	0.26	0.00	1.00	1.00	1.00
4	3	8.60	8.60	7.80	0.02	0.26	15.32	0.33	0.02	1.00	1.30	1.40
	5	10.40	10.40	9.40	0.03	0.33	131.70	0.33	0.01	1.00	1.40	1.40
	1	7.13	7.13	7.13	0.00	0.12	0.01	0.18	0.00	1.00	1.00	1.00
5	3	9.39	9.26	9.26	0.01	0.15	0.02	0.20	0.01	1.00	1.10	1.19
	5	11.10	11.39	11.39	0.01	0.18	0.05	0.24	0.04	1.00	1.16	1.32
	1	8.10	8.10	8.10	0.00	0.16	0.03	0.31	0.00	1.00	1.00	1.00
6	3	10.25	10.25	10.25	0.01	0.32	0.04	0.35	0.01	1.00	1.00	1.00
	5	11.85	12.50	12.50	0.01	1.15	0.08	0.64	0.06	1.00	1.20	1.40
	1	9.00	9.00	8.47	0.01	0.87	14.69	1.68	0.00	1.00	1.00	1.00
7	3	11.06	11.06	10.41	0.02	1.01	15.66	1.63	0.01	1.00	1.00	1.00
	5	13.47	13.47	12.71	0.03	2.11	33.70	2.55	0.13	1.00	1.18	1.82
	1	10.08	10.08	10.08	0.01	0.81	0.02	1.19	0.00	1.00	1.00	1.00
8	3	12.08	12.08	12.08	0.01	0.63	0.04	1.13	0.01	1.00	1.08	1.08
	5	14.23	14.23	14.23	0.01	1.55	0.06	3.53	0.02	1.00	1.08	1.08
	1	11.00	11.00	11.00	0.03	3.36	0.04	10.86	0.00	1.00	1.00	1.00
9	3	13.05	13.05	13.05	0.03	5.30	0.06	11.15	0.01	1.00	1.00	1.00
	5	15.10	15.10	15.10	0.03	4.32	0.09	8.43	0.02	1.00	1.00	1.00

TABLE 7.3: Summary of the results of our experiments for the minimal mediated graph.

In Figure 7.3 we show the performance profiles (in log-scale to ease its reading) for our experiments on the minimal mediated graph distinguishing by dimension n, size of the set $\mathcal{B}$, s, and domain. Each of those lines was constructed by indicating the percent of instances optimally solved in less than a given number of seconds (in log-scale). The less time-consuming approach (the superior lines) seems to be the domain $(2\mathbb{Z})^n$ for $s = 1$ (solid blue lines). In contrast, the more challenging problems were the continuous domain (green) and some of those in the $\mathbb{Z}^n$ domain (red).

In conclusion, our approach to compute minimal mediated graphs was capable of solving all the instances (even the $n = 9$ ones) in more than reasonable CPU time, both to compute a single mediated graph or all the graphs

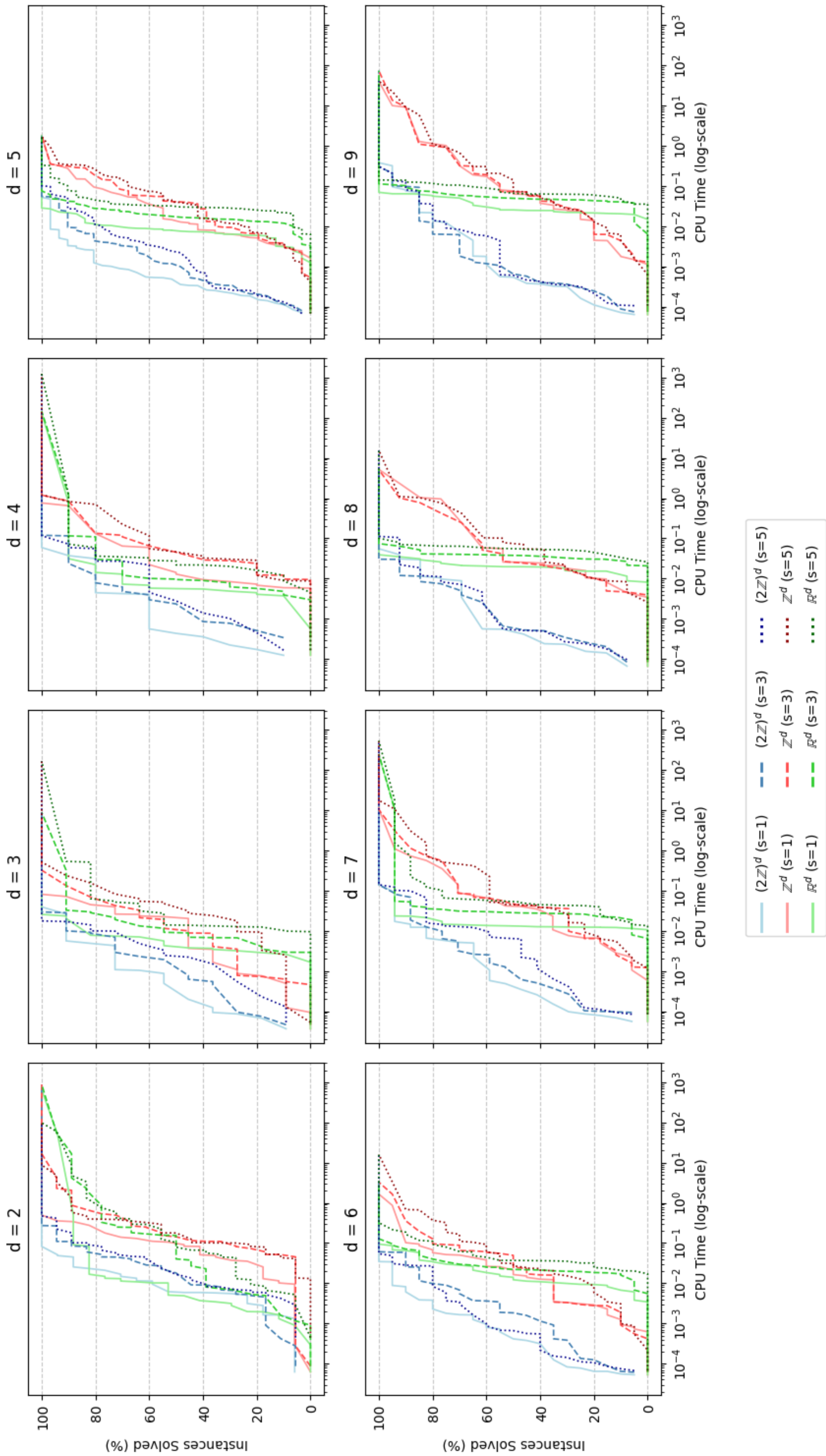

FIGURE 7.3: Performance profile for our experiments on the minimal mediated graphs. Blue lines represent $\mathbb{M} = (2\mathbb{Z})^n$, green lines $\mathbb{M} = \mathbb{R}^n$ and red lines $\mathbb{M} = \mathbb{Z}^n$. Solid lines indicate the case $s = 1$, dashed lines $s = 3$, and dotted lines $s = 5$.

in the family $\mathrm{MinMG}_A(\mathcal{B})$, for all the domains that we consider. Thus, this novel approach with multiple applications in conic decomposition has been proven to be useful and can be practically applied to these problems.

Computational Experiments for the MαMGP

We have run a series of experiments to analyze the performance of solving M$\boldsymbol{\alpha}$MGP on randomly generated instances. Note that the only input for M$\boldsymbol{\alpha}$MGP is the vector $\boldsymbol{\alpha} \in \Delta_d$. Thus, we randomly generate sequences of d integers in $[1, q]$, with d ranging in $\{2, 3, 4\}$ and q ranging in $\{10, 20, 30, 40\}$. For each combination of d and q, we generate 5 instances. Each of these instances results in a vector $\boldsymbol{\alpha} \in \Delta_d$ normalizing the resulting vector by the sum of its coordinates. In total, 60 instances were generated.

For each of these instances, we run the model described in Section 4.1.2. The formulation has been coded in Python 3.8 in a Huawei FusionServer Pro XH321 (`https://supercomputacion.ugr.es/arquitecturas/albaicin/albaicin` at Universidad de Granada) with an Intel Xeon Gold 6258R CPU @ 2.70GHz with 28 cores. We used Gurobi 10.0.3 as an optimization solver. A time limit of 5 hours was fixed for all the instances.

In the results of our preliminary experiments, we observed that in most of the instances, the minimal cardinality of the mediated graph was reached in the lower bound. Thus, instead of fixing $\Lambda_{\boldsymbol{\alpha}}$ as the upper bound, which results in an optimization problem with an overestimated number of variables, we proceed by fixing, initially $\Lambda_{\boldsymbol{\alpha}}$ to the value of the lower bound, and in case the problem is infeasible, we increase by one unit this bound, until the problem is feasible. This strategy dramatically reduces the size of the optimization problem.

The set of instances used in our experiments is available at the GitHub repository `https://github.com/vblancoOR/extended-representations`.

In Table 7.4 we summarize the results of our experiments. For each value of d (dimension of $\boldsymbol{\alpha}$) and q (maximum value of s), we report in the table the minimum, average, and maximum CPU time (in seconds) required by Gurobi to solve the problem (columns bellow `CPU Time`); the number of nodes in the branch and bound approach for solving the feasible problem (`#Nodes`); the deviations of the optimal value with respect to both the lower bound (`DevLB`) and the upper bound (`DevUB`). Finally, in column `Opt` we report the average optimal value for the problem, i.e., the cardinality of the minimal

		CPU Time (secs)						
d	q	Min	Av	Max	#Nodes	DevLB	DevUB	Opt
2	10	0.02	0.04	0.04	0	0.00%	19.67%	3.8
	20	0.06	0.16	0.35	1028	0.00%	27.88%	5.2
	30	0.06	0.24	0.61	2659	0.00%	20.48%	5.4
	40	0.15	0.3	0.41	2901	0.00%	19.52%	5.8
3	10	0.13	0.43	0.96	1415	0.00%	26.93%	4.6
	20	0.89	69.67	179.97	6101	12.38%	26.49%	6.2
	30	1.28	2.11	3.67	19319	0.00%	35.67%	6
	40	1.38	58.2	281.54	73464	2.86%	29.13%	6.4
4	10	0.69	344.76	850.48	2884667	18.10%	20.08%	6.2
	20	397.14	8551.05	18000*	63662316	22.14%	22.94%	7.2
	30	412.06	6343	18000*	4063237	15.87%	30.00%	7.6
	40	2.85	815.54	1628.23	2542017	7.14%	15.00%	6.5

TABLE 7.4: Summary of our computational experiments for the M$\boldsymbol{\alpha}$MGP.

$\boldsymbol{\alpha}$–mediated graph minus d. For $d = 4$ we highlight with an asterisk ($*$) in the Max CPU time column that for one of the instances summarized in that row reached the time limit in one of the runs, and in that case, the minimum cardinality of the $\boldsymbol{\alpha}$-mediated graph might be smaller but Gurobi was not able to find a feasible solution within the time limit and then, the problem for a larger value of $\Lambda_{\boldsymbol{\alpha}}$ was successfully solved.

Several observations can be drawn from the obtained results. First, that the M$\boldsymbol{\alpha}$MGP is a computationally challenging problem. As the dimension of $\boldsymbol{\alpha}$, d, increases, solving the M$\boldsymbol{\alpha}$MGP becomes more computationally costly. Additionally, in the planar case ($d = 2$), the optimal cardinality of the mediated set in the mediated graph coincides with the lower bound ($\max\{d-1, \lceil \log_2(\hat{s}) \rceil\}$) (Morenko et al., 2013, Section 3.2), which establishes an upper bound equal to this lower bound for this case (both representations are equivalent in terms of complexity). This is no longer the case for $d \geq 3$, but still in 75% of the instances for $d = 3$ the lower bound coincides with the optimal value. For $d = 4$, the situation becomes different, since in only 20% of the instances the solver was able to check that the lower bound is the optimal cardinality of the mediated set. It can be the case that although the lower bound is reached, the solver was not able to prove it within the time limit.

Finally, one can also observe that the integer linear problem is challenging and requires branching, being the number of nodes in the branch-and-bound required to certify optimally really large for some of the instances.

The most interesting observation, that validates the study in Section 4.1, is that the deviations with respect to a myopic representation of the cones (as a tree-based mediated graph) are large (see `DevUB`, i.e., the savings in the number of mediated vertices, or equivalently, in the number of variables required to represent the cones as second order cones.

Note that although solving the M$\boldsymbol{\alpha}$MGP might require a significant amount of CPU time, the problems requiring the representation of a given power cone would need to represent the cone several times (as in most continuous location problems) but the M$\boldsymbol{\alpha}$MGP is solved just once. It is advisable then to solve optimization problems restricted to these cones, since the minimal representation results in a reduction in the CPU time required to solve them, as can be observed in the following section.

In figures 7.4 and 7.5 we show some of the optimal mediated graphs obtained in our experiments for the cases $d = 3$ (in $\mathbb{R}^2$) and $d = 4$ (in $\mathbb{R}^3$), respectively. In the plots, we represent with red dots the elements in $\mathcal{A}_{\boldsymbol{\alpha}}$, with a green dot the point $\boldsymbol{b}_{\boldsymbol{\alpha}}$, and with blue dots the rest of the elements in the mediated set. The arrows represent the arcs of the mediated graph. An intriguing question, that will be the goal of our further research, is to determine the topological structure of the mediated graphs and to exploit it into the above mathematical optimization problem.

7.2 Continuous Location Problems via Conic Programming

7.2.1 Results on Gravitational Covering Location Problem

We have run a series of experiments to analyze the performance of solving this problem with an optimal SOC representation of the generalized power cone with respect to the usual representation that provides the upper bound described in Remark 4.13. The chosen inputs are a random generation of four planar datasets of demand points in plane ($n = 2$) with $|I| \in \{25, 50, 75, 100\}$. The parameters ω_i were randomly chosen as integers in $[0, 10]$. We assume that the m-variables are bounded in $[0, 1]$ where $d = 3$; that the budget, B, is

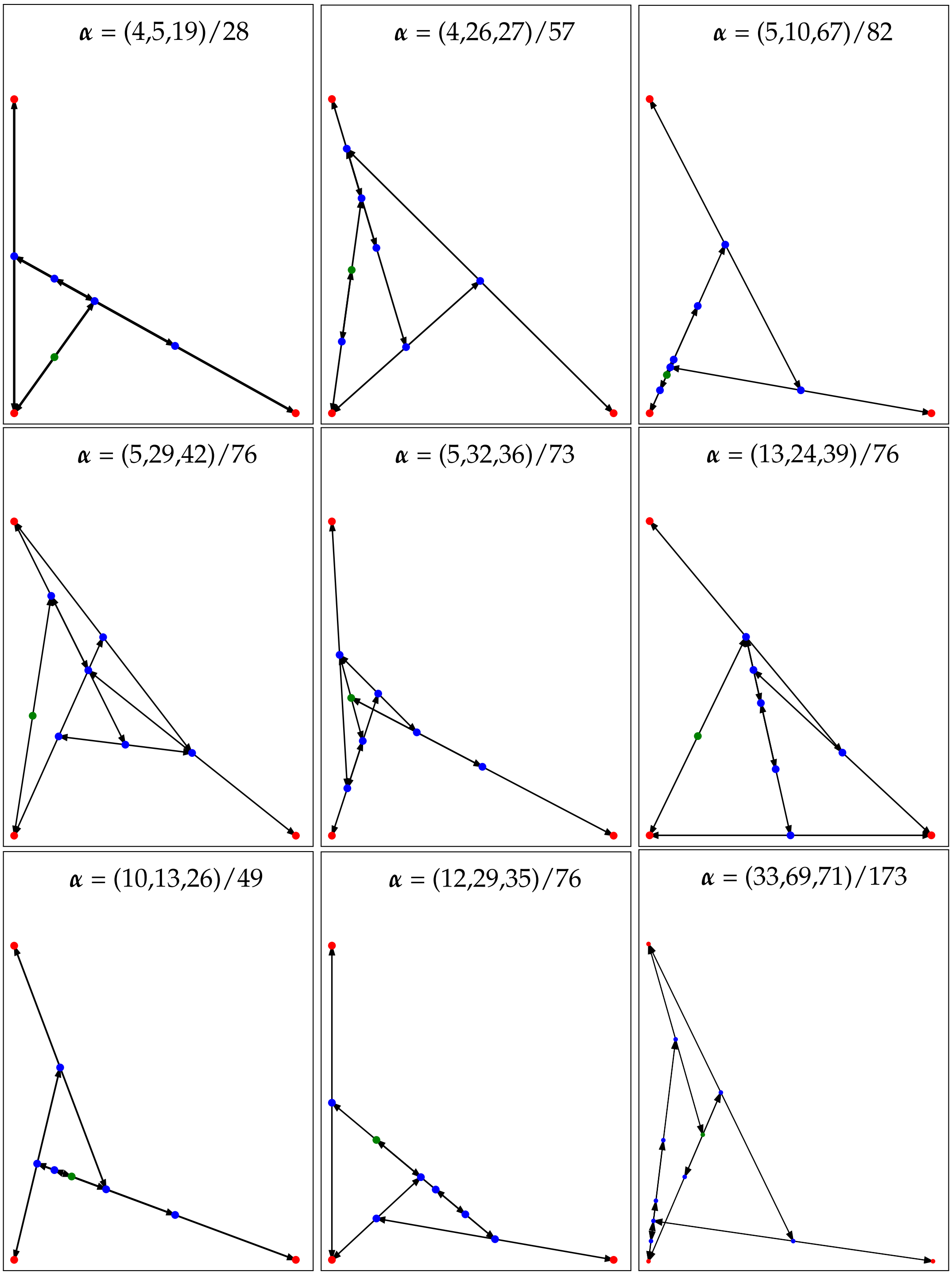

FIGURE 7.4: Some examples of minimal α–mediated graphs for $d = 3$.

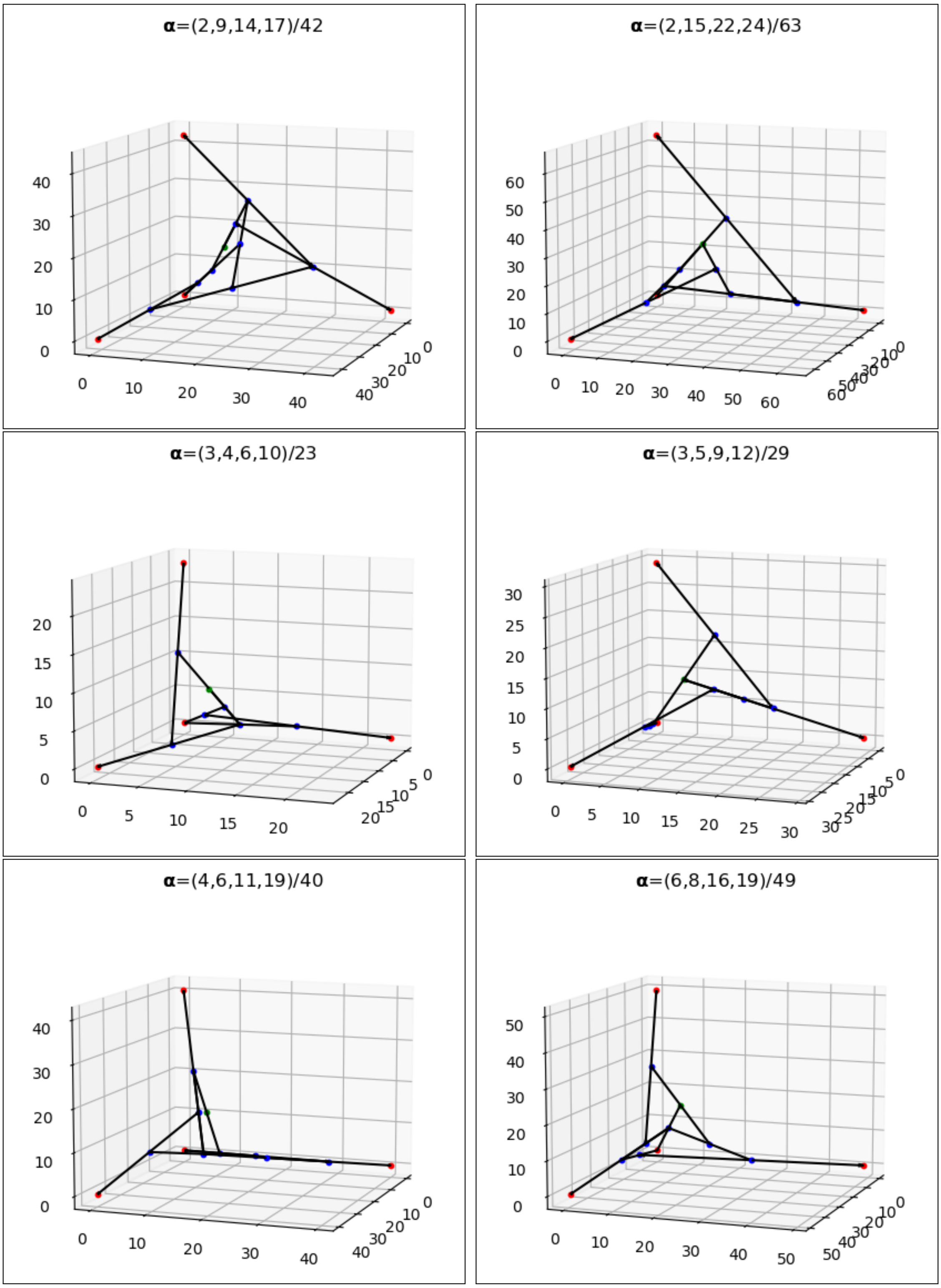

FIGURE 7.5: Some examples of minimal $\boldsymbol{\alpha}$–mediated graphs for $d = 4$.

$\gamma(2|I|+|J|)$, where $\gamma = \frac{1}{4}$; and the constants G_{ij} are all equal to 1. We solved the problem for $|J| \in \{2,3,5\}$.

We run the experiments for all the combinations of ℓ_p–norms and $\boldsymbol{\alpha}$ values described in Table 7.5:

p	$\boldsymbol{\alpha}$
$\frac{43}{31}$	$\left(\frac{2}{26}, \frac{5}{26}, \frac{19}{26}\right)$
2	$\left(\frac{13}{80}, \frac{33}{80}, \frac{34}{80}\right)$
	$\left(\frac{6}{60}, \frac{19}{60}, \frac{35}{60}\right)$
$\frac{17}{3}$	$\left(\frac{35}{180}, \frac{58}{180}, \frac{87}{180}\right)$

TABLE 7.5: Norms and $\boldsymbol{\alpha}$ used in our computational experiments.

In total, 144 instances were generated. A time limit of 2 hours was fixed for all the instances.

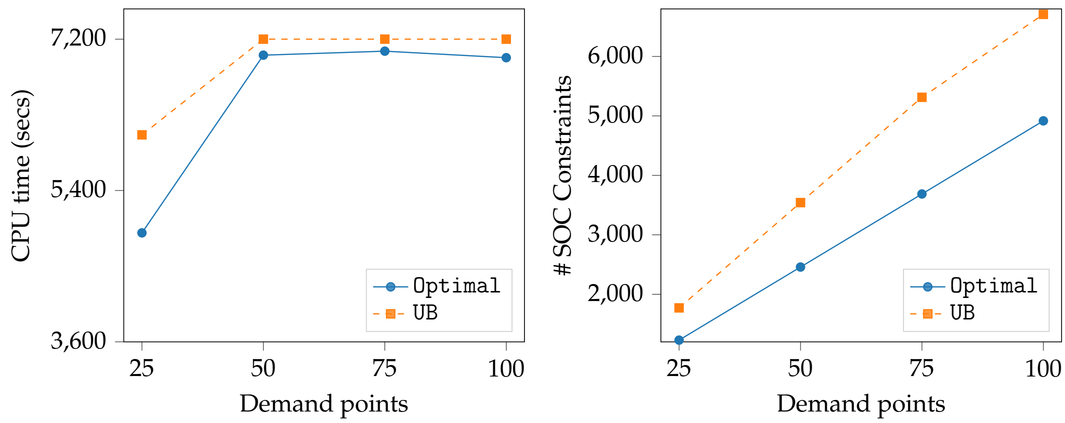

FIGURE 7.6: Average CPU times (left) and number of constraints (right) of the optimal SOC representations of the gravitational maximal covering location problem with respect to UB SOC representantions.

In figures 7.6 and 7.7 we summarize the main results obtained in our experiments. In Figure 7.6 we represent, for each number of demand points in the experiments, in the left plot, the average CPU time (in seconds) required by Gurobi to solve the problem (or 7200 seconds if the time limit was reached without guarantying optimality), and, in the right plot, the number of SOC constraints in the formulation, both for the optimal representation

(`Optimal`) and the one that provides the upper bound (`UB`). As can be observed, using the optimal cones is advisable since it reduces, significantly, the computational resources required to solve the problems. Specifically, the upper bound representation was able to solve optimally only 9 out of the 144 instances within the time limit (all of them form 25 demand points), whereas the optimal representation was able to solve 21. The main reason for such a gain is the number of SOC constraints in the models (on average 30% less of these constraints in the optimal representation model).

Since most of the instances were not optimally solved within the time limit, in what follows we compare the quality of the best solution obtained after two hours. In the obtained results, the optimal model always reaches a coverage at least as good as the one obtained with the upper bound representation. In 94 out of the 144 instances (65% of the instances), the optimal representation model obtained a strictly better coverage than the upper bound model.

In Figure 7.7 we represent the percent deviation, in coverage, of the best solution obtained with the optimal representation with respect to the one obtained with the upper bound representation for those instances where the solutions are different. They represent 55% of the instances for $|I| = 25$, 72% of the instances for $|I| = 50$, 64% of the instances for $|I| = 75$, and 69% of the instances for $|I| = 100$. Observe that the average gain is impressive in the quality of the solution. Although the average deviation is 26%, in some instances the optimal representation obtained solutions with 82% more coverage than those obtained with the upper bound representation.

7.2.2 Computational Experiments for Network Covering

In this section, we report on the results of a series of computational experiments performed to empirically assess our methodological contribution to the k-MNLCLP and PSNLCLP presented in the previous sections. We use six real networks obtained from two different sources: one based on the networks developed by the University of Exeter's (UOE) Centre for Water Systems available in `https://emps.exeter.ac.uk/engineering/research/cws/resources/benchmarks/` and other privately provided by Prof. Ormsbee from the University of Kentucky (UKY). These networks, which are called `gessler`, `jilin`, `richmond`, `foss`, `rural` and `zj`, have $14, 34, 44, 58, 60$ and 85 edges, respectively. The networks have been scaled to fit in a disk of radius 5. The networks are drawn in Figure 7.8.

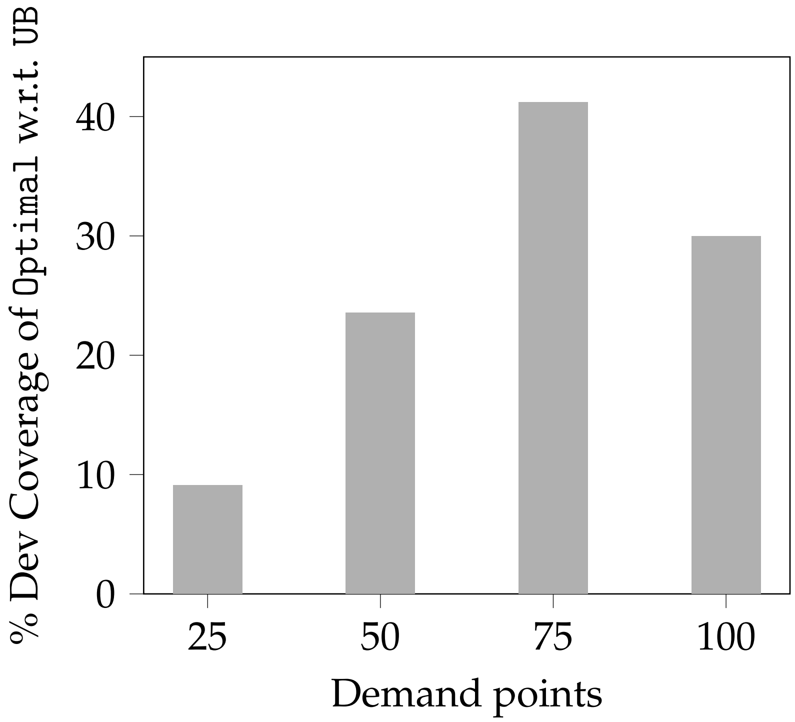

FIGURE 7.7: Average coverage deviations of the optimal SOC representations of gravitational maximal covering location problem with respect to UB SOC representantions.

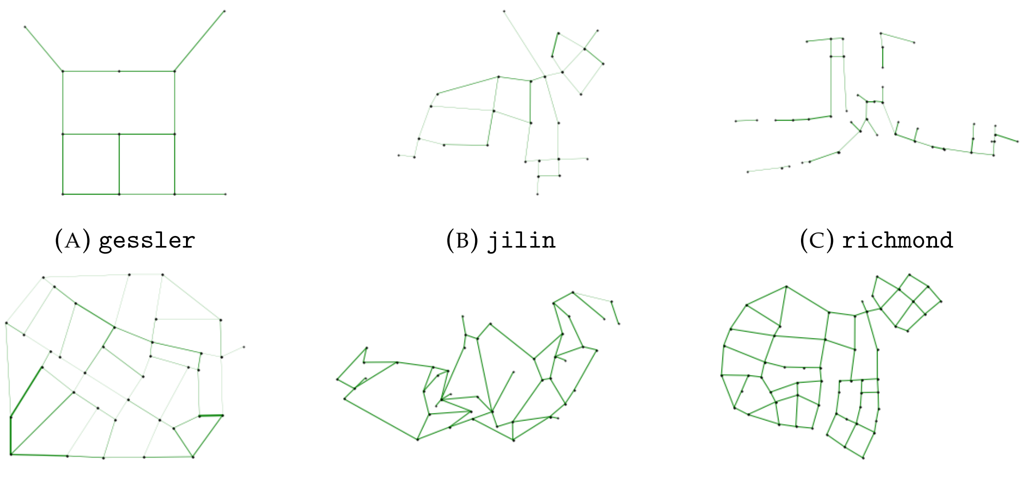

(A) gessler (B) jilin (C) richmond

(D) foss (E) rural (F) zj

FIGURE 7.8: Networks used in our computational experiments.

We have run the different approaches for the MNLCLP and the PSNLCLP for disk-shaped coverage areas with radii ranging in $\{0.1, 0.25, 0.5\}$. For the MNLCLP the number of devices to locate, k, ranges in $\{2, 5, 8\}$, whereas for the PSNLCLP the values of γ range in $\{0.5, 0.75, 1\}$.

All the experiments have been run on a virtual machine in a physical server equipped with 12 threads from a processor AMD EPYC 7402P 24-Core Processor, 64 Gb of RAM, and running a 64-bit Linux operating system. The models were coded in Python 3.7 and we used Gurobi 9.1 as optimization solver. A time limit of 5 hours was set for all the experiments.

In Tables 7.6 and 7.7 we show the average results obtained in our experiments. We report average values of the consumed CPU time (in seconds), and percent of unsolved instances, and the MIP Gap within the time limit. Both tables are similarly organized. In the first block (first three columns), the name of the instance together with its number of vertices and edges is provided. In the second block (next two columns) we write the values of k (for the MNLCLP) or γ (for the PSNLCLP) and the radius. The next three blocks are the results obtained with each of the approaches. For the MNLCLP we run the MISOCP formulation, and also the exact and math-heuristic solution approaches detailed in sections 6.3.3, Constructing Initial Feasible Solutions (MNLCLP_1, for short) and 6.3.3, Math-heuristic Approach (MNLCLP_2), respectively. We do not report results on the Unsolved instances and MIPGap for the MNLCLP_2 since all the instances were solved within the time limit with that approach. In Table 7.7 the results are organized similarly for the PSNLCLP, but we do not generate initial solutions since that strategy only applies to the MNLCLP, and only the strategy PSNLCLP_2. The flag `TL` indicates that all the instances averaged in the row reach the time limit without certifying optimality. The flag `OoM` indicates that the solver outputs *Out of Memory* at some point when solving the instance.

The first observation from the results that we obtain is that both problems are computationally challenging since they require large CPU times to solve even the small instances. Actually, the exact MNLCLP was only able to solve up to optimality, small instances with small values of k, and the exact PSNLCLP only solved a few instances, and in many of them, the solver outputs Out of Memory when solving them.

The first alternative (and exact) strategy, MNLCLP_1, based on constructing initial solutions to the problem, had a slightly better performance with respect to those instances that were solved with the initial formulation, both in CPU time and MIPGap. Some of the instances were not able to be solved with MNLCLP but were able to be solved with the initial solutions that we construct.

With respect to the heuristic approach, the consumed CPU times are tiny compared to the times required by the exact approaches and was able to construct feasible solutions for all the instances, even for those that the exact approaches flagged Out of Memory. In terms of the quality of the obtained solutions, in figures 7.9 and 7.10 we show the average deviations (for each instance) of the alternative approaches with respect to the original one. This measure provides the percent improvement of the alternative method with respect to the best solution obtained by the original formulation of the problem. We observed that the solutions that we obtained with the two strategies are significantly better than those obtained with the original formulation for the MNLCLP within the time limit. Providing initial solutions to the problem allows us to obtain solutions with 20% more coverage than the initial formulation, whereas the heuristic approach gets solutions with more than 25% more coverage. In the case of the PSNLCLP, in most of the instances, the heuristic solutions are even better than those obtained with the exact approach. Nevertheless, in the instance `jilin`, the solutions are almost 50% worse than those obtained with the exact approach.

In Figure 7.11 we plot boxplots for the average of the best weighted coverages obtained by each of the approaches within the time limit for each of the six instances. Regarding the distribution of the results, one cannot infer that the results are significantly different. Nevertheless, in terms of the central tendencies, there is a clear improvement in the results obtained with the two alternative methods with respect to the original formulation, especially for the larger instances (see figures 7.9 and 7.10).

Vertex and Edge-Restricted Models

Finally, we run some experiments to validate our proposal regarding the coverages obtained with our approaches and those obtained by the vertex and edge-constrained versions of our model. In those models, the devices are allowed to be located only at the vertices or edges of the network instead of the whole space as in our model. We have run these restricted versions of the maximal covering model, for the same instances and parameters as in the previous section.

First, in Figure 7.12 we plot the average deviations of the weighted volume coverages of these approaches with respect to those obtained with our model (the best solution obtained with our solution approaches). One can observe that, in some of the instances, the deviations are close to 40%, that is, our model obtained solutions covering 40% more volume of the network

Instance	$\|V\|$	$\|E\|$	k	R	CPU Time (secs) MNLCLP	MNLCLP_1	MNLCLP_2	Unsolved MNLCLP	MNLCLP_1	GAP (%) MNLCLP	MNLCLP_1
gessler	12	14	2	0.1	151.53	13.69	0.89	0%	0%	0%	0%
				0.25	48.97	11.87	1.34	0%	0%	0%	0%
				0.5	26.28	10.59	0.62	0%	0%	0%	0%
			5	0.1	TL	TL	2.26	100%	100%	86%	84%
				0.25	TL	TL	2.92	100%	100%	69%	62%
				0.5	TL	TL	1.61	100%	100%	24%	31%
			8	0.1	TL	TL	3.54	100%	100%	90%	87%
				0.25	TL	TL	5.59	100%	100%	74%	69%
				0.5	TL	TL	2.92	100%	100%	41%	35%
jilin	28	34	2	0.1	167.25	39.10	1.99	0%	0%	0%	0%
				0.25	196.56	144.30	3.37	0%	0%	0%	0%
				0.5	164.83	152.10	2.45	0%	0%	0%	0%
			5	0.1	TL	TL	2.95	100%	100%	86%	85%
				0.25	TL	TL	6.64	100%	100%	72%	64%
				0.5	TL	TL	3.17	100%	100%	40%	42%
			8	0.1	TL	TL	6.07	100%	100%	88%	84%
				0.25	TL	TL	10.34	100%	100%	72%	73%
				0.5	TL	TL	4.67	100%	100%	70%	37%
richmond	48	44	2	0.1	1180.62	133.99	8.75	0%	0%	0%	0%
				0.25	717.09	121.90	7.47	0%	0%	0%	0%
				0.5	184.63	244.25	2.32	0%	0%	0%	0%
			5	0.1	TL	TL	23.22	100%	100%	78%	77%
				0.25	TL	TL	13.79	100%	100%	62%	59%
				0.5	TL	TL	3.70	100%	100%	42%	41%
			8	0.1	TL	TL	33.64	100%	100%	88%	85%
				0.25	TL	TL	23.89	100%	100%	86%	71%
				0.5	TL	TL	5.82	100%	100%	71%	56%
foss	37	58	2	0.1	561.98	39.61	2.77	0%	0%	0%	0%
				0.25	380.54	38.42	1.99	0%	0%	0%	0%
				0.5	196.92	86.40	1.83	0%	0%	0%	0%
			5	0.1	TL	TL	6.49	100%	100%	82%	80%
				0.25	TL	TL	5.46	100%	100%	64%	62%
				0.5	TL	TL	4.31	100%	100%	61%	56%
			8	0.1	TL	TL	9.33	100%	100%	88%	86%
				0.25	TL	TL	7.99	100%	100%	87%	71%
				0.5	TL	TL	9.11	100%	100%	78%	64%
rural	48	60	2	0.1	12263.72	1169.41	16.94	0%	0%	0%	0%
				0.25	TL	559.93	15.69	100%	0%	23%	0%
				0.5	5054.64	1612.73	13.98	0%	0%	0%	0%
			5	0.1	TL	TL	26.46	100%	100%	92%	91%
				0.25	TL	TL	32.19	100%	100%	83%	82%
				0.5	TL	TL	21.99	100%	100%	79%	77%
			8	0.1	TL	TL	40.89	100%	100%	97%	94%
				0.25	TL	TL	49.51	100%	100%	91%	86%
				0.5	TL	TL	40.66	100%	100%	94%	84%
zj	60	85	2	0.1	TL	TL	13.12	100%	100%	49%	65%
				0.25	TL	5235.81	7.29	100%	0%	51%	0%
				0.5	TL	9603.61	9.33	100%	0%	5%	0%
			5	0.1	TL	TL	25.56	100%	100%	96%	95%
				0.25	TL	TL	27.48	100%	100%	90%	89%
				0.5	TL	TL	18.32	100%	100%	87%	86%
			8	0.1	TL	TL	37.85	100%	100%	98%	96%
				0.25	TL	TL	31.05	100%	100%	94%	90%
				0.5	TL	TL	20.45	100%	100%	91%	85%

TABLE 7.6: Computational results for the MNLCLP approaches.

Instance	$\lvert V\rvert$	$\lvert E\rvert$	γ	R	CPU Time (secs) PSNLCLP	CPU Time (secs) PSNLCLP_1	Unsolved PSNLCLP	GAP (%) PSNLCLP
gessler	12	14	0.5	0.1	TL	19.15	100%	96%
				0.25	TL	6.28	100%	89%
				0.5	TL	1.90	100%	75%
			0.75	0.1	TL	30.27	100%	98%
				0.25	TL	10.94	100%	93%
				0.5	TL	3.39	100%	86%
			1	0.1	TL	39.76	100%	97%
				0.25	TL	13.67	100%	93%
				0.5	TL	4.74	100%	89%
jilin	28	34	0.5	0.1	TL	26.40	100%	96%
				0.25	TL	13.29	100%	87%
				0.5	TL	3.44	100%	67%
			0.75	0.1	OoM	54.77	100%	-
				0.25	TL	20.00	100%	95%
				0.5	TL	4.60	100%	88%
			1	0.1	OoM	78.69	100%	-
				0.25	TL	24.36	100%	97%
				0.5	TL	7.05	100%	95%
richmond	48	44	0.5	0.1	TL	57.79	100%	94%
				0.25	TL	14.49	100%	92%
				0.5	TL	3.90	100%	71%
			0.75	0.1	OoM	91.99	100%	-
				0.25	TL	21.33	100%	93%
				0.5	TL	5.62	100%	91%
			1	0.1	OoM	116.10	100%	-
				0.25	TL	25.68	100%	94%
				0.5	TL	7.67	100%	96%
foss	37	58	0.5	0.1	TL	41.95	100%	96%
				0.25	TL	14.21	100%	92%
				0.5	TL	6.83	100%	75%
			0.75	0.1	OoM	111.96	100%	-
				0.25	TL	26.74	100%	97%
				0.5	TL	11.54	100%	94%
			1	0.1	OoM	230.93	100%	-
				0.25	OoM	61.73	100%	-
				0.5	OoM	19.59	100%	-

TABLE 7.7: Computational results for the PSNLCLP approaches.

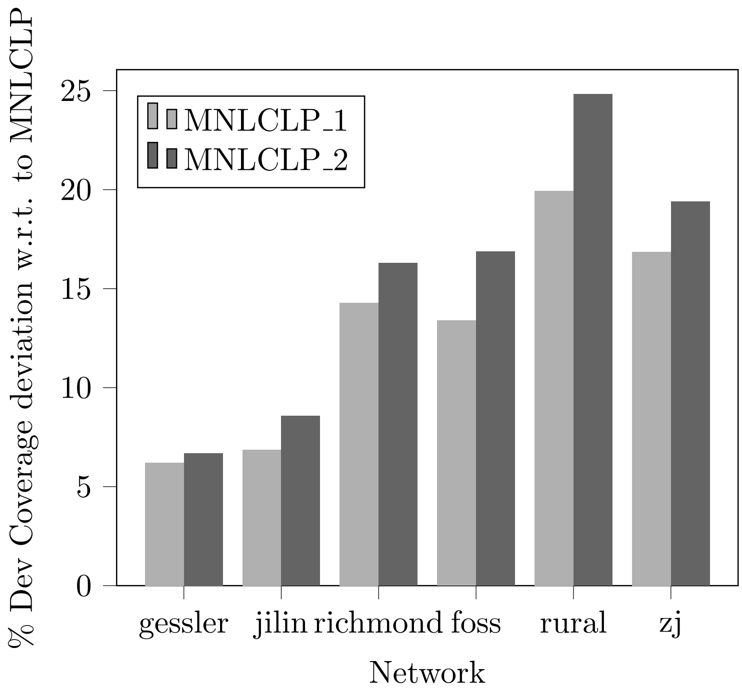

FIGURE 7.9: Average coverage deviations of the MNLCLP_1 and MNLCLP_2 approach with respect to MNLCLP.

than the restricted versions. As expected, the edge-restricted version covers more network length than the vertex-restricted model, although, in most instances, the differences are less than 5%.

The detailed average results for the different values of k and R are shown in Table 7.8. As can be observed, as larger the number of devices to be located the larger the deviations with respect to the two restricted models. Nevertheless, the deviations do not seem to follow a clear pattern with respect to the radii. For some instances, the deviations are larger for smaller values of R whereas for others the deviations are larger for the larger values.

In Figures 7.13 and 7.14 we show the best solutions obtained with the three models for two of the instances (`foss` with $k = 5$ and `rural` with $k = 8$ both of them with $R = 0.5$). In the left plot of both figures, we show the optimal solution of our model. The center and right plots are the solutions obtained with the edge-restricted and vertex-restricted versions of the MNLCLP, respectively. As can be observed, the optimal location of the devices differs for the different models. Specifically, the MNLCLP takes advantage of locating devices outside the edges of the network to cover edges with a high volume, whereas the restricted versions do not have such flexibility. In

Network	k	R	Dev_Vertex	Dev_Edges	Network	k	R	Dev_Vertex	Dev_Edges
gessler	2	0.1	9.94%	1.20%	foss	2	0.1	32.77%	2.14%
		0.25	9.84%	1.11%			0.25	32.82%	2.08%
		0.5	9.82%	1.10%			0.5	26.36%	4.32%
	5	0.1	11.99%	2.78%		5	0.1	32.80%	22.35%
		0.25	13.92%	6.22%			0.25	36.47%	9.38%
		0.5	11.66%	4.51%			0.5	19.12%	9.55%
	8	0.1	23.46%	22.10%		8	0.1	60.73%	40.86%
		0.25	20.47%	19.13%			0.25	61.87%	17.85%
		0.5	21.42%	14.82%			0.5	57.66%	32.72%
jilin	2	0.1	22.72%	0.97%	rural	2	0.1	19.94%	0.67%
		0.25	19.88%	1.53%			0.25	19.42%	0.43%
		0.5	20.38%	10.49%			0.5	6.03%	1.14%
	5	0.1	24.89%	16.42%		5	0.1	23.77%	22.78%
		0.25	18.26%	17.48%			0.25	20.44%	45.94%
		0.5	21.50%	9.88%			0.5	16.37%	39.60%
	8	0.1	49.72%	45.95%		8	0.1	40.18%	58.42%
		0.25	24.79%	38.00%			0.25	80.81%	31.23%
		0.5	29.79%	11.23%			0.5	31.41%	30.54%
richmond	2	0.1	12.62%	2.32%	zj	2	0.1	1.32%	0.97%
		0.25	9.53%	3.53%			0.25	1.31%	0.08%
		0.5	16.67%	9.03%			0.5	5.86%	2.59%
	5	0.1	13.98%	6.72%		5	0.1	14.70%	9.53%
		0.25	19.83%	9.30%			0.25	5.67%	8.58%
		0.5	14.48%	17.60%			0.5	12.35%	8.18%
	8	0.1	27.39%	32.84%		8	0.1	69.01%	26.19%
		0.25	23.76%	38.96%			0.25	33.11%	27.69%
		0.5	33.90%	29.89%			0.5	32.38%	27.59%

TABLE 7.8: Average deviations of vertex and edge-restricted MNLCLP with respect to MNLCLP for the different values of k and R.

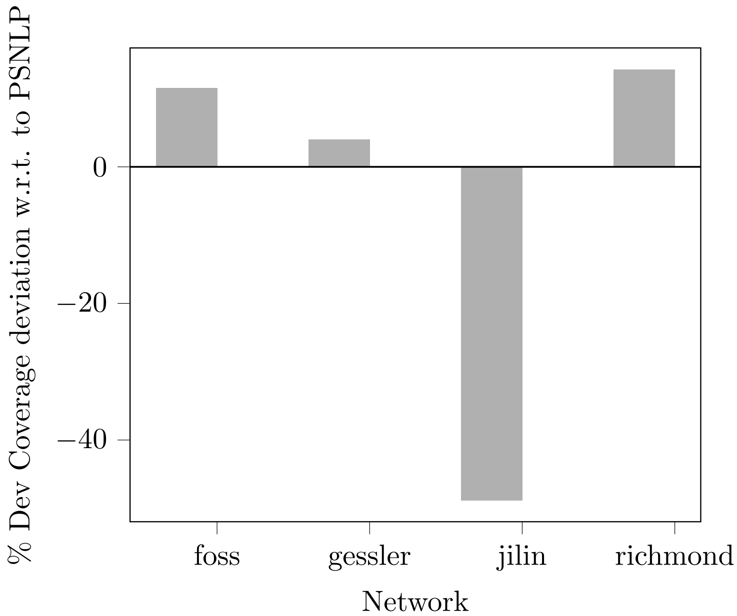

FIGURE 7.10: Average coverage deviations of the PSNLCLP_1 approach with respect to PSNLCLP.

Figure 7.13, one can observe that, for the `foss` network, there is a high concentration of weighted volume at the edges in the bottom right corner of the network. Thus, the three models try to locate the devices to cover that demand. In the MNLCLP, a single device (outside the edges and vertices) suffices to cover most of the demand, whereas the restricted models require two or three devices to cover a similar amount of volume. This flexibility directly affects global coverage. For this network, our model was able to cover 10% and 20% more volume than the edge and vertex-restricted models, respectively. The situation for the `rural` network (Figure 7.14) is even more impressive since our model obtained a solution with more than 30% coverage than the restricted models.

One can conclude that our model is adequate to locate devices that maximize the volume coverage of a network in case they can be located at any place of the space where the network lives, as in the case of leak detection devices, since the obtained solutions significantly outperform (in coverage) the classical vertex and edge-restricted versions of the problem.

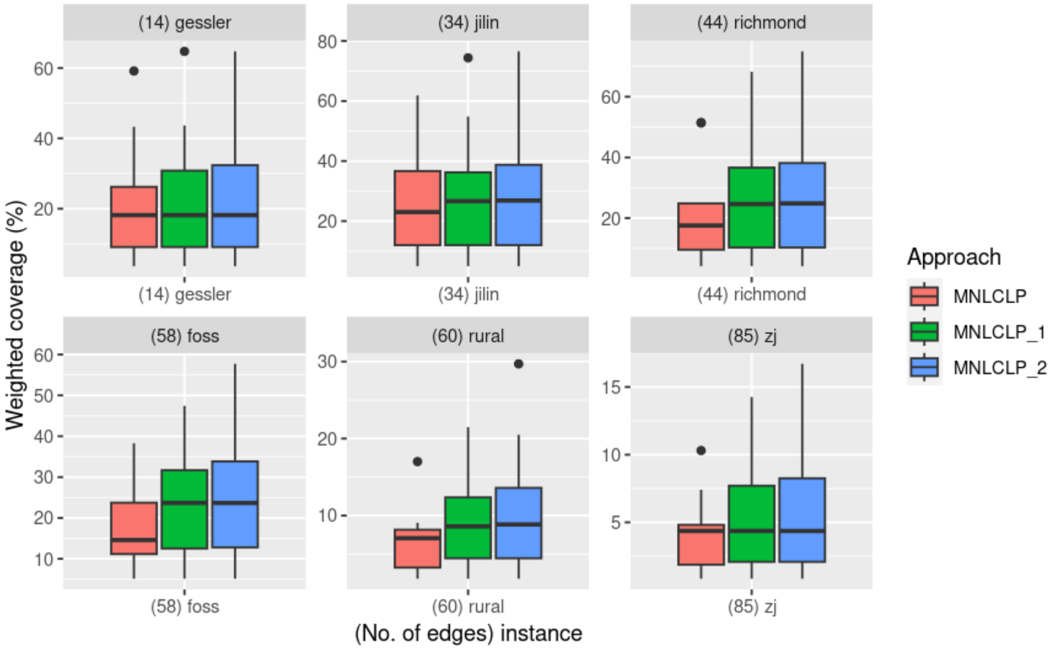

FIGURE 7.11: Weighted coverage comparison between the solutions of the three approaches MNLCLP, MNLCLP_1, and MNLCLP_2.

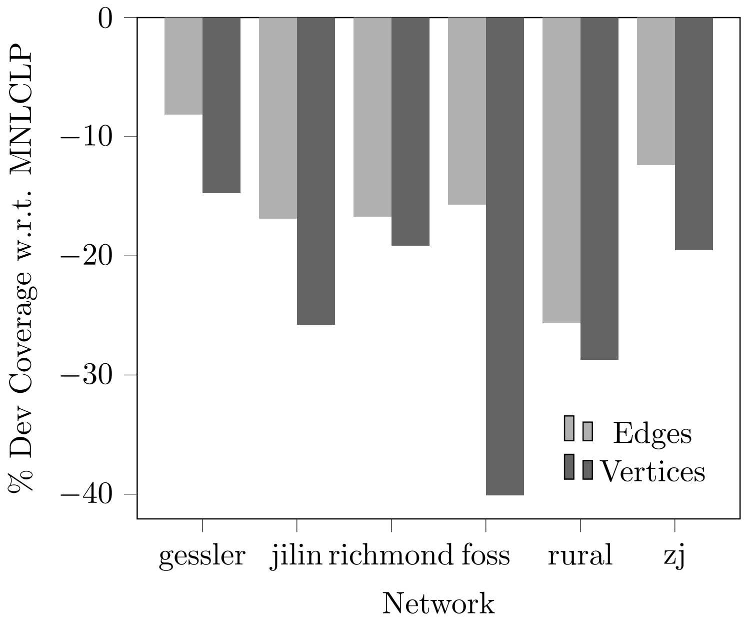

FIGURE 7.12: Average deviations of the coverages obtained with the vertex and edge-restricted versions of MNLCLP with respect to MNLCLP.

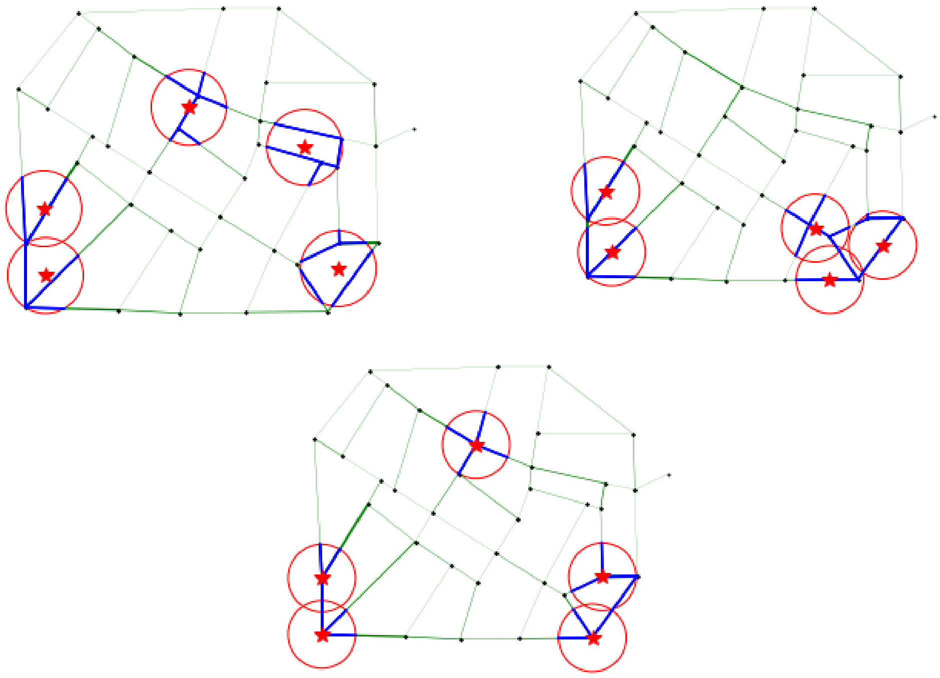

FIGURE 7.13: Solutions of the MNLCLP (left), MNLCLP-edge restricted (center), and MNLCLP-vertex restricted (right) for instance `foss` ($k = 5$).

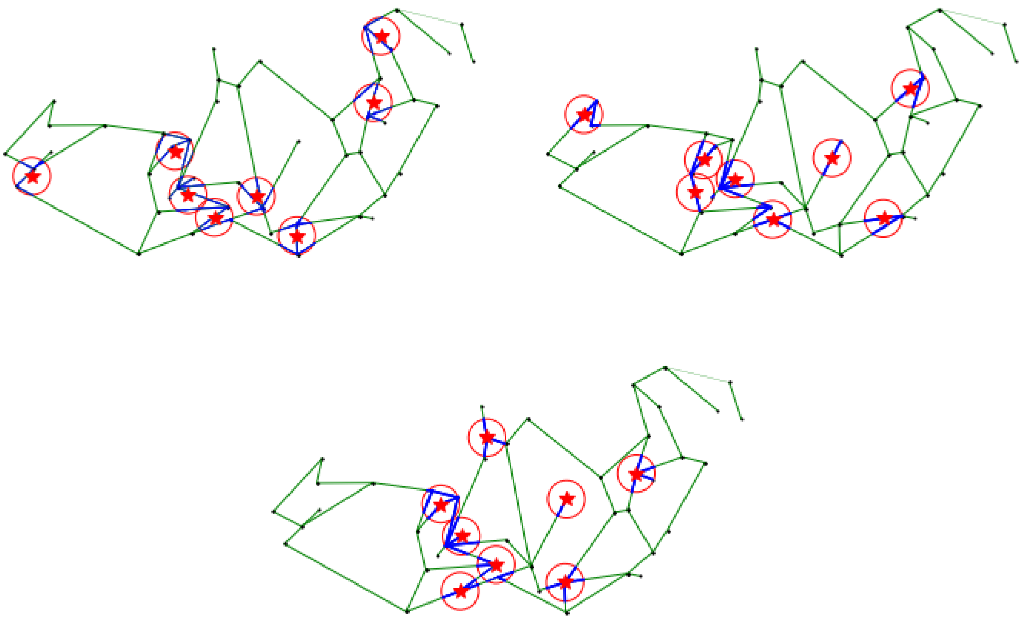

FIGURE 7.14: Solutions of the MNLCLP (left), MNLCLP-edge restricted (center), and MNLCLP-vertex restricted (right) for instance `rural` ($k = 8$).

Chapter VIII

Conclusion

Yo no robé del Olimpo este fuego, mi amor.
Fue del infierno este invierno buscando calor.

— Robe. *Lo que aletea en nuestras cabezas*, Guerrero

In this closing chapter, we reflect on the conclusions and further research lines derived from this work. For the sake of the understanding, we will split these thoughts by the chapters they are referred to.

Chapter III: Mediated Graphs

In this work, we formally introduce the notion of mediated graphs, motivated by their numerous applications in convex algebraic geometry. We take a first step in analyzing their theoretical properties, focusing particularly on optimal mediated graphs, which are extremal with respect to the partial order induced by the cardinality of their vertex sets. To efficiently compute these minimal and maximal graphs across different domains, we propose mixed integer linear optimization models, strengthened by the theoretical properties we establish.

Despite these advances, several open questions remain. The structure of optimal mediated graphs requires further analysis, particularly regarding specific sets $\mathcal{A}$ and $\mathcal{B}$ where computing minimal mediated graphs may be simplified. For maximal mediated graphs, a conjecture initially posed by Reznick (1989) and empirically tested by Hartzer et al. (2022) suggests that, in dimension two, all simplices are either H-simplices or M-simplices. The polyhedral analysis of our integer programming formulations could provide insight into proving this conjecture. Moreover, in applications such as sum of squares (SOS) decompositions or second–order cone (SOC) representations, large mediated graphs might hinder computational efficiency, necessitating relaxed conditions to find approximate structures. The role of integer linear programming in these approximations remains an open question.

Chapter IV: Conic Algebraic Geometry

Expanding on this framework, we analyze extended representations of general cones, particularly generalized power cones, which are crucial for modeling constraints in optimization problems. We study different representations of these cones, simplifying them into second–order cones when parameters $\boldsymbol{\alpha}$ and p have rational entries. To construct minimal representations —those using the fewest additional variables and constraints— we introduce the minimal $\boldsymbol{\alpha}$–mediated graph problem (M$\boldsymbol{\alpha}$MGP) and develop a mixed integer linear programming formulation. Computational experiments demonstrate that minimal representations are not only mathematically intriguing but also practically beneficial, significantly improving optimization efficiency. The geometric properties of minimal mediated graphs have a direct impact on deriving valid inequalities for M$\boldsymbol{\alpha}$MGP, which could accelerate solution times. Further research will focus on identifying particular values of p and $\boldsymbol{\alpha}$ that allow for easier derivation of minimal representations, as well as formally proving the conjecture that M$\boldsymbol{\alpha}$MGP is NP-hard, reinforcing its significance as a complex combinatorial problem.

Additionally, we exploit both continuous and discrete, minimal and maximal mediated graph structure to obtain minimal second–order cones representations of sums of circuits polynomials. This means another efficient way to tackle unconstrained polynomial optimization. On the other hand, one can fully characterize the intersection between SOS and SONC cones, that is SOBS. We yield an explicit sum of binomial squares decomposition for each polynomial that lies on this intersection.

Chapter V: Complexity

We investigate the complexity of mathematical optimization problems involving ℓ_p–norms. While these problems can be reformulated as second–order cone (SOCP) or semidefinite programming (SDP) problems, leveraging the explicit structure of p–order cones —especially SOC— results in improved complexity bounds. Specific choices of p allow for further refinements in complexity analysis.

Our findings contribute to a deeper understanding of p–order cones and their role in optimization. Many problems involving ℓ_p–norm constraints also include integer or binary variables, modeling on/off or disjunctive constraints. While these problems lose convexity, efficiently solving their continuous relaxations has been key to developing branch-and-bound algorithms for mixed integer second order cone programming (MISOCP). However, mixed integer p–order cone programming (MIpOCP) problems have so far been tackled only through reformulations as MISOCP problems. Future research will explore direct methods to address MIpOCP problems, potentially leading to more efficient solution techniques.

Chapter VI: Applications

We also examine upper bounds on the norm of feasible solutions and explore the implications in applications such as ℓ_p-support vector machines, robust optimization with ℓ_p–norm uncertainty sets, and single-facility ordered continuous location problems. These applications have gained increasing attention in recent years.

Finally, we examine two different covering location problems. First, gravitational covering location problem was introduced as a novel location problem to optimally locate a given number of facilities in the Euclidean space, and decide their coverage radii based on different features to maximize the overall coverage of a given set of users. The radii will represent an attraction measure based on Newton's law of universal gravitation. For solving it, we propose a generalized power cone program.

Besides, we introduced a novel network covering problem with direct applications in optimizing the placement of leak detection devices in urban pipeline networks. We develop a general framework for two problem variants: the maximal network length covering location problem, which maximizes the network length covered by a given number of devices, and the partial set network length covering location problem, which minimizes the number of devices needed to cover a specified percentage of the network. We propose a method for constructing initial solutions and introduce a matheuristic algorithm, which we test on real-world urban water supply networks.

Future research in this area includes incorporating more sophisticated coverage shapes for detection devices, such as polyellipsoids or nonconvex shapes formed by unions of polyhedral and ℓ_p–norm balls. This would necessitate a deeper study of p–order cone constraints and disjunctive representations, posing challenges for real-world implementation. Developing efficient heuristic approaches capable of scaling to large networks remains an essential direction for further study.

All of our extensive computational results, which were drawn in Chapter VII, validate the efficiency of our approaches, showing that our framework significantly reduces CPU time compared to previous methods and highlighting the practical performance of our models.

Bibliography

Alizadeh, F. (1995). Interior point methods in semidefinite programming with applications to combinatorial optimization. *SIAM Journal on Optimization*, 5(1):13–51.

Alizadeh, F. and Goldfarb, D. (2003). Second–order cone programming. *Mathematical Programming*, 95(1):3–51.

Anjos, M. F. and Lasserre, J. B. (2011). *Handbook on semidefinite, conic and polynomial optimization*, volume 166. Springer Science & Business Media.

Averkov, G. (2019). Optimal size of linear matrix inequalities in semidefinite approaches to polynomial optimization. *SIAM Journal on Applied Algebra and Geometry*, 3(1):128–151.

Avriel, M. and Williams, A. C. (1971). An extension of geometric programming with applications in engineering optimization. *Journal of Engineering Mathematics*, 5(2):187–194.

Balas, E. (1998). Projection with a minimal system of inequalities. *Computational Optimization and Applications*, 10:189–193.

Barnes, J. A. (1969). Graph theory and social networks: A technical comment on connectedness and connectivity. *Sociology*, 3(2):215–232.

Barvinok, A. (2002). *A course in convexity*, volume 54. American Mathematical Society.

Basu, A. and Blanning, R. W. (1997). A graph-theoretic approach to analyzing knowledge bases containing rules, models and data. *Annals of Operations Research*, 75(0):3–23.

Basu, S., Pollack, R., and Coste-Roy, M. (2007). *Algorithms in Real Algebraic Geometry*. Algorithms and Computation in Mathematics. Springer Berlin Heidelberg.

Bektaş, T. and Letchford, A. N. (2020). Using ℓ_p-norms for fairness in combinatorial optimisation. *Computers & Operations Research*, 120:104975.

Bell, T. L. and Church, R. L. (1985). Location-allocation modeling in archaeological settlement pattern research: Some preliminary applications. *World Archaeology*, 16(3):354–371.

Ben-Tal, A. and Nemirovski, A. (1999). Robust solutions of uncertain linear programs. *Operations Research Letters*, 25(1):1–13.

Ben-Tal, A. and Nemirovski, A. (2001a). *Lectures on modern convex optimization: analysis, algorithms, and engineering applications*. SIAM.

Ben-Tal, A. and Nemirovski, A. (2001b). On polyhedral approximations of the second-order cone. *Mathematics of Operations Research*, 26(2):193–205.

Berman, O., Kalcsics, J., and Krass, D. (2016). On covering location problems on networks with edge demand. *Computers & Operations Research*, 74:214–227.

Berman, O. and Wang, J. (2011). The minmax regret gradual covering location problem on a network with incomplete information of demand weights. *European Journal of Operational Research*, 208(3):233–238.

Bertsimas, D. and Copenhaver, M. S. (2018). Characterization of the equivalence of robustification and regularization in linear and matrix regression. *European Journal of Operational Research*, 270(3):931–942.

Bertsimas, D., Pachamanova, D., and Sim, M. (2004). Robust linear optimization under general norms. *Operations Research Letters*, 32(6):510–516.

Bie, T. D. and Cristianini, N. (2006). Fast SDP relaxations of graph cut clustering, transduction, and other combinatorial problems. *The Journal of Machine Learning Research*, 7:1409–1436.

Blanco, V. (2019). Ordered p-median problems with neighbourhoods. *Computational Optimization and Applications*, 73(2):603–645.

Blanco, V. and Gázquez, R. (2021). Continuous maximal covering location problems with interconnected facilities. *Computers & Operations Research*, 132:105310.

Blanco, V. and Gázquez, R. (2023). Fairness in maximal covering location problems. *Computers & Operations Research*, 157:106287.

Blanco, V., Gázquez, R., and Saldanha-da-Gama, F. (2023a). Multi-type maximal covering location problems: Hybridizing discrete and continuous problems. *European Journal of Operational Research*, 307(3):1040–1054.

Blanco, V., González, G., Hinojosa, Y., Ponce, D., Pozo, M. A., and Puerto, J. (2022). Network flow based approaches for the pipelines routing problem in naval design. *Omega*, 111:102659.

Blanco, V., González, G., Hinojosa, Y., Ponce, D., Pozo, M. A., and Puerto, J. (2023b). The pipelines and cable trays location problem in naval design. *Ocean Engineering*, 286:115525.

Blanco, V., Japón, A., and Puerto, J. (2020a). Optimal arrangements of hyperplanes for SVM-based multiclass classification. *Advances in Data Analysis and Classification*, 14(1):175–199.

Blanco, V., Magron, V., and Martínez-Antón, M. (2025). On the complexity of p–order cone programs. *arXiv preprint arXiv:2501.09828*.

Blanco, V. and Martínez-Antón, M. (2024a). On minimal extended representations of generalized power cones. *SIAM Journal on Optimization*, 4(3):3088–3111.

Blanco, V. and Martínez-Antón, M. (2024b). Optimal coverage-based placement of static leak detection devices for pipeline water supply networks. *Omega*, 122:102956.

Blanco, V. and Puerto, J. (2022). On hub location problems in geographically flexible networks. *International Transactions in Operational Research*, 29(4):2226–2249.

Blanco, V., Puerto, J., and El-Haj Ben-Ali, S. (2014). Revisiting several problems and algorithms in continuous location with ℓ_τ norms. *Computational Optimization and Applications*, 58(3):563–595.

Blanco, V., Puerto, J., and El-Haj Ben-Ali, S. (2016). Continuous multifacility ordered median location problems. *European Journal of Operational Research*, 250(1):56–64.

Blanco, V., Puerto, J., and Rodriguez-Chía, A. M. (2020b). On ℓ_p-support vector machines and multidimensional kernels. *The Journal of Machine Learning Research*, 21(1):469–497.

Blanquero, R., Carrizosa, E., Boglárka, G., et al. (2016). Maximal covering location problems on networks with regional demand. *Omega*, 64:77–85.

Blekherman, G., Parrilo, P. A., and Thomas, R. R. (2012). *Semidefinite optimization and convex algebraic geometry*. SIAM.

Bondy, J. A. and Murty, U. S. R. (1976). *Graph theory with applications*, volume 290. Macmillan London.

Boyd, S. P. and Vandenberghe, L. (2004). *Convex optimization*. Cambridge University Press.

Boykov and Kolmogorov (2003). Computing geodesics and minimal surfaces via graph cuts. In *Proceedings of the 9th IEEE International Conference on Computer Vision*, pages 26–33. IEEE.

Brar, J. K. and Hare, W. (2020). Portfolio optimization using second order conic programming approach. *Math. Finance Lett.*, 2021:Article–ID.

Buchheim, C. and Kurtz, J. (2018). Robust combinatorial optimization under convex and discrete cost uncertainty. *EURO Journal on Computational Optimization*, 6(3):211–238.

Burer, S. and Chen, J. (2009). A p-cone sequential relaxation procedure for 0-1 integer programs. *Optimization Methods & Software*, 24(4-5):523–548.

Carathéodory, C. (1907). Über den variabilitätsbereich der koeffizienten von potenzreihen, die gegebene werte nicht annehmen. *Mathematische Annalen*, 64(1):95–115.

Casillas, M. V., Puig, V., Garza-Castanón, L. E., and Rosich, A. (2013). Optimal sensor placement for leak location in water distribution networks using genetic algorithms. *Sensors*, 13(11):14984–15005.

Chiang, M., Tan, C. W., Palomar, D. P., O'neill, D., and Julian, D. (2007). Power control by geometric programming. *IEEE Transactions on Wireless Communications*, 6(7):2640–2651.

Chuong, T. D. (2022). Second-order cone programming relaxations for a class of multiobjective convex polynomial problems. *Annals of Operations Research*, 311(2):1017–1033.

Church, R. and ReVelle, C. (1974). The maximal covering location problem. *Papers of the Regional Science Association*, 32(1):101–118.

Clarkson, K. L. (1995). Las Vegas algorithms for linear and integer programming when the dimension is small. *Journal of the ACM*, 42(2):488–499.

Cody, R. A., Dey, P., and Narasimhan, S. (2020a). Linear prediction for leak detection in water distribution networks. *Journal of Pipeline Systems Engineering and Practice*, 11(1):04019043.

Cody, R. A., Tolson, B. A., and Orchard, J. (2020b). Detecting leaks in water distribution pipes using a deep autoencoder and hydroacoustic spectrograms. *Journal of Computing in Civil Engineering*, 34(2):04020001.

Cooper, L. (1963). Location-allocation problems. *Operations Research*, 11(3):331–343.

Dantzig, G. B. (1948). *Programming in a linear structure*. Washington, DC: Comptroller, USAF.

Danzer, L., Grünbaum, B., and Klee, V. (1963). Helly's theorem and its relatives. In *Convexity: Proceedings of the 7th Symposium in Pure Mathematics of the American Mathematical Society*, volume 7, page 101. American Mathematical Society.

Dhyani Bhatt, S., Jayaswal, S., Sinha, A., and Vidyarthi, N. (2021). Alternate second order conic program reformulations for hub location under stochastic demand and congestion. *Annals of Operations Research*, 304:481–527.

Dijkstra, E. W. (1959). A note on two problems in connexion with graphs. *Numerische Mathematik*, 1:269–271.

Dressler, M., Iliman, S., and De Wolff, T. (2017). A positivstellensatz for sums of nonnegative circuit polynomials. *SIAM Journal on Applied Algebra and Geometry*, 1(1):536–555.

Dwyer, F. R. and Evans, J. R. (1981). A branch and bound algorithm for the list selection problem in direct mail advertising. *Management Science*, 27(6):658–667.

El-Abbasy, M. S., Mosleh, F., Senouci, A., Zayed, T., and Al-Derham, H. (2016). Locating leaks in water mains using noise loggers. *Journal of Infrastructure Systems*, 22(3):04016012.

El-Abbasy, M. S., Senouci, A., Zayed, T., Mirahadi, F., and Parvizsedghy, L. (2014). Condition prediction models for oil and gas pipelines using regression analysis. *Journal of Construction Engineering and Management*, 140(6):04014013.

El Ghaoui, L. and Lebret, H. (1996). Robust least squares and applications. In *Proceedings of the 35th IEEE Conference on Decision and Control*, volume 1, pages 249–254. IEEE.

El-Zahab, S. and Zayed, T. (2019). Leak detection in water distribution networks: an introductory overview. *Smart Water*, 4(1):1–23.

Erdős, P. and Rényi, A. (1960). On the evolution of random graphs. *Publ. Math. Inst. Hung. Acad. Sci*, 5(1):17–60.

Fantozzi, M., Calza, F., and Lambert, A. (2009). Experience and results achieved in introducing district metered areas (DMA) and pressure management areas (PMA) at Enia utility (Italy). In *Proceedings of the 5th IWA Water Loss Reduction Specialist Conference*, pages 153–160.

Fekete, S. P., Mitchell, J. S., and Beurer, K. (2005). On the continuous Fermat-Weber problem. *Operations Research*, 53(1):61–76.

Ford, L. R. and Fulkerson, D. R. (1956). Maximal flow through a network. *Canadian Journal of Mathematics*, 8:399–404.

Gaar, E. and Rendl, F. (2020). A computational study of exact subgraph based SDP bounds for max-cut, stable set and coloring. *Mathematical Programming*, 183(1):283–308.

Gaar, E., Siebenhofer, M., and Wiegele, A. (2022). An SDP-based approach for computing the stability number of a graph. *Mathematical Methods of Operations Research*, 95(1):141–161.

García, S. and Marín, A. (2019). Covering location problems. In *Location Science*, pages 99–119. Springer.

Gilbert, E. N. (1959). Random graphs. *The Annals of Mathematical Statistics*, 30(4):1141–1144.

Glineur, F. et al. (2000). Computational experiments with a linear approximation of second order cone optimization. *Image Technical Report*, 1.

Goemans, M. X. and Williamson, D. P. (1995). Improved approximation algorithms for maximum cut and satisfiability problems using semidefinite programming. *Journal of the ACM*, 42(6):1115–1145.

Góez, J. C. and Anjos, M. F. (2019). Second-order cone optimization formulations for service system design problems with congestion. In *Modeling and Optimization: Theory and Applications: MOPTA, Bethlehem, PA, USA, August 2017, Selected Contributions*, pages 97–120. Springer.

Hakimi, S. L. (1964). Optimum locations of switching centers and the absolute centers and medians of a graph. *Operations Research*, 12(3):450–459.

Hamilton, S. and Charalambous, B. (2013). *Leak detection: technology and implementation*. IWA Publishing.

Hartzer, J., Röhrig, O., de Wolff, T., and Yürük, O. (2022). Initial steps in the classification of maximal mediated sets. *Journal of Symbolic Computation*, 109:404–425.

Helly, E. (1923). Über mengen konvexer körper mit gemeinschaftlichen punkte. *Jahresbericht der Deutschen Mathematiker-Vereinigung*, 32:175–176.

Henrion, D., Korda, M., and Lasserre, J. B. (2020). *Moment-SOS hierarchy, the: lectures in probability, statistics, computational geometry, control and nonlinear PDEs*, volume 4. World Scientific.

Hien, L. T. K. (2015). Differential properties of Euclidean projection onto power cone. *Mathematical Methods of Operations Research*, 82(3):265–284.

Hilbert, D. (1888). Über die darstellung definiter formen als summe von formenquadraten. *Mathematische Annalen*, 32(3):342–350.

Hosseininezhad, S. J., Jabalameli, M. S., and Naini, S. G. J. (2013). A continuous covering location model with risk consideration. *Applied Mathematical Modelling*, 37(23):9665–9676.

Hurwitz, A. (1891). Über den vergleich des arithmetischen und des geometrischen mittels. *Journal für die Reine und Angewandte Mathematik*, 108:266–268.

Iliman, S. and De Wolff, T. (2016a). Amoebas, nonnegative polynomials and sums of squares supported on circuits. *Research in the Mathematical Sciences*, 3:1–35.

Iliman, S. and De Wolff, T. (2016b). Lower bounds for polynomials with simplex newton polytopes based on geometric programming. *SIAM Journal on Optimization*, 26(2):1128–1146.

Kaibel, V. and Walter, M. (2015). Simple extensions of polytopes. *Mathematical Programming*, 154(1-2):381–406.

Khulief, Y., Khalifa, A., Mansour, R. B., and Habib, M. (2012). Acoustic detection of leaks in water pipelines using measurements inside pipe. *Journal of Pipeline Systems Engineering and Practice*, 3(2):47–54.

Kian, R., Berk, E., and Gürler, U. (2019). Minimal conic quadratic reformulations and an optimization model. *Operations Research Letters*, 47(6):489–493.

König, D. (1922). Über konvexe körper. *Mathematische Zeitschrift*, 14(1):208–210.

Kostreva, M. M., Ogryczak, W., and Wierzbicki, A. (2004). Equitable aggregations and multiple criteria analysis. *European Journal of Operational Research*, 158(2):362–377.

Krokhmal, P. A. and Soberanis, P. (2010). Risk optimization with p-order conic constraints: A linear programming approach. *European Journal of Operational Research*, 201(3):653–671.

Kruskal, J. B. (1956). On the shortest spanning subtree of a graph and the traveling salesman problem. *Proceedings of the American Mathematical Society*, 7(1):48–50.

Kucukyavuz, S., Shojaie, A., Manzour, H., Wei, L., and Wu, H.-H. (2023). Consistent second-order conic integer programming for learning bayesian networks. *Journal of Machine Learning Research*, 24(322):1–38.

Kuhn, H. W. (1967). On a pair of dual nonlinear programs. *Nonlinear Programming*, 1:38–45.

Laporte, G., Nickel, S., and Saldanha-da-Gama, F. (2019). Introduction to location science. In *Location Science*, pages 1–21. Springer.

Lasserre, J. B. (2001). Global optimization with polynomials and the problem of moments. *SIAM Journal on Optimization*, 11(3):796–817.

Lasserre, J. B. (2009). *Moments, positive polynomials and their applications*, volume 1. World Scientific.

Lee, J. and Leyffer, S. (2011). *Mixed integer nonlinear programming*, volume 154. Springer Science & Business Media.

Li, R., Huang, H., Xin, K., and Tao, T. (2015). A review of methods for burst/leakage detection and location in water distribution systems. *Water Science and Technology: Water Supply*, 15(3):429–441.

Li, W., Ling, W., Liu, S., Zhao, J., Liu, R., Chen, Q., Qiang, Z., and Qu, J. (2011). Development of systems for detection, early warning, and control of pipeline leakage in drinking water distribution: A case study. *Journal of Environmental Sciences*, 23(11):1816–1822.

Liu, T., Saldanha-da-Gama, F., Wang, S., and Mao, Y. (2022). Robust stochastic facility location: sensitivity analysis and exact solution. *INFORMS Journal on Computing*, 34(5):2776–2803.

Lobo, M. S., Vandenberghe, L., Boyd, S., and Lebret, H. (1998). Applications of second-order cone programming. *Linear Algebra and its Applications*, 284(1-3):193–228.

López, J. and Maldonado, S. (2016). Multi-class second-order cone programming support vector machines. *Information Sciences*, 330:328–341.

Lu, Y., Yang, C.-Y., Chen, J.-S., and Qi, H.-D. (2020). The decompositions with respect to two core non-symmetric cones. *Journal of Global Optimization*, 76(1):155–188.

Lu, Z. (2006). A new cone programming approach for robust portfolio selection. *Optimization Methods & Software*, 26(1):89–104.

Lubin, M., Yamangil, E., Bent, R., and Vielma, J. P. (2018). Polyhedral approximation in mixed-integer convex optimization. *Mathematical Programming*, 172:139–168.

Magron, V. and Wang, J. (2023). SONC optimization and exact nonnegativity certificates via second-order cone programming. *Journal of Symbolic Computation*, 115:346–370.

Maldonado, S. and López, J. (2014). Imbalanced data classification using second-order cone programming support vector machines. *Pattern Recognition*, 47(5):2070–2079.

Marshall, M. (2008). *Positive polynomials and sums of squares*. Number 146. American Mathematical Society.

Mignotte, M. (1982). Some useful bounds. In *Computer Algebra: Symbolic and Algebraic Computation*, pages 259–263. Springer.

Mirkil, H. (1957). New characterizations of polyhedral cones. *Canadian Journal of Mathematics*, 9:1–4.

Mohamed, I. N., El-Hamawi, M., Al Hassan, R. A., Aslanyan, A., Filenev, M., Aslanyan, I., Bargouthi, J., and Salim, B. (2012). Leak detection by temperature and noise logging. In *Abu Dhabi International Petroleum Exhibition and Conference*, pages SPE–161983. SPE.

Mohammadisiahroudi, M., Fakhimi, R., Augustino, B., and Terlaky, T. (2024). Generating linear, semidefinite, and second-order cone optimization problems for numerical experiments. *Optimization Methods & Software*, 39(4):725–755.

Morenko, Y., Vinel, A., Yu, Z., and Krokhmal, P. (2013). On p-norm linear discrimination. *European Journal of Operational Research*, 231(3):784–789.

Motzkin, T. S. (1967). The arithmetic-geometric inequality. In *Inequalities (Proc. Sympos. Wright-Patterson Air Force Base, Ohio, 1965)*, pages 205–224.

Muramatsu, M. and Suzuki, T. (2003). A new second-order cone programming relaxation for max-cut problems. *Journal of the Operations Research Society of Japan*, 46(2):164–177.

Murasugi, K. (1989). On invariants of graphs with applications to knot theory. *Transactions of the American Mathematical Society*, 314(1):1–49.

Murray, A. T. (2021). Contemporary optimization application through geographic information systems. *Omega*, 99:102176.

Murray, A. T. and Tong, D. (2007). Coverage optimization in continuous space facility siting. *International Journal of Geographical Information Science*, 21(7):757–776.

Nestorenko, T., Nestorenko, O., Morkunas, M., Volkov, A., Balezentis, T., Streimikiene, D., and Cai, J. (2022). Optimization of production decisions under resource constraints and community priorities. *Journal of Global Information Management*, 30(12):1–24.

Newton, I. (1687). *Philosophiæ naturalis principia mathematica*. Jussu Societatis Regiæ ac Typis Josephi Streater, London.

Nickel, S. and Puerto, J. (2006). *Location theory: a unified approach*. Springer Science & Business Media.

Orecchia, L. and Vishnoi, N. K. (2011). Towards an SDP-based approach to spectral methods: A nearly-linear-time algorithm for graph partitioning and decomposition. In *Proceedings of the Twenty-second Annual ACM-SIAM Symposium on Discrete Algorithms*, pages 532–545. SIAM.

Ota, R. R., Pati, J. C., and Ojha, A. K. (2019). Geometric programming technique to optimize power distribution system. *OPSEARCH*, 56(1):282–299.

Parrilo, P. A. (2003). Semidefinite programming relaxations for semialgebraic problems. *Mathematical Programming*, 96:293–320.

Parrilo, P. A. and Lall, S. (2003). Semidefinite programming relaxations and algebraic optimization in control. *European Journal of Control*, 9(2-3):307–321.

Pauwels, E., Henrion, D., and Lasserre, J. B. (2017). Positivity certificates in optimal control. In *Geometric and Numerical Foundations of Movements*, pages 113–131. Springer.

Pelegrín, M. and Xu, L. (2023). Continuous covering on networks: Improved mixed integer programming formulations. *Omega*, 117:102835.

Porkolab, L. and Khachiyan, L. (1997). On the complexity of semidefinite programs. *Journal of Global Optimization*, 10(4):351–365.

Powers, V. and Reznick, B. (2021). A note on mediated simplices. *Journal of Pure and Applied Algebra*, 225(7):106608.

Prim, R. C. (1957). Shortest connection networks and some generalizations. *The Bell System Technical Journal*, 36(6):1389–1401.

Puerto, J. (2020). An exact completely positive programming formulation for the discrete ordered median problem: an extended version. *Journal of Global Optimization*, 77(2):341–359.

Puust, R., Kapelan, Z., Savic, D., and Koppel, T. (2010). A review of methods for leakage management in pipe networks. *Urban Water Journal*, 7(1):25–45.

Qing, H. and Wang, J. (2020). Dual regularized laplacian spectral clustering methods on community detection. *arXiv preprint arXiv:2011.04392*.

Radon, J. (1921). Mengen konvexer körper, die einen gemeinsamen punkt enthalten. *Mathematische Annalen*, 83(1):113–115.

Ramírez-Arroyo, A., Zapata-Cano, P. H., Palomares-Caballero, Á., Carmona-Murillo, J., Luna-Valero, F., and Valenzuela-Valdés, J. F. (2020). Multilayer network optimization for 5g & 6g. *IEEE Access*, 8:204295–204308.

Renegar, J. (1992a). On the computational complexity and geometry of the first-order theory of the reals. Part I: Introduction. Preliminaries. The geometry of semi-algebraic sets. The decision problem for the existential theory of the reals. *Journal of Symbolic Computation*, 13(3):255–299.

Renegar, J. (1992b). On the computational complexity of approximating solutions for real algebraic formulae. *SIAM Journal on Computing*, 21(6):1008–1025.

Reznick, B. (1989). Forms derived from the arithmetic-geometric inequality. *Mathematische Annalen*, 283(3):431–464.

Reznick, B. (2000). Some concrete aspects of Hilbert's 17th problem. *Contemporary Mathematics*, 253(251-272).

Rockafellar, R. T. (1970). Convex analysis. *Princeton University Press, Princeton, New Jersey*.

Roy, S. and Xiao, L. (2022). On self-concordant barriers for generalized power cones. *Optimization Letters*, 16(2):681–694.

Royal, A. C., Atkins, P. R., Brennan, M. J., Chapman, D. N., Chen, H., Cohn, A. G., Foo, K. Y., Goddard, K. F., Hayes, R., Hao, T., et al. (2011). Site assessment of multiple-sensor approaches for buried utility detection. *International Journal of Geophysics*, 2011(1):496123.

Schrijver, A. (1998). *Theory of linear and integer programming*. John Wiley & Sons.

Seckler, D. W. et al. (1998). *World water demand and supply, 1990 to 2025: Scenarios and issues*, volume 19. IWMI.

Smith, H. K., Laporte, G., and Harper, P. R. (2009). Locational analysis: highlights of growth to maturity. *Journal of the Operational Research Society*, 60(sup1):S140–S148.

Tedeschi, D. and Andretta, M. (2021). New exact algorithms for planar maximum covering location by ellipses problems. *European Journal of Operational Research*, 291(1):114–127.

Tijani, I., Abdelmageed, S., Fares, A., Fan, K., Hu, Z., and Zayed, T. (2022). Improving the leak detection efficiency in water distribution networks using noise loggers. *Science of the Total Environment*, 821:153530.

Toregas, C., Swain, R., ReVelle, C., and Bergman, L. (1971). The location of emergency service facilities. *Operations Research*, 19(6):1363–1373.

v. Neumann, J. (1928). Zur theorie der gesellschaftsspiele. *Mathematische Annalen*, 100(1):295–320.

Vajda, S. (2009). *Mathematical programming*. Courier Corporation.

Venkateswaran, P., Han, Q., Eguchi, R. T., and Venkatasubramanian, N. (2018). Impact driven sensor placement for leak detection in community water networks. In *2018 ACM/IEEE 9th International Conference on Cyber-Physical Systems (ICCPS)*, pages 77–87. IEEE.

Vielma, J. P., Ahmed, S., and Nemhauser, G. L. (2008). A lifted linear programming branch-and-bound algorithm for mixed-integer conic quadratic programs. *INFORMS Journal on Computing*, 20(3):438–450.

Vinel, A. and Krokhmal, P. A. (2014). On polyhedral approximations in p-order cone programming. *Optimization Methods & Software*, 29(6):1210–1237.

Walski, T. M. (1987). Water supply system rehabilitation. In *Task Committee on Water Supply Rehabilitation Systems of the Water Supply and Resources Management Committee of the Environmental Engineering Division of ASCE*, page 336. American Society of Civil Engineers (ASCE).

Wang, J. (2022). Nonnegative polynomials and circuit polynomials. *SIAM Journal on Applied Algebra and Geometry*, 6(2):111–133.

Wang, J. (2024). Weighted geometric mean, minimum mediated set, and optimal simple second-order cone representation. *SIAM Journal on Optimization*, 34(2):1490–1514.

Wang, X., Fan, N., and Pardalos, P. M. (2018). Robust chance-constrained support vector machines with second-order moment information. *Annals of Operations Research*, 263:45–68.

Weber, A. (1909). Über den standort der industrien. 1. Teil: Reine theorie des standorts. *JCB Mohr, Tübingen, (English ed. by CJ Friedrichs, Univ. Chicago Press, 1929).*

Wei, R. and Murray, A. T. (2015). Continuous space maximal coverage: Insights, advances and challenges. *Computers & Operations Research*, 62:325–336.

Wesolowsky, G. O. (1993). The Weber problem: History and perspectives. *Computers & Operations Research.*

Weyl, H. (1934). Elementare theorie der konvexen polyeder. *Commentarii Mathematici Helvetici*, 7(1):290–306.

Xue, G. and Ye, Y. (2000). An efficient algorithm for minimizing a sum of p-norms. *SIAM Journal on Optimization*, 10(2):551–579.

Zhen, J., de Ruiter, F. J., Roos, E., and den Hertog, D. (2022). Robust optimization for models with uncertain second-order cone and semidefinite programming constraints. *INFORMS Journal on Computing*, 34(1):196–210.